THE UNIVERSITY OF CALGARY

Extraction of Peace River Bitumen Using Supercritical Ethane

by

Jeffrey Lawrence Rose

A DISSERTATION
SUBMITTED TO THE FACULTY OF GRADUATE STUDIES
IN PARTIAL FULFILMENT OF THE REQUIREMENTS FOR THE

DEGREE OF DOCTOR OF PHILOSOPHY

DEPARTMENT OF CHEMICAL AND PETROLEUM ENGINEERING

CALGARY, ALBERTA
OCTOBER, 1999

Abstract

As the supply of conventional crude oil continues to decline, petroleum companies are looking for alternative hydrocarbon sources. The vast reserves of heavy oil and bitumen located in northern Alberta are among the alternatives. The challenge facing engineers is to develop a process for recovering this oil which is economic, efficient and environmentally acceptable. Supercritical fluid extraction is one method being investigated which could potentially meet all of these criteria.

In this study, Peace River bitumen was extracted using supercritical ethane. The bitumen was mixed with sand and packed into a semi-batch extractor. Ethane contacted the oil/sand mixture and the fraction of the bitumen soluble in the ethane was removed and subsequently collected in a two phase separator. The flow of ethane was such that the experiments were governed by equilibrium and not mass transfer. Experimental temperatures and pressures were varied in order to observe the effect of these parameters on the mass and composition of the extracted material. The extraction yields increased as the temperature decreased and pressure increased. Samples were collected at various time intervals to measure changes in the properties of the extracted bitumen over the duration of the process. As the extraction proceeded, the samples became heavier and more viscous.

The bitumen feed was characterised and the experimental data was then modelled using the Peng-Robinson equation of state. The characterisation process involved the distillation of the bitumen into five fractions. The distillation curve and density of each fraction was measured and this data was used in conjunction with correlations to determine the critical properties of the bitumen. Interaction parameters in the equation of state were then optimised until the predicted composition of extracted bitumen matched the experimental results.

Acknowledgements

I would like to take this opportunity to thank my supervisor, Bill Svrcek for all of his help and guidance over the years. Not only did he give me the opportunity to learn in the academic sense, he also gave me the chance to experience a great many things beyond the walls of the university.

I would also like to express my gratitude to my parents, Bud and Pat, my sister Jenn, and Marline. Their support and encouragement during my studies were always appreciated and valued.

I would also like to thank Wayne Monnery for his advice and input in this project. His door was always open and he was willing to share his knowledge and experience with me.

I am also indebted to Ken Chong of Core Laboratories Ltd., in Calgary. His assistance in co-ordinating all of the lab analysis and assistance with understanding the results was greatly appreciated.

Thanks must also be given to the great people and graduate students in the Department of Chemical and Petroleum Engineering. Your help and friendships will always be fondly remembered.

a, b	Parameters in the Peng-Robinson equation of state
A,B	Dimensionless forms of a and b
c	Volume correction factor
C	Concentration mol/L
C_v	Valve flow coefficient
d_0, d_1....	Constants for the translated Peng-Robinson equation of state
d_p	Particle diameter, m
D	Extractor diameter, m
D/uL	Dispersion number
f	Function used in Twu correlations to calculate critical properties
f_i	Fugacity for component i
k_{ij}	Interaction parameter for the i^{th} and j^{th} component
k_0, k_1....	Constants for the translated Peng-Robinson equation of state
K	Watson characterisation factor
K_i	Equilibrium constant for component I
l_0, l_1	Constants for the translated Peng-Robinson equation of state
L	Length of extractor, m
m	Dimensionless function in the Peng-Robinson equation of state
M	Mass, g
MW	Molecular weight, g/gmol
OSR	Oil to solvent ratio, g/Std L
P	Pressure, kPa
PCi	Pseudocomponent i
Q_i	Quadrupole for component i, $\mu J^{1/2}cm^{5/2}$
R	Universal Gas Constant, kPa L/mol K
SG	Specific gravity at 60°F relative to water at 60°F

t	Time, min
t	Translation factor for Peng-Robinson equation of state
T	Temperature, K
T_{10}	Saturation temperature at 10 mmHg, K
T_b	Normal boiling temperature, K or °R
v	Molar volume, L/mol
V	Solvent volume at standard conditions, L
x, y	Mole fraction
X	Weight fraction
z_i	Mole fraction of component i in feed to flash
z_{RA}	Racket compressibility factor
Z	Compressibility factor

Greek Symbols

α	Dimensionless function in the Peng-Robinson equation of state
β	Vapour phase fraction
ε	Sand porosity
ϕ	Fugacity coefficient
ψ	Value of objective function used to optimise binary interaction parameters
ρ	Density, kg/m^3
σ	Variance used in residence time distribution study
θ	Convergence criteria
ϖ	Acentric factor

Subscripts

C	Critical property
i,j	Component index

R	Reduced property

Superscripts

0	Reference property for n-alkane in the Twu correlations
k	Phase k

Chapter One

Introduction

As conventional light crude oil reserves continue to decline, oil companies are relying on alternative sources as means of satisfying the world's demand for petroleum and petrochemical products. The new sources of hydrocarbons include bitumens, heavy oils, oil shales and coal. The problem with these energy sources is that the properties of the fluids differ from the properties of light crude oils, which have been the traditional feed stocks for refineries. Therefore, in order to utilise these reserves, new processes are required for the recovery and refining of these heavier hydrocarbon mixtures. In addition to economic and process constraints, there are increased demands that these processes have a reduced impact on the environment. The development of new technologies that will meet these criteria requires additional experimental research in order to provide a sound basis for their design.

Bitumens and heavy oils have properties that are much different than the conventional crude oils. Light crude oils have °API gravities from 25 to 37 and viscosities less than 140 cSt at 38°C (Speight, 1991). In comparison, Athabasca bitumen found in northern Alberta, has an °API gravity of 8.6 and a viscosity of 7560 cSt at 38°C (Speight, 1991). The higher densities and viscosities of heavy oils and bitumens mitigate the production and transport of these fluids, as well as requiring additional upgrading into a suitable refinery feedstock. Upgrading is required in order to increase the hydrogen to carbon atomic ratio of heavy oils from approximately 1.491, to 1.818, typical of light crude oils (Speight, 1991). Hence, new recovery methods and improved upgrading technologies are

required if these reserves are to become viable alternatives to conventional lighter crude oils.

1.1 Setting the Scene

Based on the crude oil production rates for 1989, it has been estimated that the known conventional oil reserves are capable of lasting until the year 2020 (Altgelt et al., 1994). Because the demand for petroleum products has increased, oil companies have been expanded their production by developing new reserves which are considerably different from the traditional light crude oil supplies. The resulting change in refinery feed stocks is reflected in the increase in density of oils being refined in the United States during the 1980's, shown in Figure 1.1.

One of the reasons for the decrease in the °API gravity for the crude oils being refined is the increased amount of bitumen and heavy oils being produced. Figure 1.2 shows the location of the four main reserves of bitumen and heavy oil found in Alberta, Canada. As of 1995, it was estimated that these reserves contained 1.7 trillion barrels of bitumen in place, which is more oil than the proven reserves in Saudi Arabia (Hyndman, 1995). Due to the incredible size of these reserves, a great deal of time and money is being spent on developing these resources. It is estimated that present recovery methods are only capable of recovering 300 billion barrels of Alberta's known bitumen and heavy oil reserves (Hyndman, 1995).

The term "bitumen" has been used to describe many different types of unconventional petroleum reserves. Phrases used to define bitumen include: "A thick tar-like hydrocarbon substance" (Bentein, 1996) and "Any natural mixture of solid and semi-solid hydrocarbons" (Gray, 1994). In 1992, UNITAR developed criteria to classify heavy

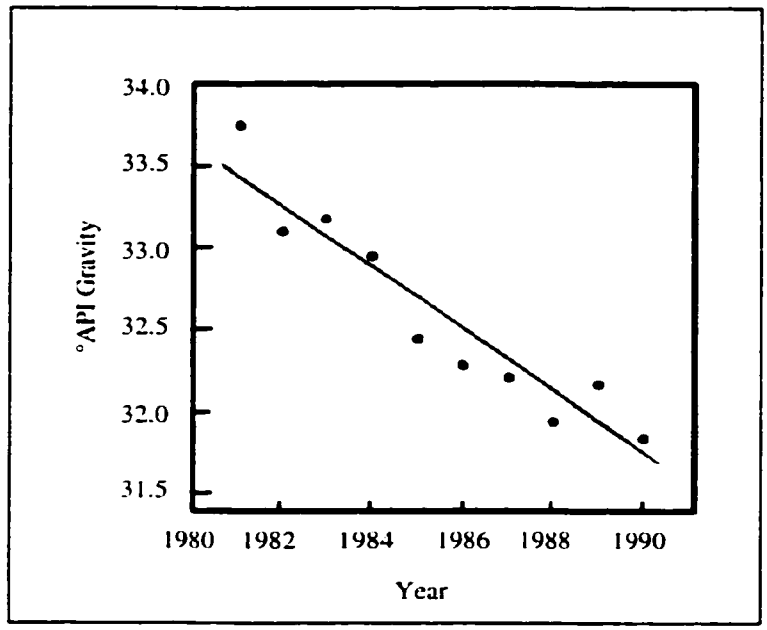

Figure 1.1 – The °API gravity of crude oils refined in the United States during the 1980's (Altgelt et al., 1994).

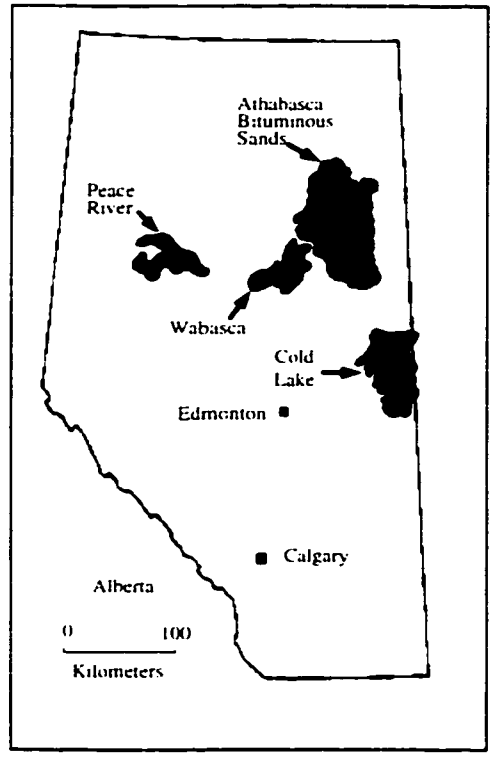

Figure 1.2 – Location of the four principle bitumen and heavy oil reserves in Alberta (Capeling et al., 1979).

hydrocarbon reserves based on their physical properties (Miller, 1994). If the mixture has a viscosity greater than 10 000 cP on a gas free basis at reservoir conditions, then it is considered an immobile bitumen. Fluids with viscosities less than 10 000 cP are considered heavy oils and are further classified based on their density using the guidelines shown in Table 1.1.

Density, kg/m^3		Classification
Minimum	Maximum	
1000		Extra Heavy
966	1000	Heavy
934	966	Less Heavy
904	934	Intermediate
	904	Conventional

Table 1.1 – UNITAR sub-classification criteria for heavy oils (Miller, 1994).

The methods used to recover bitumen and heavy oil can be divided into two catagories, surface mining and *in situ* methods. Athabasca bitumen is separated from mined tar sand using the Clark Hot Water Extraction process and then upgraded into a light synthetic crude. *In situ* production methods for producing heavy oils involve the reduction of the fluid's viscosity, often using heat supplied by steam, such that it can be produced using horizontal and vertical wells. The oil is then diluted with light hydrocarbons to facilitate its transportation to upgrading facilities.

While surface mining and steam injection are the most common processes for recovering bitumen and heavy oil, they are not without their share of problems. For example, surface mining is hindered by process and environmental concerns such as the availability of fresh water supplies, heat losses to tailings, accumulation of tailing sludge in large ponds and high equipment maintenance costs (Houlihan, 1984; Pruden, 1997). The efficiency of thermal *in situ* processes utilising steam declines dramatically when applied to thin

reservoirs or reservoirs with bottom aquifers (Frauenfeld et al., 1998). Therefore, new technologies which may address these problems while meeting economic constraints would be appealing to petroleum production companies.

1.2 Objectives of This Study

In this study, it was necessary to design and construct an apparatus capable of collecting data for bitumen and supercritical fluid systems. Extensive data exists regarding the solubility of light gases such as nitrogen, ethane and carbon dioxide in bitumens at subcritical conditions (Mehrotra et al., 1985; Svrcek et al., 1989; Eastick et al., 1992). A void exists in the literature with respect to the composition of the solvent rich phase for bitumen/supercritical fluid systems. The composition of the light phase is important for the design of an extraction process using supercritical fluids. Thus, the first phase of the project was to design, construct and validate an apparatus that was easy to operate and would provide data for the extraction of bitumen using a supercritical fluid.

The goal of the experimental phase of the project was to partially fill the void in the literature by providing solubility data for bitumen/supercritical fluid systems. Experiments were conducted to examine how temperature and pressure impacted the extraction of bitumen from a bitumen/sand mixture using supercritical ethane. Samples of extracted bitumen were analysed in order to determine how their properties, such as composition, viscosity and SARA fractions were affected by changing the extraction temperature and pressure and how they changed over the duration of an extraction. A second set of extractions using supercritical carbon dioxide were used to provide an indication of the ability of supercritical ethane to extract bitumen with respect to another common supercritical fluid.

The last stage of this study was the development of a computer model of the extraction process. A relatively simple, well studied equation, the Peng-Robinson equation of state, was chosen to be the thermodynamic basis of the model and would be used to predict the phase behaviour of the system. Different methods for the characterisation of hydrocarbon mixtures needed to be evaluated to determine which set of existing correlations was suitable for the Peace River bitumen. In addition, optimal binary interaction parameters for the bitumen fractions and ethane would be provided.

1.3 Dissertation Structure

Chapter Two provides background information regarding supercritical fluids and their properties. Examples of the enhanced solvent capabilities of supercritical fluids are discussed and examples of successful industrial processes utilising supercritical fluids are provided. A summary of the present literature on supercritical fluids and heavy hydrocarbon systems, such as bitumens, is presented. The Peng-Robinson equation of state and its application to supercritical fluid systems is also presented in Chapter Two.

The design and evaluation of the experimental apparatus used in this study is discussed in Chapter Three. Specifications for the equipment comprising the experimental apparatus are provided. The flow pattern of the solvent through the extractor was studied and the results are presented in this chapter. The performance of the apparatus is verified against published data to confirm that the data produced is consistent with that of other researchers.

Chapter Four presents the experimental results for the Peace River-supercritical ethane system. An extensive study was conducted in order to determine whether this system was dominated by thermodynamic equilibrium or mass transfer resistances. The effects of

temperature and pressure on extraction rates and the composition and properties of the extracted oil are discussed. A comparison was made of the capabilities of supercritical ethane and carbon dioxide to act as solvents for the extraction of bitumen from a mixture of bitumen and sand. Mass transfer considerations with respect to the system and operation conditions studied are highlighted in this chapter.

Chapter Five deals with the characterisation of the Peace River bitumen. This is necessary if an equation of state is to be used to model the experimental data. Furthermore, suitable procedures for estimating the complete boiling point curve for Peace River bitumen were evaluated. Methods for calculating the critical properties for complex mixtures of hydrocarbons are evaluated using a translated form of the Peng-Robinson equation of state.

The results from the thermodynamic modelling phase of the project are presented in Chapter Six. Details such as liquid volume shift method, optimisation routine and the sensitivity of the results to different input data are discussed. The ability of the model to reproduce the experimental results is presented in this chapter.

In Chapter Seven, conclusions are drawn based on the experimental and modelling results for the Peace River bitumen/supercritical ethane system. Recommendations are made regarding further areas of research which if explored may lead to the application of supercritical fluids for the processing and recovery of bitumens and heavy oils that are economically appealing to the petroleum industry.

Chapter Two

Literature Review and Background

Supercritical fluids were first discovered in 1822 by Baron Cagniard de la Tour in 1822 (McHugh et al., 1994; Taylor, 1996). Using a modified piece of a cannon and later a visual cell, he was able to detect and record the conditions at which the gas-liquid interface disappeared for different fluids. During the late 1800s, researchers used various techniques, such as building mercury columns that ran the length of the Eiffel Tower, in order to achieve higher pressures (McHugh et al., 1994). The ability to operate at higher pressures enabled the detection of critical temperatures and pressures for a much wider range of compounds.

During the following 100 years much has been discovered regarding the behaviour of supercritical fluids. Attempts have been made to exploit the characteristics in a number of industrial applications and in many cases, such as deasphalting of oils and decaffeination of coffee beans, the results have been quite successful.

In this chapter, the unique characteristics of supercritical fluids are discussed along with how these affect the solvent properties. Industrial applications of supercritical fluids are highlighted with focus on their uses in the petroleum industry. Finally, modelling of supercritical fluid systems using cubic equations of state is reviewed and methods for the characterisation of heavy hydrocarbon mixtures are presented.

2.1 Supercritical Fluid Characteristics

Figure 2.1 shows a pressure-temperature diagram for a typical pure fluid (McHugh et al., 1994). The critical point is located at the end of the vapour-liquid equilibrium line and has a corresponding critical temperature (T_c) and critical pressure (P_c). At the critical point, increasing the pressure will not result in the formation of a liquid phase and increasing the temperature will not result in the formation of a gas phase. When both the T_c and P_c are exceeded, the phase is no longer considered a liquid nor a vapour and is defined as a supercritical fluid.

The critical point can also be distinguished by dramatic changes in the properties of the fluid. To illustrate this, density data from the NIST Thermophysical Properties of Pure Fluids Database (National Institute of Standards and Technology, 1992), was plotted in its reduced form as a function of reduced pressure for ethane and is shown in Figure 2.2. In the region close to the critical point, small changes in pressure result in significant changes in the fluid density especially compared to gases or liquids just below the critical point. Temperature changes also have a greater impact on the density near the critical point. In Figure 2.2, moving from Tr = 1.0 to Tr = 1.1 results in a larger change in reduced density than from Tr = 0.9 to Tr = 1.0 at constant pressures near the critical point. Thus the density of a supercritical fluid is a much stronger function of temperature and pressure than the corresponding gas or liquid density. Similar dramatic changes in properties such as diffusivity of solutes and viscosity are also a characteristic of supercritical fluids.

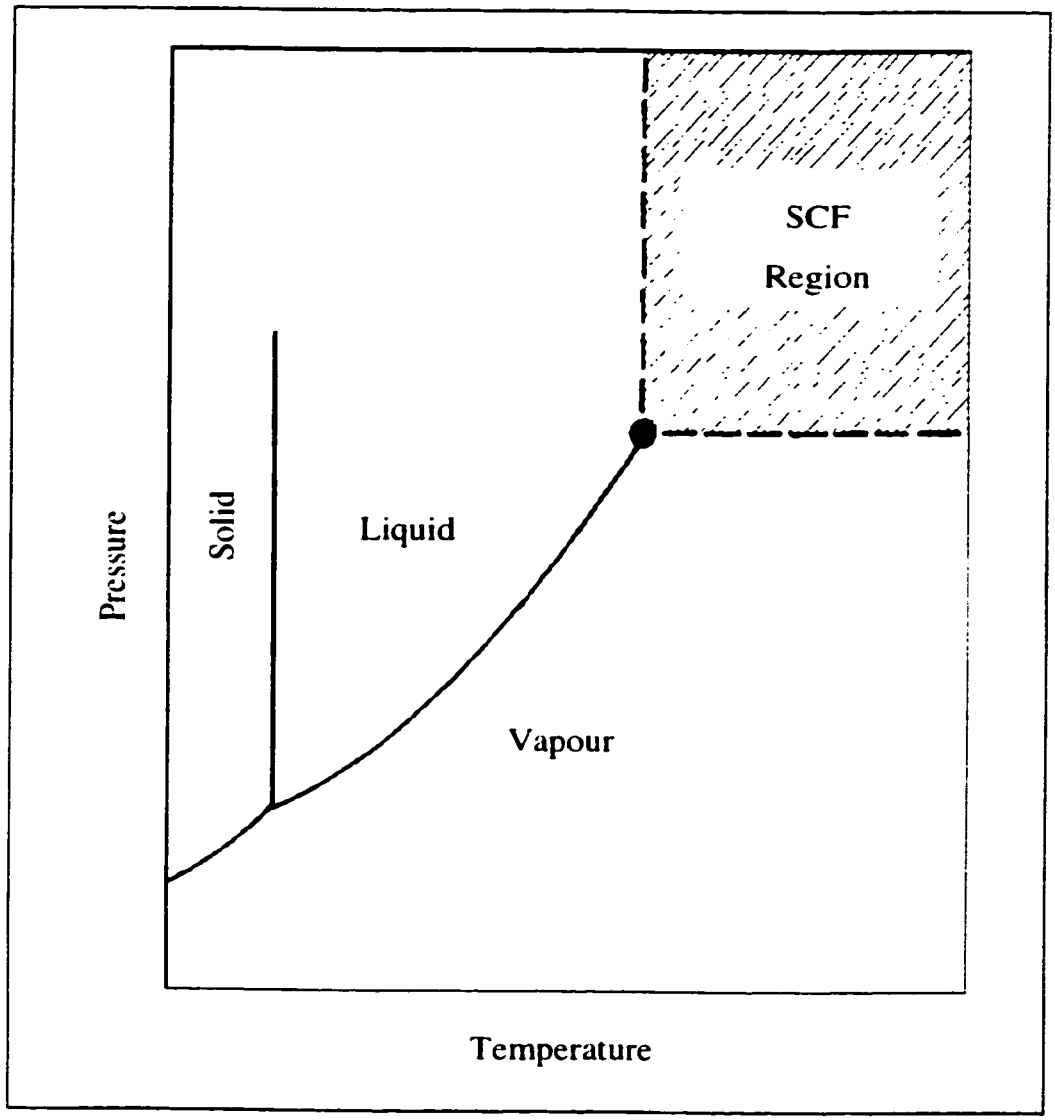

Figure 2.1 - Pressure-temperature diagram for a typical pure component (McHugh et al., 1994).

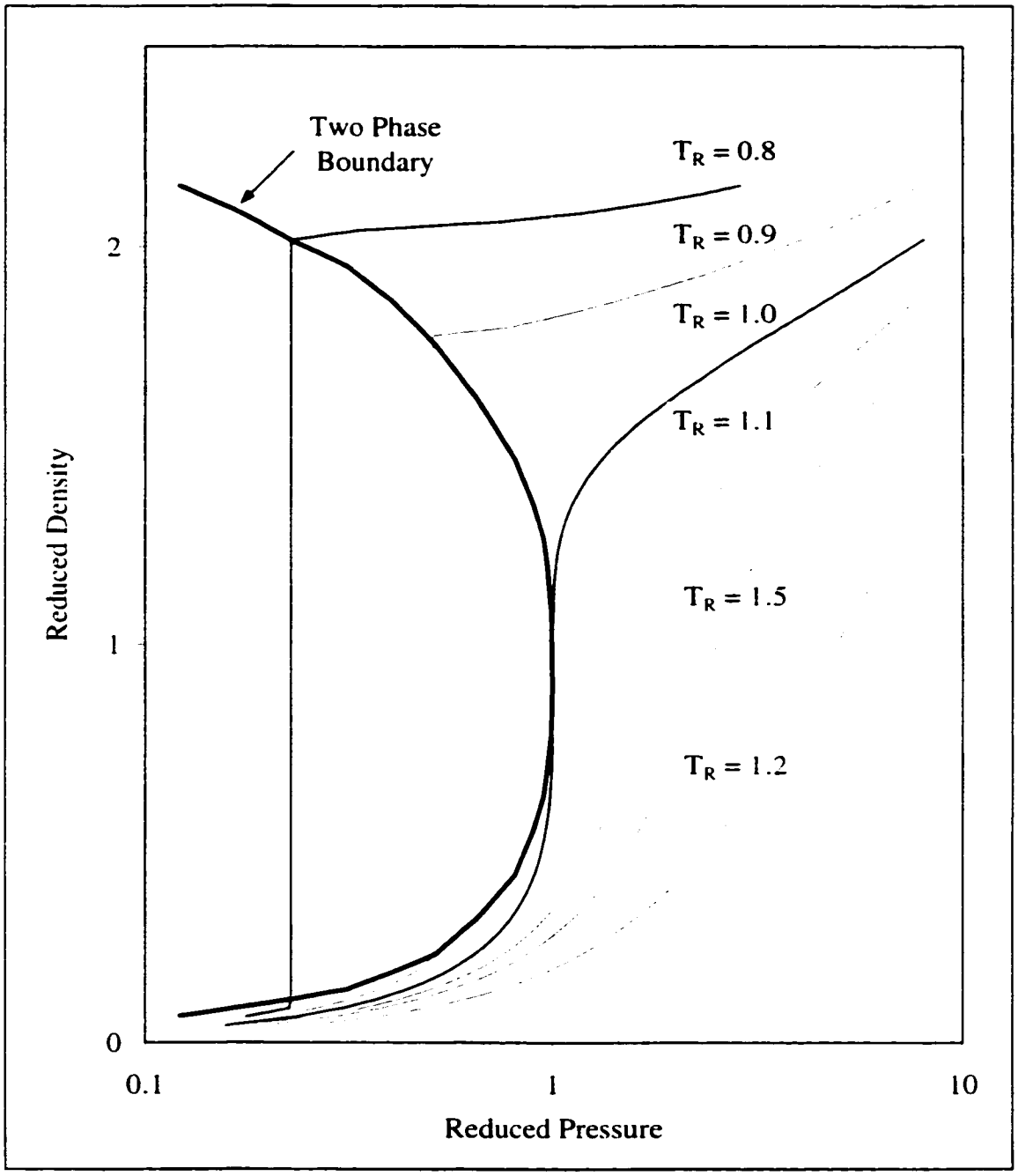

Figure 2.2 – Reduced density versus reduced pressure at different reduced isotherms for ethane.

Another unique aspect of supercritical fluids is the fact that they have both gas-like and liquid-like properties. Figure 2.2 shows that when the pressure is increased and ethane shifts from a gas to a supercritical fluid, the density rises rapidly and approaches that of liquid ethane. Figure 2.3 shows how the viscosity for ethane changes as a function of temperature at a different isobars. One can see that as the temperature increases and ethane goes from the liquid phase to supercritical phase, the viscosity decreases dramatically then goes through a minimum and becomes gas-like. These observations are summarised in Table 2.1 where the values for density, viscosity and diffusion coefficient for the three phases can be compared (Taylor, 1996).

	Density, g/ml	Dynamic Viscosity, g/cm-s	Diffusion Coefficient, cm^2/s
Gas (ambient)	0.0006-0.002	0.0001-0.003	0.1-0.4
Supercritical fluid (T_c, P_c)	0.2-0.5	0.0001-0.003	0.0007
Liquid (ambient)	0.6-1.6	0.002-0.03	0.000002-0.00002

Table 2.1 – Typical physical properties for gases, liquids and supercritical fluids (Taylor, 1996).

Higher densities improve the solubility of solutes in supercritical fluids relative to gases, while gas-like transport properties assist in reducing mass transfer resistances within supercritical fluids as compared to liquids. This combination of gas-like and liquid-like properties have led to the development and use of supercritical fluids as alternatives to conventional solvents in many extraction processes.

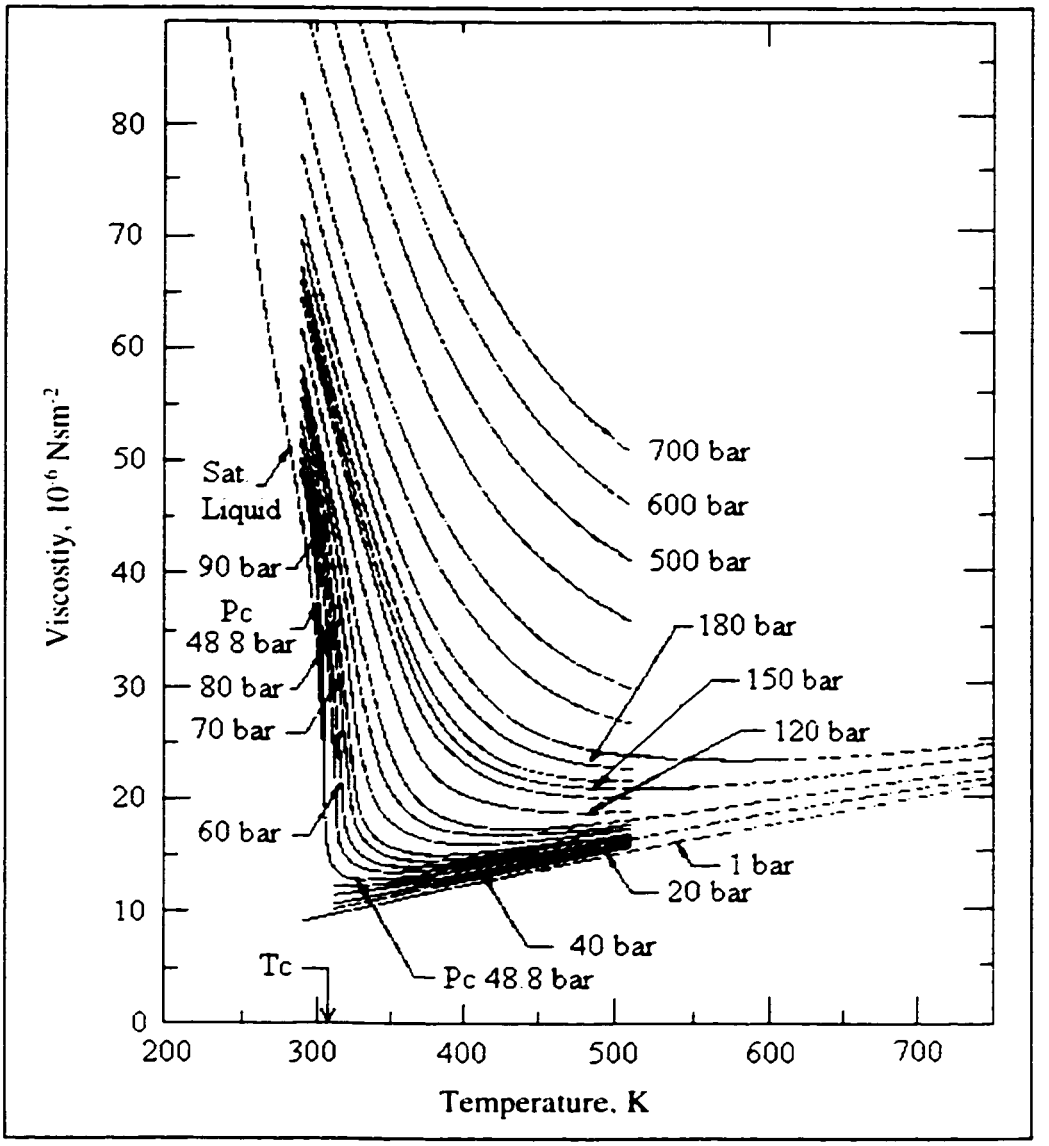

Figure 2.3 – Viscosity versus temperature for ethane (Stephan et al., 1979).

2.2 Enhanced Solvent Properties

The benefits of using supercritical fluids as solvents in extraction processes are numerous. One advantage is the behaviour of density near the critical point. Liquid-like densities result in solubility levels for supercritical fluids that approach those of liquids and are much higher than those for gas solvents. This means that supercritical solvents can perform extractions at much lower solvent to feed ratios than the corresponding gas phase extraction. In addition, the dramatic changes in density near the critical point result in easier solvent recovery. These benefits can be illustrated using the solvent-solute system of CO_2-naphthalene.

Figure 2.4 is a plot of naphthalene solubility versus pressure at two different temperatures greater than the critical temperature of CO_2. At low pressures, $P << P_c$, the solubility is governed by the vapour pressure of naphthalene and the system behaves ideally, thus as the pressure of the system increases, the solubility of naphthalene in the CO_2 decreases. As the pressure is further increased and approaches the critical pressure, the density of the CO_2 phase begins to increase rapidly similar to the behaviour of ethane observed earlier in Figure 2.2. In this region the solvent density begins to govern the solubility as opposed to the solute vapour pressure and thus there is a sharp rise in the solubility of naphthalene in the carbon dioxide. As the pressure is increased further, the solvent density begins to approach a constant value and the mole fraction of solute reaches a maximum and then declines at even higher pressures (Kurnik et al., 1981).

Figure 2.4 can also be used to illustrate the effects of temperature on the solubility of solutes in supercritical fluids. At pressures below approximately 60 atm and above 120 atm, the solubility increases as temperature increases. This results from the fact that in these regions, the vapour pressure of the solute is the dominating factor in determining solubility and at higher temperatures the solute has higher vapour pressures. From 60-120 atm, the CO_2-naphthalene system demonstrates the phenomena of retrograde

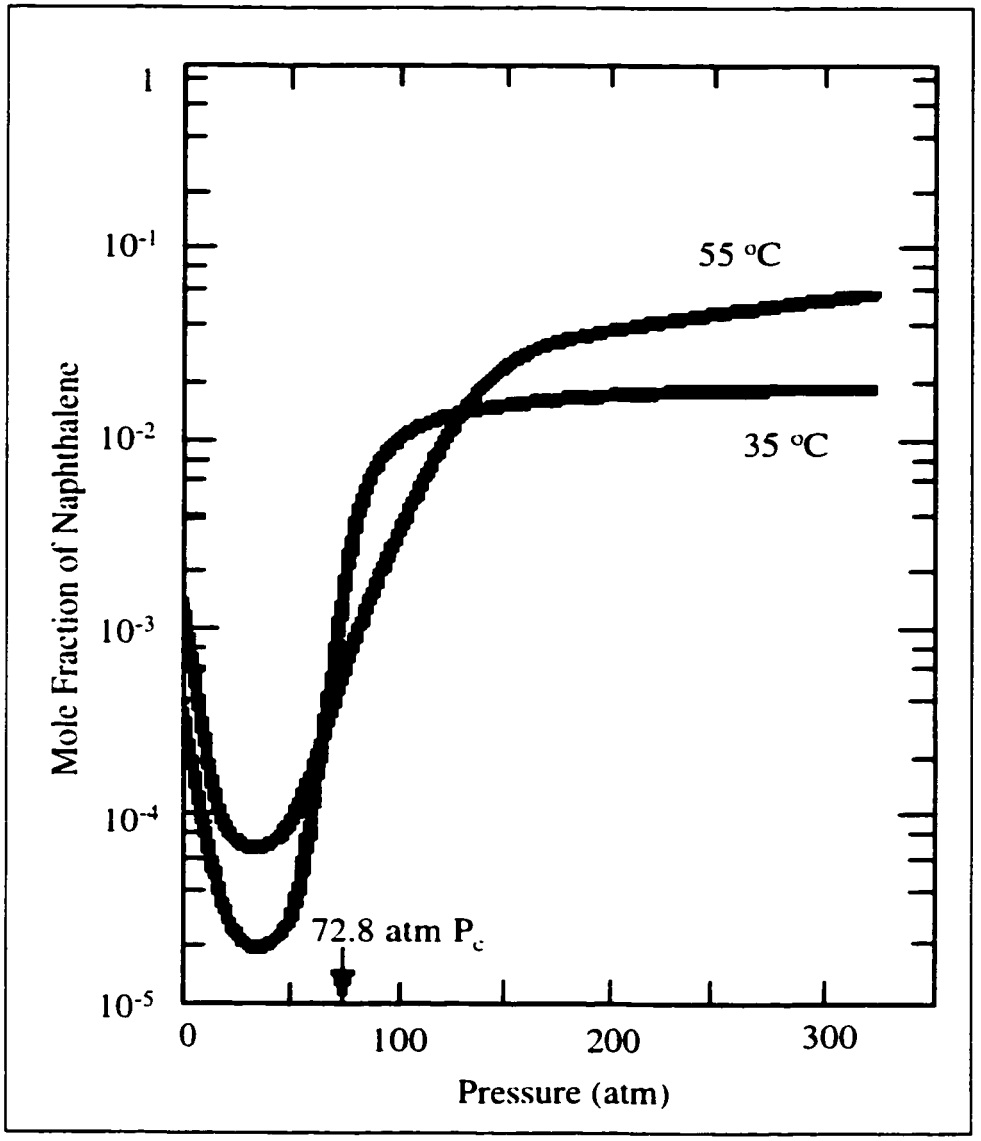

Figure 2.4 – Solubility of naphthalene in CO_2 (Hoyer, 1985).

condensation. In this region, increases in temperature result in the precipitation of the solute instead of an increase in solubility. This is due to the fact that in this range, the density of CO_2 is governing the solubility as opposed to the vapour pressure of naphthalene. As temperature is increased, density decreases and as a result, solute solubility decreases as well.

Another advantage in using supercritical solvents arises in the solvent recovery process. In Figure 2.4, the solubility of naphthalene in CO_2 changes dramatically as temperature and/or pressure is adjusted when operating near the critical point. If the extraction of naphthalene is performed at 35 °C and 100 atm, an extract phase with a composition of $1*10^{-2}$ mole fraction would be produced. If the pressure of that stream was subsequently decreased to approximately 45 atm, a solvent rich phase could be recycled that would have a naphthalene composition of $2*10^{-5}$ mole fraction. In other words, 99.8% of the naphthalene would be precipitated and recovered and a solvent stream that was 99.998% pure CO_2 could be repressurised and recycled. Solvent recovery could also be achieved by adjusting the temperature of the system but the results would not be as favourable. Table 2.2 provides a summary of the effects of adjusting pressure and temperature on solvent recovery for an extraction performed at 55 °C and 150 atm which would result in an exit stream with the mole fraction of naphthalene being $2*10^{-2}$ based on data from Figure 2.4.

Solvent Recovery Action	Solvent Recovery Conditions	Solute Recovery, %	Recycled Solvent Purity, mole %
Drop Pressure Constant Temperature	Pressure: 45 atm Temperature: 55 °C	99.65	99.993
Constant Pressure Drop Temperature	Pressure: 150 atm Temperature: 35°C	50%	98.00
Drop Pressure Drop Temperature	Pressure: 45 atm Temperature: 35°C	99.9	99.998

Table 2.2 – Solute recovery and recycled solvent purity for CO_2-naphthalene.

Separations performed using supercritical fluids have an advantage over traditional methods such as distillation in terms of the operating temperature required. Table 2.3 lists the critical conditions for a number of solvents commonly used as supercritical solvents. The critical temperature for these solvents are quite low. Thus, extractions performed at or near these temperatures will have lower energy requirements than distillation (Parkinson et al.,1989). In addition, because supercritical fluid extractions can be performed at lower temperatures, they are ideal for extracting and separating solutes which are temperature sensitive and would degrade at the temperatures where conventional extractions are performed. This makes supercritical fluid extraction ideal for applications in the food, pharmaceutical and petroleum industries where product degradation is a major concern (Williams, 1981).

Solvent	Critical Temperature, K	Critical Pressure, MPa
Carbon Dioxide	304.25	7.38
Ethane	305.35	4.88
Ethylene	282.45	5.04
Propane	369.85	4.25

Table 2.3 - Critical temperature and pressure for compounds commonly used in supercritical fluid extraction.

One of the disadvantages with using liquid extraction processes is the low mass transfer rates. Table 2.1 showed that supercritical fluids have gas-like viscosities and diffusivities which reduce the mass transfer resistance in the solvent phase and increase the rate at which the solute moves into the solvent phase. For example, a supercritical fluids extraction that can be completed in 10-60 minutes may take hours or even days to be completed using a liquid solvent (Luque de Castro et al., 1994).

Supercritical fluids may also provide an alternative to processes that are subject to strict environmental legislation. Supercritical CO_2 may be an excellent candidate to replace traditional solvents which are detrimental to the environment (Brennecke et al., 1989). This is mainly because carbon dioxide is non-toxic. In the United States, the Environmental Protection Agency has developed a program to reduce the use of a number of harmful organic solvents commonly used in analytical chemistry and supercritical carbon dioxide is an excellent replacement solvent (Taylor, 1996; Luque de Castro et al., 1994).

2.3 Supercritical Fluid Applications

The potential for using supercritical fluids as solvents in extraction processes has been known for over one hundred years. In 1879, J. B. Hannay and J. Hogarth recognised that the ability of ethanol to dissolve potassium iodide increased dramatically when ethanol was in the supercritical region. (Williams, 1981). They also observed that the solute could be recovered by decreasing the pressure of the system. Villard studied the solubility of hydrocarbons such as camphor, stearic acid and paraffin wax in supercritical methane, ethylene and carbon dioxide in 1896 (McHugh et al., 1994). In the 1930's, data began to appear for many other supercritical fluid/hydrocarbon binary systems (Williams, 1981).

Auerbach filed a patent in 1927 outlining a process for treating and purifying petroleum fluids (McHugh et al., 1994). He observed that he could fractionate an oil and produce extracts that varied in both chemical structure and molecular weight. In 1943, the first commercial application involving the use of supercritical fluids was patented by H. E. Messmate in the United States for the deasphalting of petroleum streams (Williams, 1981). Research drifted away from high pressure processes during the 1940's to 1960's

and not until the energy crisis of the 1970s did scientists and engineers look to supercritical processes as viable alternatives to the existing energy intensive processes (McHugh et al., 1994). During following decades, numerous processes were developed which exploited the characteristics of supercritical fluids as solvents for separation processes.

One of the most successful applications of supercritical fluids technology was the decaffeination of coffee beans and tea. Zosel first described a process for removing caffeine from green coffee beans using supercritical carbon dioxide in 1974 (McHugh et al., 1994). Based upon Zosel's process, Kaffee HAG constructed a 30 000 tonne/y coffee decaffeination plant in the late 1970s (Körner, 1985) and SKW Trostberg AG built a 6 000 tonne/y tea decaffeination plant in 1988 (Parkinson et al., 1989). As of 1989, approximately two-thirds of Germany's decaffeinated tea was produced using supercritical technology. Supercritical carbon dioxide is more selective than ethyl acetate (the only other solvent being used commercially), resulting in a product which has a better flavour and less caffeine. The success of these plants has prompted the construction of larger plants in both Germany and the United States.

The production of hops extract is another example of a large scale process relying on supercritical fluids as the solvent (Körner, 1985; Clifford et al., 1993; Parkinson et al., 1989). In this process, a supercritical fluid solvent is used to remove acids such as the humulones which give beer a bitter taste (Williams, 1981). Hops processing plants have been constructed in Germany, the United Kingdom, Australia and the United States utilising carbon dioxide near its critical point. These plants are capable of throughputs in the vicinity of 10 000 tonne/y and have operating costs comparable to older processes. Conventional technology utilises solvents such as hexane but this results in problems with potential residual solvent left in the product. The benefits to using supercritical carbon dioxide are that it is non-toxic and thus residual solvent in the products are no

longer a serious concern. In addition, supercritical carbon dioxide is more selective and therefore, less solvent is required.

Supercritical fluids have had success in other smaller scale commercial processes including: 1) removal of nicotine from tobacco, 2) flavour extraction from vanilla, ginger, paprika and rosemary, 3) aromatic component extraction for cosmetics from basil leaf, ginger root, parsley seed, vanilla beans and chamonile flowers, 4) separation of valuable components in the pharmaceutical industry and 5) colour extraction from red pepper (Brennecke et al., 1989; Parkinson et al., 1989; Taylor, 1996). There are also many other areas in which the potential for using supercritical fluids is high such as the following: soil and water remediation, a medium for chemical reactions, removal of cholesterol from eggs and butterfat, removal of terpenes from citrus oils, pulping process for woods, activated carbon regeneration and supercritical chromatography (Taylor, 1996; Parkinson et al., 1989; and Hoyer, 1985). The chief benefit in using supercritical solvents in these extraction processes is the exploitation of the lower operation temperatures needed with supercritical fluids. These lower temperatures reduce the chance of degradation of the delicate material being extracted.

2.4 Supercritical Extraction Applications: Petroleum Industry

One of the earliest applications of supercritical fluid technology was to treat, separate and purify hydrocarbon streams. A patent detailing the use of supercritical CO_2 to achieve the separation of such mixtures as tar oil, resin oils and fatty oils was filed in 1927 by E. B. Auerbach (McHugh et al., 1994). His work in this field pioneered the development of the propane deasphalting process first discussed in 1936 and is still in use today (McHugh et al., 1994). Propane deasphalting and the Residuum Oil Supercritical Extraction (ROSE) process, developed by Kerr McGee (McHugh et al., 1994), are the most successful

example of exploiting the behaviour of fluids near their critical point in the petroleum industry.

The ROSE process was developed in 1954 and is used to remove asphaltenes and resins from resid feed using fluids near their critical point (Williams, 1981; McHugh et al., 1994). A process flow diagram is shown in Figure 2.5. The residuum feed is mixed with compressed butane or pentane solvent at a pressure above the critical pressure of the solvent but at a temperature just below the critical temperature. At these conditions, the asphaltenes are not soluble in the solvent and the solvent-resid mixture is sent to a separator where the asphaltenes are collected in the bottoms stream. If resins are to be removed as a separate product, the overhead from the asphaltene separator is heated and sent to a second separator (not shown in Figure 2.5) where the resins precipitate. The solvent is recovered by heating the solvent-oil mixture to a temperature just above the critical temperature of the solvent. The remaining deasphalted oil is insoluble and is separated from the solvent in the third tower. The solvent is cooled and compressed to return it to the initial conditions so it can be recycled. The deasphalted oil, free of solvent, is produced as the valuable product.

The ROSE process has had a great deal of commercial success. The first unit came on line in August, 1979 and plants exist that are capable of processing up to 50 000 BPD of feed. There are 16 units in operation world-wide, with capacities ranging from 1 700 to 50 000 BPD and 9 more licenses have been issued as of March 1996 (Pruden, 1997).

The main benefits of the ROSE process is in the solvent recovery step. Conventional deasphalting requires both a large pressure drop and large temperature increase separating the liquid deasphalted oil from the vapourised solvent. A large amount of energy is required to cool and repressurise the solvent to the conditions such that it can be recycled. In the ROSE process, 85-93% of the solvent is recovered by keeping the pressure relatively constant and increasing the temperature 10-15°C. The remaining solvent is

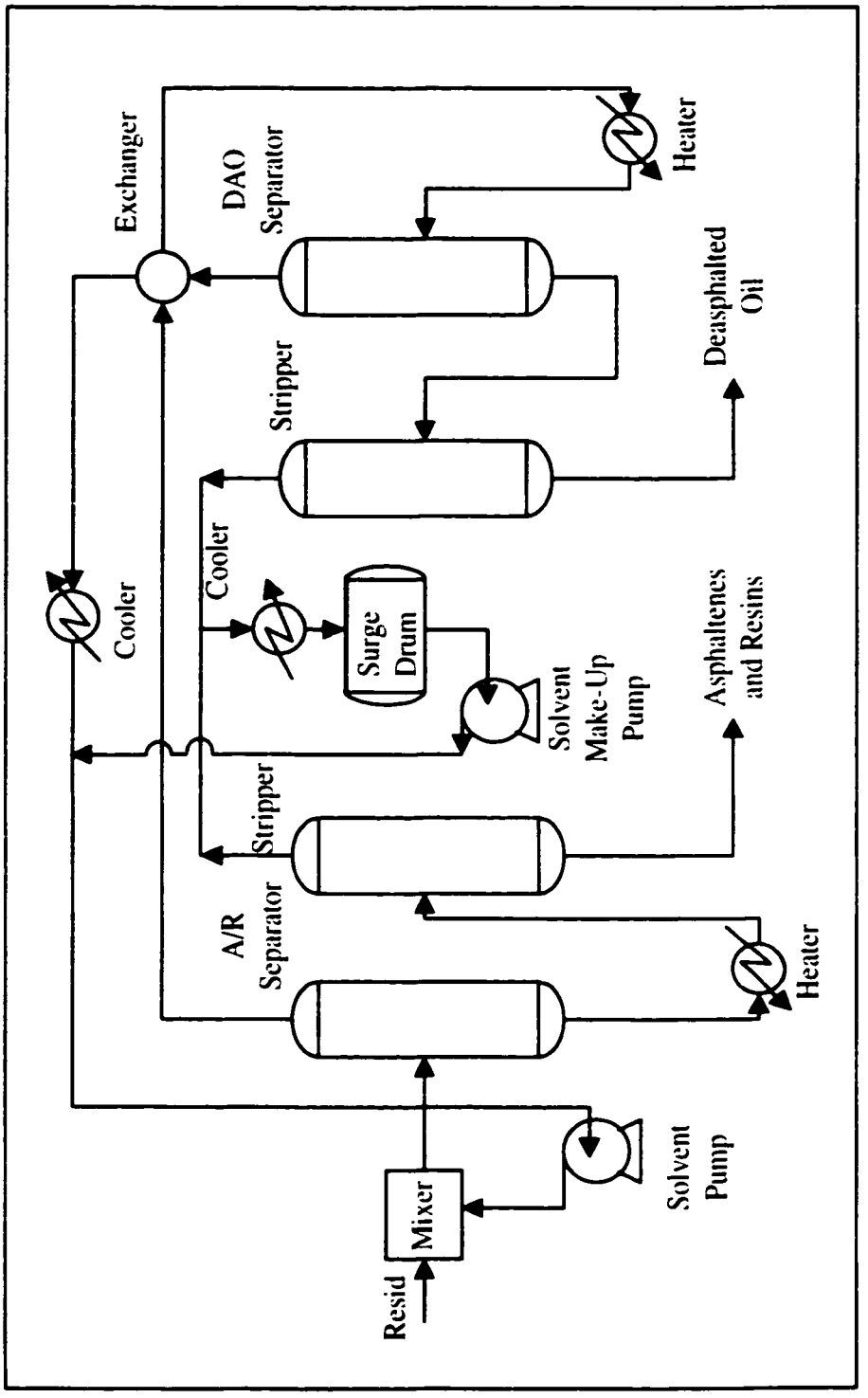

Figure 2.5 - Schematic of the ROSE process (McHugh, 1994)

recovered in the traditional manner. Using this technique, a much smaller amount of solvent is depressurised and heated, thus less energy is required to recycle the solvent. Based on a 1995 study, there was a 60% energy savings using the ROSE process as compared to conventional liquid deasphalting.

Propane deasphalting is quite similar to the ROSE process with the main differences being the solvent used and the feed processed. As the name suggests, propane deasphalting uses near critical propane to produce a light paraffin oil from a lube oil feed. The ROSE process uses compressed butane or pentane to remove the asphaltenes, and in some cases the resins, from a heavier residuum feed. Butane and pentane cannot be used to treat the lighter lube oil feed because both the desired light paraffin oil and the remaining heavier oil are highly soluble in these solvents and thus a separation would not occur. Conversely, propane would cause the precipitation for more than just asphaltenes and resins and if propane was used in place of butane or pentane in the ROSE process, a large portion of the desired product would be lost in the asphaltene and resin streams. Both processes rely on the dynamic behaviour of the solvents near their critical point to selectively precipitate various fractions of the feed at different stages in the process. This also highlights the importance of selecting the proper solvent for a given application.

Based on the success of the propane deasphalting and the ROSE processes combined with the data researchers were collecting for mixtures of supercritical fluids and pure hydrocarbon systems, engineers began looking to supercritical fluids to address other hydrocarbon processing needs. As the supply of conventional light crude oil continues to decline, petroleum companies are looking for new supplies such as oil shales, heavy oils and bitumens. The properties of these new fluids are greatly different than traditional light crude oil. Therefore, new technology is required to for the production and processing of these feedstocks because the traditional methods are not designed to process these new fluids. The application of supercritical fluid technology is one avenue being explored.

Two potentially viable sources for hydrocarbons are the vast resources of oil shales and coal reserves in countries such as Australia and Turkey. Companies such as Kerr-McGee and the National Coal Board of England have developed processes for coal liquification using supercritical fluids (Sunol et al., 1990). Researchers have looked at using supercritical fluids to extract oil from oil shales (Kesavan et al., 1988; Triday et al., 1988; and Bartle et al., 1984) and coal (Sunol et al., 1990; Kershaw et al.,, 1987). Typical experiments involved the contact of flowing supercritical solvents over a fixed bed of crushed oil shale or coal. Fluids used as solvents in these studies include water, toluene and carbon dioxide.

For example, Kesevan et al. processed Stuart oil shale from Queensland, Australia, using supercritical carbon dioxide (Kesavan et al., 1988). They studied the effects of varying the temperature and pressure on the amount and chemical composition of the extracted oil. Higher temperatures increased the yield of oil but as these temperatures were quite high, they did observe some degradation of the product. Increasing the pressure also resulted in more oil being removed from the shale. In both cases the amount of oil extracted using supercritical carbon dioxide was greater than that obtained using conventional retorting.

An example of the work being conducted to determine the ability of supercritical fluids to extract oil from coal is that being performed by Sunol et al. (Sunol et al., 1990). Using a semi-batch extractor, they observed that Wyodak 1 coal could be processed more efficiently using supercritical toluene. The toluene extracted the components which undergo decomposition and repolymerisation reactions that occur during traditional extraction processes. This aided in the reduction of product degradation and the plugging of pores in the coal. They also reported that recoveries of hydrocarbons were in excess of 30 wt% on a dry basis using supercritical toluene.

It has also been postulated that supercritical fluids could be used to fractionate heavy hydrocarbon streams produced during the processing of both conventional and heavy crude oils. Crude oils (Oschmann, et al., 1998; Deo et al., 1992; Hwang, et al., 1996), residues (Cheng, et al., 1994; Eisenbach et al., 1983; Lutz et al., 1984; and Warzinski, 1987) and bitumen-derived liquids (Deo et al., 1992) have all been separated using supercritical fluids such as propane and carbon dioxide.

The potential for using supercritical fluids to fractionate mixtures such as crude oils and vacuum residue has also been investigated (Hwang et al., 1996; Hwang et al., 1995; Deo et al., 1992). Using fluids such as propane and carbon dioxide, they investigated the effects of varying temperature and pressure on the amount of extracted material and its composition. They found that extraction yields increased as the solvent density increased and as the operating conditions moved closer to the solvent critical point. In addition, they reported that as the extractions proceeded, the material removed became heavier. This was reflected in increases in the carbon numbers and the boiling point curves for the extracted material.

Cheng et al. designed experiments in which they fractionated Sheng-Bei wax bearing residue using supercritical propane (Cheng et al., 1994). They observed that by varying the pressure during the extraction process, the yields increased from 52 wt% at 8.3 MPa to 64 wt % at 10.3 MPa. They concluded that supercritical propane was a more efficient fluid because the supercritical extraction process was more selective and gave higher yields than liquid propane deasphalting (Cheng et al., 1994).

Experiments have also been reported in which portions of different bitumens were extracted using supercritical fluids (Subramanian et al., 1998; Deo et al., 1992; Eisenbach et al., 1983). Deo et al. and Eisenbach et al. used semi-batch experimental devices in which Whiterocks bitumen (Deo et al., 1992) and Athabasca bitumen (Eisenbach et al., 1983) were initially fed into an extractor and contacted with a supercritical fluid. Deo et

al. observed that the composition of the extract changed over time as more and more of the bitumen was removed during the extraction process. They were able to report how the extracts varied in composition and yield by collecting extract samples at various stages during the course of the experiment. Both Deo et al. and Eisenbach et al. observed that the lighter fraction of the bitumens were extracted using the supercritical fluid. In addition, Deo et al. examined the effects of varying the temperature and pressure at which the extractions were performed. They found that the extract yields were highest in the vicinity of the critical temperature of the solvent and that the yields increased as pressure increased. They also noted that the carbon number of the extracted oil increased as a function of extraction time and as the operating pressure of the extractions increased. Deo et al. reported that carbon dioxide was a poor choice of solvent as it could only extract a maximum of 2 wt% of the bitumen where as propane yields approached 50 wt%.

Another application for supercritical extraction is as an analytical tool for characterising bitumens and heavy oils (Chung et al., 1996). Bench-scale supercritical extraction units have been built and are used to fractionate heavy hydrocarbon mixtures. The main advantage of this method over traditional distillation techniques is that the supercritical process operates at much lower temperatures and can cut deeper into the residue. Traditional distillation techniques can only be used to fractionate heavy hydrocarbon samples up to approximately 50 wt% (Speight, 1991). In order to cut beyond this point, it would be necessary to increase the operating temperature beyond 350°C at which point the sample begin to crack (Speight, 1991). This would produce results which would not represent the original feed. Other methods, such as gel permeation chromatography and sequential extraction fractionation, have been used to cut deeper but the samples of extracted material are much smaller than those obtained using supercritical extraction (Chung et al., 1996).

A bench-scale extraction unit was used by Chung et al. to fractionate atmospheric topped coker feed bitumen from Syncrude at the Petroleum University at Beijing, China (Chung

et al., 1996). Using vacuum distillation they were able to distil approximately 50% of the bitumen. The residue was then fed to a supercritical extraction unit. Using n-pentane at 210°C and increasing the pressure from 3.5 MPa to 12 MPa over eight hours, they were able to further fractionate the residue into ten fractions. Tests such as C/H ratio and metals content, were performed on these cuts in order to characterise the coker feed in more detail. This additional information can improve the accuracy of models used to describe bitumen processing technology.

Much of the bitumen and heavy oils that exist in northern Alberta cannot be recovered using surface mining techniques (Dunn et al., 1989). Thus the challenge for engineers is to develop a technique to recover these hydrocarbons in an efficient and environmentally sound manner. One solution is to inject a soluble gas to reduce the viscosity of the oil in place such that it becomes mobile and can be produced (Dunn et al., 1989; Lim et al., 1995; Williams, 1981). One option is to use supercritical fluids in the in situ production of heavy oils.

A bench-scale sand pack was flooded with Cold Lake bitumen and produced first using subcritical ethane and a second time using supercritical ethane (Lim et al., 1995). They compared the differences in the resulting production rates, total amount of oil produced and solvent recovered after blowdown. The results showed that by using supercritical ethane, there was an increase in the bitumen production rate by an average of 25% with the rate being almost twice that of subcritical ethane in the first cycle. If the economic cut off point for the project was 30 % recovery, using supercritical ethane reduced the project life by approximately 20%. Another important factor to consider when conducting solvent floods is the amount of solvent recovered at blowdown. The supercritical ethane experiments had 25% higher solvent recovery when the apparatus was depressurised at the end of the experiment. Based on their data, Lim et al. concluded that supercritical ethane performed better than subcritical ethane for *in situ* recovery.

If supercritical fluids are to be used in commercial applications, one of the first steps is to gain an understanding of the phase behaviour of these systems. Phase behaviour studies have been conducted involving supercritical fluids and bitumens including: various Utah bitumens with propane and carbon dioxide (Deo et al., 1992; Subramanian et al., 1998), Cold Lake bitumen and carbon dioxide (Yu et al., 1989; Huang et al., 1990), Athabasca bitumen and propane (Eisenbach et al., 1983) and Peace River bitumen and carbon dioxide (Han et al., 1992). These experiments can be divided into two types: those with constant solvent to bitumen ratios and those with semi-batch extractors where the solvent flowed through the extractor charged with a fixed sample of bitumen or heavy oil.

Han et al., Yu et al. and Huang et al. focused on measuring solubilities of their respective bitumens in supercritical phases under conditions of constant composition. Han et al. sampled the heavy (bitumen-rich phase) and light (supercritical-rich) phase under static conditions over a range of temperatures and pressures. This was used to determine the composition of each phase at a fixed solvent to bitumen ratio. Yu et al. and Huang et al. used a system in which the bitumen and solvent were continuously pumped into a mixing chamber and from there into a separator. In the separator, a heavy phase collected at the bottom and the light phase exited from the top. By analysing the heavy and light phases, they could determine the composition of bitumen in the supercritical fluid-rich phase and the amount of supercritical fluid in the bitumen-rich phase.

Eisenbach et al. and Deo et al. performed experiments of the second type. The bitumen was initially fed into the extractor and the supercritical fluid flowed through the extractor removing any of the components in the bitumen that were soluble in the solvent at the operating conditions. This data described how the supercritical fluid/bitumen system changed as portions of the bitumen were continuously extracted. Estimates for the total amount of bitumen that could be extracted at a given temperature and pressure as well as the rate at which the oil could be extracted are two examples of the data provided by this

type of experiment. In addition, characteristics of the extracted oil such as composition and viscosity, can be studied.

2.5 Thermodynamic Modelling

Numerous supercritical systems have been modelled using different equations of states. The majority of systems studied have been pure component binary systems involving a supercritical fluid and a solid hydrocarbon (Burk et al., 1992; Johnston et al., 1981; Madras et al., 1993; McHugh et al., 1980). Solid-supercritical fluid systems are popular because it allows for the assumption of a pure solid phase (Johnston, 1989) and thus the behaviour of the supercritical phase can be examined in more detail.

The performance of these equations have been reviewed in the literature (Johnston et al., 1989; Mukhopadhyay et al., 1993; Brennecke et al., 1989). Johnston et al. compiled an extensive review of the equations available to model supercritical systems. They discussed the performance of cubic equations of state, perturbed hard-sphere equations of state, lattice models, Kirkwood-Buff solution theory and mean-field theory. For liquid-supercritical systems, they concluded that the Peng-Robinson equation of state (Peng et al., 1976) could correlate a wide range of systems and extrapolate over a range of temperatures and pressures. These conclusions were consistent with those of Brennecke et al. who found "Cubic equations of state are exceedingly simple, have been remarkably successful in modelling supercritical fluid phase behaviour... the cubic equation of state must be the equation of choice for process design of any very complex system, because the interactions are too involved to justify the use of a more fundamentally-based equation." (Brennecke et al., 1989). Mukhopadhyay et al. remarked that "the Peng-Robinson (P-R) EOS performed as satisfactorily as the more complicated perturbed hard-sphere equations" (Mukhopadhyay et al., 1993). Cubic equations of state such as the

Peng-Robinson and the Soave-Redlich-Kwong (Soave et al., 1972) have been used successfully to model numerous binary systems involving supercritical fluids and heavy hydrocarbons (Benmekki et al., 1987; Bertucco et al., 1995; Mukhopadhyay et al., 1993).

2.5.1 Peng-Robinson Equation of State

The Peng-Robinson (P-R) equation of state (EOS) was developed in 1976 in an attempt to improve the prediction of liquid densities while keeping vapour pressures and equilibrium ratios accurate (Peng et al., 1976). This was done by modifying the attractive pressure term of the van der Waals equation. The P-R EOS is as follows:

$$P = \frac{RT}{v - b} - \frac{a(T)}{v^2 + 2bv - b^2} \qquad \text{Equation 2.1}$$

Where,

$$a(T) = a_p \alpha(T_R, \omega) \qquad \text{Equation 2.2}$$

$$a_p = 0.45724 \frac{R^2 T_C^2}{P_C} \qquad \text{Equation 2.3}$$

$$\alpha = \sqrt{1 + m(1 - T_R^{1/2})} \qquad \text{Equation 2.4}$$

$$m = 0.37464 + 1.54226\ \omega - 0.26992\ \omega^2 \qquad \text{Equation 2.5}$$

$$\omega = 1.000 - \log_{10}\left(\frac{P^{sat}}{P_C}\right)_{T_R = 0.7} \qquad \text{Equation 2.6}$$

$$b = 0.07780\left(\frac{RT_c}{P_c}\right) \qquad \text{Equation 2.7}$$

The above equations for a and b are used for pure components. When modelling mixtures, it is necessary to use mixing rules in order to calculate a_{mix} and b_{mix} which replace a and b in Equation 2.1. For the calculation of a, the following mixing rule is used:

$$a = \sum_i \sum_j x_i x_j a_{ij} \qquad \text{Equation 2.8}$$

Where,

$$a_{ij} = (1 - k_{ij})\sqrt{a_{ii} a_{jj}} \qquad \text{Equation 2.9}$$

In Equation 2.9, a_{ii} and a_{jj} are pure component a values calculated using Equation 2.2 after substituting the appropriate values for T_c and ω for each component.

A mixing rule is required for the parameter b in Equation 2.1. The following is the most common equation used to evaluate b.

$$b = \sum_i x_i b_i \qquad \text{Equation 2.10}$$

Where b_i is calculated using Equation 2.3 for each compound.

2.5.2 Hydrocarbon Mixture Modelling with the Peng-Robinson Equation of State

Equations have been used to model the solubility of light gas-bitumen systems under a variety of conditions and in combination with different light gases. Extensive data has been published for Peace River, Athabasca and Cold Lake bitumen saturated with sub-critical gases such as N_2, CO, CH_4, CO_2, and C_2H_6 (Jacobs et al., 1980; Svrcek et al.,

1989; Svrcek et al., 1982; Mehrotra et al., 1989; Mehrotra, 1985a; Mehrotra, 1985b; Han et al., 1992). Based on this data and using the P-R EOS, it has been demonstrated that bitumen-light gas systems can be modelled quite accurately (Mehrotra et al., 1989; Eastick et al., 1992; Mehrotra, 1985b; Sheng et al., 1991). For example, Mehrotra et al. were capable of predicting the solubility of ethane in Peace River bitumen with an average deviation of 3.3% (Mehrotra et al., 1985b).

Modelling of multi-component hydrocarbon mixtures and supercritical solvents with the Peng-Robinson equation of state has not been as widely studied. Yu et al. and Huang et al. modelled the phase behaviour of CO_2 in different cuts of bitumen and in Cold Lake bitumen using Soave and Peng-Robinson equations of state and using the Perturbed Hard Chain equation (Yu et al., 1989; Huang et al., 1990). Deo et al. modelled the dynamic extraction of a crude oil, bitumen-derived liquid and a bitumen using CO_2 and propane (Deo et al., 1992). This was performed using the Peng-Robinson EOS and was able to reproduce the experimental compositions for the bitumen experiments within an average error of 12.2%. The model was only fitted for one pair of temperature and pressure and there was no mention of the interaction parameters required to fit the equation to the experimental results.

2.6 Bitumen Characterisation

In order to use an equation of state such as Equation 2.1, it is necessary to have the critical temperature (T_c), critical pressure (P_c) and acentric factor (ω) for each component in the system. This creates a problem when modelling undefined fluids such as bitumens and crude oils which are mixtures of thousands of pure compounds. Neither the composition nor the structure of all of the hydrocarbons are known for these mixtures and as a result all of the T_c, P_c and ω are not known. In order to get around this problem, a

number of authors have proposed that the oil be subdivided into smaller fractions or pseudocomponents. T_c, P_c and ω can then be estimated using correlations that are based upon properties of the pseudocomponents such as boiling point, specific gravity and/or analysis such as paraffin/naphthene/aromatic composition.

Voulgaris et al. performed a rigorous evaluation of over 25 different methods for calculating T_c, P_c and ω for non-polar compounds, petroleum and coal liquid fractions (Voulgaris et al., 1991). The performance of the correlations was measured by using the predicted values in a translated Peng-Robinson equation of state to predict vapour pressure and liquid densities. Included in their analysis were 1, 2, 3 and 4 parameter equations, methods requiring PNA (paraffin, naphthene, aromatic) analysis and group contribution techniques. They concluded that two versions of the Riazi-Daubert ("RRD" and "RD10") modified by Magoulas et al. and later by Voulgaris et al. along with the Twu correlations performed best overall (Magoulas et al., 1990; Voulgaris et al., 1991). For petroleum fractions, Twu, RRD and Kesler-Lee gave the most accurate predictions. For the lighter coal liquid fractions Kesler-Lee and Twu were the best and for heavier coal liquids, the RRD method was the most accurate with Kesler-Lee and Twu close behind.

Stamataki et al., evaluated the performance of cubic equations of state at high pressures using systems containing heavy hydrocarbons (Stamataki et al., 1998). As part of their work, they evaluated different methods for calculating critical properties for hydrocarbons with carbon numbers greater than twenty. They noted that the predicted critical properties diverged as the carbon number was increased, with the most significant divergence occurring for critical pressure. They observed that the critical properties predicted using the revised Riazi-Daubert correlations by Magoulas et al. and those predicted using the group contribution method gave better vapour liquid equilibrium results for a system consisting of methane and nC_{24}.

The conclusions drawn by Voulgaris with respect to the RRD correlations by Magoulas et al. were reinforced by Stamataki et al. Therefore, based upon the detailed analysis of Voulgaris et al., the Kesler-Lee, Twu and RRD methods for calculating the critical properties and acentric factors for hydrocarbon mixtures were evaluated to determine the best set of correlations to use in this work.

2.6.1 Kesler-Lee Correlations

The Kesler-Lee correlations for T_c, P_c, molecular weight and acentric factor were developed in an attempt to improve enthalpy predictions for hydrocarbon fractions (Kesler et al., 1976). The equations are as follows:

$$T_C = 341.7 + 811\,SG + (0.4244 + 0.1174\,SG)T_b + (0.4669 - 3.2623\,SG)10^5 / T_b \qquad \text{Equation 2.11}$$

$$\ln(P_C) = 8.3634 - 0.0566/SG - (0.24244 + 2.2898/SG + 0.11857/SG^2)10^{-3}T_b + (1.4685 + 3.648/SG + 0.47227/SG^2)10^{-7}T_b^2 - (0.42019 + 1.6977/SG^2)10^{-10}T_b^3 \qquad \text{Equation 2.12}$$

$$MW = -12272.6 + 9486.4\,SG + (4.6523 - 3.3287\,SG)\,T_b + (1 - 0.77084\,SG - 0.02058\,SG^2)(1.3437 - 720.79/T_b)10^7/T + (1 - 0.80882\,SG + 0.02226\,SG^2)(1.8828 - 181.98/T_b)10^{12} \qquad \text{Equation 2.13}$$

Where T_c and T_b are in °R and P_c is in psia.

For the acentric factor, two equations were developed to be used depending upon the reduced temperature. They are as follows:

For T_r>0.8,

$$\omega = -7.904 + 0.1352\,K - 0.007465\,K^2 + 8.359\,T_{bR} + (1.408 - 0.01063\,K)/T_{bR} \qquad \text{Equation 2.14}$$

For T_r<0.8,

$$\omega = \left[\ln(P^S_{bR}) - 5.92714 + 6.09648/T_{bR} + 1.28862\ln(T_{bR}) - 0.169347\,T^6_{bR}\right] * \left[15.2518 - 15.6875/T_{bR} - 13.4721\ln(T_{bR}) + 0.43577\,T^6_{bR}\right] \qquad \text{Equation 2.15}$$

Where T_{br} is the reduced normal boiling point, P^S_{bR} is the reduced vapour pressure at the normal boiling point and K is the Watson characterisation factor defined as:

$$K = \frac{(CABP)^{1/3}}{SG} \qquad \text{Equation 2.16}$$

With CABP representing the cubic average boiling point for the mixture.

Using the values predicted using these correlations, Kesler et al. were able to predict enthalpies for liquid hydrocarbons with an average deviation of 1.9%.

2.6.2 Twu Correlations

The Twu correlations were developed in 1984 in an attempt to provide an accurate method for calculating T_c, P_c and molecular weight for hydrocarbon mixtures including

coal-tar liquids (Twu, 1984). Pure n-alkanes with boiling points as high as 1778 K and specific gravities up to 1.436 were used as a reference system. A critical property (i.e. temperature) is calculated for the reference n-alkane based on the boiling point for the hydrocarbon mixture. The reference critical property (i.e. T_c^o) is then transformed to the critical property for the initial hydrocarbon mixture. The equations for the reference properties are as follows:

$$T_C^o = T_b(0.533272 + 0.191017*10^{-3}T_b + 0.779681*10^{-7}T_b^2 - 0.284376*10^{-10}T_b^3 + 0.959468*10^{28}/T_b^{13})^{-1} \quad \text{Equation 2.17}$$

$$V_C^o = [1-(0.419869 - 0.505839\alpha - 1.56436\alpha^3 - 9481.70\alpha^{14})]^{-8} \quad \text{Equation 2.18}$$

$$P_C^o = (3.83354 + 1.19629\alpha^{1/2} + 34.8888\alpha + 36.1952\alpha^2 + 104.193\alpha^4)^2 \quad \text{Equation 2.19}$$

$$SG^o = 0.843593 - 0.128624\alpha - 3.36159\alpha^3 - 13749.5\alpha^{12} \quad \text{Equation 2. 20}$$

where,

$$\alpha = 1 - \frac{T_b}{T_C^o} \quad \text{Equation 2.21}$$

Twu also developed a method for calculating molecular weights. It is an iterative process using the following equations:

$$T_b = \exp\left(5.71419 + 2.71579\theta - 0.286590\theta^2 - \frac{39.8544}{\theta} - \frac{0.122488}{\theta^2}\right) - 24.7522\theta + 35.3155\theta^2 \quad \text{Equation 2.22}$$

Where,

$$\theta = \ln(MW^{o}) \qquad \text{Equation 2.23}$$

Twu provides an initial guess for MW^{o} which is shown below.

$$MW^{o} = \frac{T_b}{10.44 - 0.0052\,T_b} \qquad \text{Equation 2.24}$$

In Equation 2.17 - Equation 2.24, the critical pressure (P_c) is in psia, critical temperature (T_c) and the normal boiling point (T_b) are in °R, SG is the specific gravity of the liquid at 60 °F relative to water at the same temperature and V_c has the units of ft^3/lb/mol.

In order to obtain the desired critical properties, the values for the corresponding n-alkanes are translated using the following equations:

Critical temperature:

$$T_C = T_C^{o}\left(\frac{1 + 2f_T}{1 - 2f_T}\right)^2 \qquad \text{Equation 2.25}$$

Where f_T is:

$$f_T = \Delta SG_T\left[\frac{0.362456}{T_b^{1/2}} + \left(0.0398285 - \frac{0.948125}{T_b^{1/2}}\right)\Delta SG_T\right] \qquad \text{Equation 2.26}$$

and

$$\Delta SG_T = \exp[5(SG^{o} - SG)] - 1 \qquad \text{Equation 2.27}$$

Critical volume:

$$V_C = V_C^o\left(\frac{1+2f_V}{1-2f_V}\right)^2 \qquad \text{Equation 2.28}$$

Where f_V is:

$$f_V = \Delta SG_V\left[\frac{0.466590}{T_b^{1/2}} + \left(-0.182421 + \frac{3.01721}{T_b^{1/2}}\right)\Delta SG_V\right] \qquad \text{Equation 2.29}$$

and

$$\Delta SG_V = \exp[4(SG^o - SG)] - 1 \qquad \text{Equation 2.30}$$

Critical pressure:

$$P_C = P_C^o\left(\frac{T_C}{T_C^o}\right)\left(\frac{V_C^o}{V_C}\right)\left(\frac{1+2f_P}{1-2f_P}\right)^2 \qquad \text{Equation 2.31}$$

Where f_P is:

$$f_P = \Delta SG_P\left[\begin{array}{l} 2.53262 - \frac{46.1955}{T_b^{1/2}} - 0.00127885\,T_b + \\ \left(-11.4277 + \frac{252.140}{T_b^{1/2}} + 0.00230535\,T_b\right)\Delta SG_P \end{array}\right] \qquad \text{Equation 2.32}$$

and

$$\Delta SG_P = \exp[0.5(SG^o - SG)] - 1 \qquad \text{Equation 2.33}$$

Molecular weight:

$$\ln(MW) = \ln(MW^o)\left(\frac{1+2f_M}{1-2f_M}\right)^2 \qquad \text{Equation 2.34}$$

Where f_M is:

$$f_M = \Delta SG_M \left[|x| + \left(-0.0175691 + \frac{0.193168}{T_b^{1/2}} \right) \Delta SG_M \right] \quad \text{Equation 2.35}$$

with

$$|x| = \left| 0.0123420 - \frac{0.328086}{T_b^{1/2}} \right| \quad \text{Equation 2.36}$$

and

$$\Delta SG_v = \exp[4(SG'' - SG)] - 1 \quad \text{Equation 2.37}$$

These equations were reported by Twu to predict T_c, P_c, V_c and molecular weight with an average absolute percent deviation less than 3.75% (Twu, 1984).

2.6.3 Revised Riazi – Daubert Equations

Riazi and Daubert developed equations of the form shown in Equation 2.38 to predict the critical properties for hydrocarbon mixtures (Riazi et al., 1987).

$$\phi = a(T_b)^b SG^c \quad \text{Equation 2.38}$$

Where ϕ is the desired critical property, T_b is the normal boiling point in °R, SG is the specific gravity of the fluid at 60°F relative to water at the same temperature and a, b and c are regressed parameters.

Critical property data for 138 pure hydrocarbons was used by Riazi and Daubert to derive the constants in Equation 2.38. The hydrocarbons used had molecular weights ranging from 70-300 and normal boiling points from 80-650°F.

Magoulas et al. and later Voulgaris et al. modified the equations for T_c and P_c developed by Riazi and Daubert in 1980 to fit a wider range of components (Magoulas et al. 1990; Voulgaris et al., 1991). They expanded the database of hydrocarbons which formed the basis for regression to 258 compounds including n-paraffins, i-paraffins, naphthenes and aromatics. They called these new equations the Revised RD or RRD correlations and they are as follows:

$$T_C = 17.44265\, T_b^{0.60393} SG^{0.37671} \qquad \text{Equation 2.39}$$

$$P_C = 21.965110 * 10^6\, T_b^{-2.15711} SG^{2.28283} \qquad \text{Equation 2.40}$$

Where T_b and T_c are in K, P_c is in bar and SG is the specific gravity of the hydrocarbon mixture relative to water.

In the same paper, Voulgaris et al. modified the Riazi and Daubert equations a second time. The purpose of this was to modify them such that T_c and P_c could be calculated based on the boiling point of the fraction at 10 mmHg and the specific gravity at 25 °C (Voulgaris et al., 1991). They called these equations the RD10 correlations, and are as follows:

$$T_C = 29.618\, T_{10}^{0.5465} SG_{25}^{0.40537} \qquad \text{Equation 2.41}$$

$$P_C = 2.58016 * 10^6\, T_{10}^{-1.89598} SG_{25}^{2.34060} \qquad \text{Equation 2.42}$$

Voulgaris et al. concluded that the revised forms of the Riazi-Daubert equations, both the RRD and the RD10, improved the accuracy of the original equations and that the revised forms were one of the most accurate methods for predicting critical properties for pure components, petroleum fractions and coal liquid fractions.

2.7 Summary

The existence of supercritical fluids has been known for well over 150 years. In addition, the unique behaviour of these fluids and their enhanced solvent characteristics have been well documented. There are a number of large scale industrial applications, including hydrocarbon processing methods, which exploit the solvent properties of supercritical fluids and have been proven to be both efficient and economic.

While there is a large amount of published data for supercritical fluid and pure component systems, there is a significant void in the literature regarding the behaviour of supercritical fluids and mixtures of heavy hydrocarbons. The experimental data that does exist can be divided into two types: constant bitumen/solvent ratio and semi-batch extraction data. Limited literature of the second type can be found for bitumens from Utah and Athabasca bitumen with supercritical carbon dioxide and propane. While ethane is one of the more common solvents used in binary systems, it does not appear to be a popular choice for extracting soluble components in bitumens and heavy oils.

A variety of equations have been used in an attempt to model systems consisting of supercritical fluids and heavy oils or bitumens. Cubic equations of state, perturbed hard-sphere equations of state, lattice models, etc... have been used with mixed degrees of success. The Peng-Robinson equation of state has been proven to model these systems

with the same degree of accuracy as more complex models with the benefit of being much less complicated.

In order to use an equation of state, critical data and acentric factors for the components in the system are required. A number of different methods have been developed to estimate these values for hydrocarbon mixtures of unknown composition. Stamataki et al. found that the modified form of the Raiai-Daubert method provided the best results for a predicting critical properties (Stamataki et al., 1998). Voulgaris et al. concluded that four correlations out performed the other methods published Voulgaris et al., 1991). These methods were chosen to be evaluated for use in this work and are as follows: Kesler-Lee, Twu and the two revised Raizi-Daubert correlations.

Based on the state of the existing database for systems composed of supercritical fluids and undefined hydrocarbon mixtures, there is the need for more experimental data and the refinement of equations capable of modelling these systems. The potential for the application of supercritical fluids to the petroleum processing industry exists but the development of these processes are being hindered by the lack of data available. Therefore, this work will provide a means to fill this void by providing data for a new supercritical fluid/bitumen system.

Chapter Three

Experimental Set-up and Design

Different experimental designs have been used to collect equilibrium data for systems involving supercritical solvents in conjunction with heavy oils and bitumens. The choice of the type of apparatus depended whether the data to be collected was for constant bitumen to solvent ratios or for dynamic systems in which the composition of the bitumen or heavy oil changed as a function of the amount of solvent that had contacted the feed.

Two different techniques were reported for cases where researchers were investigating the phase behaviour of a supercritical solvent and a heavy oil or bitumen system with a constant feed to solvent ratio. The first apparatus used a "flow-cell" where both the solvent and the bitumen were continuously pumped into a mixing cell (Yu et al., 1989; Huang et al., 1990). Two syringe pumps were used to pump Cold Lake bitumen and carbon dioxide into a static mixer. Downstream of the mixer, the fluid entered a windowed cell separator from which the light and heavy phases exited through the top and bottom respectively. Each stream was depressurised and four samples were collected, a vapour and liquid sample from both the heavy and light phases. This apparatus was used to measure phase compositions for three cuts of Cold Lake bitumen at fixed CO_2/hydrocarbon ratios over a temperature range of 50 to 250°C and pressure range of 4.01 to 16.08 MPa.

A second apparatus was proposed by Han et al. to collect solubility data of supercritical solvents in heavy hydrocarbons (Han et al., 1992). In this system, a cell is charged with

bitumen or heavy oil and brought up to operating pressure using the solvent. Pressure was maintained in the extractor by the addition of solvent until the pressure remained relatively constant for at least 24 hours. During this time, the solvent was cycled through the oil using a solenoidal pump until equilibrium was achieved (i.e. constant pressure). Valves were used to manipulate the flow such that samples of both the heavy and light phases could be taken. As with the previous set-up, the solubility data collected was for the case when the ratio of bitumen to solvent remained constant. This apparatus was designed to operate from 20 to 70°C and up to a maximum pressure of 15 MPa.

Dynamic data has also been collected for supercritical solvent/heavy hydrocarbon mixtures. For this type of data, the most common type of apparatus was the semi-batch process in which the feedstock was initially charged to the extractor and the solvent flowed through the extractor removing the soluble components. A number of researchers have collected data for different combinations of solvents and heavy oils or bitumens.

Eisenbach et al. used a semi-batch system to collect dynamic extraction data for Athabasca oilsand and supercritical propane (Eisenbach et al., 1983). No mention is made in their work as to how they ensure that the solvent and bitumen was properly mixed. They reported the difference between extract obtained using the supercritical solvent and the extract removed using toluene and found that they were quite similar. Their experiment was conducted at 110°C and 2 MPa.

Researchers at the University of Utah used a semi-batch process to extract soluble fractions from a crude oil, bitumen-derived liquid and Whiterocks, Asphalt Ridge, PR Spring and Sunnyside bitumens using supercritical CO_2 and propane (Deo et al., 1992; Hwang et al., 1995; Hwang et al., 1996; Subramanian et al., 1998). The extractor was kept at a constant temperature using a heating jacket and pressure was controlled using a back-pressure control valve. A magnetic-drive packerless stirring device was used to ensure that the solvent and the feed were well mixed. The fraction of the feedstock that

was soluble was collected in two-phase separators after the pressure was decreased to atmospheric. The separators were replaced at intervals of approximately 20 minutes in order to observe how the extracted material changed with time. The temperatures and pressures for the experiments ranged from 21 to 150°C and 5.5 to 17.2 MPa, respectively.

A different type of semi-batch system was developed at the University of Petroleum in Shandong, China (Cheng et al., 1994). As with earlier designs, the bitumen was charged to the extractor, solvent continually flowed through the extractor and was depressurised to collect the soluble material. In this apparatus, the extractor was composed of two sections: the extraction cell and the fractionation column. Sheng-Bei wax-bearing residue was charged into the extraction section that was 25% shorter and 1.6 times wider than the fractionation column. Supercritical propane contacted the bitumen in the extraction cell and flowed up into the fractionation column. The fractionation column was packed with stainless steel packing and the top was kept at a higher temperature than the bottom. The increase in temperature caused the solvent density to decrease as it moved up the column and resulted in some of the extracted material precipitating out and being returned to the extraction cell. The operating pressure was increased step-wise during an experiment using a pressure controller downstream of the fractionation column. Temperatures at the top of the column were kept constant at 111°C and pressure was increased from 5.4 to 10.8 MPa.

In this work, a unique semi-batch apparatus was designed and constructed in order to perform dynamic extraction studies of solutes using supercritical fluids. The apparatus was designed such that the solvent was saturated with the soluble components in the bitumen. The extracted oil was collected and analysed to determine how different temperatures and pressures affected the extraction process. The apparatus, its verification, experimental procedure and error analysis are discussed in this chapter.

3.1 Apparatus and Procedure

A system was designed and constructed that would provide data describing the results of contacting a mixture of Peace River bitumen and sand with supercritical ethane. The experimental apparatus used in this study is shown in Figure 3.1. A photograph of a portion of the apparatus contained within the oven is shown in Figure 3.2.

At the beginning of a run, the extractor was packed with a bitumen/sand mixture and with clean sand and glass wool above the bitumen/sand feed. The sand and bitumen were mixed in the lab such that the final mixture was 15 wt% bitumen. This ratio of bitumen to sand was chosen as it was a typical ratio of oil to sand that can be found in areas such as the Peace River and the Athabasca regions located in northern Alberta, Canada (Pruden, 1997). The inclusion of the sand served two purposes: to assist in the distribution of the supercritical solvent within the extractor and to make the experiments more like a real extraction process.

A positive displacement pump was used to supply solvent and bring the system up to pressure in addition to regulating the flow of solvent through the system. The extractor and most of the tubing were placed inside the oven used to control the temperature for the duration of the experiment. The solvent flowed through a section of tubing which acted as a preheat section allowing it to reach the operating temperature before entering the extractor. The solvent entered the extractor at the bottom and flowed upwards, through the extractor removing the soluble portion of the bitumen. The resulting light phase exited the extractor and passed through a micrometer valve that was used to manually control pressure. The micrometer valve was also used to decrease the pressure from operating to atmospheric pressure which caused the extracted oil to precipitate. The extracted samples were collected in two-phase separators that were replaced at twenty minute intervals until the pump was emptied of solvent. The separators were weighed before and after to determine the mass of oil extracted. The ethane left through the top of

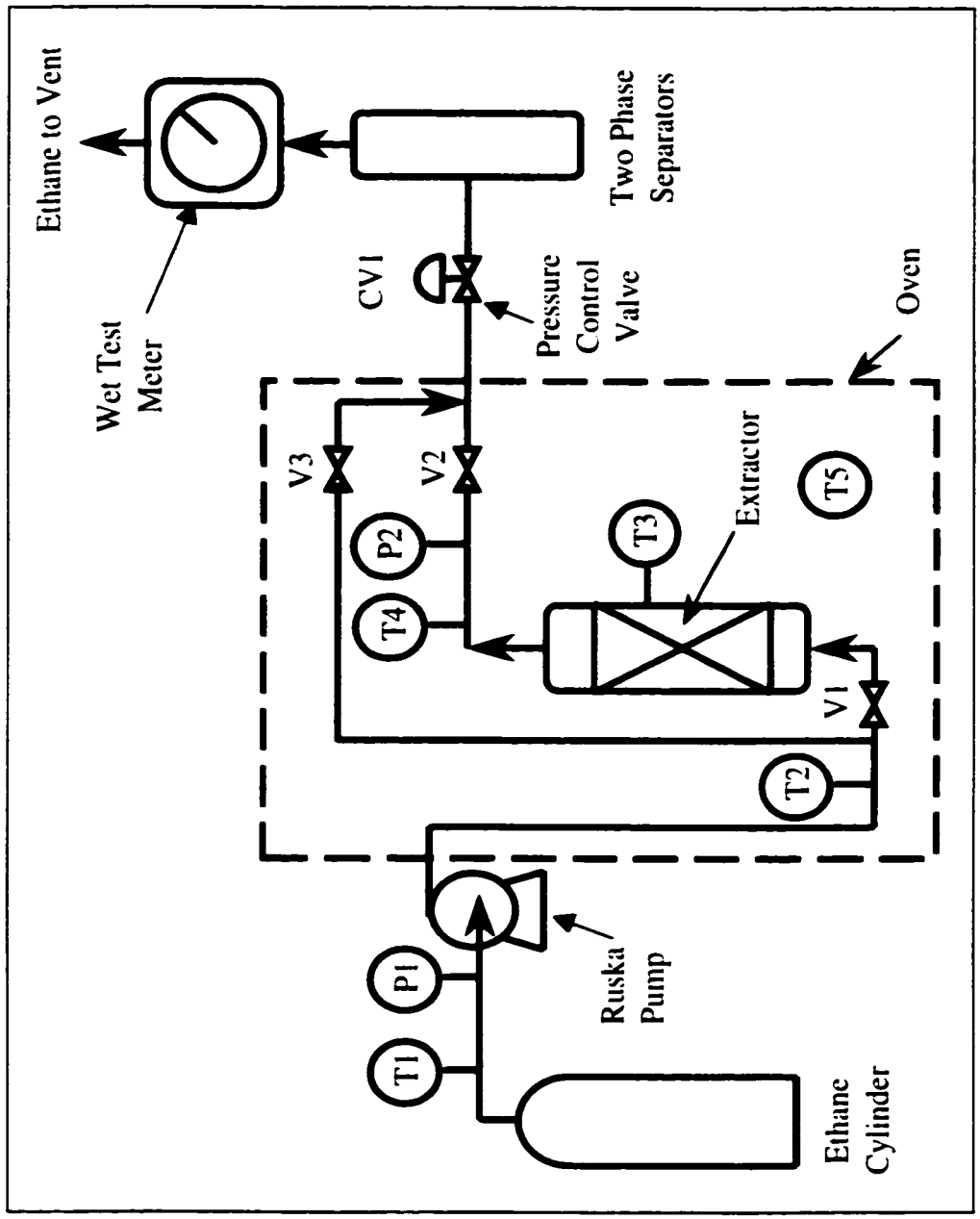

Figure 3.1 - Schematic of the supercritical extraction apparatus.

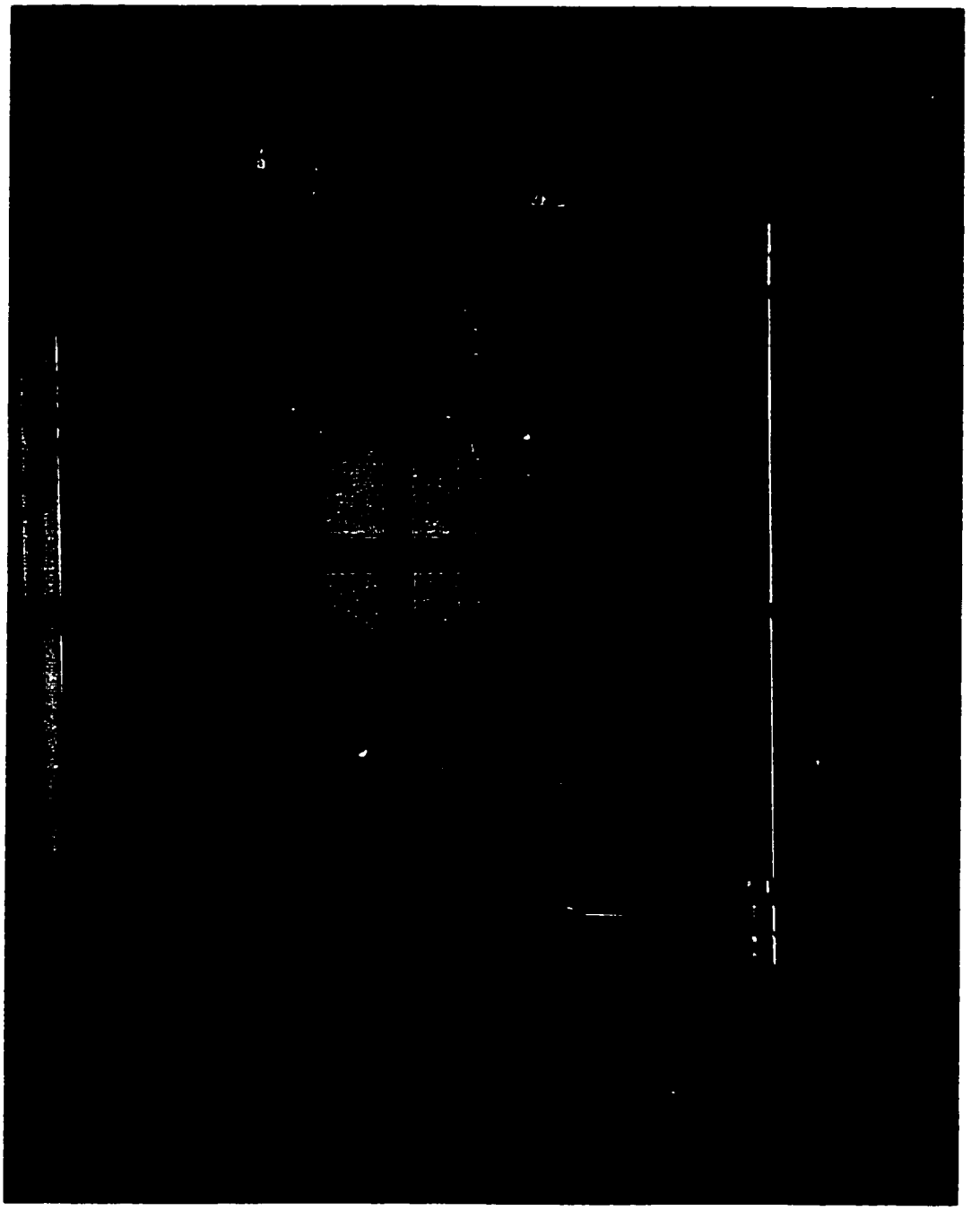

Figure 3.2 – Photograph of extractor set-up within the oven showing the extractor (right), preheat section (left) and bypass (centre).

the separators and passed through a wet test meter before being vented. At the end of a run, the system was depressurised and the bitumen/sand mixture remaining in the extractor was collected and weighed to close the mass balance.

3.1.1 Extractor

As described earlier, a semi-batch extractor was used that was packed with feed consisting of bitumen mixed in sand. A schematic of the extractor is presented in Figure 3.3.

The extractor was constructed in the Department of Chemical and Petroleum Engineering Machine Shop at the University of Calgary. The body of the extractor was constructed using 2 inch O. D. Schedule 160 pipe made of 316 stainless steel. The extractor was rated for a maximum pressure of 21.8 MPa for a temperature of 204°C based upon the calculation method outlined in the Pressure Vessel Handbook (Megyesy, 1981). At each end of the extractor, a 2.5 cm flange was welded to the body. Eight bolts, 5 cm in length were used to fasten the flange plates together. 6.67 cm O.D. by 6.03 cm I.D Viton O-rings were used to provide a seal between the flange plates. The extractor was connected to the apparatus using ¼ inch NPT/Swagelock fittings.

Gas distribution was aided by the presence of a 0.3 cm thick distributor preceded by a 4.0 cm deep wind-box section. The distributor was constructed of porous stainless steel with an average pore size distribution of 2 μm provided by Mott Corporation. The porous material was welded to the sides of the extractor to ensure that the solvent could not bypass the distributor by moving around the edges of the distributor plate. Numerous tests were performed to evaluate the ability of the porous distributor to assist the solvent in flowing in a plug flow manner through the extractor (Section 3.3).

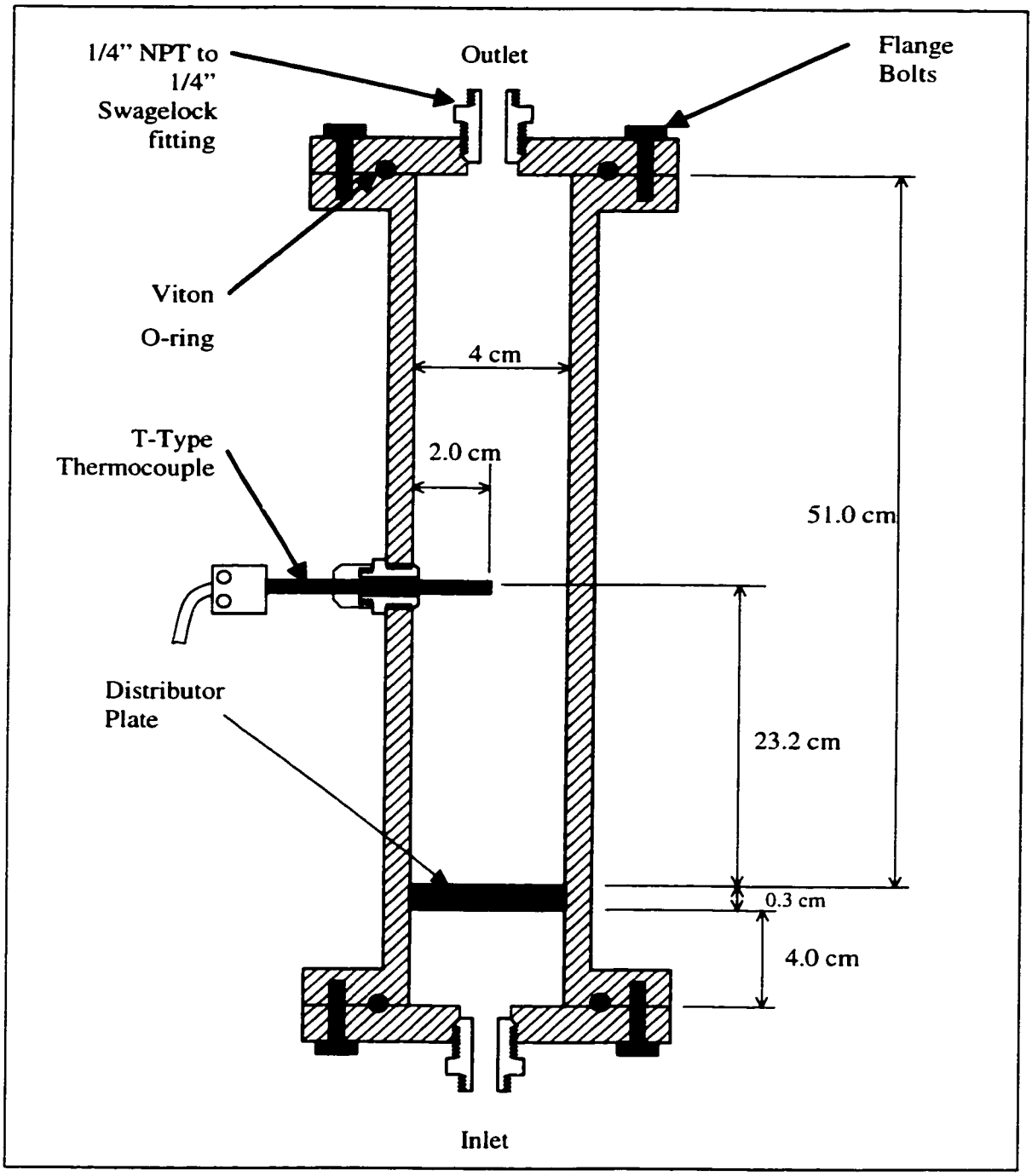

Figure 3.3 – Detailed schematic of the extractor used in equilibrium study.

A port was added to the side of the extractor to facilitate the attachment of a thermocouple that was used to monitor the temperature inside the extractor. It was located at a height of 23.2 cm above the distributor. A ¼ inch NPT/Swagelock fitting was threaded into the wall of the extractor. This thermocouple was used to determine when the bitumen/sand mixture had reached the operating temperature and to record the extractor temperature during a run.

3.1.2 Solvent Pump

A Ruska proportion pump (2248 WIII) was used to supply the solvent and regulate the flow. The pump has two cylinders, each with volumes of 0.5 L and a ¾ Hp electric motor. The pump has a quick-change transmission that allows the flow of the fluid to be fixed to one of 28 possible rates by adjusting the gears. The flow rates ranged from 0.005 – 1.12 L/h per cylinder. The maximum flow when both cylinders were engaged was 2.24 L/h. The maximum pressure that the pump could provide was 27.5 MPa.

Two safety features were built into the pump to prevent damage to the system and/or an explosion. First, the pump was equipped with electrical breakers that shut off power to the motor when the piston approached either end of the cylinders. The breakers were designed to prevent the pistons from hitting the ends of the cylinders and damaging the piston shaft, cylinder and/or motor. Secondly, pressure relief valves were installed at the discharge ends of the pump. If the pump pressure exceeded 24.1 MPa, the valves would open and prevent the pressure in the cylinders from increasing further.

3.1.3 Separators

The separators used to collect the extracted oil precipitated at atmospheric pressure were sized according to industry guidelines (Monnery et al., 1993). The separators had an internal diameter of 3.2 cm and an O.D. of 3.7 cm. The internal height was 9.4 cm with the inlet located 4.5 cm from the bottom. The separators were constructed of aluminium and were fabricated in the Machine Shop at the University of Calgary. Glass wool was used at the top of the separators to prevent any entrained oil from leaving the extractor. The separators were placed in an ice bath during operation, to reduce the temperature and enhance the precipitation of the extract.

The performance of the separators was verified by analysing the exit gas before it entered the wet test meter. Samples of the gas were taken and a gas chromatograph was used to detect the presence of any other hydrocarbons besides ethane. "Worst case" scenarios were experiments with high solvent flow and large amounts of oil extracted because these would be the situations where there would be the greatest chance of entrainment in the separators. It was assumed that if the separators performed satisfactorily under these conditions, they would be adequate for all other experiments. The operating conditions chosen for these experiments are shown in Table 3.1 with the conditions of 48°C and 10.5 MPa considered to reflect the worst cases. In addition, samples were taken as early in the run as possible. This was when the lightest components in the oil were extracted and these would be the most likely to remain entrained in the gas stream leaving the extractor.

The apparatus was modified such that a sample of the gas leaving the separator was taken before entering the wet test meter. A sample tube was used to collect a sample at the beginning of a run and a sample of this gas was immediately injected into the gas chromatograph. The gas chromatograph was temperature programmed to begin at 50°C and after two minutes, increase to a final temperature of 250°C at a rate of 15°C/min. The bitumen feed had an initial boiling point of 160°C and thus if any of the oil was not

Temperature, °C	Pressure, MPa	Flow Rate, L/h	Area % Ethane
48	7.3	0.2	99.64
48	7.3	0.2	100.00
48	7.3	0.4	100.00
48	7.3	0.4	100.00
48	10.5	0.4	100.00
48	10.5	0.4	100.00

Table 3.1 – Results verifying the performance of the separators and the conditions at which the tests were performed.

recovered in the separator, it would be detected in the chromatograph. Other details pertaining to the operation of the gas chromatograph are discussed in Section 3.1.7. The results of the study were presented in Table 3.1.

There was only one case when the sample was not pure ethane and in that instance the sample was over 99.5% ethane and when the second sample was analysed, it was found to be 100% ethane. Based upon these results, it can be concluded that the separators performed satisfactorily.

3.1.4 Pressure Monitoring and Control

Two pressure transducers were used to monitor and record the pressure in the system. These are shown as P1 and P2 in Figure 3.1 A Rosemount Alphaline Model 1151 GP pressure transducer was used to record the pressure at the pump (P1). The transducer was capable of measuring pressure from 0 to 20.67 MPa with an accuracy of ±0.25% over the calibrated range. A second transducer, P2, was attached at the outlet of the extractor and

used to measure the pressure exiting the extractor. This transducer was a Rosemount 2088 with a span of 2.76 to 20.67 MPa. The accuracy of the device was ±0.25% of span. The output from both transducers was a 4-20 mA signal that was converted to 1-5 V using a 250 Ω resistor before being received by the data acquisition system. Calibration information for these transducers is described in Appendix A.

Pressure was controlled manually using a micro-meter valve, (CV1 in Figure 3.1). The valve was constructed by Whitey (SS22RS4) and had a maximum flow coefficient, C_v, of 0.007. The low C_v was necessary to control the pressure at the low flow rates at which the experiments were conducted. During the experiments, the pressure dropped across the control valve from the operating pressure down to near atmospheric pressure causing the temperature at the valve to decrease. The valve was heated using Fibrox heat tape to prevent plugging in the casing of the valve (Cole-Parmer E-03105-20).

3.1.5 Temperature Monitoring and Control

All of the temperatures in the system were monitored using T-type special thermocouples, T1-T5 in Figure 3.1, obtained from All Temp Sensors (A11-16-E-USS-6). The thermocouples were copper-constan, metal sheathed and ungrounded with a diameter of 0.159 cm and a length of 15.24 cm. The range for these thermocouples was –59 to 93°C with an accuracy of ± 0.6°C. Thermocouple calibration is discussed in Appendix A.

A Blue M DC-166F oven was used to maintain the temperature of the extractor and solvent at the desired operating temperature. The temperature of the oven could be set to an accuracy of ± 0.5°C over an operating range of 30 – 500°C. The oven was equipped with a safety switch, which would shut the oven off if the maximum temperature was exceeded. The oven shut off was set to 150°C for all experiments conducted in this work.

3.1.6 Data Acquisition System

All temperatures and pressures were recorded using a data acquisition consisting of a Scientific Instruments LABMATE Series 7000 data board in a 80486-based computer system. The data board contained a cold junction reference that allowed the thermocouple signals to be processed as direct temperature measurements provided that the thermocouple type had been provided.

The data was managed by QMON Data Acquisition and Control software developed by Solar Calorimetry Laboratory at Queen's University. The thermocouples and pressure transducers were connected to the board using wire with a Teflon shield and copper drain wire preventing noise caused by electrostatic and electromagnetic sources. Data was recorded to a file specified by the user at 0.5 min. intervals. The software allows for measured variables to be plotted in real time. An example of the display used in this work is shown in Figure 3.4. The software enables the user to input calibration equations for measured signals. All thermocouples and pressure transducers were calibrated (see Appendix A) and the resulting equations were used by the software to improve the accuracy of the recorded data.

3.1.7 Ancillary Equipment

Tubing, Fittings and Valves

Swagelock 316 stainless steel tubing with a nominal outside diameter of 0.25 inch and a wall thickness of 0.089 cm was used throughout the apparatus. The tubing was rated to a

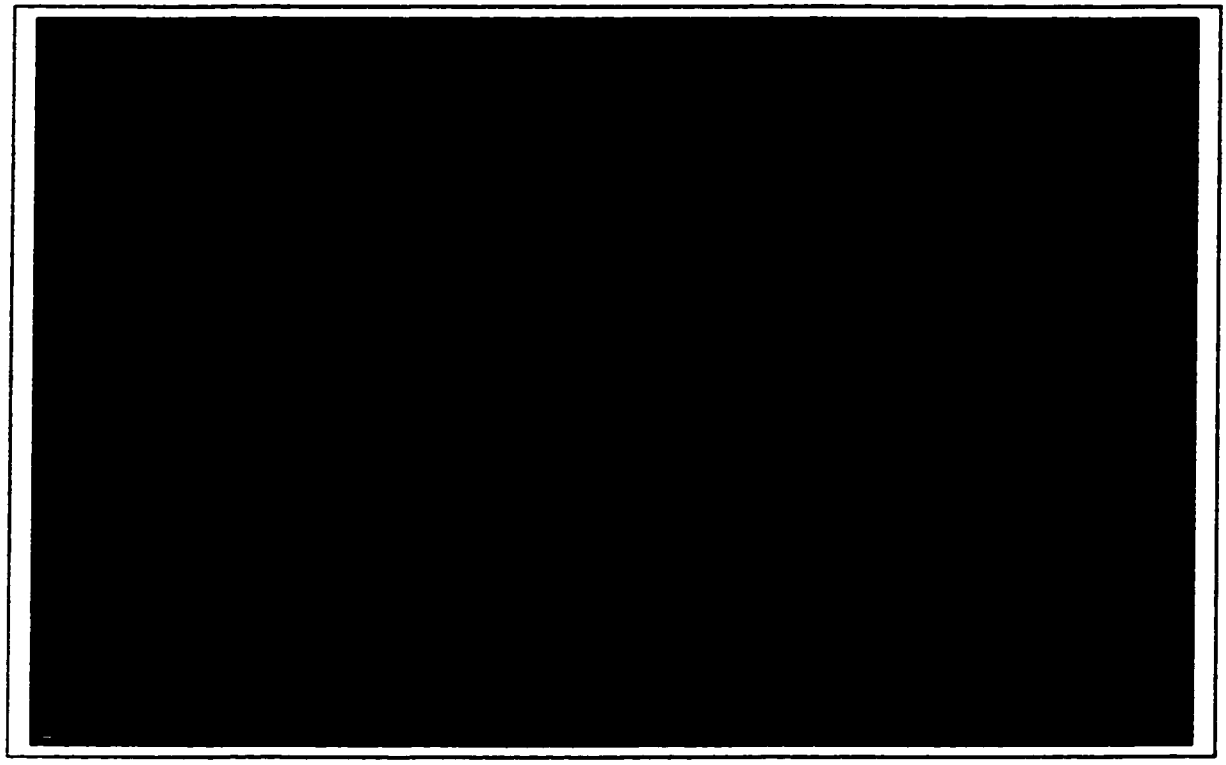

Figure 3.4 - A QMON screen as seen during a typical extraction run displaying key process variables.

maximum pressure of 33.76 MPa at a temperature of 20°C. All elbows, tees and unions were Swagelock ¼ inch and made of stainless steel. They were rated to the same maximum conditions as the tubing used.

Valves V1-V3 were Whitey Series 43 straight pattern, two-way on/off valves with quarter inch Swagelock connections (SS-4354). The valves had C_v's of 2.4 and were rated to 20.68 MPa at 65°C.

Wet Test Meter

A GCA Precision Scientific wet test meter (6312) was used to measure the cumulative outlet vapour flow from the separator. The meter could measure a maximum cumulative volume of 3000 L. One revolution was equivalent to 3 L and the volume could be measured to an accuracy of 0.01 L. The wet test meter was calibrated against a Porter mass flow controller (model 221-APASVCAA) with an accuracy of ±1% of full scale which was 0-2 standard litres per minute. Details of the wet test meter calibration can be found in Appendix A.

Mass Balance

A Mettler BasBal BB2400 balance was used to determine the mass of oil extracted during the experiments. An Ohaus Class P Metric calibration mass set was used to verify that the reading from the balance corresponded to the true weight. The readings from the scale were extremely accurate (±0.005 g).

Gas Chromatographs

Two gas chromatographs were used in this work. The first was used to test the performance of the two-phase separators (see Section 3.1.3). The second was used to

detect the composition of the stream exiting the extractor during the residence time distribution studies (see Section 3.3). Two gas chromatographs were required due to the composition of the streams being analysed.

A Hewlett Packard 5890 Series II gas chromatograph was used to evaluate the performance of the two-phase separators. Its primary function was to determine if there was any of the extracted oil leaving the separators. A packed column consisting of 3% O.V. 101 packing on Supelcoport support was used in conjunction with a thermal conductivity detector. The injector temperature was 230°C and the detector operated at 280°C. The initial oven temperature was 50°C and was programmed to remain at this temperature for two minutes and then begin to increase at a rate of 15°C per minute until 250°C was reached. A sample size of 30 μL was injected manually using a syringe.

A second gas chromatograph was used in the residence time distribution study. This gas chromatograph analysed the exit gas in order to produce the response curve for the extractor when subjected to a known disturbance. A Varian 3400 gas chromatograph with a 2 ml sample loop, thermal conductivity detector and a Chromosorb 103 packed column were used. Helium was used as the carrier gas and the column was calibrated to detect ethane. The oven temperature was held at a constant 80°C for 4.5 minutes and both the detector and injector were set to 200°C. The calibration method and results can be found in Appendix A.

Combustible Gas Detector

A combustible gas detector was installed near the pump and cylinders. The detector (MT03) was purchased from Micro Watt of Calgary. The purpose of the detector was to alert the lab personnel if any leaks from the pump, cylinders, etc... occurred.

3.2 Materials

Materials used in the experiments included Peace River bitumen, ethane and sand. In addition, a series of pure component experiments were performed using carbon dioxide and hexadecane.

3.2.1 Pure Components

The ethane used in the extraction experiments was purchased from Praxair Distribution Inc. The fluid was delivered in T-type liquid withdrawal cylinders that weighed 14.51 kg and had a pressure of 3.74 MPa. The ethane had purity greater than 99.0% and Table 3.2 lists the composition of the ethane cylinders.

Fluid	Concentration, ppm
Methane	< 50
Ethylene	< 4000
Propane	< 400
Propylene	< 1000
C3's	< 1500
Sulphur	< 1

Table 3.2 – Composition of ethane used as the solvent for the experiments.

Carbon dioxide was used as one of the solvents to extract bitumen and also used to evaluate the performance of the apparatus. The carbon dioxide was purchased from Praxair with a purity of 99.5 mol% with a maximum moisture content of 34 ppm. The cylinders were T-type liquid withdrawal.

Nitrogen used in the residence time distribution work was also purchased from Praxair Distribution Inc., and had a purity of 99.7 mol% and a maximum moisture content of 32 ppm. The cylinders were the standard T-type.

The n-hexadecane with carbon dioxide was the binary system used in the pure component solubility studies used to evaluate the apparatus. The hexadecane was obtained from Aldrich Chemical Company Inc and was 99% pure. No further purification of the n-hexadecane was performed.

3.2.2 Peace River Bitumen

The bitumen feedstock for this work was Peace River bitumen. The sample was received from the Peace River facility operated by Shell Canada Limited. The bitumen was produced using the cyclic steam production technique. After the water removal step, diluent was added to make the bitumen easier to transport. Two samples were received from Shell, one being the bitumen plus diluent and the second the diluent. The diluent was removed by distilling the diluent/bitumen mixture until the material removed from the bitumen and the diluent had matching boiling point curves. The resulting bitumen was then analysed to determine its properties that are shown in Table 3.3.

Density at 15°C		998.3 kg/m^3
		10.2 °API
Initial Boiling Point		160°C
Total Sulphur		5.5 wt%
Pour Point		+ 3°C
CCR		8.9 wt%
C_5 Asphaltenes		15.36 wt%
Viscosities		10270 cSt at 20°C
		3718 cSt at 30°C
		1506 cSt at 40°C
SARA:	Saturates	26.96 wt%
	Aromatics	42.65 wt%
	Resins	15.03 wt%
	Asphaltenes	15.36 wt%

Table 3.3 – Properties of the Peace River bitumen used in this work.

The Peace River bitumen had an initial normal boiling point of 160°C and it was possible to distil 50.5 wt% of the bitumen using the ASTM D2887 method to a maximum boiling point of 584°C. The distillation data for both the Peace River bitumen used in this work and the diluent can be found in Appendix B.

3.2.3 Sand

The sand was purchased from Target Products Ltd of Calgary and was produced at a plant in Morinville, Alberta. The sand is predominantly silica (93 wt%) with a small amount of alumina (4 wt%) and trace amounts of oxides. The complete chemical analysis is shown

in Appendix B. The sand was classified as 20-40 mesh with an average diameter of 0.663 mm. The sieve analysis is provided in Appendix B.

3.3 Extractor Flow Characterisation and Distribution

One of the key aspects considered when designing the extractor was the distribution of the solvent as it passed through the extractor. The flow pattern for an ideal extractor would be plug flow across the complete cross-section of the extractor. This would ensure that all of the bitumen in the extractor would be contacted evenly with the solvent.

Extensive research has been published on gas and liquid flow through packed beds (Carberry et al., 1958; Shah et al., 1978; Han et al., 1985; Geise et al., 1998). These studies typically use air and water as the gas and liquid to determine the effects of different packing and size of packing on the distribution of these fluids at low pressures and moderate temperatures. Shah et al. reviewed a number of papers on this subject (Shah, 1978). As part of the study, they discussed methods for conducting residence time distribution tests, how to interpret the data and reasons why flow deviated from the ideal cases of plug flow and complete mixing in reactors.

Two important considerations when analysing the flow pattern in the extractor used in this study were solvent bypass and solvent channelling. According to Shah et al., these are two of the factors that can contribute to deviation from ideal plug flow (Shah et al., 1978). Thus, a residence time distribution study was performed to examine how close the flow of the solvent was to plug flow.

A limited amount of work has been published regarding the distribution of fluids at elevated pressures and of supercritical solvents in packed columns. Benneker et al.

examined the effects of buoyant forces on the flow of gases of mixed composition at pressures as high as 1.5 MPa (Benneker et al., 1998). They found that axial dispersion was strongly affected by changes in density, especially in cases where density increased with height. It was also concluded that this is mainly a concern when scaling up process from the lab scale. The only cause for density changes in this work would be as a result of composition changes as the temperature is constant and pressure drop is very small in the extractor.

Tan et al. conducted experiments to study the axial dispersion of supercritical fluids in packed columns (Tan et al., 1989; Tan et al., 1988). They argued that because the properties of supercritical fluids were neither completely gas-like nor completely liquid-like, correlations for column diameter to particle diameter and length of packing to particle diameter for gases and liquids would not be valid for supercritical fluids. Using particles ranging from 0.1 cm to 0.4 cm, and supercritical CO_2, they developed the following criteria for uniform distribution of supercritical fluids in packed columns:

$$\frac{D}{d_p} \geq 10 \qquad \text{Equation 3.1}$$

$$\frac{L}{d_p} \geq 40 \qquad \text{Equation 3.2}$$

Thus, in this study, two checks were made to evaluate the flow of solvent in the extractor. First, a residence time distribution study was conducted to quantify the solvent flow and ensure that the sand and the porous stainless steel distributor provided sufficient distribution of solvent to assume plug flow. Second, it was also assumed that the sand would act like packing and help improve distribution of the solvent. The criteria proposed by Tan et al. were used to verify this assumption.

3.3.1 Residence Time Distribution

A residence time distribution, RTD, study was conducted in order to determine the flow characteristics of the solvent as it passed through the extractor. Methods for conducting RTD studies in order to determine the flow characteristics of fluids through packed beds have been well documented (Carberry et al., 1958; Han et al., 1985; Shah et al., 1978). RTD studies were used to describe the flow pattern in a vessel and determine if channelling or uneven flow distribution occurred. A transient response technique was used in which a step change in inlet flow composition was made. Two types of RTD runs were conducted, the first with the extractor filled with sand only and the second with bitumen and sand present.

In the first set of experiments, sand was packed in the extractor and the apparatus was brought up to temperature and system was charged with nitrogen up to the required operating pressure. The set-up was modified to enable a gas chromatograph to be connected online at the exit of the extractor after the pressure control valve. Gas compositions were measured every 4.7 minutes to detect the change in composition of the exit gas as a function of time. The feed to the extractor was stepped from pure nitrogen to pure ethane. Table 3.4 outlines the conditions at which the residence time distribution experiments were conducted.

Temperature	48°C
Pressure	10.5 MPa
Disturbance	Step in Feed Concentration
Flowrate	0.4 L/h at pump conditions

Table 3.4 – Operating conditions for the RTD studies with and without bitumen present in the extractor.

In the second set of RTD experiments, the extractor was filled with a mixture of sand and bitumen. The major concern in conducting these experiments was to prevent any of the extractable bitumen from plugging up the column in the gas chromatograph. This problem was addressed by filling the extractor with the normal bitumen feed and conducting an extraction to remove the soluble hydrocarbons. The extraction step was performed at a much higher pressure of 15 MPa because at these conditions, more of the bitumen was soluble in the solvent (see Section 4.4). The extraction was continued until negligible amounts of oil were collected in the separator. It was assumed that by operating at the higher pressure first, any of the feed left in the extractor would not be soluble in either nitrogen or ethane at the lower pressure at which the RTD experiment would be conducted. The RTD experiments were then conducted in the same manner and at the same conditions as those without the bitumen.

The outlet composition data was collected and used to characterise the flow distribution in the extractor. Figure 3.5 shows the response at the exit of the extractor to the step change in inlet composition for the system with the bitumen present. For step changes, such as those introduced in these experiments, response curves similar to the one shown in Figure 3.5 are referred to as F curves (Levenspiel, 1962).

The moment method (Levenspiel, 1962) was used to analyse the distribution data collected during the experiments. The first moment is the mean of distribution and the second is the variance. For closed systems where the fluid flows as a result of bulk flow only (no eddy diffusion), the mean and variance can be calculated using the following equations respectively:

$$\bar{t} = \sum tE(t)\Delta t \qquad \text{Equation 3.3}$$

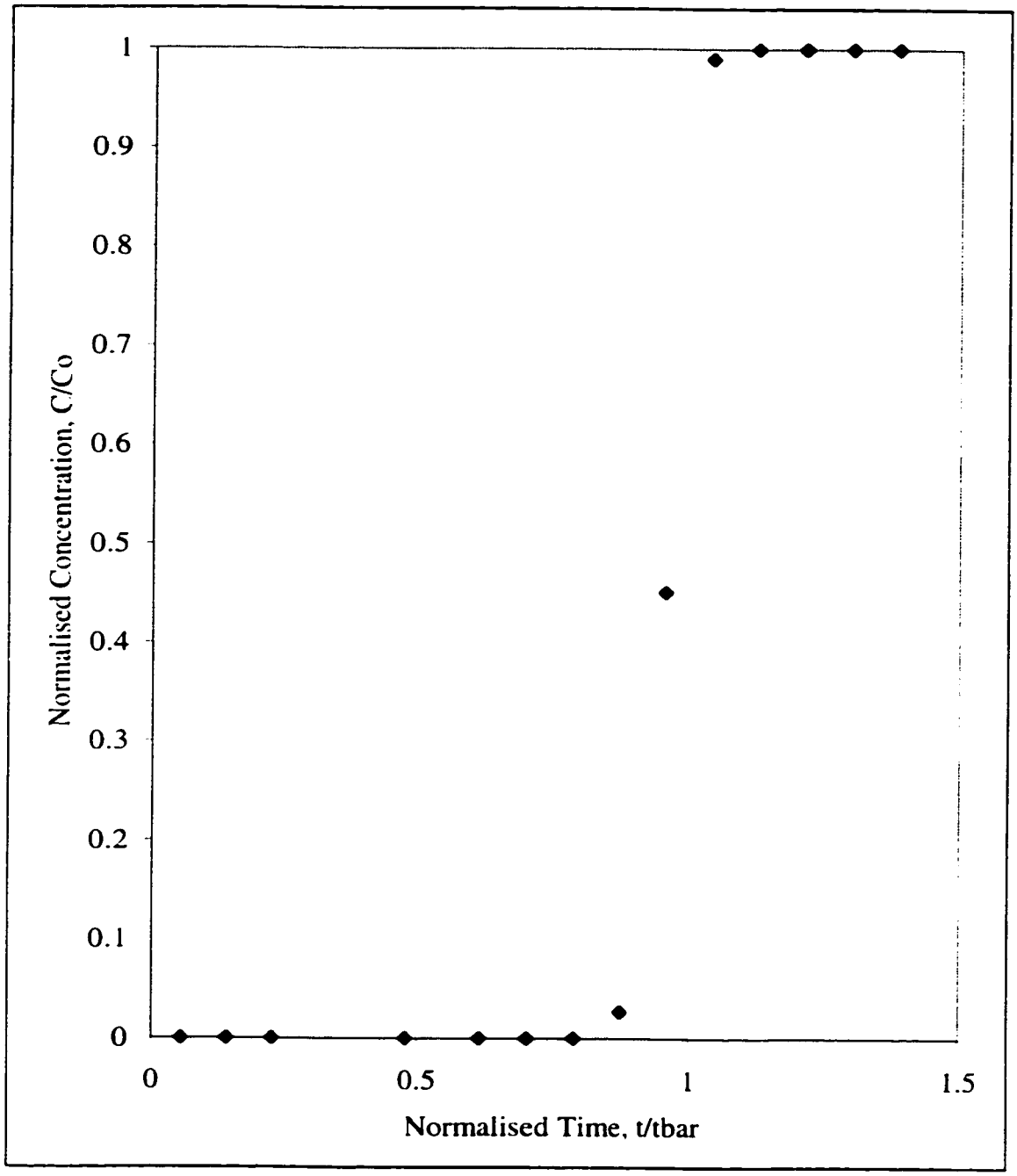

Figure 3.5 – Response curve for a step change in feed concentration (F-Curve) with no bitumen in the extractor.

$$\sigma^2 = \sum t^2 E(t)dt - \bar{t}^2 \qquad \text{Equation 3.4}$$

Where E(t) was a translated form of the output response (F curve) to a step change in the input. The E(t) and F curves were related as follows:

$$E(t) = \frac{dF}{dt} \qquad \text{Equation 3.5}$$

Procedures such as dispersion models and mixed models can be used to quantify the non-ideality of the flow through extractors (Levenspiel, 1962). In this work, the dispersion model was used to determine how close the flow of ethane through the extractor was to plug flow. For a closed extractor (one in which the disturbance was introduced at the inlet and measured at the outlet), the equation for variance in the dispersion model is as follows:

$$\sigma^2 = 2\frac{D}{uL} - 2\left(\frac{D}{uL}\right)^2 (1 - e^{-uL/D}) \qquad \text{Equation 3.6}$$

The D/uL term in Equation 3.6 is a dimensionless number called the vessel dispersion number. It was adjusted until the variance from Equation 3.6 matched the variance obtained from the experimental data (Equation 3.4). According to Levenspiel, dispersion numbers less than 0.002 indicate that a small amount of dispersion occurred.
The procedure outlined above was used to determine the flow characteristics for the extractor used in this study. The RTD experimental results yielded dispersion numbers of 0.00138 when there was no bitumen and 0.00078 for the case where bitumen was present. Based on Levenspiel's criteria, there was little backmixing and the extractor exhibited predominately plug flow behaviour. Deviations from true plug flow may be attributed to one of the following: mixing in the wind-box of the extractor, mixing due to a slight

pressure difference between the nitrogen and ethane streams when the step change was made and mixing in the line downstream of the pressure valve.

The conclusions from the RTD study verifies the assumption that the ethane flowed through the extractor in a plug flow manner. Because the vessel number indicated that the ethane flow was essentially plug flow, according to Shah et al. we can conclude that the ethane has a relatively uniform velocity profile across the complete cross section of the extractor. In addition, the system exhibited little channelling, bypassing, short-circuiting and/or back flow of solvent (Shah et al., 1978).

3.3.2 Influence of Sand

The sand acted as packing and assisted in the distribution of the solvent within the extractor. Tan et al. devised two criteria for ensuring uniform distribution of supercritical solvents in packed beds (Tan et al., 1989) as presented in Section 3.3. Using Equation 3.1 and the dimensions of the extractor and sand, the ratio of column diameter to packing diameter was 60.3. This is much greater than 40 which was the minimum value for good distribution obtained by Tan et al.

Using Equation 3.2 and the average sand diameter, L (the height of packing required to obtain complete distribution) was found to be 0.026 m. This is only 5.2% of the height of the extractor. From this, it can be concluded that even without the presence of the distributor plate, only a small portion of the bitumen would have been exposed to ethane which was not distributed evenly. With the addition of the distributor plate, this value should be much lower.

3.4 Apparatus Verification

A binary system was used to evaluate the experimental set-up. Solubility of n-hexadecane in CO_2 has been reported in literature (Deo et al., 1992; Larson et al., 1989) and used by other researchers to verify the operation of their apparatus (Deo et al., 1992; Hwang, 1996). Literature data for the CO_2/hexadecane system was published at two temperatures, 32 and 38 °C, and pressures ranging from 7.6 to 17.2 MPa (Deo et al., 1992; Larson et al., 1989). Eight experiments were performed over the above conditions. The resulting solubilities of hexadecane in CO_2 are shown in Figure 3.6. The error bars in this figure are ±3.7% of the measured solubilities which corresponds to the percent average absolute relative deviation in the measured values.

Figure 3.6 shows that the results obtained were in excellent agreement with those published by Deo et al. and Larson et al. All of the average solubilities were well within 10% of the values reported in the literature (Deo et al., 1992; Larson et al., 1989). Based on the results from the pure component study, it was concluded that the apparatus would provide reliable solubility data.

3.5 Error Analysis

Errors associated with experimental data can be divided into two categories: random errors and systematic errors (Laureshen, 1992). Random errors can be observed by fluctuations around an average value. Errors of this type are caused by judgement errors made by the experimenter or are caused by variations in parameters that cannot be controlled by the operator or the apparatus. Systematic errors are inherent to experimental apparatus and/or procedure and result in the deviation between the experimental results and the true or reported value. These errors will exist regardless

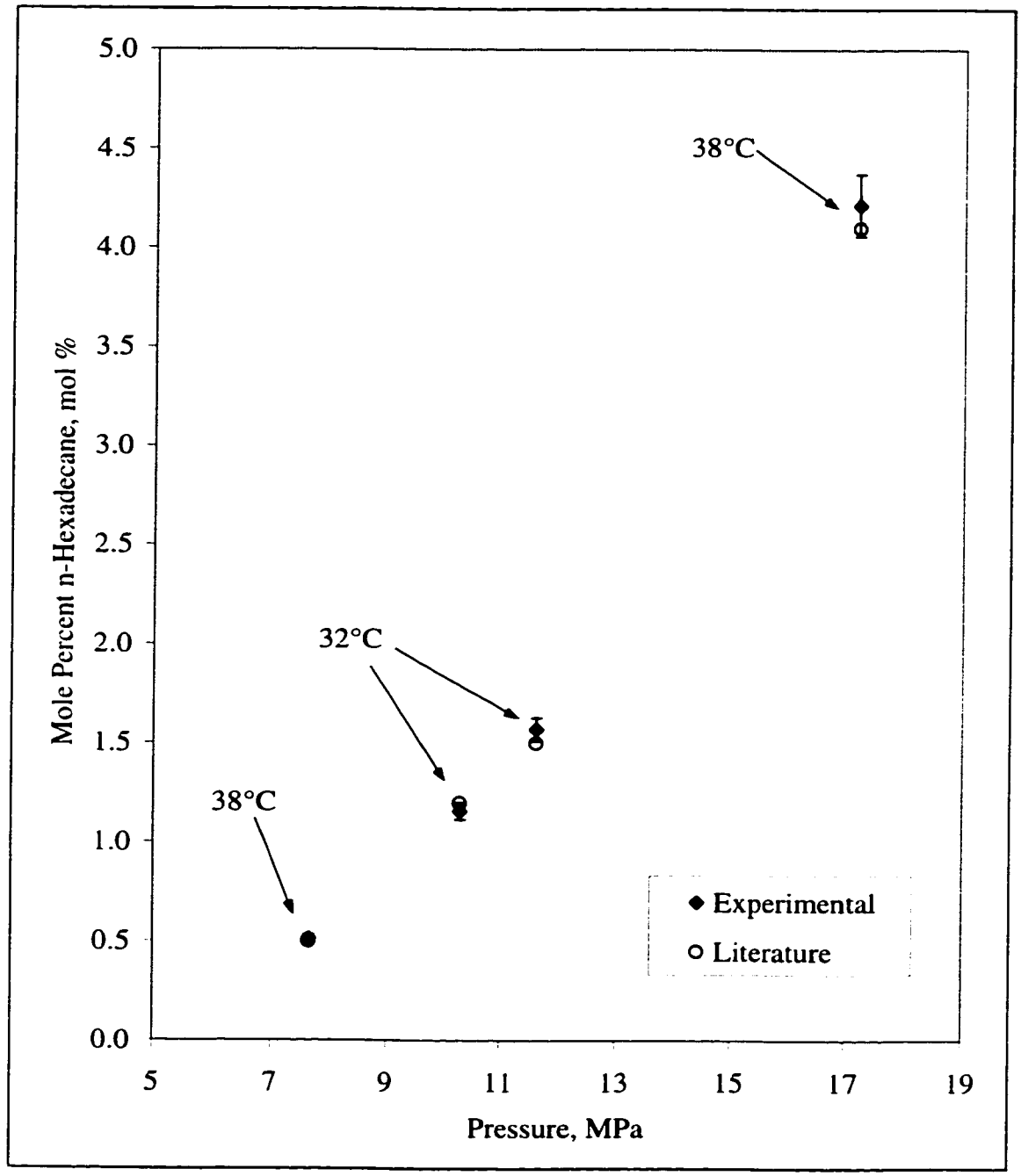

Figure 3.6 – Solubility of n-hexadecane in CO_2 as a function of pressure at temperatures of 32 and 38°C.

of the number of times the experiments are repeated and can be attributed to errors in measurement techniques and/or improper instrumentation calibration. Error analysis can be used to give an indication of the precision and accuracy of the experimental data reported. Accurate data will have low systematic error and precise data will have a small random error.

For the apparatus used in this work, error analysis was performed using the extracted oil to solvent injected ratio (g/STD L). This is a measure of the amount of oil extracted from the bitumen per standard litre of ethane injected.

3.5.1 Systematic Errors

The oil to solvent ratio (OSR) was calculated using the following equation:

$$OSR = \left(\frac{M_{sep}^{final} - M_{sep}^{initial}}{V_{C2}} \right) \qquad \text{Equation 3.7}$$

where M_{sep}'s are the separator masses of the at the beginning and end of an extraction window and V_{C2} is the volume of ethane measured by the wet test meter corrected to standard conditions.

Data from four operating conditions was used to calculate the systematic error for the apparatus. Systematic errors in the oil to solvent ratios were calculated using the values for the accuracy of the wet test meter used to measure solvent flow and the balance used to determine the mass of oil extracted. The detailed results are presented in Appendix F. The average absolute error (AAD) and average absolute relative error (%AARD) were $2.9*10^{-4}$ g/Std L and 0.128%, respectively.

3.5.2 Random Errors

The AAD and %AARD were calculated for the experimental oil to solvent ratios measured. The true value normally used in the equations to calculate AAD and %AARD was replaced with the mean oil to solvent ratio for each condition. In addition, the standard deviation was also calculated for the data and the detailed results are shown in Appendix F. The AAD was found to be $5.0*10^{-4}$ g/Std L, the %AARD was 2.12% and the standard deviation was 2.10%.

3.6 Summary

In this chapter, details regarding the design and performance of the experimental apparatus constructed has been provided. A process flow diagram and a photograph of the apparatus were included to show how the experiments were conducted. In addition, specifications for key pieces of equipment have been provided as well as information for the ancillary equipment.

A detailed study was performed to characterise the solvent flow within the extractor. The results from the residence time distribution demonstrated that the solvent moved through the extractor in a plug flow manner. It was also shown that the sand was of sufficient size to assist in the distribution of solvent across the complete cross section of the extractor.

The performance of the experimental apparatus was provided. Solubility results from a CO_2/n-hexadecane system agreed quite well with published data. The error analysis concluded that both the systematic and random errors were extremely low. As such this validates the experimental apparatus and procedure used in this work.

Chapter Four

Experimental Results and Discussion

The development of new industrial processes are greatly improved when experimental data exists that can be used as the basis for design. One of the factors that is hindering the creation of new supercritical fluid applications for industrial applications is the dearth of experimental and pilot plant data (Brennecke et al., 1989). Therefore, the first step in widening the application of supercritical fluids must be to increase the amount of data available for supercritical fluid systems.

In this chapter, experimental data is presented for the extraction of oil from Peace River bitumen using supercritical ethane. The effects of parameters such as temperature and pressure on the extraction yield, composition and characteristics of the extracted material are discussed. A comparison is made between the performance of supercritical ethane and carbon dioxide, used for the extraction of oil from bitumen.

4.1 Experimental Details

Before presenting the results from the extraction experiments, some of the technical details with respect to the operation and performance of the apparatus are highlighted.

Unless otherwise stated, 140 g of bitumen was mixed with 800 g of sand resulting in the composition of the bitumen-sand mixture to be 15 wt% bitumen. The bitumen and sand were mixed until the consistency of the mixture was uniform and then packed into the extractor prior to the start of each experiment. The composition of the feed was chosen to approximate the bitumen/sand ratio typical of the oil sands found in northern Alberta which is 6-18 wt% (Pruden, 1997).

The solvent volumetric flow rates are quoted in units of L/h. This flow rate was not at standard conditions but at the temperature and pressure of the pump. The volumes reported were measured using the wet test meter located after the two phase separator (see Section 3.1.7). The volume was then corrected to standard conditions of 15°C and 101.3 kPa using the calibration equations presented in Appendix A.

The amount of bitumen available for each extraction was limited by the volume of the pump. The positive displacement Ruska pump used in this work had a fixed volume of 1.0 L under pump conditions when both pistons were in the filled position. The volume of solvent was further reduced due to the fact the solvent was charged to the pump at the cylinder pressure and required pressurisation up to the desired pressure. This typically left 0.75 L of solvent available at the start of an extraction experiment.

The operating temperature and pressure for the extractions were controlled very accurately. The average standard deviation for the temperature over the course of an extraction was ± 0.45°C. This value was well within the accuracy of the thermocouples which was ± 0.6°C. The pressure had an average standard deviation of ± 0.040 MPa. This was also within the manufacture's stated accuracy of ± 0.045 MPa.

Mass balances were performed for each experiment. The material balances closed to within an average of -1.5 wt%, with the maximum loses being only -2.2 wt%. The majority of the losses can be attributed to the oil and sand adhering to tools such as the

spatula and packing tool required to charge and clean the extractor. The maximum loss of 2.2 wt% was less than half that reported by others performing similar experiments (Deo et al., 1992; Subramanian et al., 1998).

4.2 Equilibrium Verification

The first step in the experimental process was to determine the nature of the data collected, that is, was the amount and composition of the oil extracted governed by mass transfer effects or thermodynamic equilibrium? The answer to this question was required in order to determine the equations that would be used to subsequently model the extraction process. In order to use an equation of state it is necessary to assume that the system has achieved equilibrium. In other words, it was necessary to verify that the solvent had been completely saturated with the soluble fraction of bitumen at the exit of the extractor. If the data collected was governed by mass transfer limitations and not equilibrium, then a different model would be required, such as that presented by Cussler, (Cussler, 1996). Therefore, it was necessary to determine which regime, thermodynamic or mass transfer, was governing at the experimental conditions.

The technique used by other researchers such as Deo et al. was to evaluate their apparatus using a known binary system to check that the material extracted was limited by thermodynamics (Deo et al., 1992; Hwang et al., 1996). Deo et al. and Hwang et al. used a binary system consisting of carbon dioxide and hexadecane to test their experimental design. They hypothesised that if the weight percent extracted increased linearly with respect to cumulative volume carbon dioxide injected, the system was providing thermodynamic data over the duration of the extraction. They compared the composition of the stream leaving the extractor at two different conditions, with experimental data from literature and values predicted using the Peng-Robinson equation of state. Their

assumption was further justified based upon the fact that the compositions of the exit stream were close to both the literature and predicted values. They also assumed that, if the data for the carbon dioxide/hexadecane system was at thermodynamic equilibrium, then the experimental results for systems using propane as the supercritical solvent and fluids such as crude oils and bitumens would also yield thermodynamic data.

The major concern with this analysis was whether or not the pure components used in the validation would accurately represent the behaviour of different supercritical systems. In particular, they assumed that hexadecane and supercritical carbon dioxide would behave similarly to a system of bitumen and supercritical propane. Hexadecane has a boiling point of 286.8°C and a density of 773 kg/m^3 that are both quite different from the initial boiling point and density of the Whiterocks bitumen used in their work, 520 K and 980 kg/m^3 respectively. In addition, propane behaved differently than carbon dioxide in that the amount of bitumen extracted using carbon dioxide was negligible while propane was capable of recoveries in the range of 40 to 50 wt%. Therefore, questions arose as to whether this was a suitable approach for validating the assumption that the composition of the solvent exiting the extractor was completely saturated with oil and not limited by mass transfer restrictions.

A different approach was used to ascertain whether the apparatus used in this work could produce thermodynamic data. A series of experiments were conducted at 63°C and 10.5 MPa during which Peace River bitumen was contacted with supercritical ethane at different flow rates. The solvent flow rate was constant for each extraction and set at a rates ranging from 0.2 to 0.8 L/h. The results from these experiments were plotted as the cumulative percent of bitumen extracted as a function of cumulative volume of ethane measured by the wet test meter corrected to standard conditions. The resulting graph is shown in Figure 4.1.

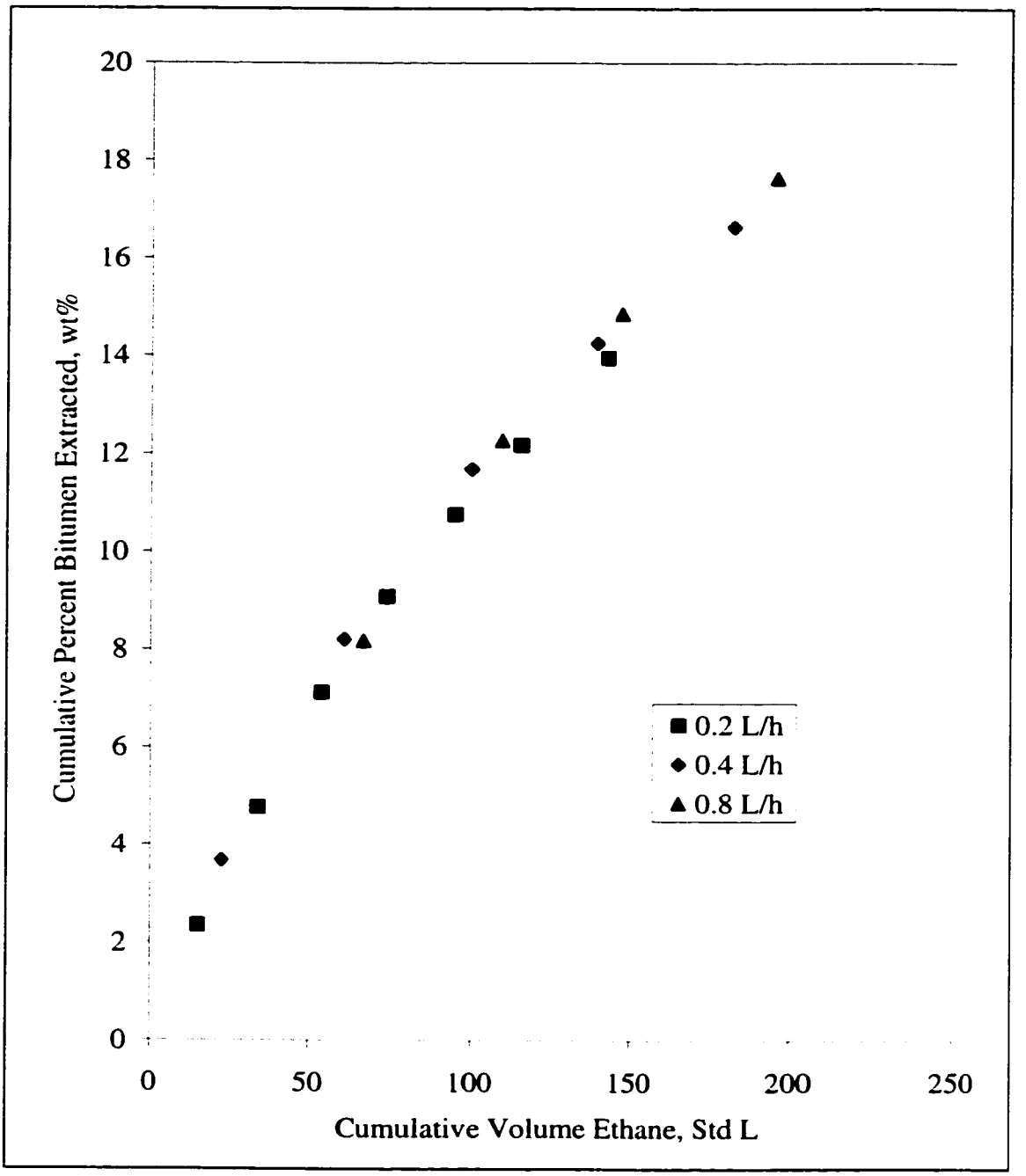

Figure 4.1 – Extraction curves for Peace River bitumen using supercritical ethane as the solvent at 63°C and 10.5 MPa.

Figure 4.1 shows that the mass extracted was independent of the rate at which the solvent flowed through the extractor. This indicated that the data collected was governed by thermodynamic equilibrium and not mass transfer resistances. If the system had been in the mass transfer dominated regime then the amount of bitumen extracted would have been a function of the solvent flow rate. As the flow rate increased, the time that the solvent was able to contact the bitumen would decrease resulting in less oil being recovered from the extractor. Since this was not the case for this system, the results indicated that when the solvent exited the extractor it was saturated with the soluble fraction of bitumen and thus governed by thermodynamic equilibrium.

Compositional analysis was conducted on samples collected when the solvent flow rate was 0.4 L/h and 0.8 L/h. This was done to verify that after having contacted the bitumen with equal amounts of ethane, both the mass of oil extracted and its composition were the same regardless of the solvent flow rate. Boiling point curves for each of the samples were obtained using the ASTM D2887 method. Using the initial boiling points and final boiling points for each of the pseudocomponents (see Section 5.1), it was possible to determine the weight percent of each pseudocomponent (PC) in the extracted oil. The results are summarised in Table 4.1.

Sample	A2	C1	A3	C2	A4	C3	A5	C4
Cumulative Ethane Volume, Std L	65.5	67.0	105.5	109.3	148.0	146.9	185.5	195.5
Composition, wt%								
PC1	38	39	33	33	28	25	24	23
PC2	39	38	43	42	44.5	46	45	46
PC3	16	16	17	17	20.5	21	23	23
PC4	5.5	6	5.5	6	5.5	6	6.5	6
PC5	1.5	1	1.5	2	1.5	2	1.5	2

Table 4.1– Comparison of the composition of samples extracted at 63°C and 10.5 MPa using flow rates of 0.4 L/h (A) and 0.8 L/h (C).

The results from the compositional analysis show that the solvent flow rate did not have an effect on the composition of extracted material. For example, even though samples A3 and C2 were extracted using solvent at flow rates of 0.4 and 0.8 L/h, respectively, their compositions were essentially the same. Therefore, at each flow rate, a given volume of solvent was becoming saturated with the same amount and composition of the soluble fraction of bitumen.

In addition to adjusting the flow rate, the apparatus was also tested using a binary system consisting of carbon dioxide and hexadecane at different temperatures and pressures. Although these experiments were performed mainly to verify the performance of the apparatus against a well documented system, they also verified that the apparatus would produce equilibrium data. The solubility of hexadecane in supercritical carbon dioxide at the conditions studied, was found to match those reported in literature (see Section 3.4).

This method was a significant improvement over the technique used by Deo et al. Results from binary system experiments were augmented with results obtained using the bitumen and solvent which was to be studied. Assumptions did not have to be made regarding how well a given binary system could be extrapolated to represent the behaviour of a complex mixture of hydrocarbons such as bitumen and supercritical ethane. Thus the assumption that the data collected using this apparatus was subject to equilibrium limitations was made with greater certainty.

One area of concern that remained was whether the equilibrium assumption could be made over the complete range of temperatures and pressures to be studied. It was conceivable that a flow rate of 0.4 L/h was low enough to achieve equilibrium at some temperatures and pressures but not for others. As a precaution, multiple runs were performed at different flow rates to check that equilibrium data was still being collected at each pair of temperatures and pressures. Experiments were performed twice at solvent flow rates of 0.4 L/h to confirm the repeatability of the results and once at a flow rate of

0.2 L/h. Performing a third run at 0.2 L/h served two objectives: Firstly, if the extraction curve for 0.2 L/h overlapped the two curves for flows of 0.4 L/h, then the oil extracted was independent of solvent flow rate and was still controlled by thermodynamic equilibrium. This was done by using a plot similar to Figure 4.1 and checking that the three curves overlapped. Based upon this check, it was observed that equilibrium was achieved for all temperatures and pressures at which the experiments were performed. Additionally, the data from this run could be used to test the repeatability of the experimental data. If the system was at equilibrium, the data collected would be independent of solvent flow and the yields should be identical to the yields at 0.4 L/h. This was the case for all of the experimental data collected.

4.3 Effect of Temperature

A series of experiments were conducted to examine how the extraction of Peace River bitumen using supercritical ethane responded to variations in operating temperature. Temperature has a strong affect on the properties of supercritical ethane especially near the critical point as discussed earlier in Section 2.1. Changes in solvent properties such as density, result in a significant variations in the solubility of different components in theses fluids as illustrated by the results of numerous pure component systems studied (Larson et al., 1989; Johnston et al., 1982; Peters et al., 1989; Moradinia et al., 1987).

Five different temperatures were investigated in this study ranging from 36.9 to 92.1°C at a constant pressure of 10.5 MPa. These temperatures, along with the corresponding solvent densities from NIST (National Institute of Standards and Technology, 1992), are summarised in Table 4.2. The temperatures were chosen with the goal of keeping the temperature as low as possible. If this process is to become a viable alternative to the conventional bitumen processing methods such as the Clark Hot Water Wash process

(Pruden, 1997), it should exploit the fact that supercritical processes can operate at low temperatures. Lower operating temperatures would reduce the operating costs required to conduct extractions in a region where ethane would be supercritical. Thus the upper temperature for operation was limited to a temperature near that of the Clark process which is 80°C (Pruden, 1997).

Temperature, °C	Reduced Temperature	Density, kg/m^3	Reduced Density
36.90	1.02	360.57	1.77
47.78	1.05	331.60	1.63
63.27	1.10	281.76	1.39
76.71	1.15	234.04	1.15
92.10	1.20	187.98	0.93

Table 4.2 – Experimental temperatures and resulting ethane densities at a pressure of 10.5 MPa.

The pressure rating for various pieces of equipment comprising the experimental apparatus constrained the maximum temperature at which experiments could be conducted. As the operating pressure increased, the maximum temperature that the fittings, valves, tubing and extractor could operate at decreased. Based upon the ratings for each piece of equipment (see Section 3.1), the maximum operating temperature was limited to 100°C.

4.3.1 Yield Variation

The effect of temperature on the amount of oil recovered from the bitumen as a function of ethane volume measured exiting the extractor is shown in Figure 4.2. The oil recovered was plotted as a cumulative percent extracted versus the cumulative volume of

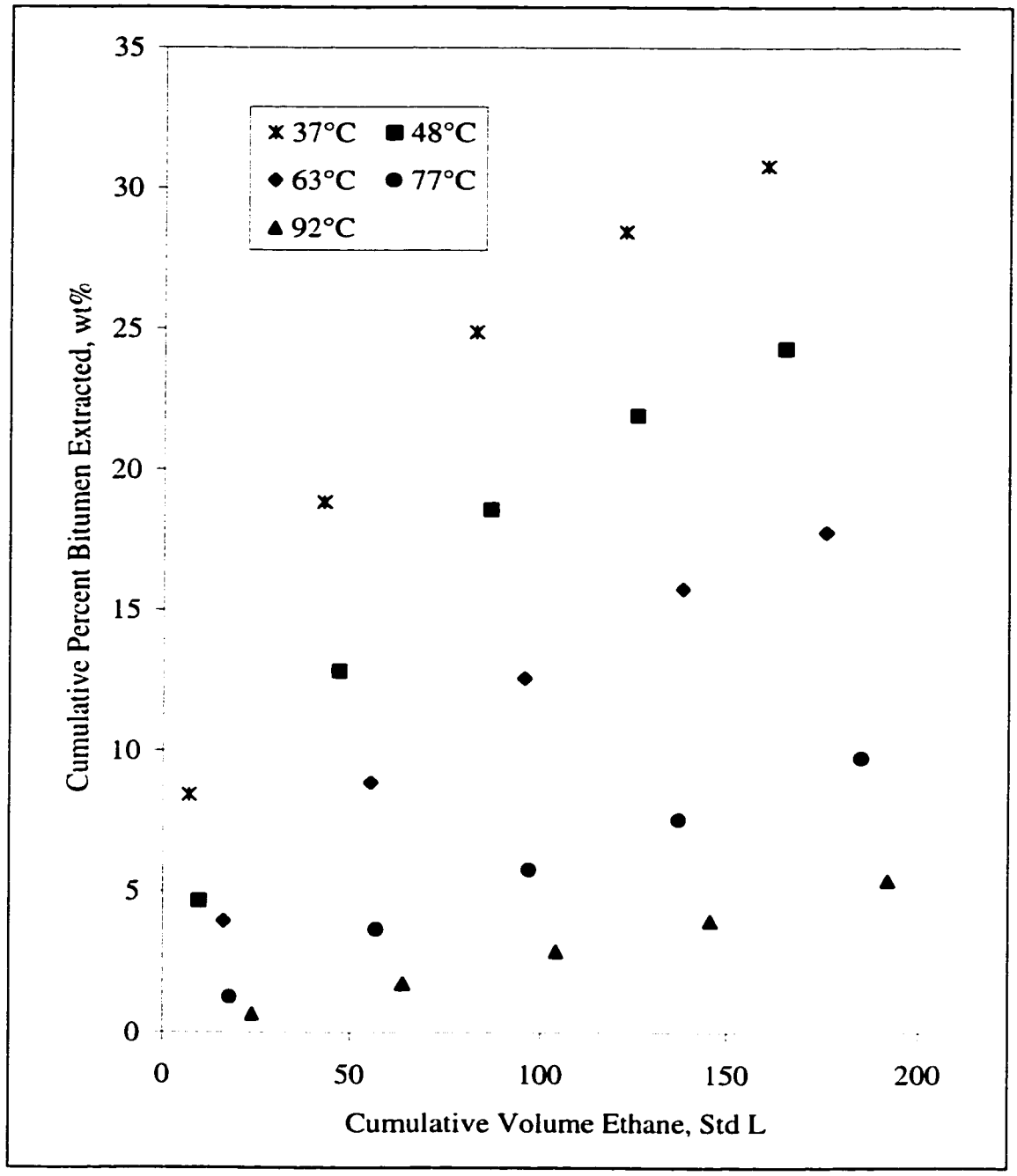

Figure 4.2 – Weight percent of extracted bitumen as a function of cumulative volume of ethane measured for extractions performed at 10.5 MPa and temperatures ranging from 37-92°C.

ethane measured using the wet test meter in standard litres. Figure 4.2 shows that as the temperature was decreased, the amount of oil extracted increased. The slope of the extraction curves revealed that the rate at which oil was extracted was also higher for experiments conducted at lower temperatures.

A comparison of the cumulative weight percent extracted after having injected approximately 175 standard litres of ethane, shows that there was a significant increase in the amount of oil recovered. The weight percent extracted increased from 4.5 wt% at 92°C to 30.7 wt% at 36.9°C, an approximate six fold increase. This large improvement in the recovery of oil can be attributed to the significant shift in the solvent reduced density over this temperature range from 0.93 to 1.77.

Figure 2.2 showed how significantly the density of supercritical ethane changed as a function of temperature near the critical point of the fluid. The data in Table 4.2 showed that the reduced density almost doubled, increasing from 0.93 to 1.77 for a relatively small temperature change of 55°C. The large density change was important because of its impact on the solubility of the hydrocarbon fractions in supercritical fluids. Hwang et al. observed that changes in solubilities of crude oil fractions in supercritical propane were proportional to changes in the solvent density (Hwang et al., 1995). As the density of supercritical propane increased, Hwang et al. observed that the solubility of crude oil increased. For example, they observed that the amount of crude oil increased from 10% to 40% when the reduced density of propane was increased from 0.2821 to 0.8385 by decreasing the extraction temperature.

Because the system studied in this work was similar to that used by Hwang et al., it was expected that a similar behaviour would be present. The results from these experiments did in fact support the observations made by Hwang et al. The solvent density increased by 92% while the amount of bitumen extracted increased by 580% over the 55°C temperature span.

The dramatic change in the amount of extractable oil can also be explained by examining the shift in the nature of the system. At 36.9°C, the density of ethane was 360.57 kg/m3 which was very close to the standard liquid density of ethane, 355.68 kg/m3 (HYSYS, 1995). Under these conditions, the system behaved similar to a liquid-liquid extraction process. Liquid solvent systems have higher solubilities due to the increased attractive forces as compared to vapour solvents (Johnston et al., 1982). Conversely, at 92.1°C, the solvent density decreased to 187.98 kg/m3, a much lower density than the liquid density. With such a low solvent density, the system now acted similar to a vapour-liquid extraction process and as a result, the extraction capacity of the solvent decreased.

The rate of extraction was observed to change depending upon the temperature at which the extraction was performed. Figure 4.2 shows that the same weight percent recovered will be achieved faster at lower temperatures for the same solvent flow rate. If the rate chosen was 100 Std L/min, 5 wt% of the bitumen would be recovered in 0.1 min at 48°C, while the same recovery would require 2 minutes at a temperature of 92°C. Therefore, not only are the yields higher at lower temperatures, the rates of extraction are also much greater.

4.3.2 Composition Variation

There was a significant difference in the composition of samples obtained after contacting the bitumen with equal volumes of solvent at different temperatures. In addition, the extent that the composition of successive samples of extracted oil changed during the course of a given extraction was also found to vary with temperature.

In Figure 4.3, boiling point curves for oil samples collected using the same amount of ethane but at two different temperatures are shown. The curves are for the first, third and fifth samples obtained at a pressure of 10.5 MPa and temperatures of 37°C (P) and 63°C (A). If the first samples, A1 and P1, are compared, it can be noticed that P1 has a much higher boiling point curve than A1. A similar trend exists for the other two pairs of samples. Generally, the heavier molecular weight hydrocarbons have higher boiling points. Therefore, the material recovered at the lower temperatures was heavier than that recovered at the higher temperature.

As the operating temperature increased, the composition of the extracted oil became more uniform. This was reflected in the initial and final boiling points for the samples shown in Figure 4.3. Comparison of the boiling point curves for samples A1 and P1 illustrates this point. These samples were obtained after contacting the bitumen/sand mixture with the same amount of ethane but at different temperatures. While both samples have the same initial boiling point, the sample produced at 63°C (A1) has an end point 120°C lower than the sample P1 which was extracted at 37°C. The greater range of the boiling point range curves meant that the oil extracted contained a wider variation of hydrocarbon constituents. Therefore, not only was more oil recovered at the lower temperature, but the variation in the components recovered was also greater.

This effect of temperature on composition can also be observed by studying the trends in the amount of each pseudocomponent present in the samples. The pseudocomponents and their properties are presented in detail in Chapter Five. Table 4.3 shows the composition of three oil samples in terms of the weight percents for each pseudocomponent. The samples shown were produced during the first extraction window at three different temperatures and a constant pressure of 10.5 MPa.

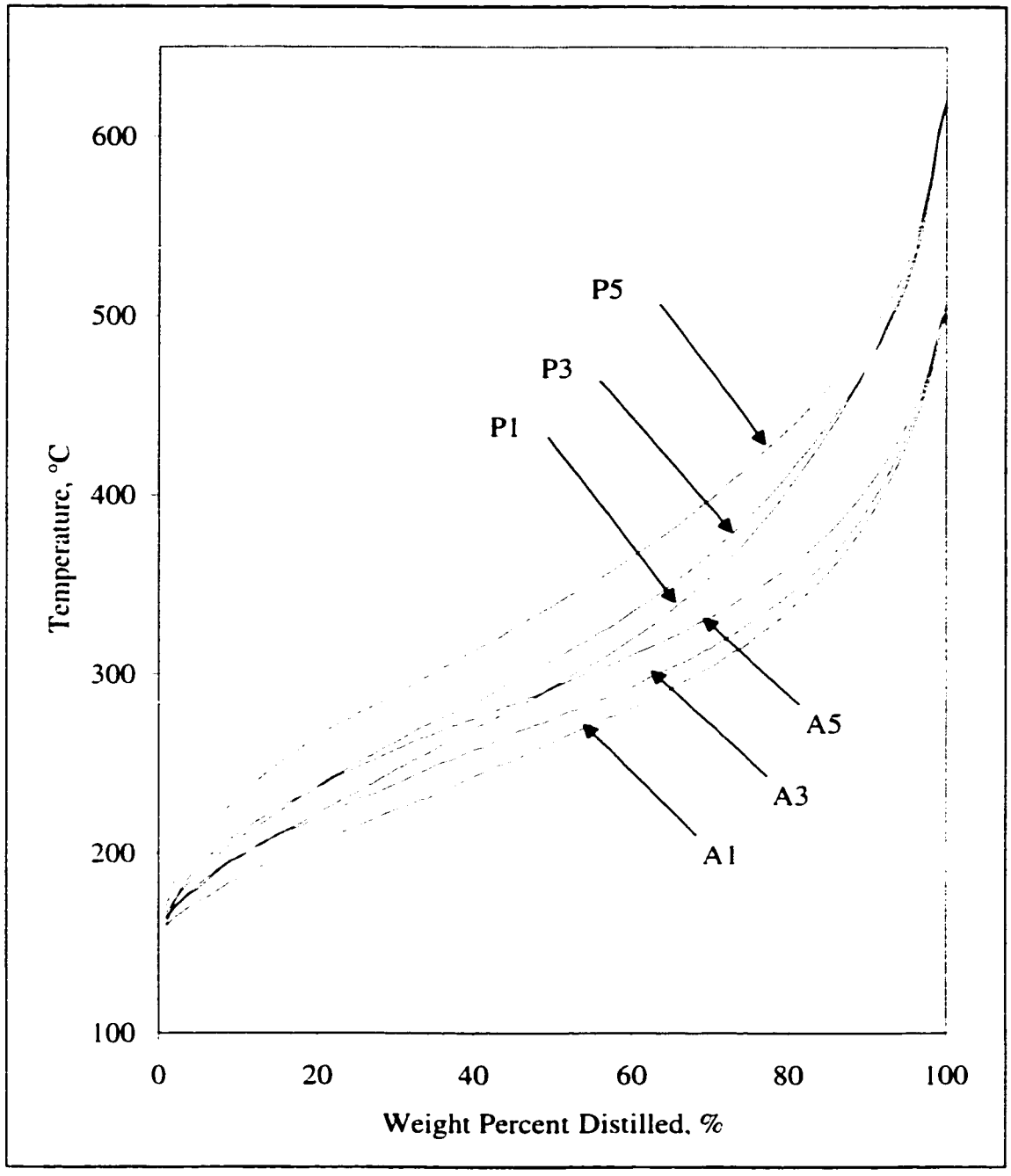

Figure 4.3 – Boiling point curves for selected samples extracted at 10.5 MPa and 37°C (P) and 63°C (A).

Temperature, °C	37	63	92
Composition, wt %			
PC1	24	39	49
PC2	34	38	40
PC3	19	16	9
PC4	9	5	2
PC5	9	2	0

Table 4.3 – Composition of the bitumen extracted during the first window at a pressure of 10.5 MPa and temperatures of 37, 63 and 92°C.

The results in Table 4.3 show that as the extraction temperature increased the composition of the oil became lighter. Shifting the operating temperature from 37°C to 92°C changed the composition of the extract dramatically. At the higher temperature, the sample was composed of twice the amount of the lightest pseudocomponent. The oil sample produced at 37°C consisted of almost 10 wt% of the PC5, but none of this pseudocomponent was collected at 92°C.

The above results were also similar to the published data for binary systems. Moradinia et al provided solubility data for heavy n-paraffins in supercritical ethane (Moradinia et al., 1987). They showed that as the molecular weight of the solute increased, the solubility decreased for a given temperature and pressure. The data shown in Table 4.3 are similar to the findings of Moradina et al. That is as the temperature increased, the oil extracted consistently had a greater weight percent of the lighter pseudocomponents because the hydrocarbons that made up these cuts were lighter and therefore more soluble.

Schmitt et al. collected solubility data for acridine, 1,4-naphthoquinone and naphthalene in a number of supercritical fluids, including ethane, over a wide range of temperatures

and pressures (Schmitt et al., 1985). For isobars above the critical but less than approximately twice the critical pressure, they observed that as the temperature increased, the solubilities decreased. Similar results were presented by McHugh et al. for naphthalene and supercritical carbon dioxide (McHugh et al., 1994). The data in Figure 4.2 for Peace River bitumen and supercritical ethane exhibited similar trends to the binary data. For a relatively low pressure, approximately twice the critical, the amount of oil extracted decreased as the temperature was increased.

Over the course of an extraction, the composition of successive oil samples extracted changed as the bitumen was contacted with increased amounts of ethane. The degree to which the composition changed was observed to be a function of the temperature at which the extractions were conducted.

In Figure 4.2, the cumulative weight percent extracted was plotted as a function of the cumulative volume of ethane injected. Unlike the curve for a binary system, the extraction curves were not linear for the bitumen-ethane system. If a plot similar to Figure 4.2 was made for a pure component solute instead of bitumen, the extraction curve would be a straight line with the slope of the curve depending on the temperature at which the extraction was performed. This was demonstrated by Deo et al. who made a plot of the cumulative weight percent of hexadecane extracted using supercritical carbon dioxide (Deo et al., 1992). The extraction curve was linear because at a fixed temperature and pressure, the solubility of hexadecane in carbon dioxide was constant.

In Figure 4.2, the extraction curves for Peace River bitumen were not linear because the fluid being extracted was a mixture. The shape of the curves changed as the extraction temperature was varied because the composition of the oil extracted changed over the course of an extraction. Since the extractor was a semi-batch system and the solute was a mixture of hydrocarbons, the composition within the extractor changed as the extraction proceeded. This in turn caused changes in the composition of the stream exiting the

extractor, which resulted in the shape of extraction curves changing as the amount of ethane which had contacted the bitumen increased. As the temperature was increased, the extraction curves eventually approached a straight line, as seen in Figure 4.2.

As temperature increased, the solubility of hydrocarbons in supercritical ethane decreased and the heavier the solute, the lower the solubility (Moradinia et al., 1987). Morandina et al. observed that for each hydrocarbon, there was a temperature beyond which the component was not soluble in ethane. In general, this temperature decreased as the component became heavier. Therefore, at higher temperatures the solvent could extract a smaller range of hydrocarbons and the amount of each component extracted was smaller. This resulted in the composition of the extracted oil becoming more uniform during the course of the extraction and the bitumen in the extractor did not change as fast as at the lower extraction temperatures. Because the compositions of successive samples were quite similar, the extraction curves in Figure 4.2 became similar to that of a binary system i.e. the composition of the extracted material is constant and the curves were linear.

The composition of selected oil samples are presented in Table 4.4 shows the composition for the first, third and fifth samples obtained at a pressure of 10.5 MPa and temperatures of 92 and 37°C. For the samples at the higher temperature of 92°C, the weight percent for each component in the samples remains relatively constant. It was this composition behaviour that resulted in the almost linear extraction curve shown in Figure 4.2.

At the lower operating temperatures, the composition of the extracted oil changed significantly between Samples 1 and 5, evident in the reduction of the weight percent for PC1 by 50%. This occurred because at this temperature, more components are soluble and the solubilities are much higher. Therefore, more components are extracted at a faster rate than at higher temperatures. By the start of the last extraction window, the weight percent of the lighter pseudocomponents, especially PC1, within the extractor

Temperature, °C	92			37		
Sample	1	3	5	1	3	5
Composition, wt%						
PC1	49	47	43	29	23	14
PC2	40	43	45	34	35	33
PC3	9	10	11	19	23	28
PC4	2	1	1	9	11	15
PC5	0	0	0	9	8	10

Table 4.4 - Composition of windows 1, 3 and 5 extracted at 92 and 37°C and at a pressure of 10.5 MPa.

have been reduced significantly. Therefore, only the heavier components remained and those that were soluble were removed at this stage of the process. The solubility levels of these heavier components were lower (Moradinia et al., 1987) resulting in a reduced amount of oil extracted. Hence, the extraction curves begin to level off as there was less soluble bitumen remaining in the extractor.

There are two consequences of these experimental results from a process design point of view. Firstly, the selectivity of the solvent can be manipulated by changes in the temperature of the extraction. High initial operating temperatures would produce an oil that was relatively light and by gradually decreasing the temperature the extracted oil would become heavier. Secondly, not only was oil being extracted from the oil/sand mixture, the composition of the extracted oil changed in a definite way. Initially, the samples were much lighter and as the extraction proceeded, the samples became heavier. This result indicates that some fractionation of the bitumen occurred at the same time as bitumen was being extracted from the bitumen/sand mixture.

4.3.3 Visual Observations

Many of the results discussed in the previous two sections can be visually substantiated by viewing photographs of the extracted oil. Figure 4.4 to Figure 4.6 are photographs showing vials containing the oil recovered after performing extractions at 10.5 MPa and three temperatures, 93, 63 and 48°C. From these photographs, it is possible to visually observe the effect of temperature on the amount of oil that was recoverable and the compositional changes of the extracted oil both as a function of operating temperature and as a function of the amount of ethane which had contacted the bitumen.

In each of these figures, Samples 2-5 were collected at twenty minute intervals and were produced using approximately the same amount of solvent. The first sample was also collected twenty minutes into the extraction run but the volume of ethane that had actually contacted the bitumen was approximately a third of that used for the other four samples. The reason for this discrepancy was that at the beginning of a run, there was a section of the apparatus downstream of the extractor that contained pure ethane. This volume of solvent had to be displaced before the ethane containing bitumen reached the separators. Therefore, a portion of the first window was spent displacing the ethane used to pressure up the system.

Figures 4.4, 4.5 and 4.6 illustrate the effect temperature had on the relative amounts of oil that could be extracted using supercritical ethane. It was visually obvious that the yields at the higher temperatures were much lower than those at the lower temperatures. The collected samples also show that the amount of oil extracted undergoes a greater change during the course of an extraction at lower temperatures. This clearly supports the results presented in Figure 4.2.

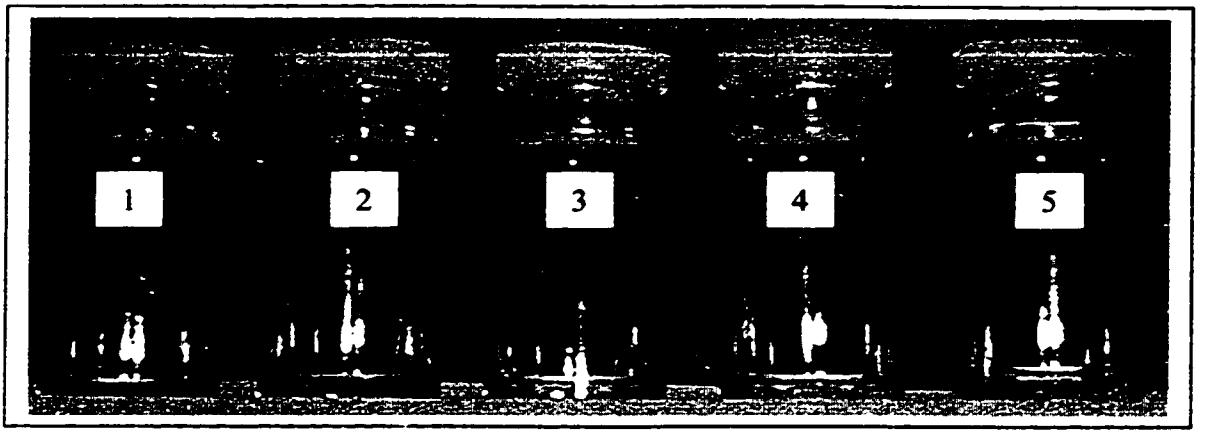

Figure 4.4 – Photograph of the samples extracted at 92°C and 10.5 MPa.

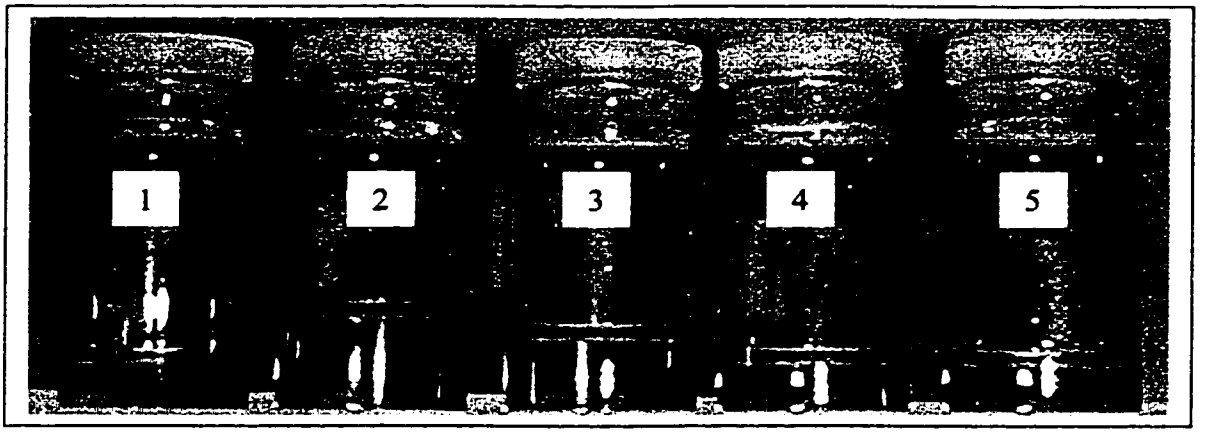

Figure 4.5 – Photograph of the samples extracted at 63°C and 10.5 MPa.

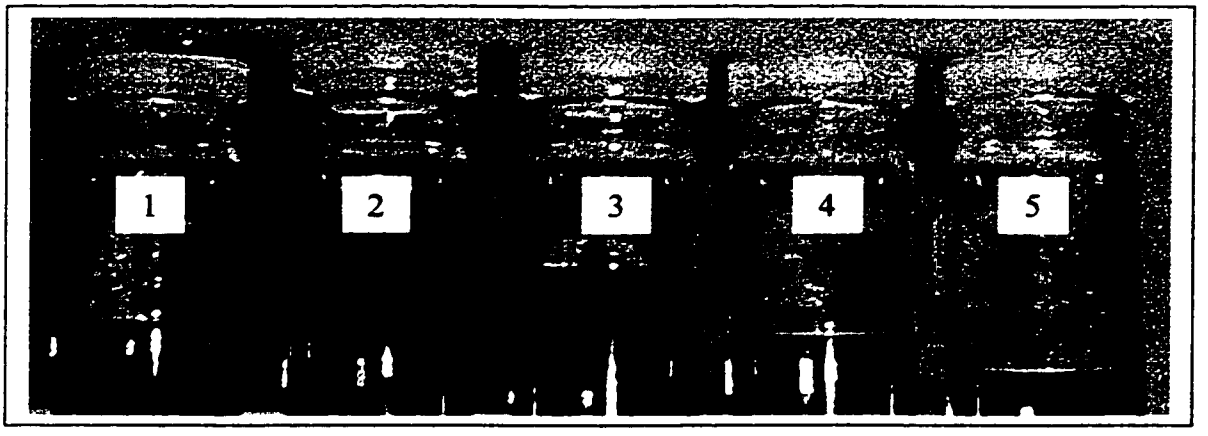

Figure 4.6 – Photograph of the samples extracted at 48°C and 10.5 MPa.

Compositional changes can be seen in Figure 4.4, 4.5 and 4.6. For instance, in Figure 4.4, the samples are all the same shade of light yellow which indicated that the oil had a similar composition. As the temperature was decreased, the colour of the samples became darker and the colour difference between successive samples visibly increased. The greatest difference is shown in Figure 4.6, with the first and last samples being the most dissimilar. These results were verified by the boiling point curves presented in Section 4.3.2 which showed that the composition of the extracted bitumen had a larger boiling point range.

It was interesting to note that for all temperatures the first sample was the lightest with respect to the boiling point curve but based upon its darker colour seemed to be the heaviest. This can be explained by examining what happens to the light solvent phase as it moves through the extractor. At the beginning of a run, all of the soluble hydrocarbons are present simply because nothing has been extracted. As the solvent passes through the extractor, it solubilises some of the lighter material, changing the properties of the solvent phase. The lighter dissolved material enhanced the solvent much like the addition of an entrainer (Lu et al., 1990). The presence of the light extract in the solvent phase allows more of the heavier material to become soluble. As the extraction proceeds, there is less of the lighter material in the extractor and as a result the solvent dissolves less which in turn results in less of the very heavy material becoming soluble. The net result is that the samples become lighter in colour but have higher boiling point curves and greater average boiling points.

There was a possibility that the darker colour of the first samples was due to entrainment of bitumen from the extractor. The solvent rich phase could have been carrying over bitumen from the upper section of the extractor and depositing it into the two phase separator. In an attempt to remove the likelihood of this occurring, clean sand followed by glass wool were used in the top of the extractor as demisters.

4.3.4 SARA Analysis

SARA analysis is used by the petroleum industry to characterise hydrocarbon mixtures based upon the weight percent of four following compound types: saturates, aromatics, resins and asphaltenes (Speight, 1991). First, pentane is added to precipitate the asphaltene fraction and the process is sped up by refrigerating the sample for approximately four hours and a centrifuge is used to collect the asphaltenes. A silica gel activated column is used to separate the remaining fractions by diluting the sample with hexane and pouring it into the column. Three solvents, hexane, methanol and a 50/50 mixture of methylene chloride/methanol, are used to recover the remaining fractions. The saturates, aromatics and eluted resins fraction weights are summed and the difference between this value and the initial weight fed to the column is used to find the weight of non-eluted resins. The results are reported as weight percent saturate, aromatic, total resin and asphaltene.

SARA analysis was performed on selected samples of extracted oil to measure the composition of the oil extracted from Peace River bitumen. Figure 4.7 shows the weight percents for these fractions in the first and fourth samples obtained at 10.5 MPa and temperatures of 47 and 63°C.

Asphaltenes were not detected in any of the samples analysed. This result was expected due to the fact that asphaltenes are the components the least soluble in the solvent and have the lowest vapour pressures. Light hydrocarbon solvents such as propane and butane are used in asphaltene precipitation processes such as propane deasphalting and the ROSE process (see Section 2.4). Therefore it was expected that ethane being lighter,

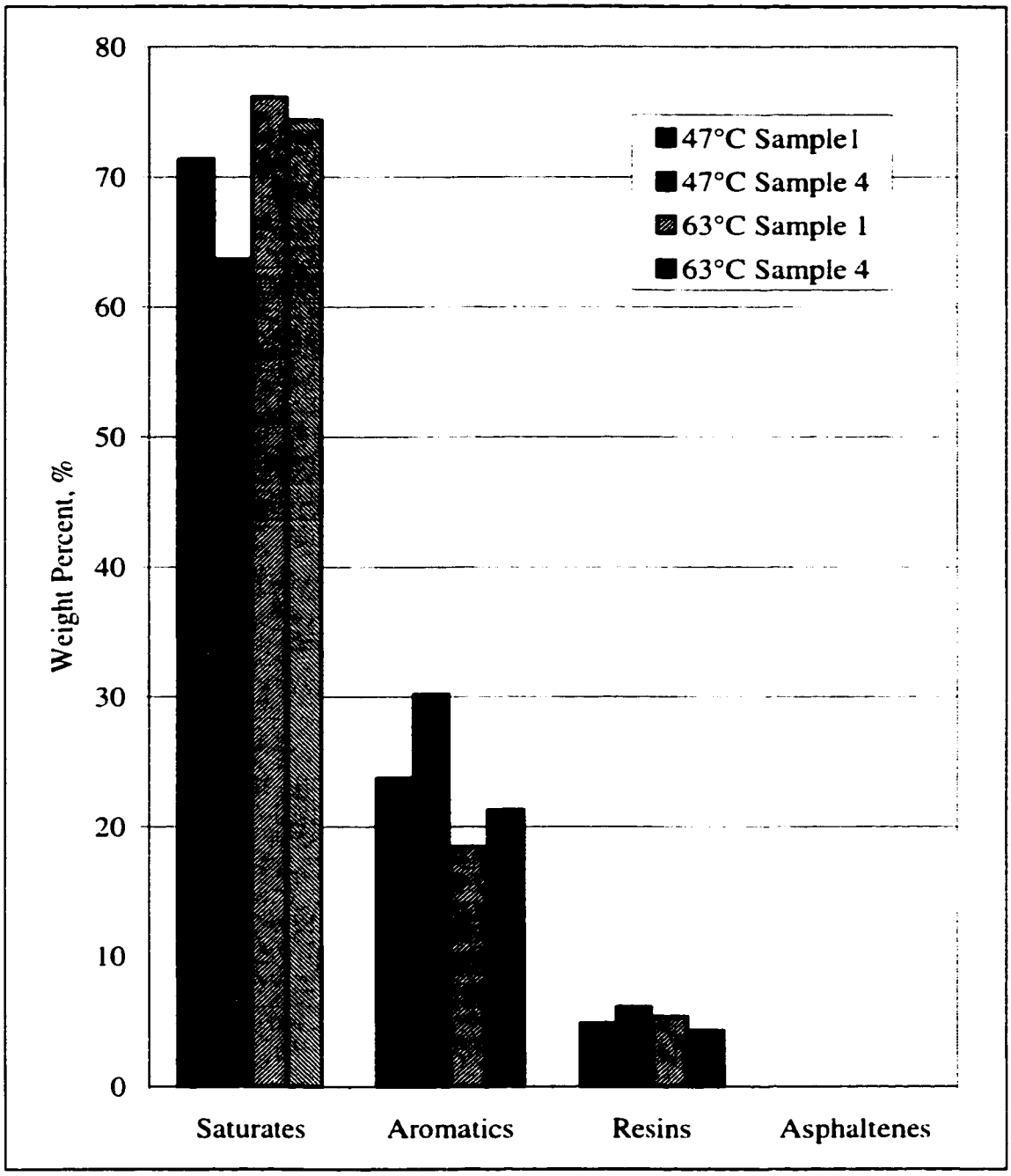

Figure 4.7 – SARA analysis for the first and fourth samples taken for extractions at a pressure of 10.5 MPa and temperatures of 47 and 63°C.

would extract oil that was free of asphaltenes and this was verified by the results presented in Figure 4.7. The samples contained mainly saturates and aromatics with approximately 5 wt% resins. The property of the supercritical ethane to preferentially extract the saturate fraction varied with changes in the extraction temperature. Selectivity values for the saturate, aromatic and resin fractions were calculated using Equation 4.1 (Treybal, 1980).

$$\text{Selectivity} = \frac{\left(\dfrac{\text{wt fraction X in Extract}}{\text{1 - wt fraction X in Extract}}\right)}{\left(\dfrac{\text{wt fraction X in Raffinate}}{\text{1 – wt fraction X in Raffinate}}\right)} \qquad \text{Equation 4.1}$$

In Equation 4.1, X is either saturate, aromatic, resin or asphaltene and extract refers to the oil that has been removed and raffinate refers to the bitumen remaining in the extractor. Selectivities for each of the fractions were calculated and are presented in Table 4.5. Note that the asphaltene fraction was not included because no asphaltenes were present in any of the fractions.

	Selectivity		
	Saturates	Aromatics	Resins
47°C, Sample 1	7.58	0.40	0.28
47°C, Sample 4	11.57	0.41	0.27
63°C, Sample 1	9.60	0.29	0.31
63°C, Sample 4	13.91	0.28	0.25

Table 4.5 – Selectivity of ethane for extracting saturates, aromatics and resins at 10.5 MPa and temperatures of 47°C and 63°C.

The results in Table 4.5 show that supercritical ethane was more selective towards the saturate fraction than either the resin or aromatic fractions. This was plausible as saturates are more "like" ethane and thus more soluble. These results are also consistent with available pure component data which shows that n-paraffins have higher solubilities in supercritical fluids such as ethane as compared to other classes of hydrocarbons such as aromatics (Schmitt et al., 1985; Moradinia et al., 1987).

While temperature had a significant effect on both the amount of oil extracted and the boiling points of the extracted oil, it had a much smaller effect on the results of the SARA analysis. From Figure 4.7, it can be perceived that the SARA analysis for the samples at the two temperatures are relatively constant with only marginal changes in the data. The largest difference was between the fourth samples where the aromatic content was approximately 9.5 wt% higher and the saturate fraction was 9.5 wt % lower for the 47°C sample compared to the same sample at 63°C.

There was also very little variance in the SARA data of the samples taken at different times during the extraction process. At 63°C, Samples 1 and 4 had essentially the same composition, there being a change of less than 5 wt% in the amounts of saturates and aromatics between the first and fourth samples. At 47°C, the resin content was relatively constant while the saturates decreased by 7.5 wt% with the aromatics increasing by the same amount. This can be attributed to the fact that at the lower temperature, the solubilities of the components are higher and the saturate fraction was preferentially extracted. Hence by the time the fourth sample was taken there was significantly less of the saturate fraction in the extractor. As a result the relative amount of aromatics increased and the amount of saturates decreased.

4.3.5 Viscosity

Tests were performed on selected samples to observe how the viscosity of the extracted oil varied with temperature. The results from these tests are presented in Figure 4.8 which show the viscosity of samples extracted at 10.5 MPa and temperatures of 47, 63 and 78°C. The viscosity was found to increase as the extraction temperature decreased. Figure 4.8 shows that the viscosity of the extracted oil also increased as the extraction proceeded, with the samples obtained later in the extraction process having the higher viscosities.

Figure 4.8 also shows that as the temperature decreased, the viscosity of the extracted samples increased. After examining the distillation curves for the extracted samples presented in Section 4.3.2 this result was expected. The distillation curves indicated that as the extraction temperature decreased, the extracted oil became heavier. According to the AOSTRA Technical Handbook on Oil Sands, Bitumens and Heavy Oils, as hydrocarbon mixtures become heavier, their viscosity increases (Hepler et al., 1989). The results shown in Figure 4.8 support these observations.

The viscosity data provided an indication of the magnitude of viscosity change during the extraction process. As the temperature increased, changes in the viscosity of the oil samples were smaller. This result was a direct reflection of the compositional changes. As the extraction temperature increased, the composition of the oil extracted during an experiment became more uniform. Therefore, the viscosity of these samples would also be similar. Figure 4.8 shows that this was in fact the case.

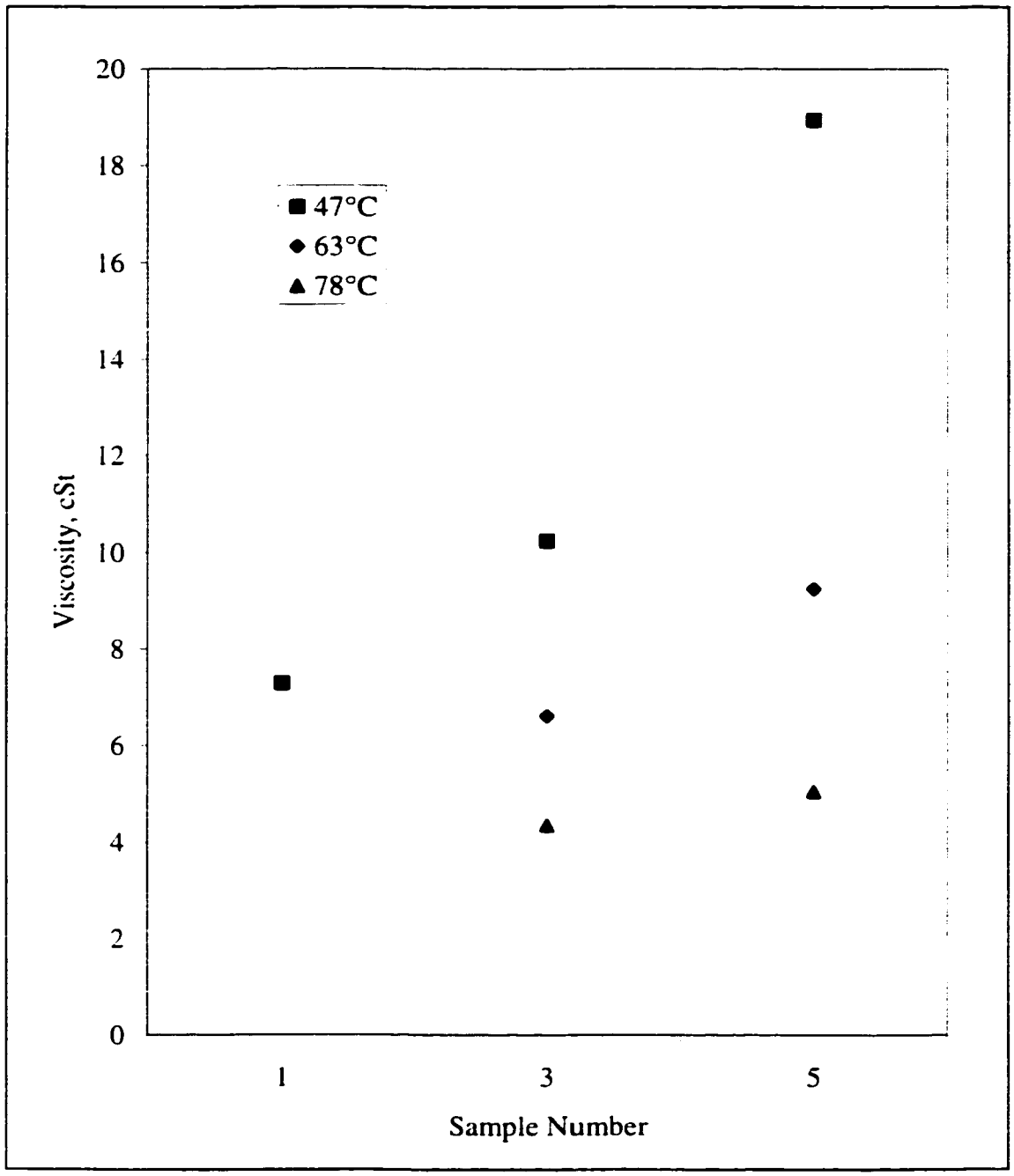

Figure 4.8 – Viscosities of selected oil samples taken at temperatures of 47, 63 and 78°C and a constant pressure of 10.5 MPa.

4.4 Effect of Pressure

The next series of experiments were performed to examine the effects of varying pressure on the behaviour of the extraction process. As discussed earlier in Chapter 2, small changes in pressure can cause significant changes in the properties of fluids near their critical points. The effect of pressure on the solubility of a wide variety of pure components in supercritical fluids has been well documented (Johnston et al., 1982; Peters et al., 1989; Schmitt et al., 1985; Moradinia et al., 1987). However, data for the solubility of complex mixtures such as bitumens is much more limited (Deo et al., 1992; Hwang et al., 1995; Subramanian et al., 1998).

The impact of pressure changes on the extraction of Peace River bitumen using supercritical ethane was examined by conducting a number of extractions at a constant temperature of 47°C and at four pressures ranging from 7.3 to 15.0 MPa. The pressures studied along with the corresponding actual and reduced densities are presented in Table 4.6.

Pressure, MPa	Reduced Pressure	Density, kg/m^3	Reduced Density
7.3	1.50	263.68	1.30
10.5	2.15	331.53	1.64
12.2	2.50	348.42	1.72
15.0	3.08	366.50	1.81

Table 4.6 – Experimental pressures and corresponding densities at a constant temperature of 47°C.

As the pressure was increased, the density of the supercritical ethane increased as expected (see Section 2.1). Although the pressure was increased stepwise by approximately 3 MPa, the density did not increase in proportional increments. Instead,

the changes in density became smaller especially for pressures significantly greater than the critical pressure for ethane. As shown in Figure 2.2, the density of ethane begins to approach a maximum at pressures much greater than the critical pressure. The range of pressures studied in this work would provide data indicating how the yields of extracted bitumen would be affected by changes in pressures where the density begins to approach a maximum.

The maximum pressure at which the experiments were conducted was limited by the pressure ratings for the experimental apparatus. At a temperature of 47°C, the safest maximum pressure that the experiments could be conducted at was 15.0 MPa. This pressure would provide a good indication of the ability of supercritical ethane at high pressures while at the same time providing a large enough margin so that the experiments could be conducted safely.

4.4.1 Yield Variation

The effect of pressure on the amount of bitumen dissolved in supercritical ethane at a constant temperature of 47°C is shown in Figure 4.9. In this figure, cumulative weight percent of bitumen extracted was plotted as a function of cumulative standard litres of ethane exiting the extractor as measured by the wet test meter downstream of the separator. Figure 4.9 clearly shows that as pressure was increased, the amount of bitumen that was extracted also increased. However, the increase in yield for successive pressures diminished as the pressure was increased.

The increase in the amount of oil extracted was expected based on the results of the numerous binary systems that have been discussed in literature. The data provided by Morandinia et al., Schmitt et al., and Johnston et al., all showed that for a given temperature, the solubility of heavy hydrocarbons in supercritical fluids increased as the

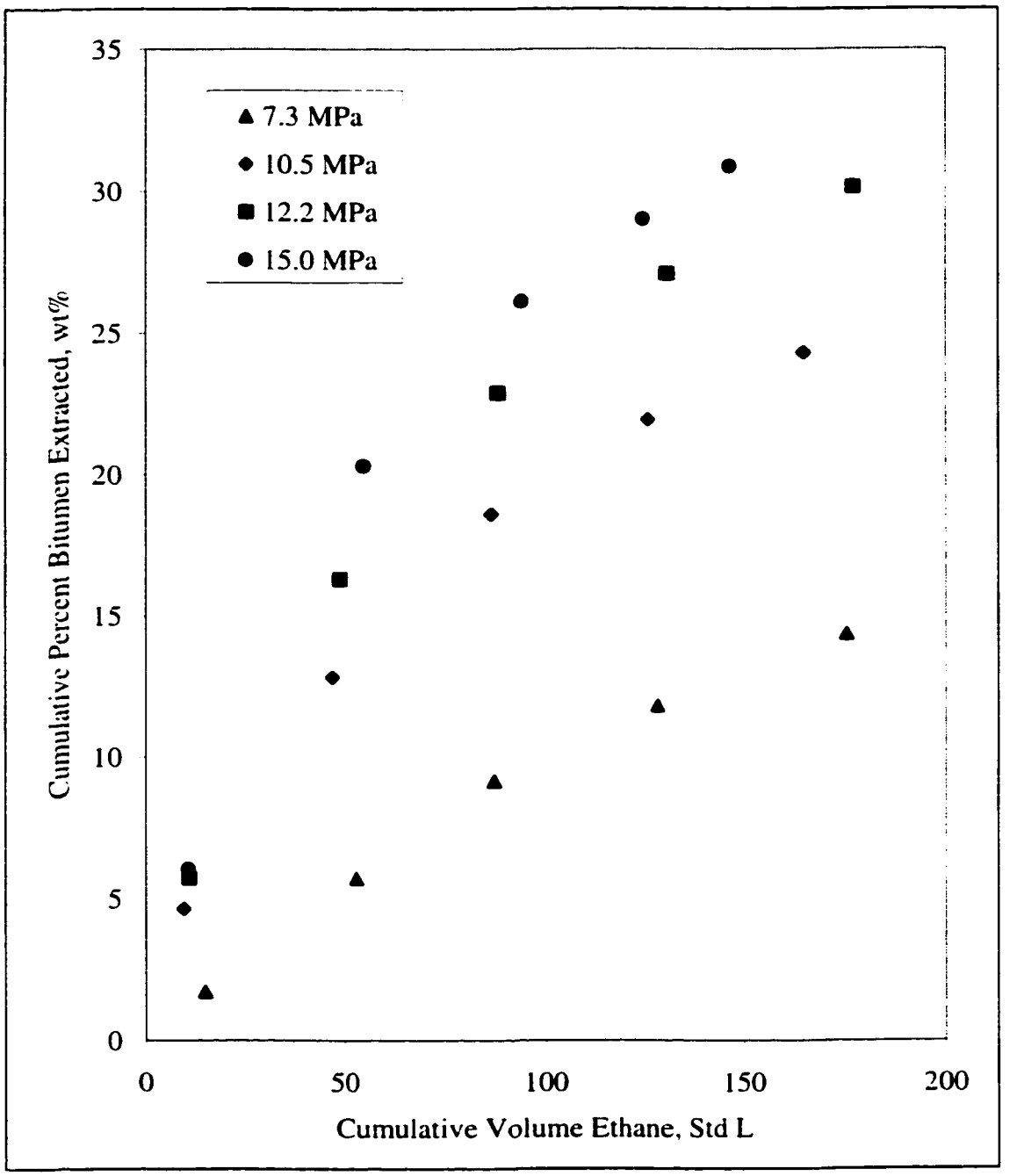

Figure 4.9 – Cumulative weight percent of bitumen extracted as a function of the cumulative volume of ethane measured at a constant temperature of 47°C and pressures ranging from 7.3 to 15.0 MPa.

experimental pressure increased (Moradinia et al., 1987; Schmitt et al., 1985; Johnston et al., 1982). This was also the trend that was observed for the solubility of Peace River bitumen in supercritical ethane as shown in Figure 4.9.

The increase in soluble bitumen can be explained by examining the behaviour of the density of supercritical ethane over the range of pressures studied. One of the characteristics of supercritical fluids is the dramatic change in their properties that results from small changes in temperature and pressure near the critical point. In this case, when the pressure was increased by 7.7 MPa, the density of ethane increased by 40%. The increase in pressure was large enough so that the density of the supercritical ethane became more liquid-like. The solvent power of ethane increased due to the increased attractive forces between the solute and solvent that result from higher solvent densities (Johnston et al., 1982). In other words, with stronger attractive forces, the solvent was capable of holding more of the solute and thus the solubility increased.

The large increase in density caused by the increase in operating pressure resulted in greater amounts of the bitumen being extracted. For example, at 7.3 MPa, approximately 5 wt% of the bitumen was extracted after contacting the bitumen with 50 Std L of ethane. When the pressure was increased to 15.0 MPa, the amount of bitumen recovered using the same amount of ethane increased to 20 wt% or approximately four times.

Figure 4.9 can also be used to provided an indication of the rate at which the oil was produced as a function of pressure. The units for the abscissa can be converted to time by dividing by the solvent flow rate while preserving the shape of the extraction curves. If this was done, then the slope of the extraction curves would become weight percent extracted per unit time. The result of this analysis is that the extractions performed at higher pressures had greater rates of oil produced, especially at the beginning of the experiment. Therefore, Figure 4.9 revealed that more oil was extracted with less solvent and it was also extracted at a faster rate. The curves begin to level off later in the

extraction due to the fact that the bitumen feed was packed batch-wise and as time proceeded, there was a reduced amount of soluble bitumen remaining in the extractor.

4.4.2 Composition Variation

The composition of the extracted fluids was measured to determine how pressure affected the composition of the oil extracted. The same method used to determine changes in the composition of the extracted oil caused by temperature was employed here. Changes in the composition were reflected in the boiling point curves measured using the ASTM D2887 method (ASTM, 1999). The higher the temperatures in the boiling point curves, the heavier the sample. Two trends were found when examining the compositional data. The first was that varying the pressure changed the composition of the oil extracted when the same volume of solvent was used. Secondly, the amount of the composition change of successive samples that occurred during the course of an extraction depended upon the there was a greater number of heavier hydrocarbons extracted at the higher pressure. Both Schmitt et al. and Moradinia et al. found that as the pressure was reduced the experimental pressure.

The first trend can be examined using the data presented in Figure 4.10 which is a plot of the boiling point curves for samples obtained performing experiments at a constant temperature of 47°C and pressures of 7.3 and 15.0 MPa. Figure 4.10 shows the boiling point curves for the first, third and fifth samples, that were produced using the same volume of ethane. The oil extracted at 15.0 MPa had boiling point curves that were all greater than those for the samples obtained at 7.3 MPa. This indicated that as the pressure increased, the recovered oil became heavier. This was consistent with binary data published by Moradinia et al. (Moradinia et al., 1987). They showed that as the

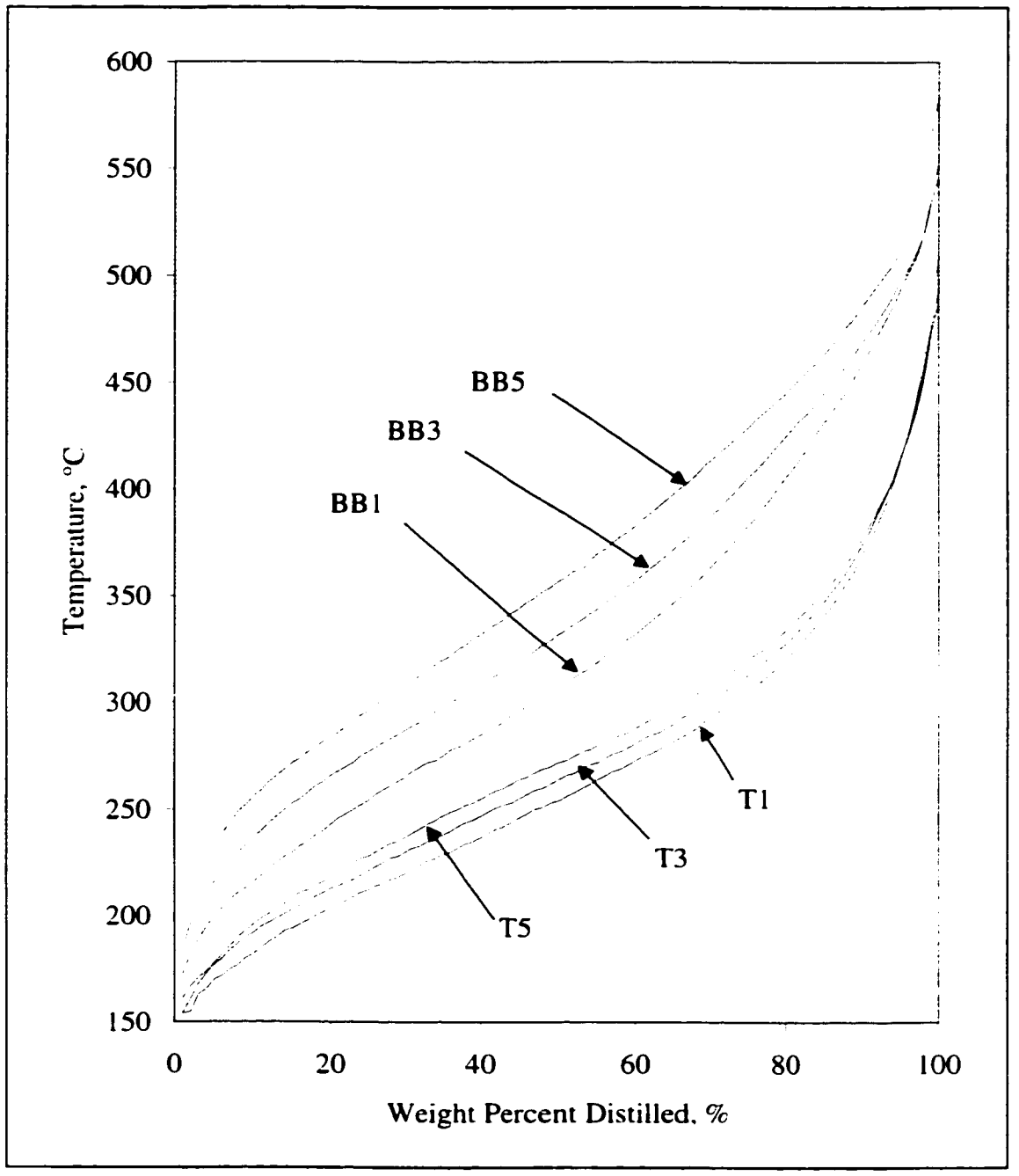

Figure 4.10 – Boiling point curves for extracted samples produced at 47°C and pressures of 15.0 MPa (BB) and 7.3 MPa (T).

pressure increased, the solubility of n-paraffins such as n-C_{28} increased for a given constant temperature. Data provided by Schmitt et al. shows a similar trend existed for aromatic compounds (Schmitt et al., 1985).

The boiling point curves shown in Figure 4.10 all have the same initial boiling points but the final boiling points differ depending on the pressure at which the experiment was performed. The oil extracted at 15.0 MPa had higher end points than that produced at 7.3 MPa. The difference between the end points for the boiling point curves indicated that there was a greater number of heavier hydrocarbons extracted at the higher pressure. Both Schmitt et al. and Moradinia et al. found that as the pressure was reduced the solubilities for pure hydrocarbons decreased and approached zero for the heavier molecular weight components. As the pressure was lowered in this system, fewer compounds were soluble in supercritical ethane and their solubility was lower. This meant that the amount of oil extracted would be less and would be composed of lighter and fewer constituents. Therefore, the boiling point curves for oil produced at lower pressures would be lower and have a narrower temperature span between the initial and final boiling points. This was the case for the data presented in Figure 4.10.

During the course of the extractions, the composition of consecutive oil samples was not constant but became heavier as the extraction proceeded. Again, the magnitude of these changes was related to the pressure at which the extraction was performed. These variations in composition were evident from the boiling point curves used to determine the weight fractions of the pseudocomponents for the samples. The changes in the composition were also reflected by the change in shape of the extraction curves. Samples produced when the experimental pressure was lower had more uniform compositions and this was reflected in a straighter extraction curve.

In Figure 4.10, at 15.0 MPa, the boiling point curves are much further apart than those for 7.3 MPa which indicated a greater compositional difference. The difference between the

curves showed that the composition of the samples produced at 7.3 MPa did not change as much as those produced at 15.0 MPa. This observation was also supported by the changes in the weight percent of the pseudocomponents listed in Table 4.7.

The compositions for samples 1,3 and 5 are presented in Table 4.7 for the oil extracted at a temperature of 47°C and pressures of 7.3 and 15.0 MPa. From the data in this table, it was obvious that the composition of the oil at 7.3 MPa did not change nearly as much as the oil extracted at 15.0 MPa. For example, PC1 decreased by 23% between samples 1 and 5 at 7.3 MPa while it decreased by more than 66% at 15.0 MPa.

Pressure, MPa	10.5			15.0		
Sample No.	1	3	5	1	3	5
Composition, wt%						
PC1	36	27	16	21	12	7
PC2	35	38	38	38	37	32
PC3	18	21	28	23	28	31
PC4	7	9	12	12	16	20
PC5	4	5	6	6	7	10

Table 4.7 – Composition of selected samples obtained at 47°C and pressures of 10.5 and 15.0 MPa.

The composition of the oil changed more at the higher pressure for two reasons: increased solubility at higher pressures and the batch nature of the experiments. The higher solubilities at higher pressures result in the depletion of the soluble components quicker than at lower pressures. According to Schmitt et al. and Morandina et al., the lighter constituents have higher solubilities and in general, the solubilities decrease as the molecular weights of the hydrocarbons increase. Therefore, during the extraction the lighter fractions were extracted early in the extraction. Due to the batch nature of the

experiments, these components could not be replaced, consequently as the extraction proceeded the remaining soluble fractions became heavier. This caused the extracted oil to become heavier over the duration of the extraction. Conversely, at lower pressure, the soluble components were lighter and the solubilities of these components were lower. The lower solubilities meant that it simply took longer to extract the oil at the lower pressure and also that the composition of the extracted oil was more uniform. As with temperature, the uniformity of the extracted oil composition was reflected in the increased linearity in the extraction curves shown in Figure 4.9.

The results of the composition analysis show the benefits of this method of extracting oil from bitumen using supercritical fluids. As the pressure was increased, the oil extracted became increasingly heavier. Hence, by manipulating pressure the characteristics of the oil extracted can be controlled. A low initial operating pressure would produce oil that was relatively light and by gradually increasing the pressure, the product could be made heavier. In addition, over the duration of the extraction the composition of the extract changed in a specific order. Initially, the samples were much lighter and as the extraction proceeded, the samples became heavier. Therefore, the composition of the extracted oil can be separated by monitoring the amount of solvent which had contacted the bitumen.

4.4.3 Visual Observations

Figure 4.11, 4.12 and 4.13 are photographs of the samples extracted at temperatures of 47°C and pressures of 7.3, 10.5 and 15.0 MPa respectively. In these figures, the numbers on the vials indicate the order in which the samples were obtained. Each sample was produced during a time interval of approximately 20 minutes. These figures provide a visual summary of the variation in the characteristics of the extractions as a function of the operating pressure.

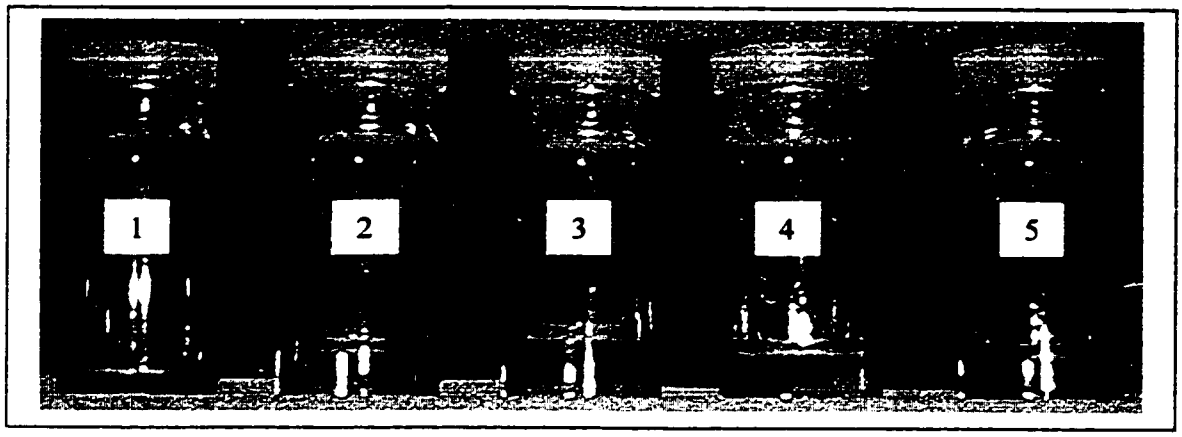

Figure 4.11 – Photograph of the samples extracted at 47°C and 7.3 MPa.

Figure 4.12 – Photograph of the samples extracted at 47°C and 10.5 MPa.

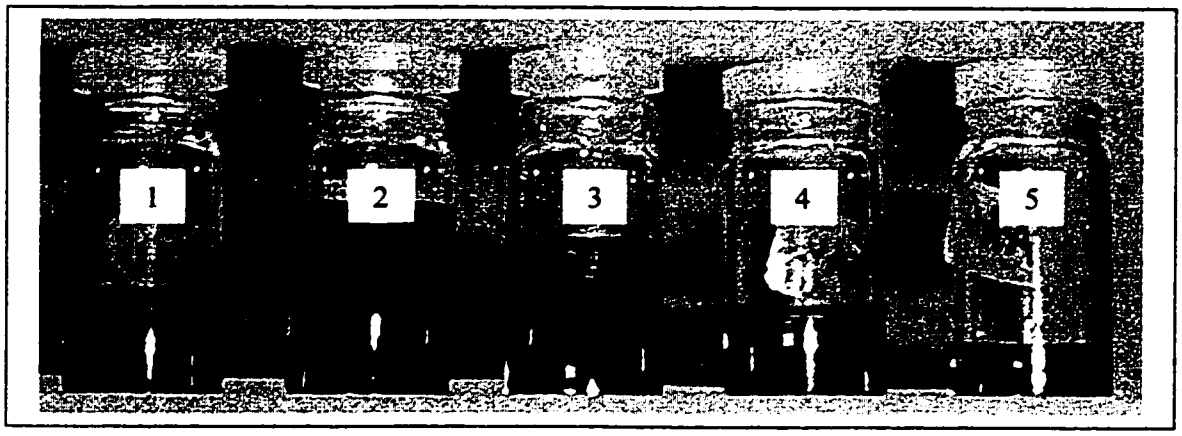

Figure 4.13 – Photograph of the samples extracted at 47°C and 15.0 MPa.

It is visually apparent that at lower operating pressures, less oil was extracted and as pressure increased so did the amount of oil extracted. One can also observe the reduced effect that changes in pressure had on the extracted material at pressures much greater than the critical pressure. The samples shown in Figure 4.12 and Figure 4.13 are quite similar in colour and amount even though the pressure differed by 5.0 MPa. This is especially evident when comparing the samples in Figure 4.11 with those in Figure 4.12. The samples in Figure 4.12 were extracted at a pressure 3.2 MPa higher than those in Figure 4.11. The smaller pressure difference between the lower operating pressures resulted in samples that are very different in both colour and volume.

A visual indication of composition of the samples was the colour of each sample and the differences in the colour of successive samples. For the samples extracted at 7.3 MPa , Figure 4.11, the colour remained relatively constant indicating that the composition did not change significantly. This is also supported by the boiling point curves for Samples 1, 3, and 5 which were presented earlier in Figure 4.10. The samples presented in Figure 4.13 vary considerably in colour and thus composition which was also verified by the boiling point curves of Figure 4.10.

As with the samples obtained at low temperatures, the higher pressures produced samples that were initially dark and became progressively lighter as the extraction proceeded. This would suggest that the heavier samples were extracted earlier which is counter to what the boiling point curves showed. The logic used to explain this behaviour for temperature changes was discussed earlier in Section 4.3.3 and will not be repeated here.

4.4.4 SARA Analysis

The results obtained from performing SARA analysis on selected samples of material extracted at 47°C and pressures of 10.5 and 15.0 MPa are presented in Figure 4.14. Samples 1 and 4 for each pressure were analysed using the standard method for SARA analysis (Speight, 1991). The samples were predominantly saturates and aromatics with small amounts of resins and no asphaltenes.

No asphaltenes were found in any of the samples analysed, even in the samples produced at pressures that were more than three times the critical pressure of pure ethane. This indicated that the asphaltenes remained in the extractor during the extraction process. In addition, there were very small levels of resins detected in the samples analysed, typically approximately 5 wt%. This result was due to the fact that both asphaltenes and resins are large, highly aromatic and polar molecules making them structurally different from the ethane.

Figure 4.14 shows that the extracted oil was composed mainly of saturates and aromatics. Early in the extractions, saturates were at their highest levels, however, as the extractions proceeded, the relative amount of saturates decreased and the difference was compensated with an increase in aromatics. The percentage of resins remained relatively constant for all samples regardless of pressure or amount of ethane that had contacted the bitumen feed. Note that the lower pressure of 10.5 MPa produced a greater weight percent of saturates for both samples analysed as compared to the samples produced at 15.0 MPa.

The selectivity of the supercritical ethane changed as the extraction pressure changed. Selectivity values for each of the three fractions were calculated using Equation 4.1 and the results are shown in Table 4.8.

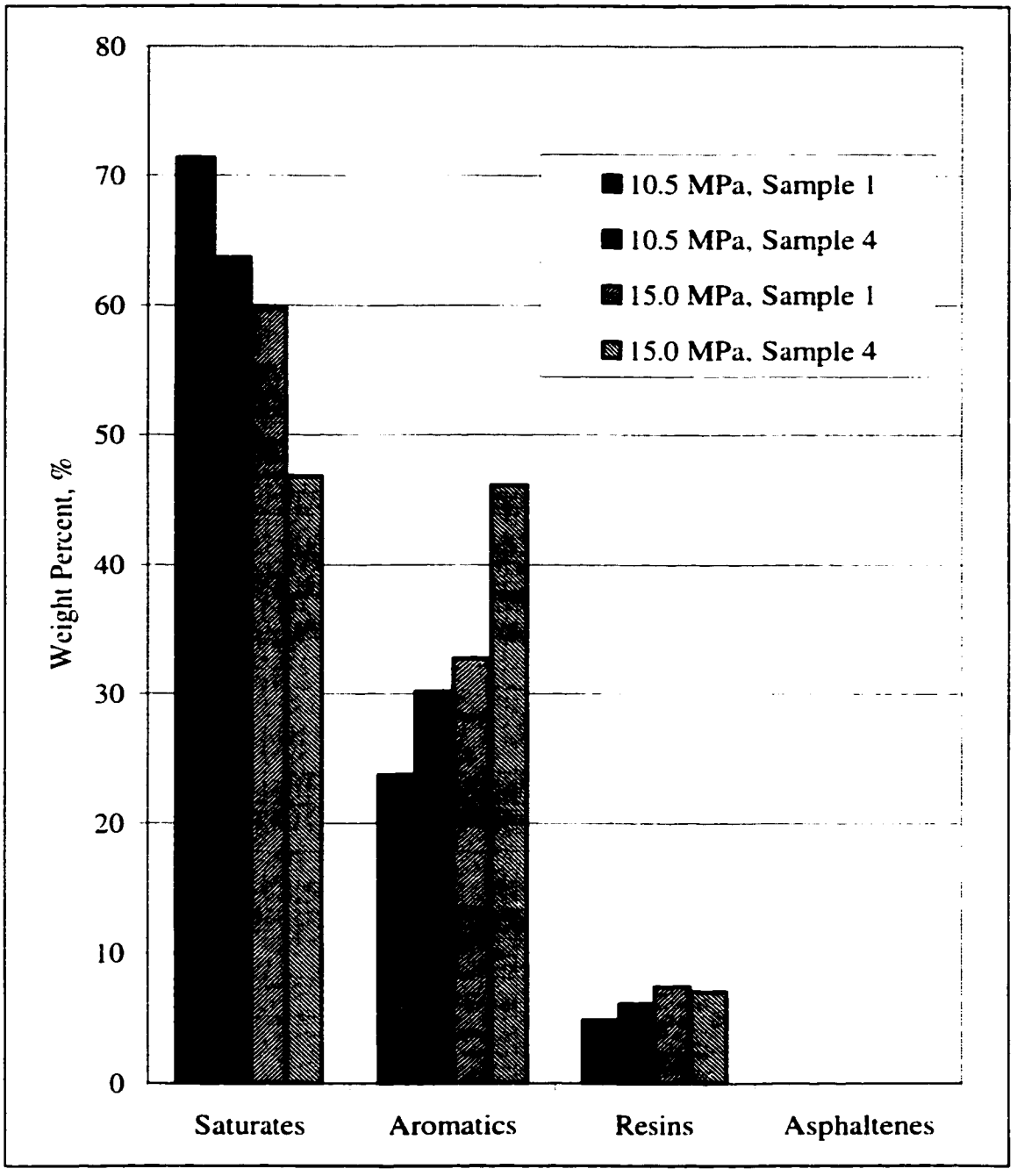

Figure 4.14 – SARA analysis of the samples produced at pressures of 10.5 and 15.0 MPa and a temperature of 47°C.

	Selectivity		
	Saturates	Aromatics	Resins
10.5 MPa, Sample 1	7.6	0.4	0.3
10.5 MPa, Sample 4	11.4	0.4	0.3
15.0 MPa, Sample 1	4.5	0.6	0.4
15.0 MPa, Sample 4	5.9	0.8	0.4

Table 4.8 – Selectivity of ethane for extracting saturates, aromatics and resins at 47°C and pressures of 10.5 and 15.0 MPa.

The results in Table 4.8 show that supercritical ethane was more selective towards the saturate fraction than either the resin or aromatic fractions. These results are consistent with the available pure component data available which show that n-paraffins have higher solubilities in supercritical fluids such as ethane as compared to other classes of hydrocarbons such as aromatics (Schmitt et al., 1985; Moradinia et al., 1987).

4.4.5 Viscosity

Tests were performed on selected samples to determine the effects of pressure on the viscosity of the extracted oil. In Figure 4.15, the viscosity of samples extracted at 47°C and pressures of 10.5 and 15.0 MPa are shown. The viscosity was found to increase with increases in the extraction pressure. Figure 4.15 shows that the viscosity of the extracted oil also increased as the extraction proceeded, with the samples obtained later in the extraction process having the higher viscosities.

The increase in viscosity with increases in pressure was expected after examining the composition of the extracted samples presented in Table 4.7. The composition indicated that as the extraction pressure increased, the extracted oil became heavier. As discussed

earlier in Section 4.3.5, the AOSTRA Technical Handbook on Oil Sands, Bitumens and Heavy Oils states that as hydrocarbon mixtures become heavier, their viscosity increases (Hepler, 1989). The results shown in Figure 4.15 support these observations. Increased pressure resulted in extracted oil that was heavier and this corresponded to samples with higher viscosities.

The viscosity analysis gave an indication of the magnitude that the viscosities changed during the course of the extraction process. As the pressure increased, the viscosity of the oil samples produced during the extraction changed more dramatically. The samples produced at 15.0 MPa were approximately three times more viscous than the samples collected at 10.5 MPa. This result was a direct reflection of the compositional changes. As the extraction pressure increased, the extracted oil became significantly heavier. The increase in the amount of heavier constituents in the extracted oil caused the viscosity to become greater.

4.5 Density Effects

In the previous two sections, changes in the amount and composition of extracted oil due to temperature and pressure were presented. Differences in the yields and composition were attributed to the changes in density of the solvent caused by pressure and temperature changes. Increases in temperature caused the density of the solvent to decrease which resulted in a decrease in the solubility of the bitumen. Decreases in pressure caused the solvent density to decrease which in turn produced lower bitumen recoveries.

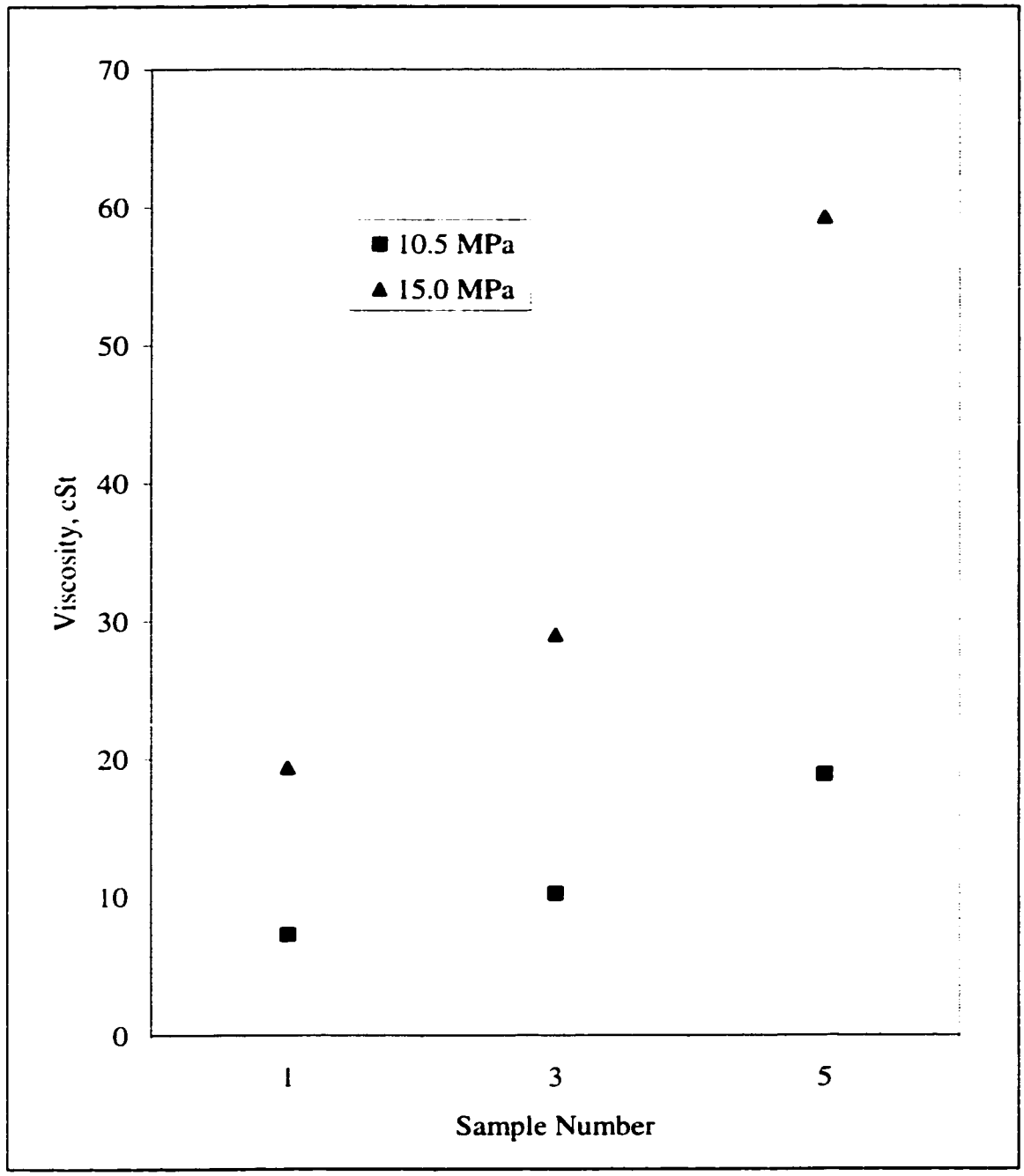

Figure 4.15 – Viscosities of selected extracted samples obtained at pressures of 10.5 and 15.0 MPa and a temperature of 47°C.

The remaining question is whether the amount and composition of the extracted oil changed solely due to density changes or did the temperature and pressure cause other changes to the system besides solvent density. Deo et al. reported that temperature had additional effects on the yields produced for bitumen-supercritical solvent systems. (Deo et al., 1992). They reported that supercritical propane exhibited enhanced solvent properties when extractions were conducted at temperatures near the critical temperature of propane. They concluded that the increased solubilities of bitumen could be attributed to the proximity of the operating temperature to the critical temperature as well as solvent density. This was counter to the conclusions drawn by Subramanian et al. who found that for bitumen/supercritical propane systems, the extractions were dominated chiefly by the pure solvent density (Subramanian et al., 1998).

The data from this work has been presented in terms of reduced density to see which of the previous conclusions pertained to the Peace River bitumen/supercritical ethane system. The results are presented in Figure 4.16 where the extraction curves have been plotted as function of the reduced solvent densities. The extraction yields increased with increases in density for all cases. This demonstrated that the extraction yields were a strong function of the pure solvent density and that there was no enhanced solvent properties when the extractions were performed near the critical temperature as observed by Deo et al. Therefore, based upon the results from this work and Subramanian et al., it can be concluded that the extraction of bitumen was governed chiefly by the density of the pure supercritical solvent.

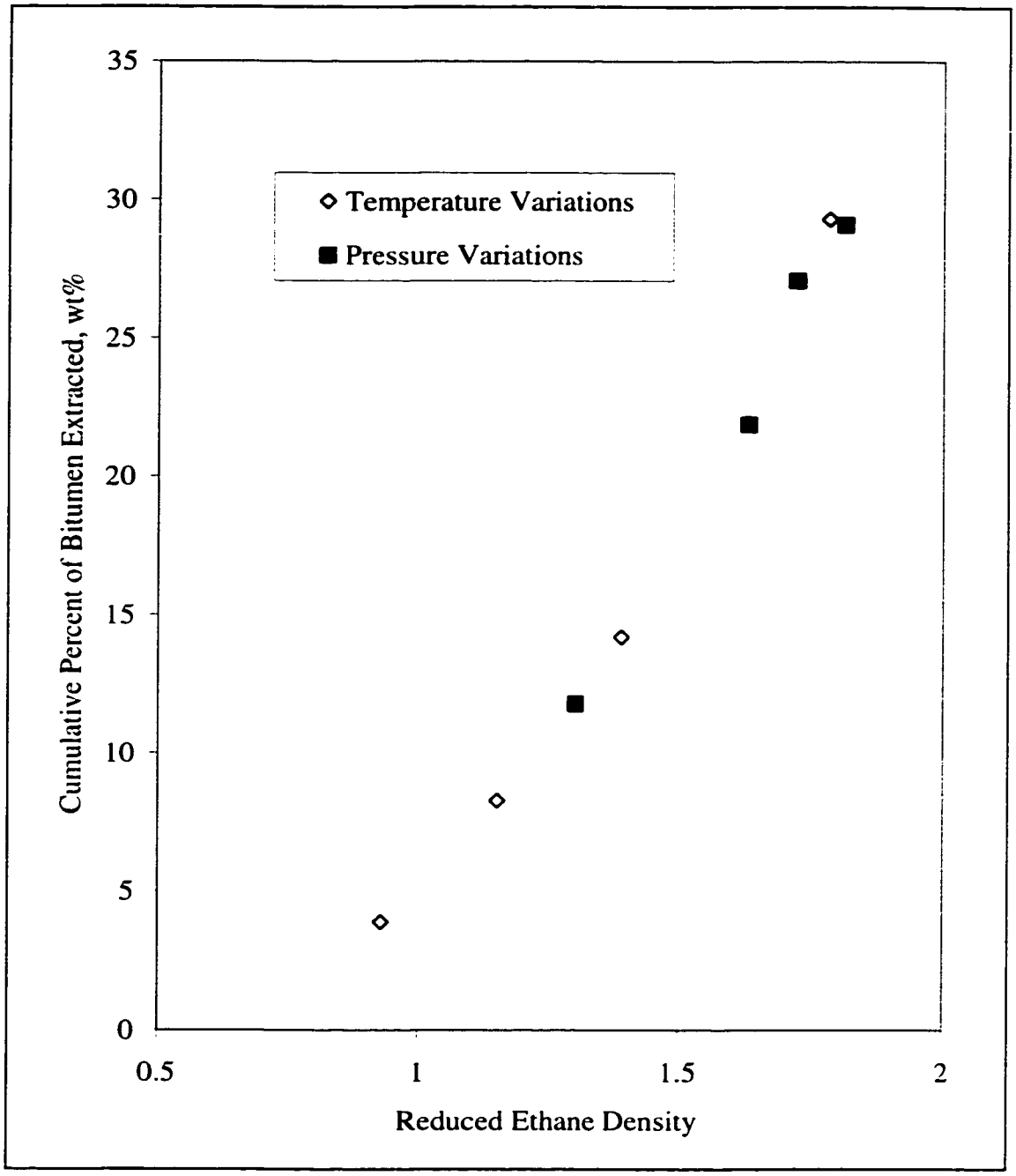

Figure 4.16 – Cumulative yield for 130 Std L solvent versus solvent reduced density.

4.6 Comparison with Carbon Dioxide

Carbon dioxide is a common fluid used in enhanced oil recovery methods (Donaldson et al., 1989) and is a popular solvent for commercial supercritical fluid extraction processes (McHugh et al., 1994). Advantages of using carbon dioxide include the low solvent cost, non-toxic, low critical temperature and readily availability (Taylor, 1996; Donaldson et al. 1989). The historical benefits of using supercritical carbon dioxide suggest that it may be an excellent choice as a solvent for the extraction of oil from bitumen. Experiments were conducted to compare the capabilities of supercritical ethane and carbon dioxide as solvents for the extraction of oil from bitumen.

Oil was extracted from Peace River bitumen using supercritical carbon dioxide over a range of temperatures and pressures. The operating conditions for the experiments were chosen in order to make meaningful comparisons between the performance of ethane and carbon dioxide. Conducting experiments at different temperatures and pressures would show if carbon dioxide behaved similar to ethane with respect to changes in the operating conditions. Temperatures and pressures were selected in order to compare the solvents under conditions where the actual and reduced densities were of the same magnitude.

4.6.1 Yields Using Carbon Dioxide

Figure 4.17 presents the extraction curves for three runs with carbon dioxide as the solvent at constant a temperature of 34°C and pressures ranging from 10.0 to 15.0 MPa. This plot shows that the yields increase as the operating pressure increased. The increase in the oil extracted was consistent with the solubility behaviour of pure hydrocarbons in supercritical carbon dioxide. The results from experiments performed by Johnston et al. and Schmitt et al. revealed that the solubility of a number of different hydrocarbons increased as the extraction pressure was increased (Johnston et al.,1982; Schmitt et al.

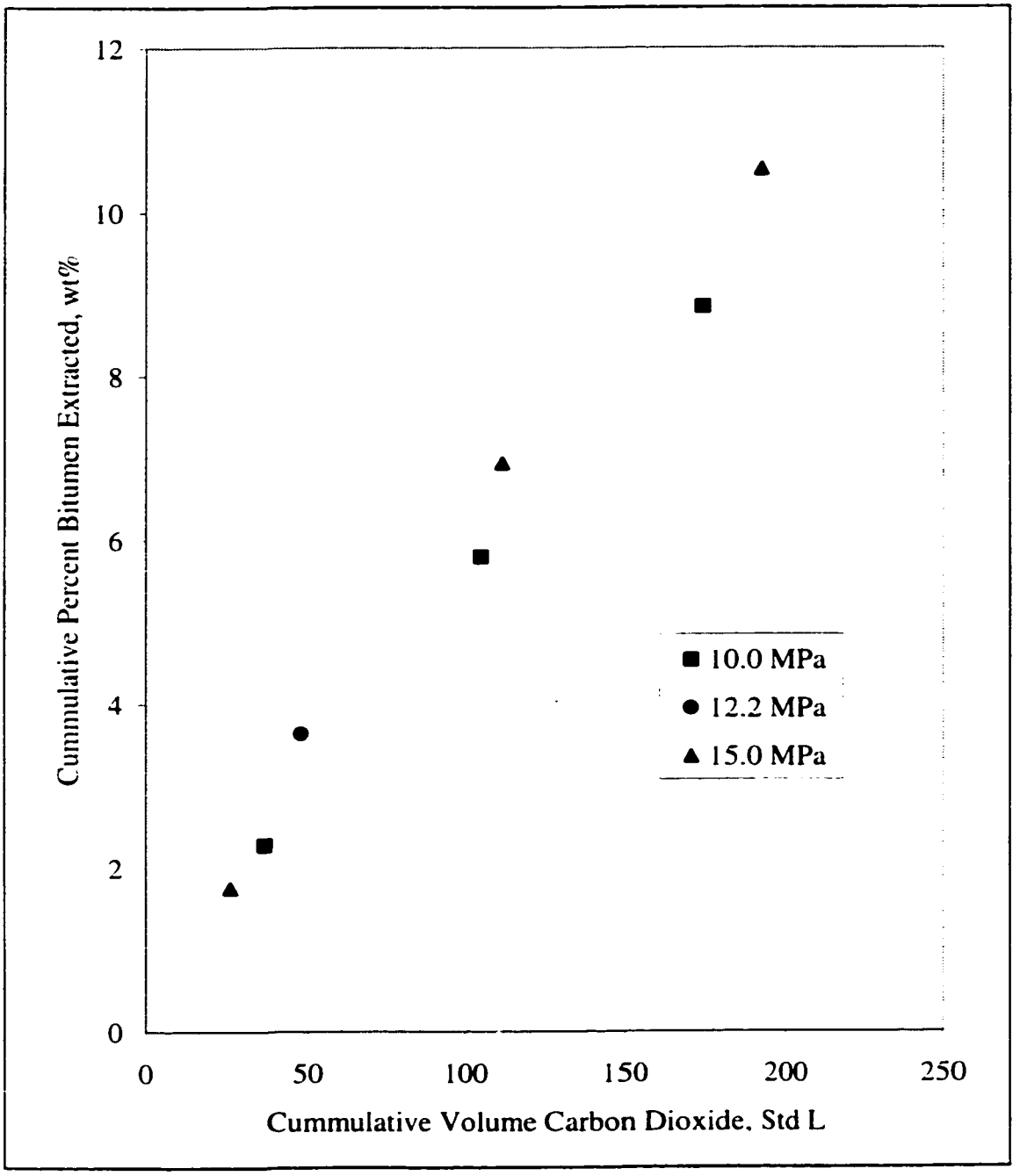

Figure 4.17 – Cumulative weight percent of bitumen extracted using supercritical carbon dioxide at a temperature of 34°C and pressures ranging from 10.0 to 15.0 MPa.

1985). The data presented in Figure 4.17 for the solubility of Peace River bitumen exhibited similar trends to pure hydrocarbon solubility data.

The magnitude of the change in extracted bitumen as a function of changes in operating pressure were very different than those for the ethane experiments. This was evident when comparing the amount of bitumen recovered after contacting the feed 50 Std L of each solvent. For ethane, when the pressure was changed from 10.5 MPa to 12.2 MPa the weight percent of bitumen extracted changed from 12.8 wt% to 16.3 wt% or a difference of 3.5 wt%. When the same pressure change was made using carbon dioxide, the amount of bitumen extracted only increased by 0.8 wt%, from 3.0 wt% to 3.8 wt %. This result showed that while the relative changes were similar, the actual solubility of bitumen in supercritical ethane was more sensitive to changes in pressure than the solubility of bitumen in supercritical carbon dioxide. These results are consistent with the data presented by Johnston et al. who showed that the solubility of a number of hydrocarbons changed more in ethane than carbon dioxide when the extraction pressure was varied over the same range (Johnston et al., 1982).

Compositions of the cumulative extracted oil produced using supercritical carbon dioxide are presented in Table 4.9. The compositions are expressed in terms of the weight percent for each pseudocomponent. It was evident from this data that the composition of the extracted material changed marginally over the range of experimental pressures. As the pressure increased, the oil became slightly heavier as indicated by the increase in the weight percent values for PC3 and PC4. It should be noted that under the conditions studied, PC5 was completely insoluble in supercritical carbon dioxide. The composition did not vary to a great extent between successive samples obtained at the same pressure, as can be seen by comparing the compositions of Samples 1 to 3 for both pressures. The oil extracted at 15.0 MPa had the largest composition change. For example, the weight percent of PC1 decreased by 11.6 wt%. The uniformity of the composition was also reflected in the linearity of the extraction curves.

Pressure, MPa	10.0		15.0	
Sample No.	1	3	1	3
Composition, wt%				
PC1	44	33	48	30
PC2	43.5	49	38.5	46
PC3	10.5	15	10.5	18
PC4	2	3	3	6
PC5	0	0	0	0

Table 4.9 – Cumulative compositional data for the oil extracted at a temperature of 34°C and pressures of 10.0 MPa and 15.0 MPa using carbon dioxide.

Experiments were also performed to examine the effects of changing temperature on the amount of bitumen extracted. The curves for these extractions are summarised in Figure 4.18. The extractions were performed at a constant pressure of 12.2 MPa and temperatures ranging from 34°C to 55°C. As with ethane, the lower temperatures produced more extracted oil while increases in temperature resulted in decreased yields. The trends in these results agreed quite well with the behaviour of binary system data. For solubilities collected under similar conditions, Johnston et al and Schmitt et al. showed that the solubility of a number of hydrocarbons in supercritical carbon dioxide decreased as temperature increased (Johnston et al.,1982; Schmitt et al, 1985). The data obtained for the solubility of Peace River bitumen in the supercritical carbon dioxide was consistent with pure hydrocarbon-carbon dioxide systems.

The decrease in the amount of oil extracted can be attributed to a decrease in the solvent density as the operating temperature increased. At 34°C, the density of carbon dioxide was 778.62 kg/m^3 which was much closer to the standard liquid density of 825.34 kg/m^3. than the density at 55°C which was 520 kg/m^3. At the lower temperature, the solvent was

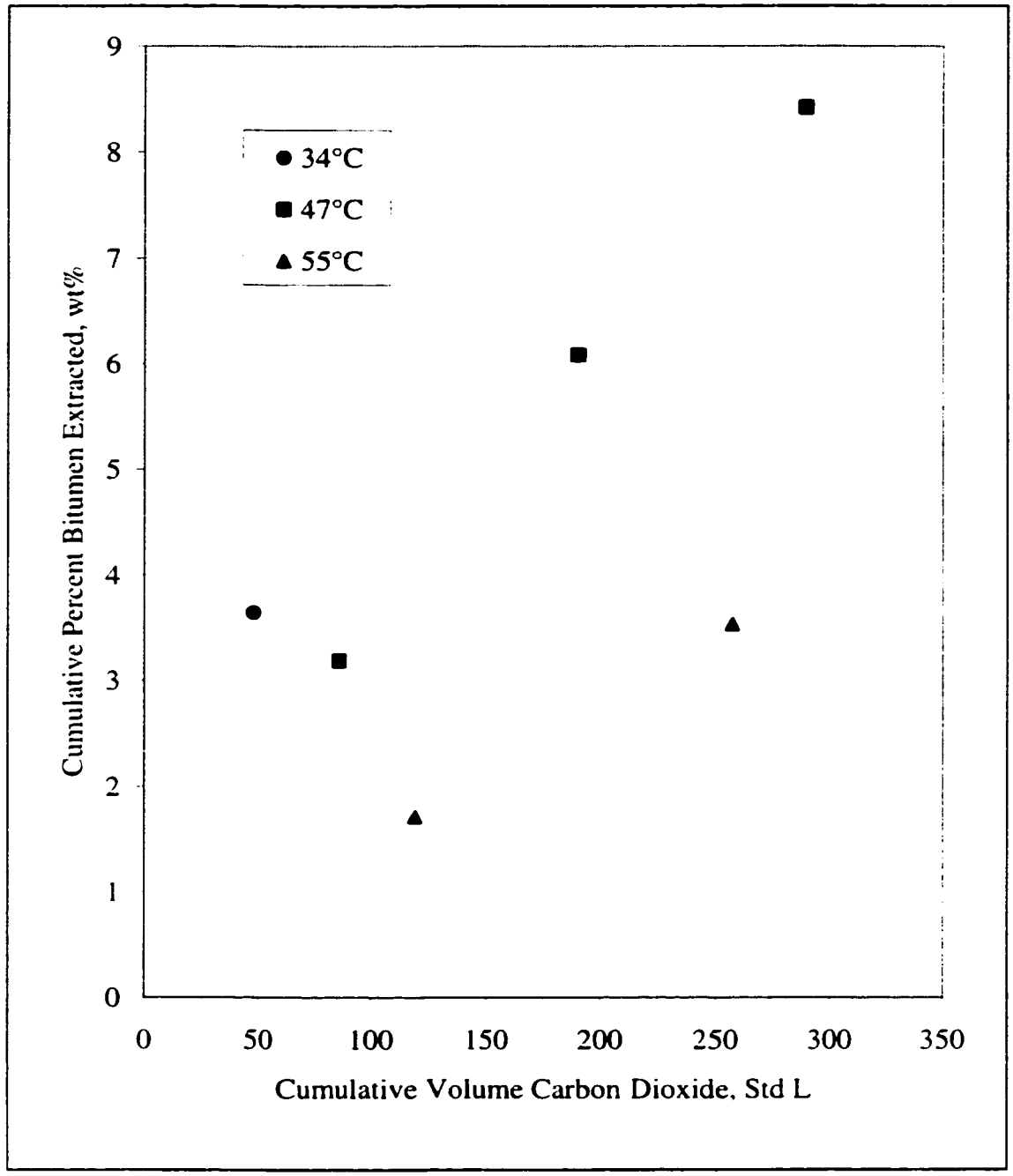

Figure 4.18 - Cumulative weight percent of bitumen extracted using supercritical carbon dioxide at a pressure of 12.2 MPa and temperatures ranging from 34°C to 55°C.

liquid-like and the higher density resulted in an increase in the oil due to a rise in the attractive forces between the solvent and bitumen fractions (Johnston et al.,1982).

Compositions of the extracted oil from these experiments were determined and the results are presented in Table 4.10. At the higher temperature, the composition of the extracted oil exhibited only small changes in the weight percent values for the pseudocomponents. As the temperature was reduced, changes in the composition of successive samples became more apparent. The changes in the extracted oil composition were greater at

Temperature, °C	47		55	
Sample Number	1	3	1	2
Composition, wt%				
PC1	39	32	32	29
PC2	47	50	53	55
PC3	12	15	13	14
PC4	2	3	2	2
PC5	0	0	0	0

Table 4.10 – Composition and yields of the oil extracted at a constant pressure of 12.2MPa and temperatures of 47 and 55°C using carbon dioxide.

lower temperatures due to higher solubilities. This resulted in faster depletion of the soluble constituents within the extractor affecting the composition of the oil extracted. At the higher temperature, fewer constituents were soluble and those that were had lower solubilities. Hence, the composition of the oil became more uniform because the composition within the extractor did not change as much.

4.6.2 Comparison at the Same Operating Conditions

The experimental conditions at which the carbon dioxide experiments were performed were chosen to provide a realistic comparison of the two solvents. Experiments were performed using both solvents at the same temperature and pressure. Data was generated which was used to compare the solvents at conditions where their reduced and actual densities were the same.

Figure 4.19 shows the two extraction curves produced when supercritical ethane and carbon dioxide were used as the solvent contacting the bitumen at 47°C and 12.2 MPa. The supercritical ethane extracted almost six times more oil than carbon dioxide for the same volume of solvent. Even after injecting more than 1.5 times more carbon dioxide than ethane, the cumulative weight percent extracted was only 7 wt% for the carbon dioxide compared to approximately 30 wt% for ethane. This was not overly surprising as studies of binary systems showed that hydrocarbons had higher solubilities in supercritical ethane than carbon dioxide for the same temperature and pressure increase (Johnston et al.,1982; Schmitt et al, 1985).

The composition of the oil was reflected by the weight percent of each of the pseudocomponents as shown in Table 4.11. The material extracted using carbon dioxide was much lighter and more uniform in composition than the oil obtained using ethane. Hence, the boiling point curves for the samples produced using ethane cover a wider range of temperatures indicating a wider range of hydrocarbon constituents in these samples.

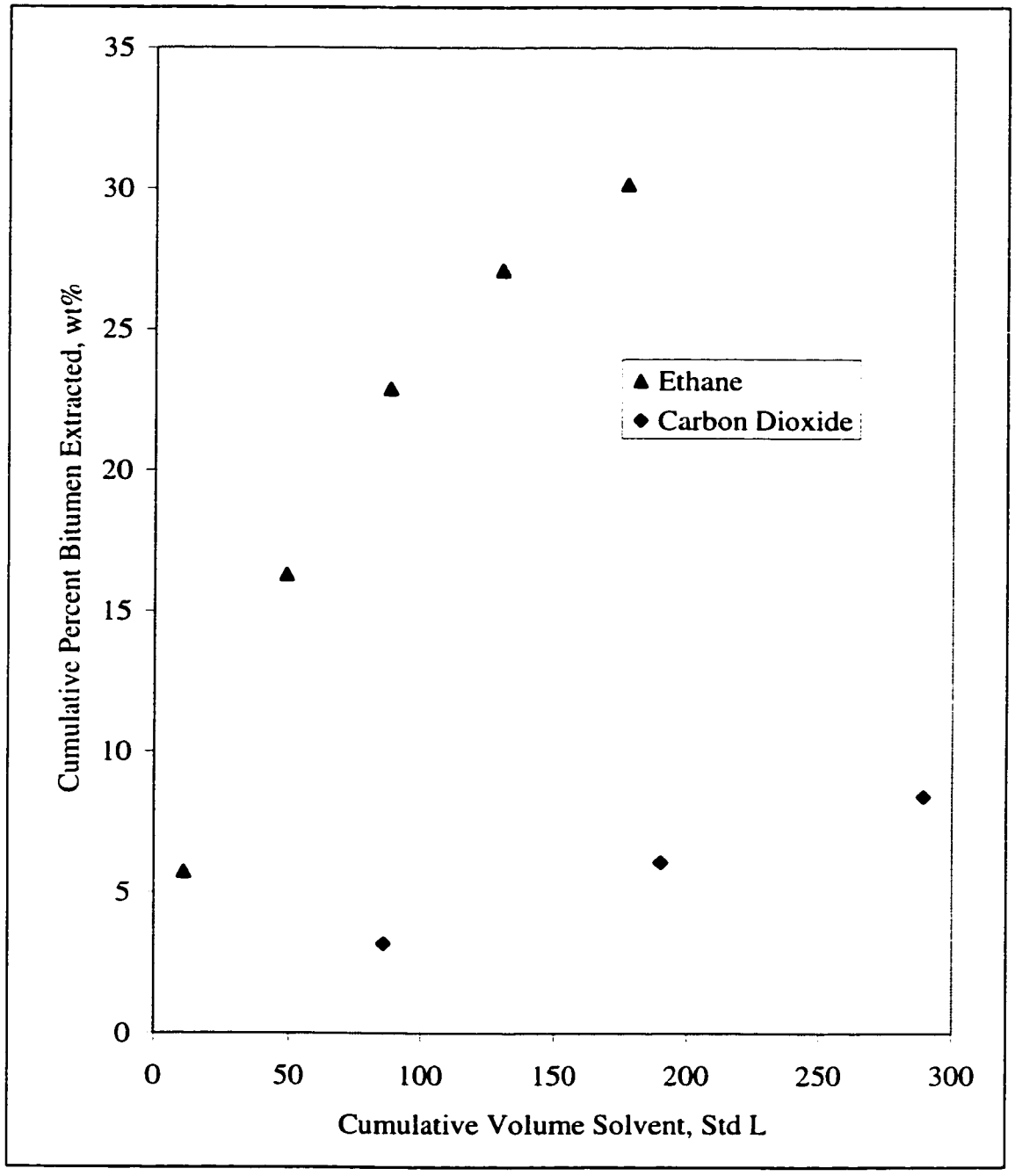

Figure 4.19 – Comparison of extraction yields using supercritical ethane and carbon dioxide at 47°C and 12.2 MPa.

Solvent	Carbon Dioxide		Ethane	
Sample Number	1	3	1	2
Composition, wt%				
PC1	39	32	31	14
PC2	47	50	35	35
PC3	12	15	19	29
PC4	2	3	9	15
PC5	0	0	6	7

Table 4.11 – Composition of the first and last samples extracted using supercritical ethane and carbon dioxide at 47°C and 12.2 MPa.

The composition of the individual samples obtained using ethane changed more over the duration of the extractions than when carbon dioxide was the solvent as evident in Table 4.11. These compositional changes were also reflected in the shape of the extraction curves which are plotted in Figure 4.19. As discussed earlier in Section 4.3.2, the more linear the extraction curve, the more uniform the composition of the material being extracted. It was obvious from Figure 4.19 that the curves for carbon dioxide were more linear which was consistent with the compositional analysis presented in Table 4.11 for the oil extracted using carbon dioxide.

4.6.3 Density Comparisons

The next phase in the comparison of the two solvents was to compare the results when the operating conditions were such that the density of the two solvents were the same. The maximum ethane density used was 366.8 kg/m^3. Using the NIST database (National Institute of Standards and Technology, 1992), it was possible to calculate a set of temperatures and pressure which would result in the density of supercritical carbon

dioxide being 366.8 kg/m^3. Unfortunately, experiments performed using carbon dioxide at this density resulted in negligible amounts of oil being extracted. Therefore it can be concluded that bitumen was not significantly soluble in supercritical carbon dioxide when the solvent density was of a similar density to supercritical ethane.

The lowest carbon dioxide density used in these experiments was 520.3 kg/m^3. At these conditions, only 3 wt% of the bitumen was extracted. To achieve such a high density for ethane, the temperature would have to be as low as possible and the pressure as high as possible. The temperature could not be reduced below the critical temperature if ethane was to remain supercritical. At 32°C, the critical temperature of ethane, the operating pressure required to achieve the desired density would be well over 70 MPa. This was above the pressure rating for the apparatus and thus these experiments could not be performed.

It was possible to produce extraction data for carbon dioxide and ethane at the same reduced densities. Data from these experiments are presented in Figure 4.20 for two cases where the reduced densities of both solvents were the same. The data shows the extraction curves for reduced solvent densities of 1.37 and 1.76. Ethane consistently extracted more bitumen than carbon dioxide, even though the reduced densities were equal. Approximately three times more oil was produced using supercritical ethane than that removed using the same amount of carbon dioxide.

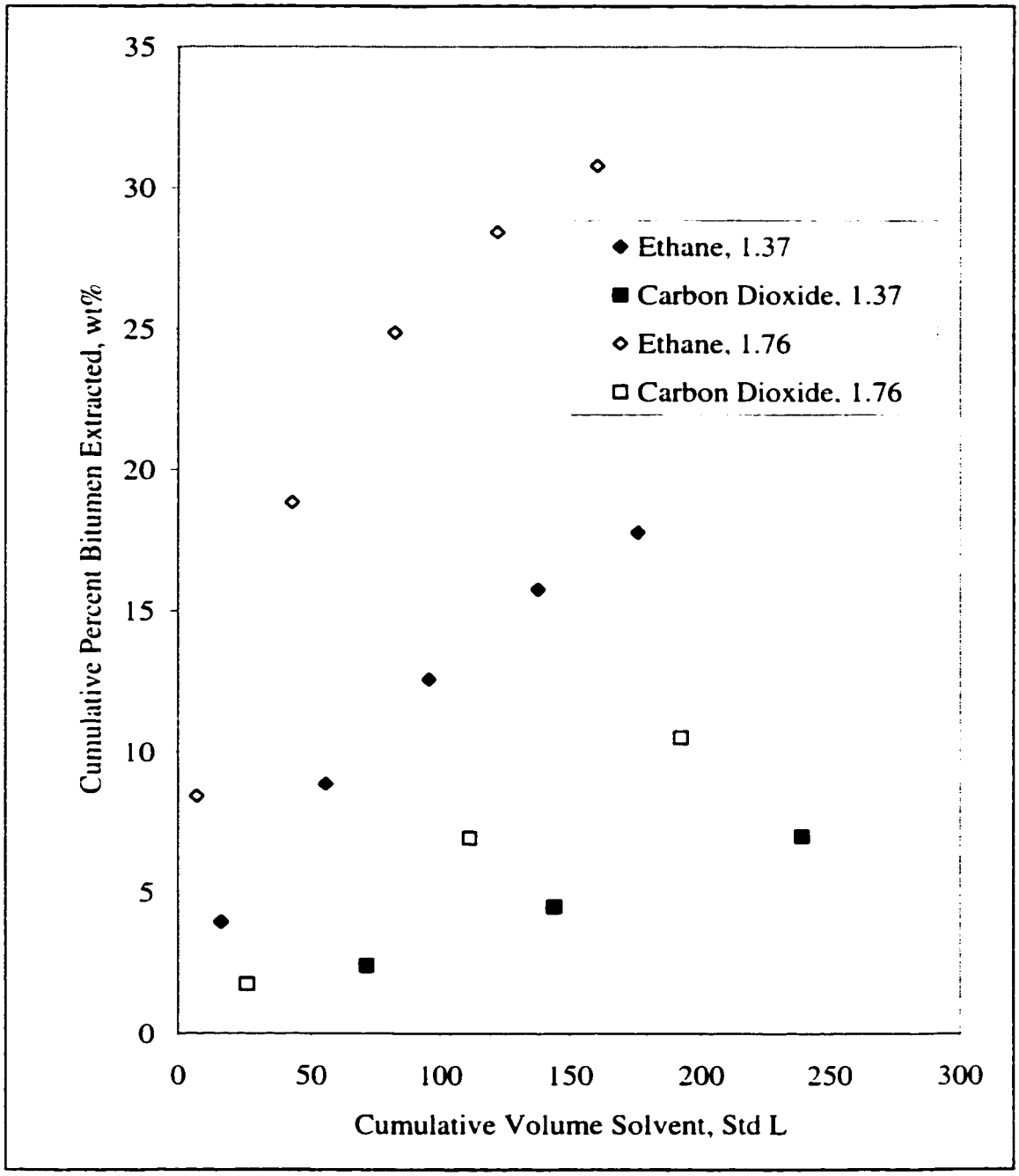

Figure 4.20 – Comparison of yields between carbon dioxide and ethane at the same reduced densities of 1.37 and 1.76.

Solvent	Ethane	Carbon Dioxide
Mass Extracted, g	21.99	6.32
Composition, wt%		
PC1	38.1	37.1
PC2	39.1	47.9
PC3	16.1	12.5
PC4	5.2	2.5
PC5	1.5	0.0

Table 4.12– Composition of samples extracted using 150 Std L of ethane and carbon dioxide at the same reduced density of 1.37.

Table 4.12 shows that ethane extracted oil that was heavier than that produced using carbon dioxide. Where carbon dioxide only removed 2.5 wt% of PC4 and 0 wt% of PC5, oil extracted using ethane contained more than twice as much PC4 and 1.5 wt% of PC5.

4.7 Mass Transfer Considerations

After completing the equilibrium experiments, modifications were made to the experimental apparatus that consisted of reducing the volume of the extraction vessel and doubling the pump capacity. The changes allowed for the adjustment of the time that the supercritical ethane contacted the bitumen, and hence the behaviour of the system would move from the equilibrium governed region to a mass transfer dominated regime. The contact time was varied using two methods, adjusting the solvent flow rate and changing the amount of bitumen in the extractor.

The new extractor had a diameter of 2.8 cm and was 28.5 cm in height resulting in a volume of 55.86 cm^3 compared to 204 cm^3 for the initial extractor. This extractor had a distributor constructed out of the same porous stainless steel as the distributor used in the larger extractor. For the equilibrium study, 140 g of bitumen were mixed with sand and charged to the extractor. For these extractions, 35 g of bitumen was mixed with sand such that the composition of the feed remained 15 wt% bitumen. Because the extractor was smaller, there was less bitumen packed in the extractor and the resulting contact time was only one quarter the base time used for the equilibrium extractions for the same solvent flow rate. At a pump flow rate of 0.8 L/h, the solvent was still saturated with soluble bitumen when it exited the extractor since the extraction curves from these experiments overlapping the original curves as shown in Figure 4.21.

The next step was to increase the solvent flow beyond 0.8 L/h. The pump was modified, doubling the maximum flow and experiments were performed using the small extractor and the higher flows of 0.96 and 2.24 L/h. At the new maximum flow rate and the amount of bitumen reduced the contact time by more than an order of magnitude. The results were plotted in terms of the weight percent extracted as a function of volume of ethane divided by initial mass of bitumen feed. The results are shown in Figure 4.21. A second pump was incorporated to allow for flow rates greater than 2.24 L/h. The higher flow rates actually caused the solvent to displace the bitumen and push it into the two phase separators. Therefore, the maximum flow rate was limited to 2.24 L/h for these experiments.

Figure 4.21 shows that the amount of bitumen recovered was not dependent upon either the solvent flow rate nor the amount of bitumen in the extractor. Hence, the only conclusion that can be reached as demonstrated by the results shown in Figure 4.21 is that the extraction process is controlled by thermodynamic equilibrium and not mass transfer resistances (see Section 4.2).

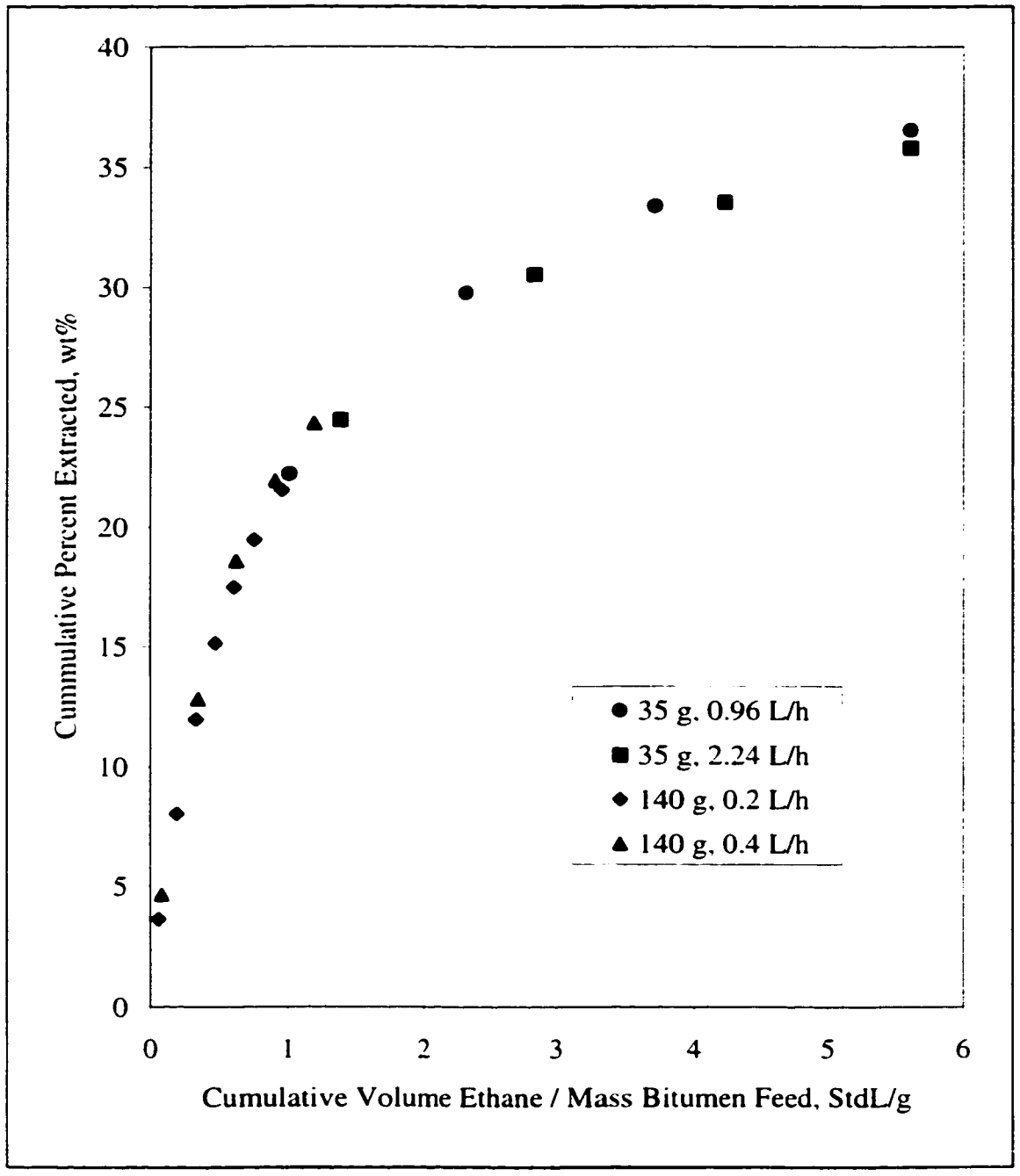

Figure 4.21 – Extraction curves for experiments performed at 47°C and 10.5 MPa using different amounts of bitumen and different solvent flow rates.

These results indicate that the fluxes of the soluble bitumen fractions into the supercritical ethane were large. High fluxes for solutes into supercritical fluids have been reported for binary systems. For example, Rance et al. observed flux rates of iodine into carbon dioxide and found that there was a significant increase in the fluxes when in the supercritical region (Rance, et al., 1974).

The diffusivities are higher for solutes in supercritical fluids than liquids as discussed in Chapter 2. Lim et al. modelled the lab scale solvent extraction of Cold Lake bitumen using near critical ethane (Lim et al., 1996). They observed that the diffusivities of ethane into the bitumen that were calculated based on their experimental data were two to three orders of magnitude greater than literature values for molecular diffusivities. Lim et al. concluded that the higher diffusivities could be attributed to the increase in contact area between the solvent and bitumen caused by the dispersion of the solvent in the porous media. The high contact area would also result in enhanced diffusion of bitumen into the solvent phase. In Chapter 3, it was shown that the presence of the distributor and sand acted to distribute the solvent such that it passed through the extractor in a plug flow manner. Thus for systems such as the extractor used in this study or the bench scale reservoir apparatus used by Lim et al., there was sufficient interfacial surface area that the mass transfer resistances were negligible.

4.8 Summary

Extensive testing was performed to confirm that the data collected for the Peace River bitumen and supercritical ethane system was governed by thermodynamic equilibrium. Instead of using a pure component solute and assuming that behaviour of this system would represent the actual bitumen-solvent system, Peace River bitumen was used in these experiments. It was observed that the solvent flow rate did not affect the amount

nor composition of the bitumen extracted over the range of rates examined, hence the data generated was controlled by thermodynamic equilibrium and not mass transfer limitations.

The effects of temperature and pressure were observed by varying the operating conditions at which the extractions were conducted. When the temperature was increased or the pressure decreased, the amount of bitumen recovered decreased. This was attributed to the fact that the density of ethane approaches gas-like behaviour at these experimental conditions which tends to reduced the solubility of hydrocarbons in the solvent. For experiments conducted at the higher temperatures or lower pressures, the oil that was produced was lighter and had lower viscosities. SARA analyses revealed that the extracted oil was predominantly saturates and aromatics with small amounts of resins present. The samples became heavier over the duration of the extractions and the degree to which the compositions changed depended on the temperature and pressure at which the extractions were performed.

A comparison was made between supercritical ethane and carbon dioxide to extract Peace River bitumen. Both solvents exhibited the same relative response to changes in temperature and pressure. Supercritical ethane proved a better solvent than carbon dioxide as more oil was recovered for the same amount of solvent. The recovered oil using ethane as a solvent was significantly heavier indicating that heavier bitumen components were extracted.

The apparatus was modified to determine if mass transfer data could be collected for the Peace River bitumen-supercritical ethane system. The flow rate was increased and the amount of bitumen in the extractor was decreased in order to reduce the solvent contact time. These changes could not overcome the high degree of mixing of the solvent and bitumen, the conclusion being that this experimental apparatus and its modified version would only generate equilibrium data.

Chapter Five

Bitumen Characterisation

Crude oils, heavy oils and bitumens are exceedingly complex, undefined mixtures. In addition to numerous hydrocarbons (paraffins, naphthenes and aromatics), there exist many non-hydrocarbon components such as sulphur, oxygen, nitrogen and porphyrin (metal) compounds (Speight, 1991). The sheer number of components comprising these fluids makes it next to impossible to measure the composition of these mixtures and determine all of the corresponding critical properties. Without the critical properties, acentric factors and feed composition it is not possible to predict thermodynamic and physical properties using cubic equations of state.

To address this problem, researchers have developed procedures for estimating the critical properties of hydrocarbon mixtures of unknown composition. The oil is first divided into a number of cuts or pseudocomponents and, using correlations such as Kesler-Lee or Twu (Section 2.5), estimations of the properties necessary to characterise the mixture are made thus allowing engineers to thermodynamically model the process.

This approach was used to characterise the Peace River bitumen used in this work. First, the oil was distilled that produced four cuts plus the remaining residue. The boiling point curve and specific gravity for each cut were measured and the critical properties, molecular weights, and acentric factors were estimated using different correlation

methods. This data was then used to characterise the feed to the extraction unit.

5.1 Pseudocomponents

The first step in characterising the Peace River bitumen was to determine how many cuts would be needed to accurately describe the complete bitumen. For modelling purposes, the boiling point for the whole mixture can be subdivided using different "rules of thumb" such as the Whitson's lumping procedure (Whitson, 1983) . The pseudocomponents act as imaginary components with properties representing the range of hydrocarbons within its portion of the boiling point curve. The small temperature intervals create pseudocomponents that better reflect the boiling point range they are to represent and typically increase the accuracy of the equation of state predictions being used to model the process.

Having a large number of pseudocomponents may increase the accuracy of the calculations but this may not always be practical. As the number of pseudocomponents increases so does the computation time and the number of interaction parameters required by the equation of state. In some cases, an alternative technique is used to characterise a mixture of hydrocarbons of unknown composition. The fluid was fractionated using a laboratory distillation procedure to separate the feed into different fractions with each cut becoming a pseudocomponent. Properties of the cut, such as density or a boiling point curve, can be measured and used in correlations to calculate the critical properties for the fraction. If such an approach is taken, producing a large number of cuts is not realistic. In most cases, the number of pseudocomponents used ranged from treating the mixture as one (Sheng et al., 1990) to five (Mehrotra et al., 1985). For example, Mehrotra et al. used four components to accurately model the solubilities of a number of gases, including ethane, in Peace River bitumen within 3.3%.

In this work, the bitumen was distilled with four cut points resulting in five cuts, four distilled fractions of oil plus the remaining residue. The residue formed the fifth cut and comprised the largest portion of the bitumen, approximately 50 wt%. In order to obtain these cuts, a portion of the Peace River bitumen used in the experiments was distilled under vacuum using the ASTM D1160 method (ASTM, 1999). The distillation was performed using the apparatus at Core Laboratory Canada, Calgary, Alberta. The first two cuts were produced using an operating pressure of 10 mmHg, the third at 5 mmHg and the last at 1 mmHg. The distillation pressure was reduced as the cuts became heavier so that the temperatures could be kept low to prevent any of the bitumen from cracking. Table 5.1 shows the operating pressure, vapour temperature at operating pressure and the equivalent normal boiling range for the four cuts and the residue.

	Pressure, mmHg	Vapour Temperature Range, °C	Equivalent Normal Boiling Point Range (°C)
Cut 1	10	45.0 – 113.5	160-245
Cut 2	10	113.5 – 184.0	245-330
Cut 3	5	168.0 – 239.0	330-415
Cut 4	1	204.0 – 261.0	415-484
Residue	1	261.0+	484+

Table 5.1 – Operating pressures and equivalent boiling points used to produce the five fractions of Peace River Bitumen.

Conversion between the vapour temperature and the normal boiling point were performed using the charts provided in the test method description for the ASTM D1160 distillation technique (ASTM, 1999). Using the vapour temperatures shown in Table 5.1, four cuts and residue were produced with the resulting weight percent of each cut shown in Table 5.2.

	Boiling Point Range, °C	Weight Percent, %
Cut 1 (PC1)	160-245	6.09
Cut 2 (PC2)	245-330	16.04
Cut 3 (PC3)	330-415	12.09
Cut 4(PC4)	415-484	9.86
Residue (PC5)	484 Plus	55.84
Losses	-	0.08

Table 5.2 – Boiling point ranges and weight percents for Peace River cuts and resid.

The losses reported in Table 5.2 correspond to the amount of hydrocarbons which were carried over by the vacuum and collected in the cold trap downstream of the receiver where the distilled sample accumulated. These losses were well within the accepted limits as outlined in the ASTM method (ASTM, 1999).

5.2 Boiling Point Extrapolation

One of the problems in dealing with heavy hydrocarbon mixtures is that distillations can only be performed up to a maximum temperature of approximately 340°C at atmospheric pressure (Nelson, 1968). Beyond this temperature, decomposition of hydrocarbons begins and the validity of the results becomes questionable. Even under vacuum, distillations can only reach a maximum equivalent normal boiling temperature of approximately 500°C (ASTM D1160). Using the simulated distillation technique (ASTM D2887) the maximum temperature for Peace River bitumen was 584°C and this corresponded to 50 wt% distilled. Figure 5.1 shows the distillation curve obtained for Peace River bitumen using the simulated distillation technique.

If characterisation methods that rely on boiling point data are to be used, then a problem exists because the best techniques can only produce partial distillation curves for heavy hydrocarbon mixtures such as bitumens. Therefore, the only way to use conventional characterisation methods to calculate critical properties for the heavy fractions is to estimate the shape of the distillation curves to 100 wt% distilled. Care must be taken when extrapolating the boiling point curves because the resulting curve may have a large influence on the phase behaviour data predicted. This is especially important for systems that operate in regions where the resid fraction is undergoing phase transitions. Methods for the extrapolation of boiling point curves has been addressed by a number of authors (Nelson, 1968; Denchfield, 1981; Pedersen, 1984).

Nelson observed that in most cases, when distillation curve data was plotted on "actuarian" or probability paper, a relatively straight line was observed in most cases. It was then possible to extrapolate a distillation curve and determine the final boiling point by plotting the known data on the probability scale and drawing a line of best fit through the data points. Denchfield adapted this technique and provided an analytical method for the calculation of the extrapolated curve as opposed to reading from charts.

Pedersen developed a different process for extrapolating boiling point curves for hydrocarbon mixtures. This procedure utilises equations to predict the distillation temperatures for the 80 and 100 wt% points based on the density of the mixture and the temperature corresponding to 50 wt% distilled. Equation 5.1 was based on North Sea heavy oil experimental data while Equation 5.2 was completely empirical. The original distillation data plus the two new points were used as the basis for fitting a 5^{th} order

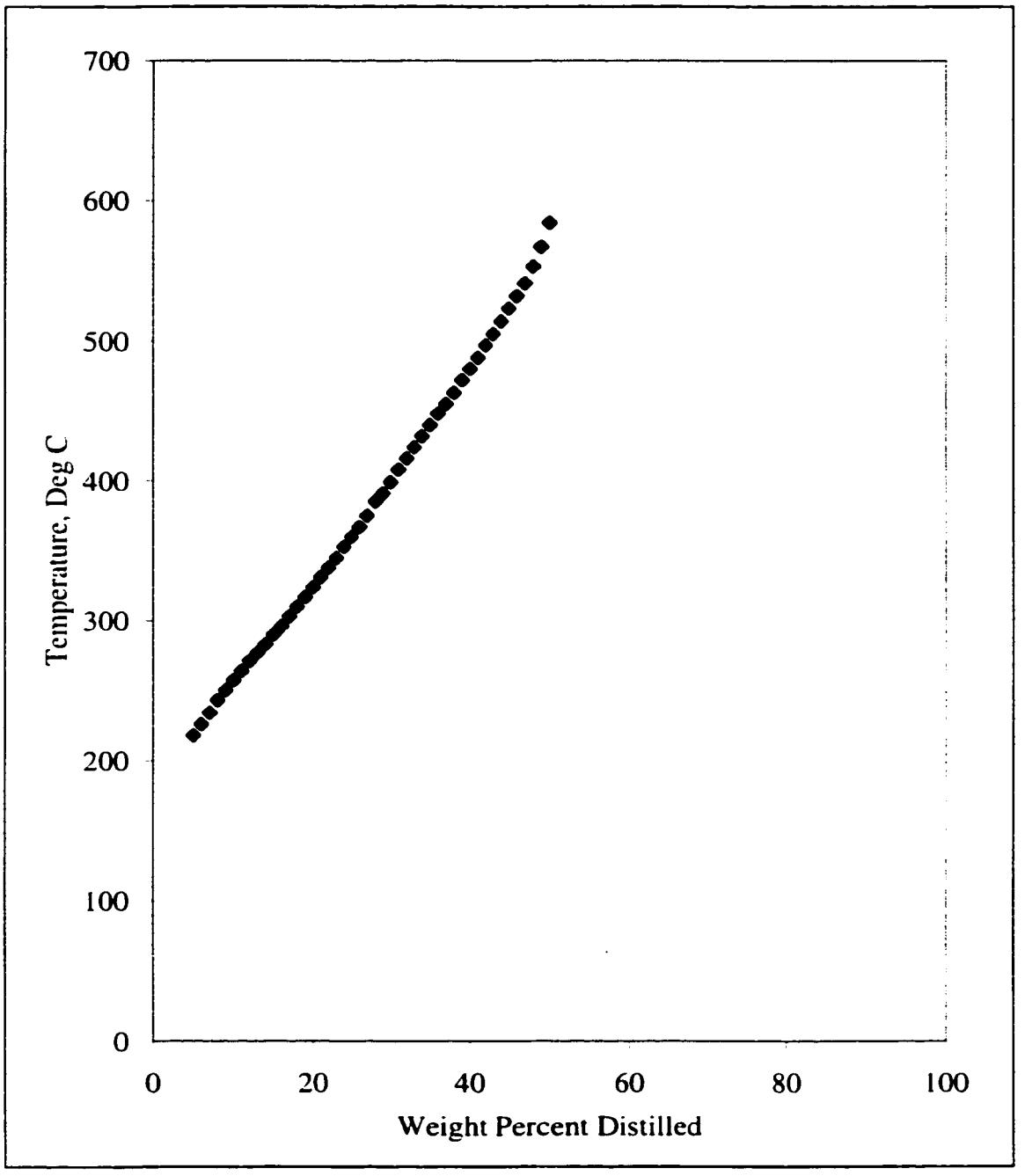

Figure 5.1 – Simulated distillation curve for the Peace River bitumen used in this study.

polynomial equation which described the complete distillation curve. The resulting equations are as follows:

$$T_{80\,wt\%} = 10^{-0.2127}\, T_{50\,wt\%}^{1.103}\, SG^{-0.6495} \qquad \text{Equation 5.1}$$

$$T_{100\,wt\%} = 10^{1.083}\, T_{50\,wt\%}^{10.7097}\, SG^{0.6717} \qquad \text{Equation 5.2}$$

Both Denchfield's and Pedersen's extrapolation methods were used to extend the boiling point curve for the Peace River bitumen used in this study. The results are shown in Figure 5.2. This plot shows that Pedersen's equations predicted a higher boiling point curve than that produced using the Denchfield method. The final boiling point temperatures predicted by each method differ by 132°C and the 80 wt% temperatures differ by 60°C. The discrepancy in the results were attributed to the ability of each method to operate beyond the range over which it was developed.

When the distillation data was transformed to the probability scale, it exhibited a degree of non-linearity. This technique was developed to extrapolate curves to 760°C and was expected to have an accuracy of ±14°C at that temperature. Because this data was extrapolated to such high temperature (1054°C), any deviation in the linearity might have a significant effect on the latter part of the extrapolated portion of the curve. In addition, this data was extrapolated based on temperature data up to only 50 wt% distilled where as the lighter oils for which this method was developed, have distillation data up to approximately 70 wt% distilled.

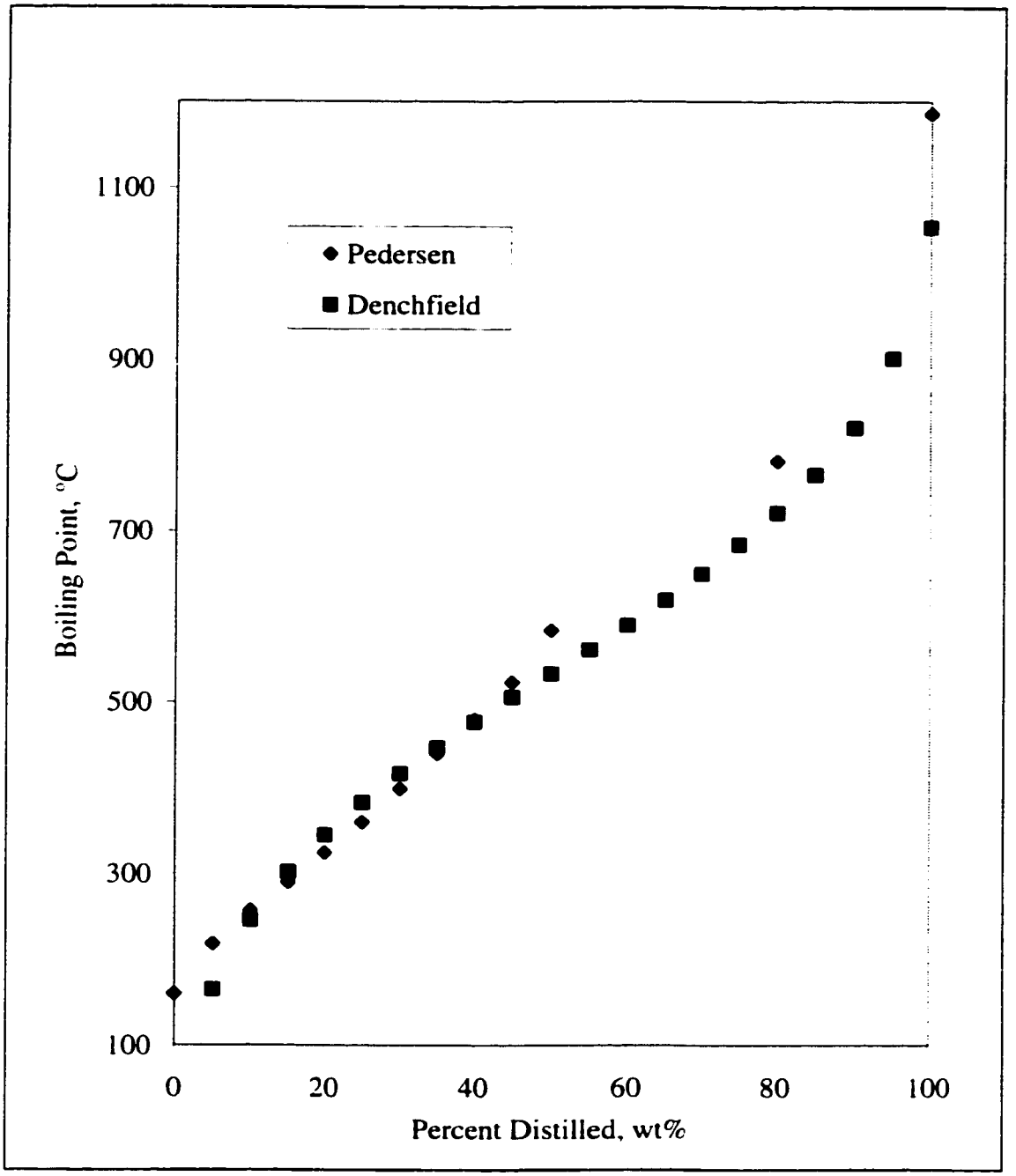

Figure 5.2 – Extrapolated distillation curves for Peace River bitumen produced using the methods developed by Denchfield and Pedersen.

Pedersen's method relied on predicting two data points based on one specific gravity measurement and a distillation temperature that was much lower than the final boiling point. Any error in this point will affect the predicted temperatures. Pedersen's correlation was developed with lighter hydrocarbon mixtures with the heaviest being North Sea crude. This is evident in the fact that Equation 5.1 was based on the regression of temperature data for 80 wt% distilled which was measured. For Peace River bitumen, the 80 wt% distilled temperature is well above the cracking temperature and cannot be measured. Lastly, the final boiling point is completely empirically based, therefore there is no way to evaluate how accurate this equation is for heavy hydrocarbons such as bitumen.

Although uncertainties exist with both methods, they provide the only indication of the possible shape of the distillation curve beyond the measurable temperature limits. The ability of both methods to describe the resid portion of Peace River bitumen are evaluated in Section 5.4.

5.3 Critical Property Estimation

Three methods were used to calculate properties for the fractions of Peace River bitumen, Twu, Kesler-Lee (K-L) and revised Raizi-Daubert (RRD) (see Section 2.5). Each of these methods required the specific gravity and cubic average normal boiling points as inputs to calculate the properties of the cuts. The average normal boiling points were calculated using the distillation data for each cut. Table 5.3 shows the normal boiling point and the specific gravity for each of the five cuts. The pseudocomponents had average boiling points and specific gravities that were similar to those chosen by Mehrotra et al. to model the solubility of light gases in Peace River bitumen (Mehrotra et

al., 198). The variation in the pseudocomponents was attributed to the fact that they used four pseudocomponents to characterise the bitumen while five were used in this work.

	Specific Gravity	Average Normal Boiling Point, °C
PC1	0.8395	207.53
PC2	0.8958	282.70
PC3	0.9629	377.01
PC4	0.9922	465.12
PC5 - P	1.0643	844.5
PC5 - D	1.0643	747.77

Table 5.3 – Specific gravity and average normal boiling point for the pseudocomponents used to characterise Peace River bitumen.

Specific gravity (SG) values were obtained experimentally using ASTM 5002 test method (ASTM, 1999). The average normal boiling point was calculated based on the distillation curves for each of the cuts. In the case of the resid, two average normal boiling points exist, each based on different distillation curve extrapolation methods as discussed in Section 5.2. PC5-P and PC5-D denote the average normal boiling point based on the Pedersen and Denchfield methods respectively.

The data in Table 5.3 was used with the K-L, Twu and RRD correlations outlined in Section 2.5 to determine the T_c and P_c for each of the cuts. The resulting values are listed in Table 5.4. It should be noted that the acentric factors presented in these tables were all calculated using the K-L correlation (Section 2.5) and the critical data predicted by the corresponding correlation.

	Critical Temperature, °C			Critical Presssure, kPa			Acentric Factor		
	K-L	Twu	RRD	K-L	Twu	RRD	K-L	Twu	RRD
PC1	400.42	407.67	407.03	2474.2	2460.1	2416.1	0.487	0.428	0.424
PC2	478.31	488.21	487.76	2085.4	2152.8	2047.6	0.618	0.551	0.528
PC3	572.99	586.28	586.34	1716.5	1889.6	1721.7	0.785	0.721	0.664
PC4	647.24	644.04	665.56	1310.5	1527.6	1402.5	0.991	0.929	0.850
PC5-P	927.20	973.70	964.99	331.1	507.7	672.9	1.809	1.572	1.615
PC5-D	866.20	901.58	899.12	519.6	755.6	818.1	1.588	1.407	1.419

Table 5.4 - Critical properties for Peace River pseudocomponents calculated using the K-L, Twu and RRD correlations.

Comparison of the results for the first four cuts showed that there was relatively good agreement between the critical data predicted by all methods. Critical temperatures for the first four cuts were quite similar, with an average deviation of ± 8.7°C, with those predicted using RRD and Twu's method consistently greater than those predicted by Kesler-Lee. The T_c's calculated for the fifth component using the Denchfield extrapolation were lower (61-72°C) than those using Pedersen's method.

Predicted critical pressures using the three methods also gave good agreement for PC1-PC4, with an average deviation of ± 92 kPa. The P_c's determined using Twu were greater than the RRD values which were in turn, greater than those from the K-L correlation. As the cuts became deeper, the predicted P_c's showed an increased deviation between correlations. P_c's for the PC5-D were 20-25% greater than P_c's for PC5-P. According to Voulgaris et al. critical pressures reported for pure components are much less certain and as a result the correlations vary to a greater degree (Voulgaris et al., 1991). Thus it was not that surprising that the critical pressures predicted spanned such a large range.
The acentric factors exhibited patterns similar to those observed in the T_c's which was not surprising as they are a function of T_c (see Section 2.5). Acentric factors for the first four components had average deviations of ±0.07. The acentric factors for the Twu and RRD correlations were quite close while ω using K-L data were consistently higher.

The greatest discrepancies came when comparing the critical properties for the resid using the two extrapolated distillation curves. Pedersen's technique predicted critical temperatures that were higher by approximately 60°C. The critical pressures deviated even more, with those predicted using Denchfield being higher by over 400 kPa in some cases. This demonstrated that the method chosen for extrapolating the boiling point curves has a significant impact on the resulting critical properties.

Molecular weights were predicted using Twu's equations and Watson K factors were calculated using the equations outlined in Section 2.5. The results for each cut are shown in Table 5.5.

	Watson K Factor	Molecular Weight
PC1	11.35	159.49
PC2	11.17	205.49
PC3	10.94	287.39
PC4	11.08	386.35
PC - P	11.86	985.28
PC - D	11.51	808.45

Table 5.5 – Watson K factors and molecular weights for the Peace River pseudocomponents.

As with previous values, there is a significant difference between the values predicted for molecular weight using data from the Pedersen extrapolation method versus the Denchfield method.

The average molecular weight was calculated using the above values. The resulting molecular weight for the whole bitumen was 560 g/mol. This compares well with the molecular weights reported by Mehrotra et al., who reported the molecular weight of the Peace River bitumen used in their work to range from 529-542 g/mol, (Mehrotra et al., 1989).

5.4 Evaluation of Predicted Critical Properties

Section 5.3 demonstrated that the critical properties estimated can vary significantly depending upon the average normal boiling point used and the correlation method chosen. It was necessary to determine which combination would best represent the system. In this study, liquid densities were predicted using a translated Peng-Robinson equation of state and each set of critical properties. The correlation that predicted the theoretical densities closest to the experimental densities was deemed to represent the cuts most accurately and was thus used in the modelling of the thermodynamic properties.

5.4.1 Translated Peng-Robinson Equation of State

The form of the translated equation of state used to predict the liquid volumes for each of the fractions of the Peace River bitumen was developed by Magoulas et al. (Magoulas et al., 1990). The modified version of the Peng-Robinson equation of state was developed by regressing the translated parameters to minimise the error between the predicted and literature values for vapour pressure and liquid density for n-alkanes from C_1 to C_{20}. The equation is shown below:

$$P = \frac{RT}{(V + t - b)} - \frac{a\alpha}{(V + t)(V + t + b) + b(V + t - b)} \qquad \text{Equation 5.3}$$

Where,

$$\alpha = [1 + m(1 - T_R^{0.5})]^2 \qquad \text{Equation 5.4}$$

$$m = d_0 + d_1\omega + d_2\omega^2 + d_3\omega^3 + d_4\omega^4 \qquad \text{Equation 5.5}$$

$$t = t_o + (t_c - t_o)\exp(B|1 - T_R|) \qquad \text{Equation 5.6}$$

$$t_o = \frac{RT_C}{P_C}(k_0 + k_1\omega + k_2\omega^2 + k_3\omega^3 + k_4\omega^4) \qquad \text{Equation 5.7}$$

$$B = l_0 + l_1\omega \qquad \text{Equation 5.8}$$

$$t_c = \frac{RT_C}{P_C}(Z_c' - Z_C) \qquad \text{Equation 5.9}$$

$$Z_C = 0.289 - 0.701\omega - 0.0207\omega^2 \qquad \text{Equation 5. 10}$$

In Equation 5.9, Z_C' is equal to 0.3074. The constants used in the above equations are listed in Table 5.6.

Equation 5.5		Equation 5.7		Equation 5.8	
d_0	0.384401	k_0	-0.14471	l_0	-10.24470
d_1	1.522760	k_1	0.067498	l_1	-28.63120
d_2	-0.213808	k_2	-0.084852		
d_3	0.034616	k_3	0.067298		
d_4	-0.001976	k_4	-0.017366		

Table 5.6 – Parameters used in the translated Peng-Robinson equation (Magoulas et al., 1990).

The translated form of the Peng-Robinson equation of state predicted values of the saturated liquid volumes for the data set that were significantly better than the original Peng-Robinson equation. The new form of the equation calculated molar volumes that had an average absolute error of less than 4% while the original equation predicted values with errors that in some cases exceeded 15%.

5.4.2 Critical Property Prediction Evaluation

The values for T_c, P_c and ω from Table 5.4 for each pseudocomponent were used in the PR EOS to predict the liquid molar volumes at standard conditions. The experimental densities were converted to molar volumes using the molecular weights from Table 5.5 and compared to the theoretical liquid molar volumes. The average absolute relative errors are presented in Figure 5.3.

The molecular weight were varied by ±10% in order to observe if variations in the molecular weights affected the comparison of molar volumes. Because the molar volumes predicted by the translated equation of state were consistently below the experimental values, varying the molecular weights did not impact on the results of the comparison. In addition, the molecular weights were calculated using the method proposed by Riazi et al. for heavy petroleum fractions (Riazi et al., 1996). Using these molecular weights, the error in the predicted molar volumes were much higher. Overall, using the Twu critical properties and molecular weights to calculate the molar volumes remained the best choice.

The molar volumes predicted using all three correlations agreed extremely well for the lighter cuts but as the cuts became heavier the difference between the predicted volumes and the experimental volumes increased for all correlations. For the three lightest components, the correlations all predicted liquid volumes that were within average absolute relative deviations of less than 12%.

Relative to the Twu and RRD results, the K-L correlations performed the worst using data for the two lightest cuts with absolute errors of greater than 9.5%. As the cuts became heavier the volumes predicted using K-L critical properties improved relative to the other predicted results. The overall %AARD for the K-L predictions was 12%. The errors observed can be attributed to the fact that the K-L correlations were developed mainly to

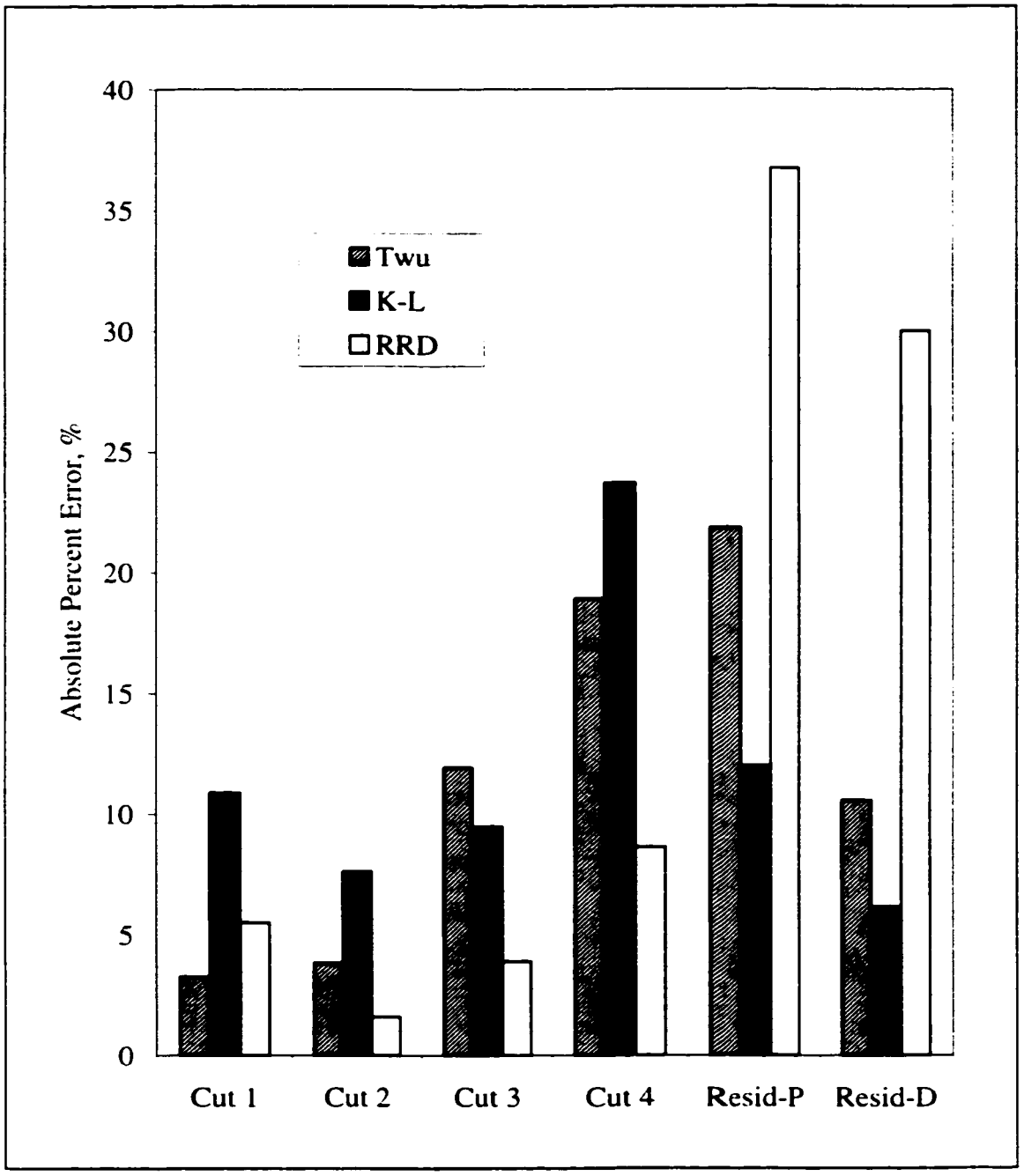

Figure 5.3 – Average errors in the predicted molar volumes for Peace River pseudocomponents using the K-L. RRD and Twu correlations.

improve enthalpy predictions for fluids such as fuel oil and naphtha, not to characterise heavy hydrocarbon mixtures.

The RRD was the most accurate in predicting the volumes for Cuts 2-4 with an average error of 4.7%. The error in the prediction of the heavier volumes was significantly greater when compared to the K-L and Twu results with absolute errors of over 30%. The overall %AARD for the RRD correlations was 14%. The errors were due in part to the fact that the RRD correlations were based on a database of critical properties for 252 hydrocarbons with carbon numbers up to C_{60} (Voulgaris et al., 1991). The main goal of these correlations was to predict T_c and P_c and not to predict liquid volumes. The molar volumes predicted using the Twu equations for the Cuts 1 and 2 were all well within 4%. The errors generally increased as the cuts became heavier (excluding Resid-D). Cut 3 was the only case where the Twu correlations did not perform the best but was only marginally poorer than K-L (the error was 2% greater). Overall, the %AARD for the Twu results was 12%.

These results were similar to those found by Voulgaris et al (Voulgaris et al., 1991). They recommended that RRD and Twu be used where heavy petroleum fractions and coal liquids are being characterised. The data collected for this system showed that both the Twu or the K-L correlations provided critical properties that could be used equally well to characterise the Peace River bitumen used in this work. Based on the volume prediction results and the conclusions drawn by Voulgaris et al., the critical properties calculated using the Twu method were chosen to characterise Peace River bitumen.

5.5 Summary

Unlike systems with known compositions and where the critical properties provided for all of the chemical species can be provided, fluids such as bitumens are undefined and contain many compounds with unknown critical properties. Modelling these processes requires the lumping together of species and representing them using pseudocomponents. Techniques used to estimate critical properties for these pseudocomponents are used to provide the data required by equations of state. These pseudocomponents were then used in equations, such as the Peng-Robinson equation of state to model a given process.

Most of the critical property prediction correlations utilise boiling point data for the hydrocarbon mixture to predict the critical properties. Unfortunately, complete distillation curves for fluids such as bitumens and heavy oils cannot be produced using conventional distillation techniques. The high temperatures required would cause the samples to crack affecting the accuracy of the results. Methods have been developed to extrapolate the boiling point curves for these fluids in order to estimate the complete distillation data. The method chosen has a significant impact on the estimated critical properties for the heavy oil.

The critical properties were also seen to be dependant on the correlations used for their calculation. The Peace River bitumen used in this study was fractionated into five cuts. Critical properties were calculated for each cut using three methods, Kesler-Lee, Twu and the revised Riazi-Daubert. In order to determine which set of correlations predicted the best critical properties, a comparison was made between the experimentally measured molar volume and the volume calculated using a volume translated Peng-Robinson equation of state. The results showed that all three were relatively similar but based upon the average absolute errors and the observations made by Voulgaris et al., it was concluded that the critical properties predicted by the Twu correlations were the most accurate.

Chapter Six

Thermodynamic Modelling

The enhanced solvent properties of supercritical fluids have been known for many years, yet the number of large-scale industrial processes utilising supercritical solvents remains small. One of the reasons for this has been the lack of equations capable of accurately modelling supercritical fluid behaviour. An accurate model can provide a means of acquiring a great deal of information about a system without undergoing the time consuming and costly process of conducting experiments. The ability to predict the behaviour of a supercritical system would allow engineers to evaluate novel processes and determine the most viable and economic process designs.

There are several different approaches that can be taken when attempting to model experimental data. For example, it would be possible to take the extraction curves presented in Chapter Four and determine emperical equations matching the data at each experimental condition studied. The equations could be made a function of independent variables such as temperature and pressure and the experimental data regressed to get the best set of constants for the equation(s). If this is done properly, the equations would be capable of accurately reproducing the experimental data.

The problem with this method of modelling data is that the equations are seldom based on a theoretical foundation, instead, equation development involves regression of the data to fit a given type of function. As a result, the equations are usually only applicable for equipment similar to that used for data collection and at the same operating conditions.

The accuracy of the emperical equations tends to become poor when applied to other systems i.e. extrapolation is not possible. The usefulness of such equations is greatly reduced because the range of situations to which the model can be applied is limited.

To address this problem, more general equations based on theory have been developed for modelling the system phase behaviour. These equations include cubic equations of state such as Peng-Robinson and Souve-Redlich-Kwong, lattice models and group contribution methods. All of the above equations use a theoretical basis in an attempt to describe the behaviour of a large number of physical systems over a range of temperatures and pressures. However, the problem with these equations is that as they become more complex, they generally become more difficult to use or require more information in order to characterise the system. Thus a balance exists between generality and complexity of the equation(s) chosen to model a given system.

In this study, a computer program was written to model the extraction data presented in Chapter Four. The Peng-Robinson equation of state was used to calculate the phase behaviour of the supercritical ethane/Peace River bitumen system. The binary interaction parameters were optimised using the experimental data in order to match the model to the data, thus providing accurate correlations. Results from the extraction program were used to verify the accuracy of the simulation using a set of constant binary interaction parameters for the complete range of conditions studied.

The computer simulation along with the algorithm used to simulate the extractions are described in this chapter. In addition to the successive substitution flash routine which incorporated the Peng-Robinson equation of state, the method used to improve the liquid density results is presented. The method used to optimise interaction parameters is described and the optimisation results are discussed. Finally, results from the simulation of the extraction process are compared to a wide range of experimental data and the sensitivity of the model to changes in the input data are investigated.

6.1 Simulation Development

A computer program was written to model the extraction process in order to reproduce the experimental results. The heart of the program was the routine simulating the semi-batch extractor. The model was required to simulate the complete experimental process, including the pressurisation procedure and the contact of the bitumen/sand feed which passed upwards through the extractor in a plug flow manner.

6.1.1 Algorithm Structure

A computer simulation of the extraction process was written using a software package developed by The Mathworks Inc. called Matlab® version 5.0. The complete Matlab code for the simulation and the compliment of subroutines are included in Appendix C. The program simulates the extraction of oil from the original bitumen feed using the Peng-Robinson equation of state to determine the phase behaviour of the bitumen-supercritical ethane system. The calculations are based on the extraction conditions and feed properties provided by the user as input. A flow chart outlining the program structure is shown in Figure 6.1.

In Block 1, all of the inputs necessary to describe extraction conditions, the bitumen and the solvent were provided as input. The following information was required: critical properties, acentric factors and molecular weights for the bitumen pseudocomponents calculated in Chapter Five, solvent properties, mass of bitumen/sand feed, sand properties and the extraction temperature and pressure.

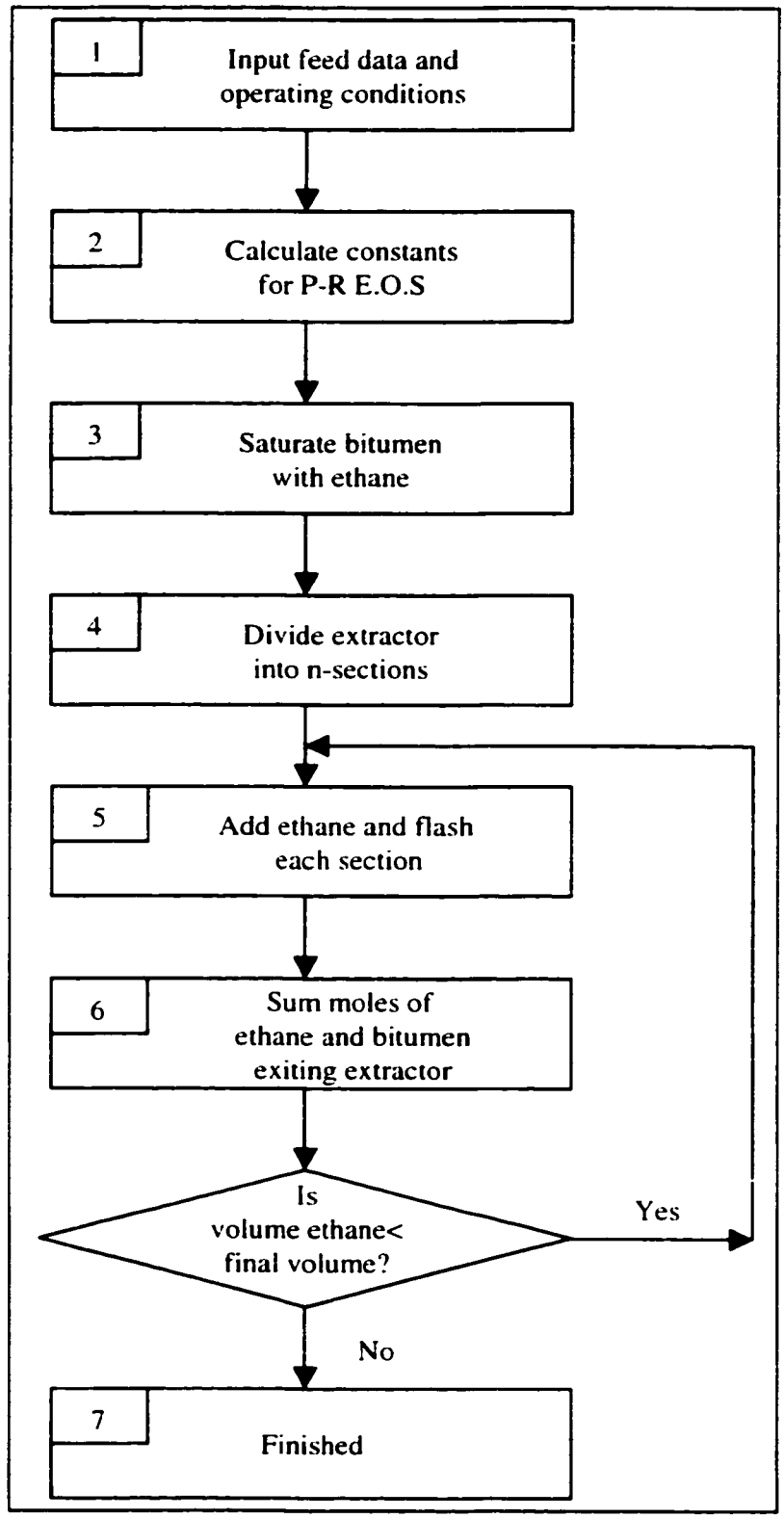

Figure 6.1 – Flowchart of the main program used to simulate extraction process.

The pure component constants required by the Peng-Robinson equation of state were calculated in Block 2. These include the pure component values for "a" and "b" as well as the parameter "a_{ij}" which were all presented in Section 2.5.1. These variables are functions of component critical properties, binary interaction parameters and extraction temperature and pressure and were all constant for a given extraction process. Since the values were required at several stages throughout the simulation, they were therefore calculated at the beginning of the program.

In Block 3, calculations were undertaken to determine the amount of ethane required to saturate the bitumen at the given extraction conditions. Essentially, this block simulated the beginning of an experiment when the system was being pressurised prior to the commencement of the extraction process. Experimentally, pressurisation was achieved by keeping the extractor exit valve (V2 in Figure 3.1) closed while the inlet valve (V1) was opened. The pump supplied solvent to the extractor causing the system pressure to increase until the desired operating pressure was achieved.

The program simulated the pressurisation using the algorithm outlined in Figure 6.2. The necessary data, such as sand characteristics, operating conditions, feed data and the properties of solvent and bitumen, were passed to this subroutine from the main program. The total void volume of the sand in the extractor was calculated using the sand properties in Block 3b. An initial guess for the amount of ethane required to saturate the bitumen was made and combined with the bitumen. The mixture was flashed to determine the molar volume of the solvent-rich phase, the translated solvent-rich phase molar volume and the number of moles comprising each phase. The molar volumes and the moles of each phase were used to determine the volume for each phase. A volume balance was performed in Blocks 3f and 3g to determine if the combined volume of

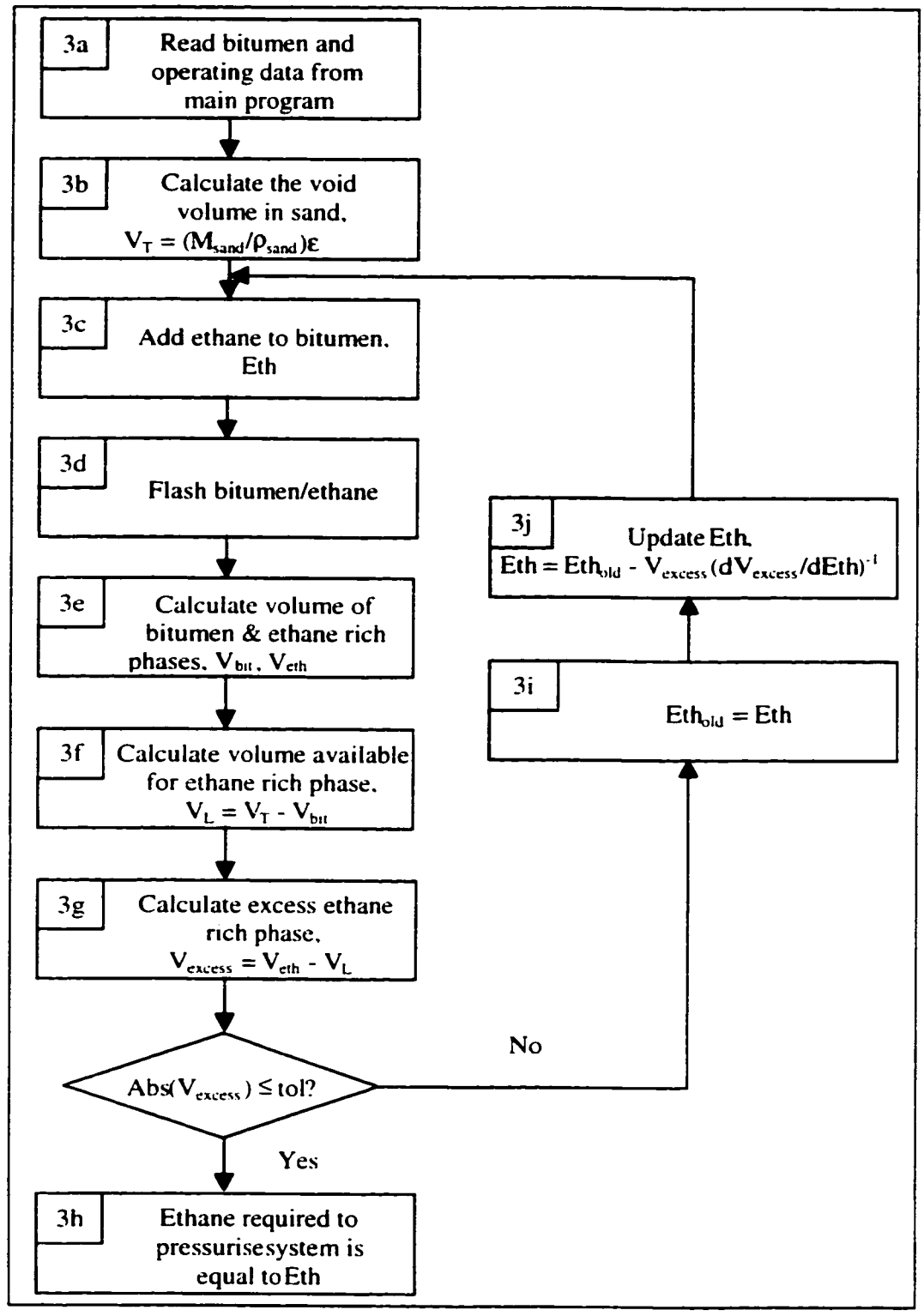

Figure 6.2 – Flowchart of the pressurisation algorithm used in Block 3 of the extraction simulation.

the bitumen-rich and ethane-rich phases was equal to the total void volume. The amount of ethane needed to pressurise the system and saturate the bitumen was adjusted using the Newton-Raphson method, until the absolute value of the excess volume was less than the given tolerance. When the amount of ethane added was sufficient to saturate the bitumen and the volume tolerance was met, the system was "pressurised" and the results were then passed back to the main program.

In order to simulate the extraction process, the extractor was divided into ten sections. Each section was considered to be completely mixed and the ethane-rich phase moved in a plug flow manner from one section to the next. In Block 4, the bitumen/sand/ethane mixture calculated during the pressurisation step was divided into ten sections, with Section 1 at the bottom of the extractor and the tenth section at the top, that is in the direction of solvent flow. The extraction process was then simulated using the algorithm shown in Figure 6.3.

The extraction began by adding a given amount of ethane to the first section of the extractor. The amount of ethane was a function of the size of the time step and the solvent flow rate. The bitumen-rich and ethane-rich phases, already calculated during the pressurisation step, were combined with the fresh ethane and then flashed to determine the moles of heavy and light phases, as well as their respective molar volumes. A volume balance, similar to the one performed in the pressurisation step, was performed for each phase. The total void volume of the sand, V_T' in the given section was calculated using Equation 6.1:

$$V_T' = \left(\frac{M_{sand}}{\rho_{sand}} \right) \varepsilon_{sand} \qquad \text{Equation 6.1}$$

where, ρ_{sand} M_{sand} and ε_{sand} are the sand density, mass of sand in the section and sand porosity, respectively.

The total volume for each of the phases, V_{bit} and V_{eth} was calculated by multiplying the number of moles in each phase by the phase molar volume calculated by the flash routine. These volumes, along with the total void volume calculated by Equation 6.1 were used to determine the amount of solvent-rich phase remaining in the section and the amount entering the next section. The equations used to complete the volume balance are presented below. First, the section volume available for the solvent-rich phase was found using the following equation:

$$V'_L = V'_T - V'_{bit} \qquad \text{Equation 6.2}$$

Next, in order to conserve the volume, the volume of the light phase exiting the section was determined using Equation 6.3:

$$V'_{exit} = V'_{eth} - V'_L \qquad \text{Equation 6.3}$$

The moles of ethane and the bitumen pseudocomponents which exited Section 1 as V'_{exit} were mixed with the existing phases in Section 2. The flash and volume balances were repeated, and the simulation moved sequentially up the extractor. If the simulation was accurate, the composition and amount of light phase exiting the last section of the extractor would match the fluid collected in the separator. The moles of pseudocomponents in the simulated exit stream were converted to mass values and summed to determine the mass of bitumen extracted. The moles of ethane in this stream were converted to a volume at standard conditions and then summed. This total volume

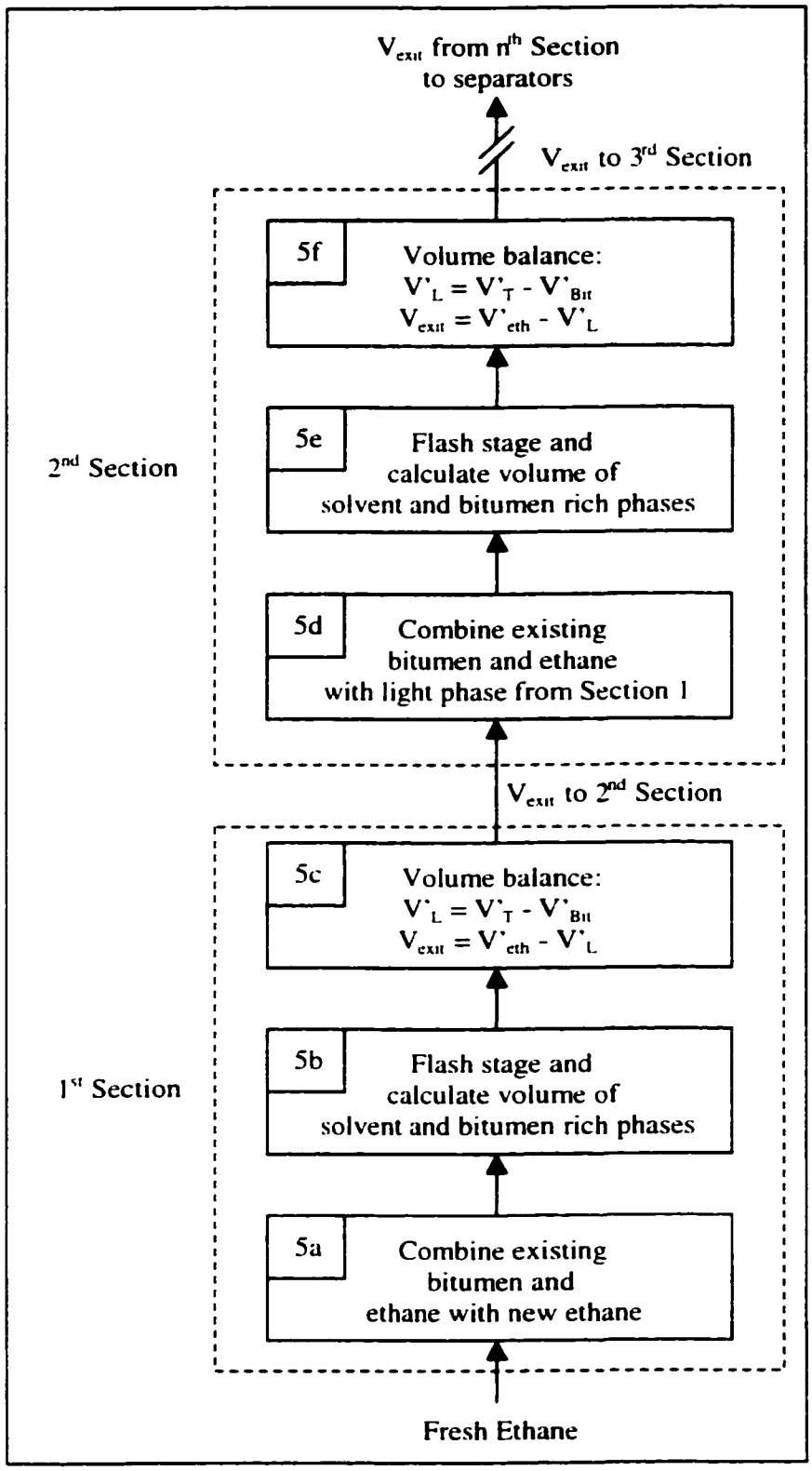

Figure 6.3 – Flowchart showing the algorithm used to simulate the extraction process.

of ethane corresponds to the cumulative amount of ethane measured by the wet test meter during the experiments. If the cumulative volume of ethane was less than final volume specified by the user, then the simulation returned to Block 5 in Figure 6.1 and the procedure outlined in Figure 6.3 was repeated.

When the upper limit for the cumulative amount of ethane was reached, the extraction process simulation ended and the program proceeded to Block 7. The final cumulative volume of ethane was reported along with the cumulative mass of bitumen extracted and the composition of the extract on an ethane free basis. These results were then compared with the experimental results to determine the fidelity of the process simulation.

6.1.2 Flash Routine

A successive substitution flash algorithm was used to calculate the phase equilibria and stability of existing phases for the extraction process simulation. The routine incorporated the Peng-Robinson equation of state as the basis for the initial pressurisation calculations as well as the phase calculations in the extraction portion of the program. The general two phase flash and stability routine was presented by Bishnoi (Bishnoi, 1996). The basic algorithm for this procedure is shown in Figure 6.4.

In Block F1, the data is passed from the main program to the flash routine. The information required by the flash routine includes the following: operating conditions, composition of the mixture being flashed, the ethane/pseudocomponent interaction parameters and the pure component constants for the Peng-Robinson equation of state calculated in Block 2 of Figure 6.1.

In Block F2, initial guesses for the equilibrium constants, K_i, were calculated using the Wilson equation (Wilson, 1968) as Equation 6.4:

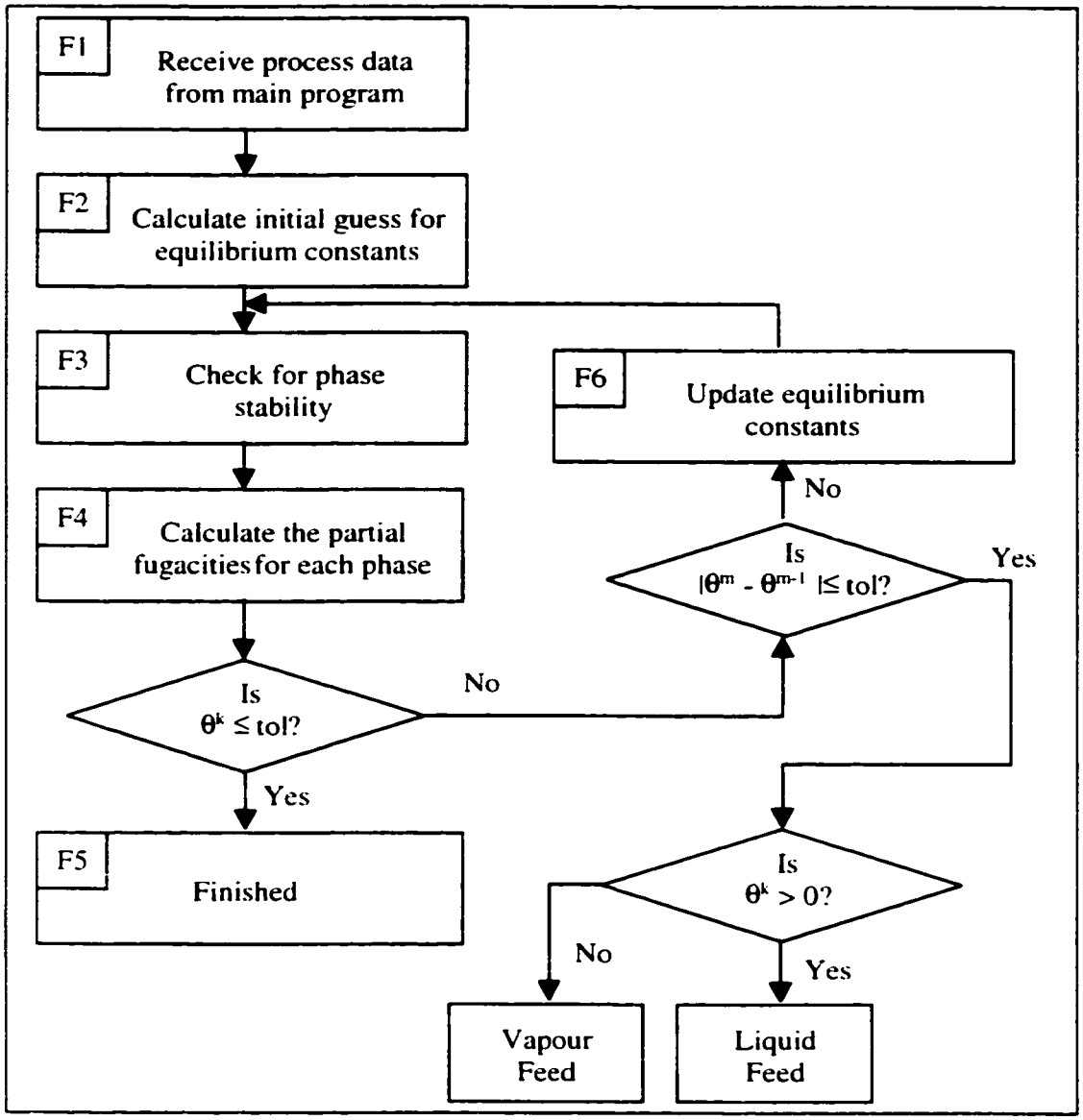

Figure 6.4 – Flowchart for the successive substitution method used to calculate the phase behaviour of the extraction process.

$$K_i = \frac{P_{Ci}\exp[5.373(1+\omega_i)(1-T_{Ci}/T)]}{P}$$ Equation 6.4

where, at equilibrium:

$$K_i = \frac{y_i}{x_i}$$ Equation 6.5

A stability check was performed in Block F3 to determine the number of thermodynamically stable phases present based on the operating conditions and equilibrium constants. For a given feed composition, z_i, and set of equilibrium constants, K_i, an equation, based on the mole balance of the two phases, can be derived which is a function of the phase split, β and is shown below:

$$Q(\beta) = \sum_{i=1}^{N} \frac{z_i(K_i - 1)}{1 + \beta(K_i - 1)} = 0$$ Equation 6.6

This function is monotonically decreasing and if two phases exist, then a phase split between zero and one is required to satisfy Equation 6.6. Equation 6.6 was evaluated for β equal to one and equal to zero. If Q(0) was greater than zero and Q(1) was less than zero, then two phases existed. If Q(0) was less than or equal to zero then the phase was a liquid or if Q(1) was greater than or equal to zero then the system was in the vapour phase.

The next step in the flash calculation was to determine the fugacities for the predicted phase(s). Using the Peng-Robinson equation of state, the expression for the partial fugacity coefficient for component i in phase k and calculated using Equation 6.7:

$$\ln\hat{\phi}_i^k = \frac{B_i}{B^k}(Z^k - 1) - \ln(Z^k - B^k) + \frac{A}{2\sqrt{2}}\left[\frac{B_i}{B^k} - \frac{2}{a\alpha}\sum_j^k (a\alpha)_{ij}\right]\ln\left[\frac{Z^k + (1+\sqrt{2})B^k}{Z^k - (1-\sqrt{2})B^k}\right] \quad \text{Equation 6.7}$$

where B_i, B and A are the dimensionless forms of b_i, b and a for phase k; i.e. $B_i \equiv b_iP/RT$, $B \equiv bP/RT$ and $A \equiv aP/R^2T^2$. It should be noted that the expression for the partial fugacity coefficients was derived using a linear mixing rule for "b" and a quadratic mixing rule for "a" as presented earlier in Chapter Two.

The variable Z in Equation 6.7 is the compressibility factor for phase k and is defined as $Z \equiv PV/RT$. The Peng-Robinson equation of state can be rearranged and expressed in the form of a cubic equation in terms of Z by substituting V for ZRT/P. The form of the revised equation of state is shown below:

$$(Z^k)^3 - (1 - B^k)(Z^k)^2 + (A^k - 3(B^k)^2 - 2B^k)Z^k - (A^kB^k - (B^k)^2 - (B^k)^3) = 0 \quad \text{Equation 6.8}$$

where, A and B are the dimensionless forms of a and b for phase k.

Three roots occur when Equation 6.8 is solved. If Equation 6.8 was solved for the lighter phase, then the largest, real, positive root was chosen. If the root to be calculated was for the heavier phase, then the smallest, real, positive root was chosen.

It was then possible to solve Equation 6.7 for each component in the phase(s). The partial fugacities for the components in the respective phase(s) were determined by taking the exponential of the partial fugacity coefficients and using the definition of the partial fugacity shown as Equation 6.9:

$$\hat{f}_i^k = x_i P\hat{\phi}_i^k \quad \text{Equation 6.9}$$

where x_i is the mole fraction of component i in phase k.

The condition for equilibrium is that the partial fugacity for component i in the light phase, $\hat{f}_i^v$, is equal to the partial fugacity for component i in the heavy phase, $\hat{f}_i^l$. The iterative flash routine adjusted the set of equilibrium constants until partial fugacity condition was met. Equation 6.10 was evaluated after each iteration and when it was less than the tolerance, the routine had converged.

$$\theta^m = \left[\sum_{i=1}^{N} y_i \left(\frac{\hat{f}_i^v}{\hat{f}_i^l}\right)\right]^2 \leq 1\times10^{-20} \qquad \text{Equation 6.10}$$

The flash was also solved for the case when only one stable phase existed, i.e. if $\left|\theta^m - \theta^{m-1} \leq \text{tol}\right|$. If θ^k was greater than zero, then the phase was a stable liquid otherwise the mixture was a stable vapour.

If Equation 6.10 was not satisfied, then the equilibrium constants were updated so that the calculations could be repeated. The updating of the set of K_i's was performed using a successive substitution method. New estimates for the equilibrium constants were found using the latest K_i's and fugacities. The equation used to update the equilibrium constants was as follows:

$$K_i^{new} = K_i^{old}\left(\frac{\hat{f}_i^l}{\hat{f}_i^v}\right) \qquad \text{Equation 6.11}$$

The flash routine then returned to Block F3 in Figure 6.4 and repeated the flash calculations using the updated equilibrium constants. The process was repeated until convergence was reached and the number of phases, the phase split and compositions of the phases were calculated and the results returned to the main routine.

6.1.3 Liquid Volume Calculation

Cubic equations of state are capable of predicting densities of liquid and vapour phases for pure components and mixtures. Equations of state such as the Peng-Robinson equation can calculate vapour densities which are in excellent agreement with experimentally determined values, but predicted liquid densities which are not as accurate (Kokal et al., 1990). In order to mitigate this problem, techniques have been developed employing the method of corresponding states to determine liquid densities of hydrocarbon mixtures. The problem with this approach is that two different methods must be used for cases when both liquid and vapour densities are required.

Kokal et al. developed a method to improve the accuracy of liquid densities predicted using the Peng-Robinson equation of state (Kokal et al., 1990). Their approach was to translate the liquid volume root predicted by the equation of state using the Racket compressibility factor, z_{RA}. The Racket compressibility factor can be calculated using the following equation:

$$v_s = \left[\frac{RT_c}{P_c}\right](z_{RA})^{[1+(1-T_R)^{2/7}]} \qquad \text{Equation 6.12}$$

where v_s is the molar volume of the desired fluid at a reduced temperature of T_R.

The liquid density for each of the five pseudocomponents was measured experimentally and these results were used in conjunction with the critical properties for each pseudocomponent to calculate the Racket compressibilities for each pseudocomponent. The compressibility for ethane was also calculated using Equation 6.12 and is presented in Table 6.1 along with the calculated compressibility of each pseudocomponent.

Component	Racket Compressibility
PC1	0.2606
PC2	0.2562
PC3	0.2609
PC4	0.2608
PC5	0.2290
Ethane	0.2833

Table 6.1 – Racket compressibility factors for the five Peace River bitumen pseudocomponents and ethane.

After having calculated z_{RA} for each component in the system, the volume correction, c, could be determined. For cases when the system temperature was below the critical temperature of the component, the equation for calculating c was as follows:

$$c = \tilde{v} - \left(\frac{RT_c}{P_c}\right)(z_{RA})^{[1-(1-T_R)^{2/7}]} \qquad \text{Equation 6.13}$$

Where $\tilde{v}$ is the liquid volume predicted using the Peng-Robinson equation of state at the reduced temperature T_R. When the system temperature was greater than the component critical temperature Equation 6.14 was used:

$$c = \left(\frac{RT_c}{P_c}\right)(0.307 - z_{RA}) \qquad \text{Equation 6.14}$$

For mixtures, the individual c_i's were calculated using either Equation 6.13 or Equation 6.14 and then combined using Equation 6.15 to determine c for the mixture.

$$c = \sum c_i x_i \qquad \text{Equation 6.15}$$

where x_i is the mole fraction of component i in the liquid mixture. The translated mixture or component volume was then determined using the equation shown below:

$$v_s = \tilde{v} - c \qquad \text{Equation 6.16}$$

The use of the Racket compressibility factor translation method improved the predicted liquid density values dramatically. Kokal et al. reported that for light gas/bitumen systems, the average error was less than 1% using the translated method as opposed to errors of 18% to 22% using the value predicted by the Peng-Robinson equation alone (Kokal et al., 1990). The density of the bitumen-rich phases in the computer program were calculated using this volume-translation method.

6.1.4 Assumptions

The first assumption made was that during the extraction process, ethane exiting the extractor was saturated with the soluble fractions of bitumen remaining in the extractor at any given time. In other words, the system was controlled by thermodynamic equilibrium and not mass transfer resistances. Experimental work was performed to validate this assumption, and the results of this phase of the project were discussed in Chapter Four and will not be repeated here except to say that the experimental results validated this assumption.

The stability calculations in the flash subroutine were performed in order to check for the existence of two phases, an ethane rich vapour-like phase and a bitumen rich liquid-like phase. It was assumed that a second liquid phase, rich in ethane, did not exist. This is a

valid assumption because vapour-liquid-liquid behaviour has not been reported for either bitumen-ethane or binary systems consisting of ethane and a heavy hydrocarbon in the temperature/pressure regions studied in this work.

A temperature/pressure region is known to exist where three phases are in equilibrium for systems consisting of a light hydrocarbon and one or more heavy hydrocarbon(s). Figures 6.5 and 6.6 illustrate the phase diagram for a binary hydrocarbon systems where the molecular weights of the components differs greatly (Miller et al., 1989; Raeissi et al., 1998). According to Miller et al., binary systems consisting of ethane and heavy n-alkanes such as C_{18}-C_{23} exhibit phase behaviour classified by van Konynenburg and Scott as Type IV, shown in Figure 6.6 (van Kronynenburg et al., 1980). For ethane and n-alkanes beyond C_{24}, the system exhibits the Type III behaviour shown in Figure 6.5 (Miller et al., 1989).

The important feature of these types of systems is that their phase diagrams show that there is a region near the critical point of the more volatile component, C_1, where two liquid phases and a vapour phase exist in equilibrium. In Figures 6.5 and 6.6, this equilibrium is represented by the liquid/liquid/vapour equilibrium line. For Type IV systems, there is a break in the LLV equilibrium line for this type of system at lower temperatures where increases in pressure cause the critical formation of a single liquid phase. This phenomenon is represented by the upper critical solution temperature or the UCST Line in Figure 6.6. For Type III systems, the UCST line merges continuously into the critical mixture curve and there is no break in the liquid/liquid/vapour equilibrium line, as shown in Figure 6.5.

For systems consisting of ethane and heavy hydrocarbons the three phase region occupies a very small temperature range. Kohn et al. and Rodrigues et al. studied binary systems comprised of ethane and hydrocarbons such as n-nonadecane, n-eicosane and n-docosane (Kohn et al., 1966; Rodrigues et al., 1967). Depending on the identity of the heavier

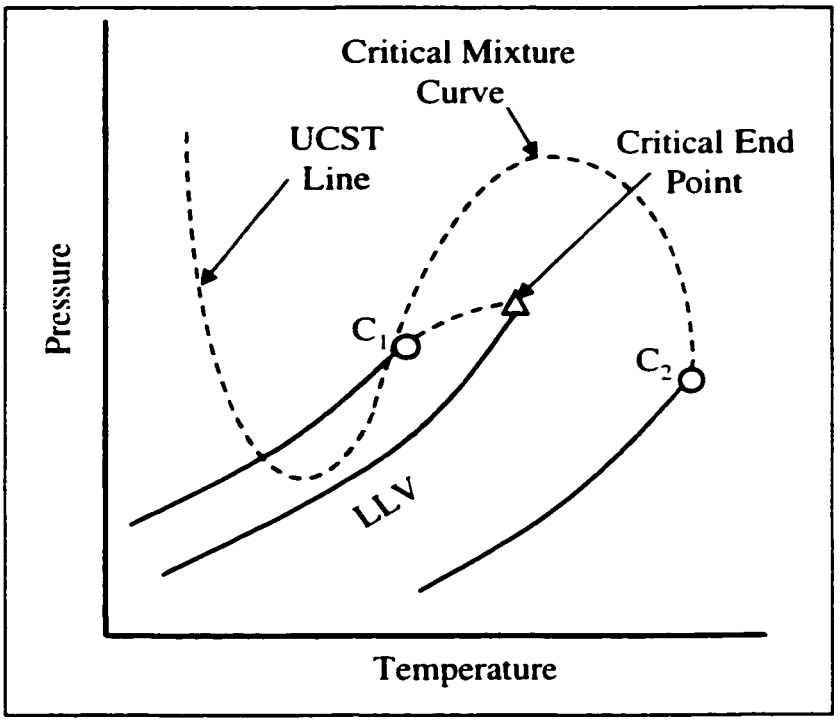

Figure 6.5 – Type III phase behaviour typical for ethane and n-alkanes with carbon numbers greater than 24 (Miller et al., 1989).

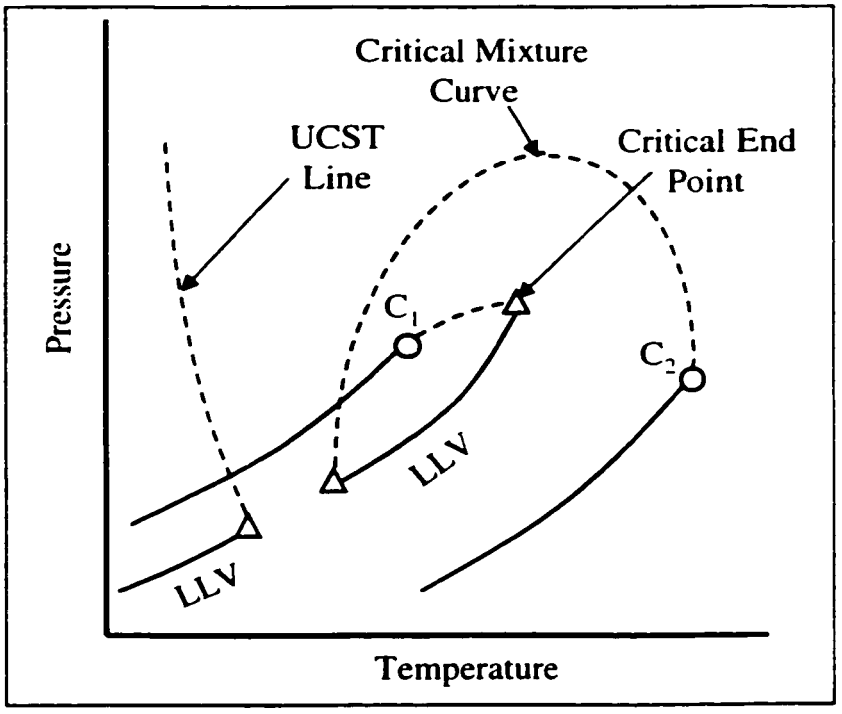

Figure 6.6 – Type IV phase behaviour for ethane and n-alkanes with carbon numbers between 18 and 23 (Miller et al., 1989).

compound, the liquid/liquid/vapour equilibrium line was observed to start at temperatures from 27.57 to 36.60°C and end at upper temperatures ranging from 34.83 to 37.78°C. The pressures for the three phase line were near the critical pressure of ethane, 4.88 MPa, and ranged between a lower bound of 4.38 to 5.25 MPa and a maximum pressure of 5.39 to 5.14 MPa.

Mehrotra et al. reported the possible existence of a three phase region for ethane and Peace River bitumen (Mehrotra et al., 1985). Although they did not have experimental data confirming a three phase region, they performed a number of three phase stability calculations and three phase flash calculations to determine if three phases could exist. Their calculations revealed that for temperatures of 12 and 25°C and pressures from 3.5 MPa to slightly greater than 4.0 MPa, a three phase region was predicted. When the temperature was increased to 50°C, their calculations indicated the existence of only two phases. Therefore, according to their calculations, the Peace River/ethane system exhibited behaviour similar to that shown in Figure 6.6.

Pressures used in this study ranged from 7.3 to 15.0 MPa and temperatures were varied from 37 to 92 °C. It should be noted that the data gathered at 37°C was at a pressure of 10.5 MPa and the data collected at 7.3 MPa was at a temperature of 47°C. All of the experimental operating conditions were well beyond the predicted three phase region for ethane and heavy hydrocarbon systems. Therefore, it was assumed that only two phases existed for supercritical ethane and Peace River bitumen over the complete range of operating conditions over which the extractions were performed.

The volume balance performed by the simulation assumed that the bitumen remained immobile over the course of an experiment. In order to validate this assumption, a verification was made during one of the experiments. A beaker containing a layer of the bitumen/sand mixture packed on top of a 3 cm layer of sand was placed inside the oven

and remained there over the course of the entire extraction process. It was observed that the bitumen level in the beaker remained constant throughout the test.

Mobility of the bitumen was also checked using experimental data from similar systems. Studies have been performed in which bitumen was recovered by gravity drainage enhanced by the presence of a light hydrocarbon solvent (Dunn et al., 1989; Das et al., 1996). The experiments lasted upwards of 2000 minutes with early bitumen flow rates of approximately 0.6 mL/min for ethane and Athabasca bitumen (Dunn et al., 1989), corresponding to a downward superficial velocity of 0.04 mm/min. Since the longest time required to complete an extraction in this work was 180 min., in the worst case senario the bitumen could have moved approximately 7.2 mm.

The mobility of the bitumen would be further impeded as the experiments proceeded due to the nature of the bitumen extraction process. During the experiments, the lighter, more mobile fractions of the bitumen were extracted first, leaving the heavier fractions in the extractor. The bitumen remaining would have a much higher viscosity than the initial sample, and would therefore be much less mobile.

The mass and composition of the oil extracted, as predicted by the model, were compared to the experimental results in order to optimise the interaction parameters and evaluate the accuracy of the model. This required the assumption that all of the bitumen extracted was collected in the separators and that no extract was carried in the overhead flow from the separators or lost when separators were changed. Experimental results showed that there was no entrainment in the overhead vapours of extracted bitumen from the separators. The results of the mass balances, discussed in Chapter Four, demonstrated that the balances closed within experimental error. Therefore, the experimental results accurately reflected the mass and composition of the extracted oil and thus used to evaluate the model results.

6.2 Interaction Parameters

In fluid mixtures, there are interactions between the various mixture constituents. The greatest interactions occur between the most "unlike" pairs while interactions between like components or between three or more species can be considered much less significant (Walas, 1985). The binary interactions impact the behaviour of the system and affect how it responds to condition changes such as temperature or pressure. The interactions between pairs of molecules are modelled by interaction parameters or the k_{ij}'s used in equations of state. The interaction parameters are used to calculate the a_{ij} term in the Peng-Robinson equation of state defined earlier in Chapter Two.

There are two ways to determine the interaction parameters between two components. Either one can use existing correlations or regress experimental data to determine the optimum parameters. Both methods were used in this study in order to determine the interaction parameters necessary to model the process.

6.2.1 Optimisation

In order to improve the performance of equations of state it is common practice to regress a set of interaction parameters on the basis of experimental data. Only interactions for the ethane/pseudocomponent pairs were optimised because these interactions are the most significant (Walas, 1985). The interaction parameters between pairs of bitumen pseudocomponents were set to zero because these interactions have a negligible effect when compared to ethane/pseudocomponent interactions (Walas, 1985).

The extraction model presented in Section 6.1 was incorporated into an optimisation routine in order to determine the optimal set of interaction parameters for this system to be used in the Peng-Robinson equation of state. An initial guess for the parameters was

provided, and the simulation was used to calculate the resulting composition of extracted oil after a set amount of ethane had flowed through the extractor. An objective function, based on the composition of the extracted oil, was evaluated after the extraction simulation was completed. This objective function is shown below:

$$\psi = \frac{1}{N}\sum_{i=1}^{n}\frac{\left|y_i^{expt} - y_i^{calc}\right|}{y_i^{expt}} \qquad \text{Equation 6.17}$$

where N is the total number of compositions used in the objective function and y_i is the mole fraction of component i in the extracted bitumen.

The interaction parameters were then updated by the optimisation routine. The composition of the extracted oil was recalculated and the error evaluated. The interaction parameters were continually adjusted until the objective function was minimised. The set of binary interaction parameters corresponding to this minimum were considered to be the optimum for the given experimental conditions. This procedure was repeated for each set of experimental data.

6.2.2 Optimisation Routine

The Simplex Method developed by Spendley, Hext and Himsworth in 1962 and further refined by Nelder and Mead in 1965 was used as the routine to modify the interaction parameters (Edgar, 1988). A simplex, a regular geometric figure, is constructed with n+1 vertices, where n is the number of parameters, x, in the function f(x) to be optimised. For example, when n = 2, a two dimensional simplex or triangle is constructed, in three dimensions (n = 3), a regular tetrahedron is formed. The routine then calculates the value of f(x) at each of the vertices to determine which vertex has the maximum value. The

routine determines a new vertex which moves the search away from the maximum value. The procedure is repeated until the difference between the objective function at each of the vertices is within a set tolerance.

6.2.3 Optimisation Results

Binary interaction parameters were regressed for six sets of operating conditions using the experimental data presented in Chapter Four. The resulting pseudocomponent/ethane interaction parameters are shown in Table 6.2 along with the average and standard deviation for each pseudocomponent.

Temperature, °C	Pressure, MPa	Interaction Parameters, k_{ij}				
		PC1	PC2	PC3	PC4	PC5
37	10.5	0.0051	0.0434	0.0494	0.0640	0.1463
47	10.5	0.0050	0.0430	0.0410	0.0874	0.1500
63	10.5	0.0060	0.0419	0.0447	0.0891	0.1525
47	7.3	0.0040	0.0330	0.0377	0.1051	0.1700
47	12.2	0.0064	0.0427	0.0444	0.0842	0.1366
47	15.0	0.0060	0.0491	0.0500	0.0890	0.1410
Average		0.0054	0.0422	0.0445	0.0865	0.1494
Standard Deviation		0.0009	0.0052	0.0047	0.0132	0.0116

Table 6.2 – Interaction parameters regressed for the operating conditions studied.

The interaction parameters shown in Table 6.2 are consistent with parameters for similar systems found in the literature. Walas reported that interaction parameters usually range from 0 to 0.2 (Walas, 1985). Mehrotra et al. used interaction parameters to predict the

solubility of ethane in Peace River bitumen at subcritical conditions (Mehrotra et al., 1985). Using four pseudocomponents, they found that the interaction parameters ranged from 0 for the lightest component to 0.1 for the heaviest. The interaction parameters in Table 6.2 are of the same order of magnitude as the interaction parameters reported by Mehrotra et al. and fall within the range suggested by Walas.

The interaction parameters listed in Table 6.2 are based on the experimental data and the characterisation data presented in Chapter Five. As a result, any errors implicit to the model or the characterisation will be built into the regressed interaction parameters. Hence, it may be difficult to generalise these interaction parameters in order to use them to model other fluid systems.

6.2.4 Calculation of Interaction Parameters

Interaction parameters for the bitumen/ethane system were calculated using the correlation developed by Trebble et al. (Trebble et al., 1990). The binary interaction parameter equation was developed for systems in which the lighter component was a supercritical fluid. The equation uses the critical volumes, dipole moments and quadrupoles of the components to calculate the interaction parameter. The equation is as follows:

$$(1 - k_{ij}) = \left[\frac{V_{ci}V_{cj}}{V_{cij}^2}\right]^{\varphi} - \eta\left[\frac{V_{ci}\mu_j^2 + V_{cj}\mu_{ci}^2}{V_{cij}^2} + \frac{1.5(V_{ci}Q_j^2 + V_{cj}Q_i^2)}{V_{cij}^{8/3}}\right] \qquad \text{Equation 6.18}$$

where, V_c is the critical volume, Q is the quadrupole, μ is the dipole moment and V_{cij} was a combined critical volume found by using Equation 6.19:

$$V_{cij} = \left[\frac{V_{ci}^{1/3} + V_{cj}^{1/3}}{2} \right]^3 \qquad \text{Equation 6.19}$$

In Equation 6.18, both η and φ were optimised to fit regressed binary interaction parameters for 78 systems comprised of 28 different compounds. Trebble et al. found that bubble point pressure data could be reproduced using the interaction parameters from their model with an average deviation of 5.66% using values for η and φ of 0.2 and 90 $\mu J^{-1}mol^{-1}$, respectively.

Both the data for the five pseudocomponents used to characterise the Peace River bitumen and the ethane were used in Equation 6.18 to calculate interaction parameters. The quadrupole for ethane was set as $-0.206\ \mu J^{1/2}cm^{3/2}$ and the dipole moments for the pseudocomponents and ethane were set to zero as recommended by Trebble (Trebble et al., 1990). The results are shown in Table 6.3 along with the average interaction parameters determined by the procedure outlined in Section 6.2.2.

	Interaction Parameters				
	PC1	PC2	PC3	PC4	PC5
Trebble	0.033	0.041	0.051	0.065	0.120
Averaged	0.0054	0.0422	0.0445	0.0865	0.1494

Table 6.3 – Interaction parameters calculated using the Trebble correlation and the average values from the regression procedure.

The results of the two methods for determining interaction parameters are quite similar. The greatest discrepancy exists between the interaction parameters for the lightest pseudocomponent, while the other parameters show good agreement.

6.3 Simulation Results

The simulations were re-run using the interaction parameters presented in Table 6.3 in order to observe the accuracy of the simulation when averaged interaction parameters were used in the flash routine. The averaged interaction parameters were used to predict extraction curves beyond the temperature range of the data, i.e. to test the ability of the simulation to extrapolate extraction data. The simulation was also run using the parameters calculated using the Trebble correlation. These results were compared to both the experimental data and the curves produced using the averaged parameters.

6.3.1 Comparison With Experimental Data

Figure 6.7 and Figure 6.8 show the results from simulations performed using the averaged interaction parameters. These figures show the cumulative weight percent of bitumen extracted as a function of cumulative ethane volume measured experimentally and predicted by the simulation. The extraction curves for experiments performed at a constant pressure of 10.5 MPa and temperatures ranging from 37 to 63°C are shown in Figure 6.7, while the results from the constant temperature extractions and different pressures are presented in Figure 6.8. It should be noted that the magnitude of the error bars shown on these figures is ±10% of the predicted data in order to give an indication of the accuracy of the model.

Using the averaged interaction parameters, the simulation was capable of reproducing the experimental extraction data with a percent average absolute relative percent deviation of 13%. The %AARD was calculated using the following equation:

$$\%AARD = \left(\frac{M_{ext}^{calc} - M_{ext}^{expt}}{M_{ext}^{expt}} \right) * 100 \qquad \text{Equation 6.20}$$

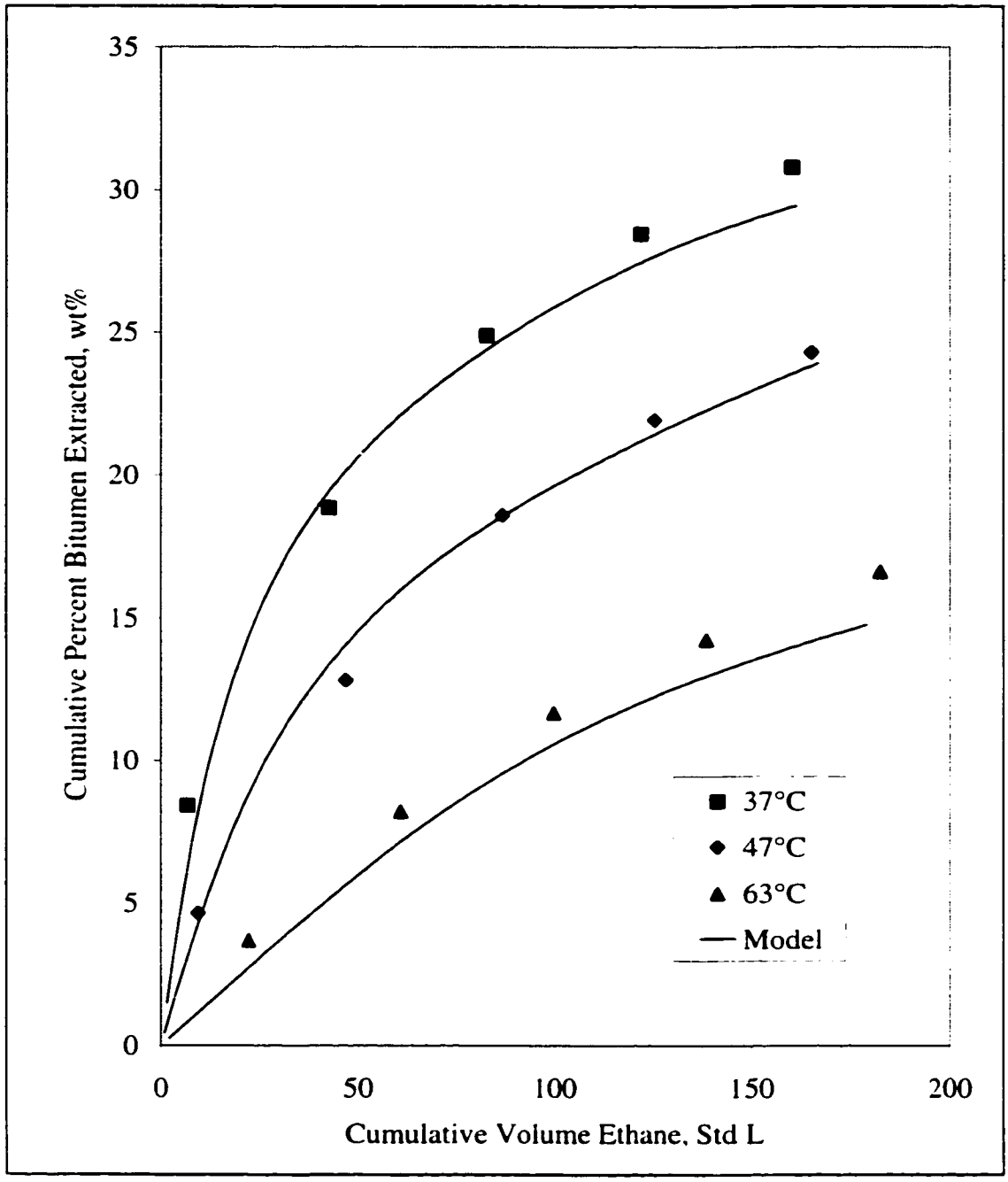

Figure 6.7 – Experimental and simulation extraction curves for a constant pressure of 10.5 MPa and temperatures ranging from 37 to 63°C.

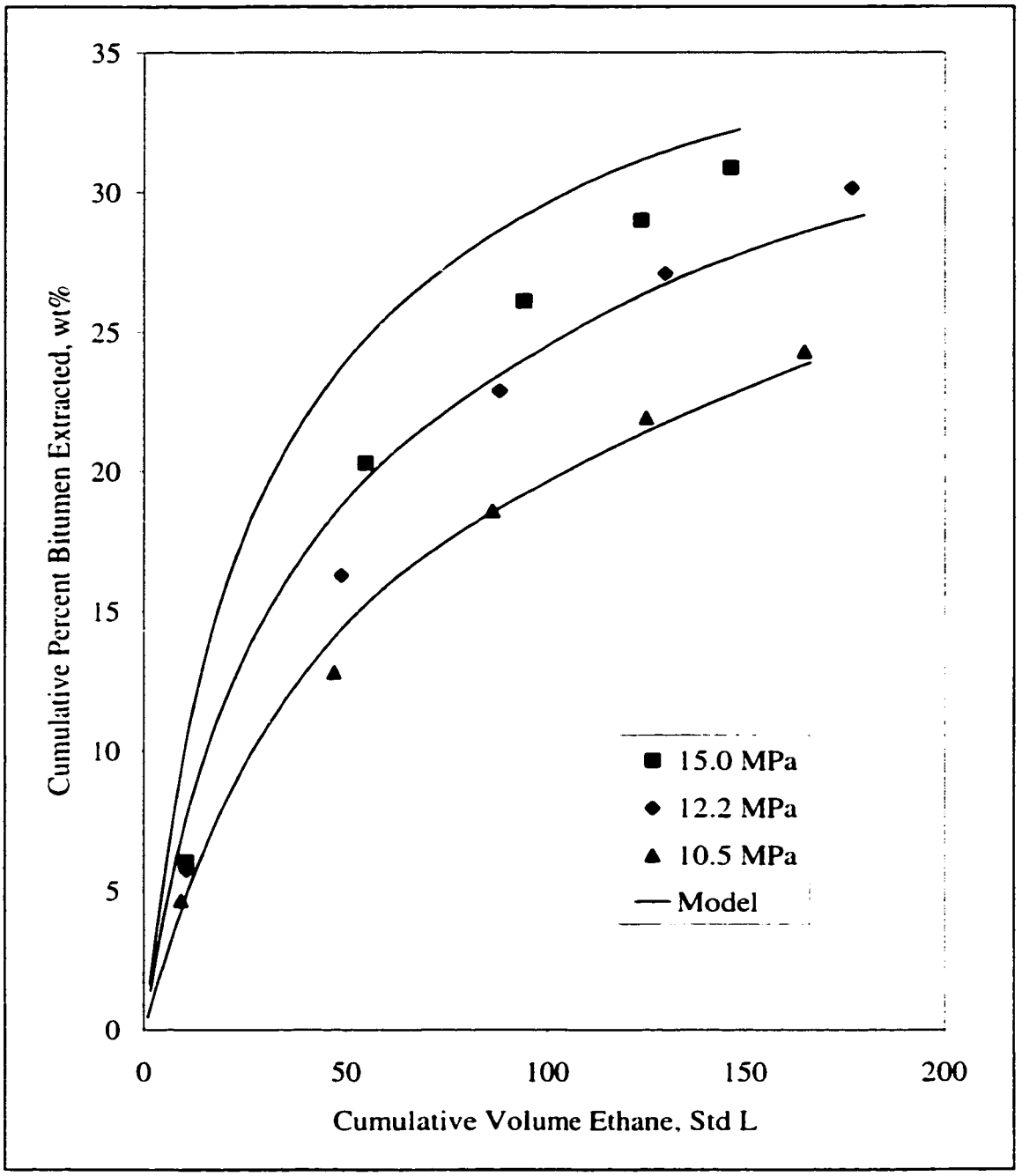

Figure 6.8 - Experimental and simulation extraction curves for a constant temperature of 47°C and pressures ranging from 10.5 to 15.0 MPa.

Where, M_{ext}^{expt} is the mass of bitumen extracted for a given amount of ethane measured experimentally. M_{ext}^{calc} is the mass of bitumen predicted by the model to be extracted using the same volume of ethane as for M_{ext}^{expt}.

The model predicted the composition of the extracted oil with a %AARD in the predicted compositions of 24.8%. The error in the mole percents greater than 0.1 mol% was 15%. The error associated with the overall composition was much higher because the model consistently under predicted the mole percent of the two heaviest pseudocomponents. These values were quite low, typically 0.01 or smaller and the model usually predicted that the heaviest pseudocomponents were insoluble in supercritical ethane under the extraction conditions. As a result, the relative error for these components was 100%. While these components constituted only a small fraction of the extracted oil, the error associated with their compositions had a significant impact on the overall error in the composition results. Table 6.4 provides examples of the composition results predicted by the model as compared to the experimentally measured compositions. The complete set of compositional data is presented in Appendix E.

	Window 1			Window 3			Window 5		
	Expt.	Calc.	% Error	Expt.	Calc.	% Error	Expt.	Calc.	% Error
PC1	3.42	2.92	13.45	1.33	1.37	3.01	0.84	0.75	10.71
PC2	2.58	3.01	18.99	1.24	1.65	33.06	0.87	1.25	43.68
PC3	0.95	0.84	9.47	0.48	0.38	18.75	0.36	0.28	22.22
PC4	0.27	0.11	59.26	0.14	0.04	71.43	0.11	0.03	72.73
PC5	0.08	0.00	100.00	0.04	0.00	0.00	0.03	0.00	100.00
Ethane	92.7	93.1	0.35	96.8	96.6	0.23	97.8	97.7	0.11
Avg.			33.59			37.75			41.58

Table 6.4 – Predicted and experimental mole percents for the oil extracted at 47°C and 10.5 MPa.

The model was used to predict extraction curves for two sets of conditions beyond the temperature range at which data was used for the interaction parameter regression. The simulation was run using the averaged interaction parameters at a pressure of 10.5 MPa and two temperatures, 78 and 93°C. The results from these simulations are shown in Figure 6.9 where both the experimental and predicted extraction curves are plotted.

The results show that the model was capable of accurately predicting data for the extraction process beyond the range for which the interaction parameters were developed. The average absolute relative deviation between the experimental and predicted values for the amount of bitumen extracted were calculated for both temperatures. The %AARD for the 78°C data was 11.2% while for 93°C the %AARD was 21.0%. The compositions of the extracted oil for the first window was measured for both temperatures and the results are shown in Table 6.5.

	78°C		93°C	
	Expt.	Calc.	Expt.	Calc.
PC1	0.0047	0.0063	0.0270	0.0039
PC2	0.0028	0.0033	0.0246	0.0018
PC3	0.0004	0.0003	0.0098	0.0001
PC4	0.0000	0.0000	0.0035	0.0000
PC5	0.0000	0.0000	0.0017	0
Ethane	0.9918	0.9901	0.9335	0.9942
%AARD		14.18		22.34

Table 6.5 – Composition of the oil extracted during the first window at 10.5 MPa and 78 and 93°C.

The simulation predicted the compositions for these samples with %AARD's of 14.2% and 22.3% at 78 and 93°C, respectively. Thus, as the extraction temperature was

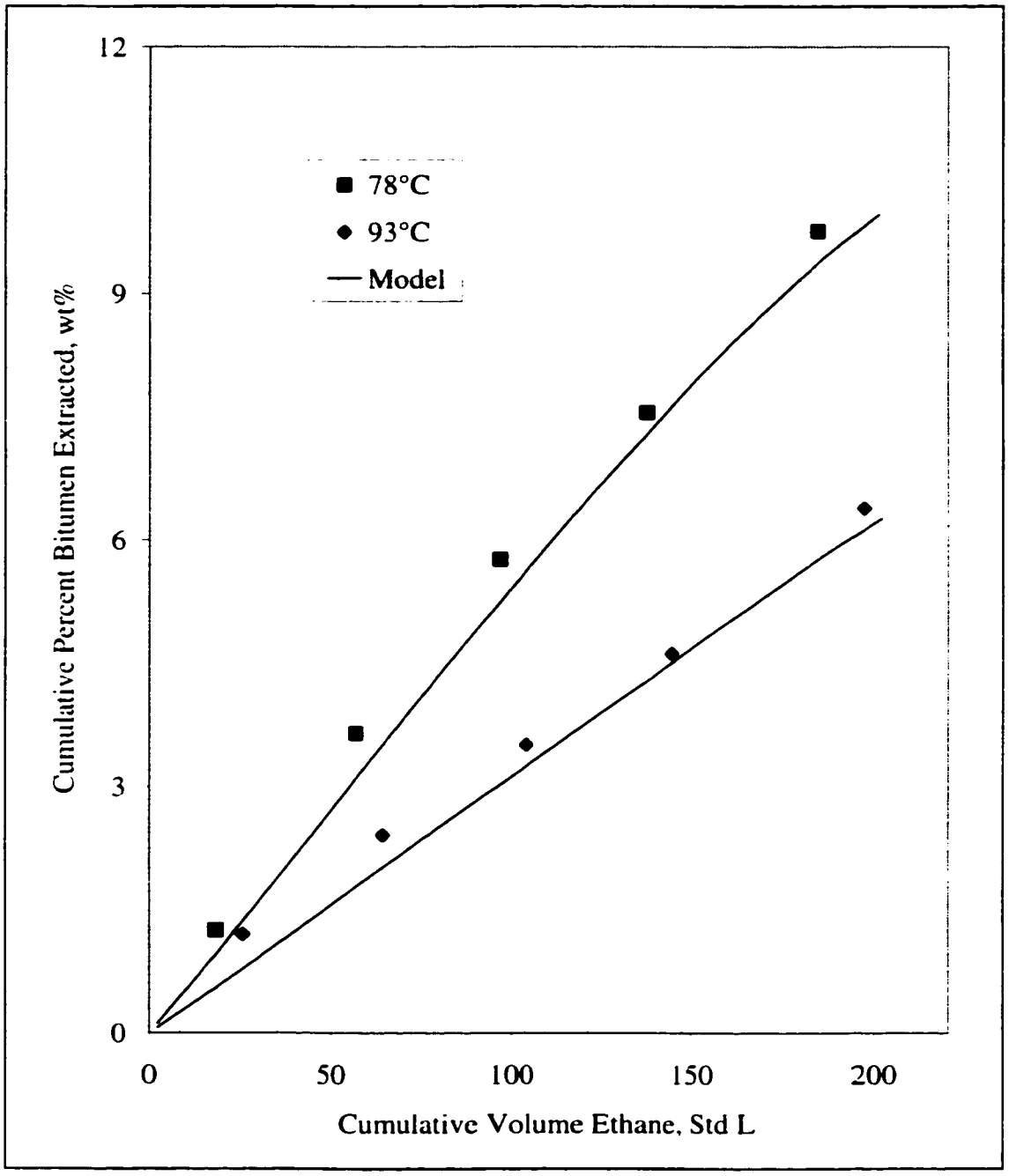

Figure 6.9 – Experimental and predicted extraction curves for a pressure of 10.5 MPa and temperatures of 78 and 93°C.

increased further out of the range for which the parameters were regressed, the errors in the model for both extraction curves and compositions increased.

In Section 4.7 the effect of changing the amount of bitumen/sand mixture packed into the extractor was experimentally measured. The results showed that a single continuous extraction curve was produced when the results were plotted as the cumulative mass percent extracted as a function of the cumulative volume of ethane divided by the initial mass of bitumen in the feed. These conditions were simulated using the model with the averaged binary interaction parameters from Table 6.2. The results are shown in Figure 6.10.

The model results were for extractions performed at 47°C and 10.5 MPa and different masses of bitumen. These results clearly show that the model was capable of matching the experimental data. The predicted extraction data falls within ± 10% of the experimental data.

The model's overall performance is excellent considering the myriad of potential sources for error, existing in both the experimental data and the model results. As discussed in Chapter 3, the experimental apparatus had systematic and random errors of 0.078% and 2.89%, respectively. Uncertainties in the extrapolation of the boiling point curve, the number of pseudocomponents chosen to characterise the bitumen and the calculation of critical properties, acentric factors and molecular weights all contributed to the errors in the model results. Even with these potential sources of error, on average the predicted results agreed to with experimental data to within 15%.

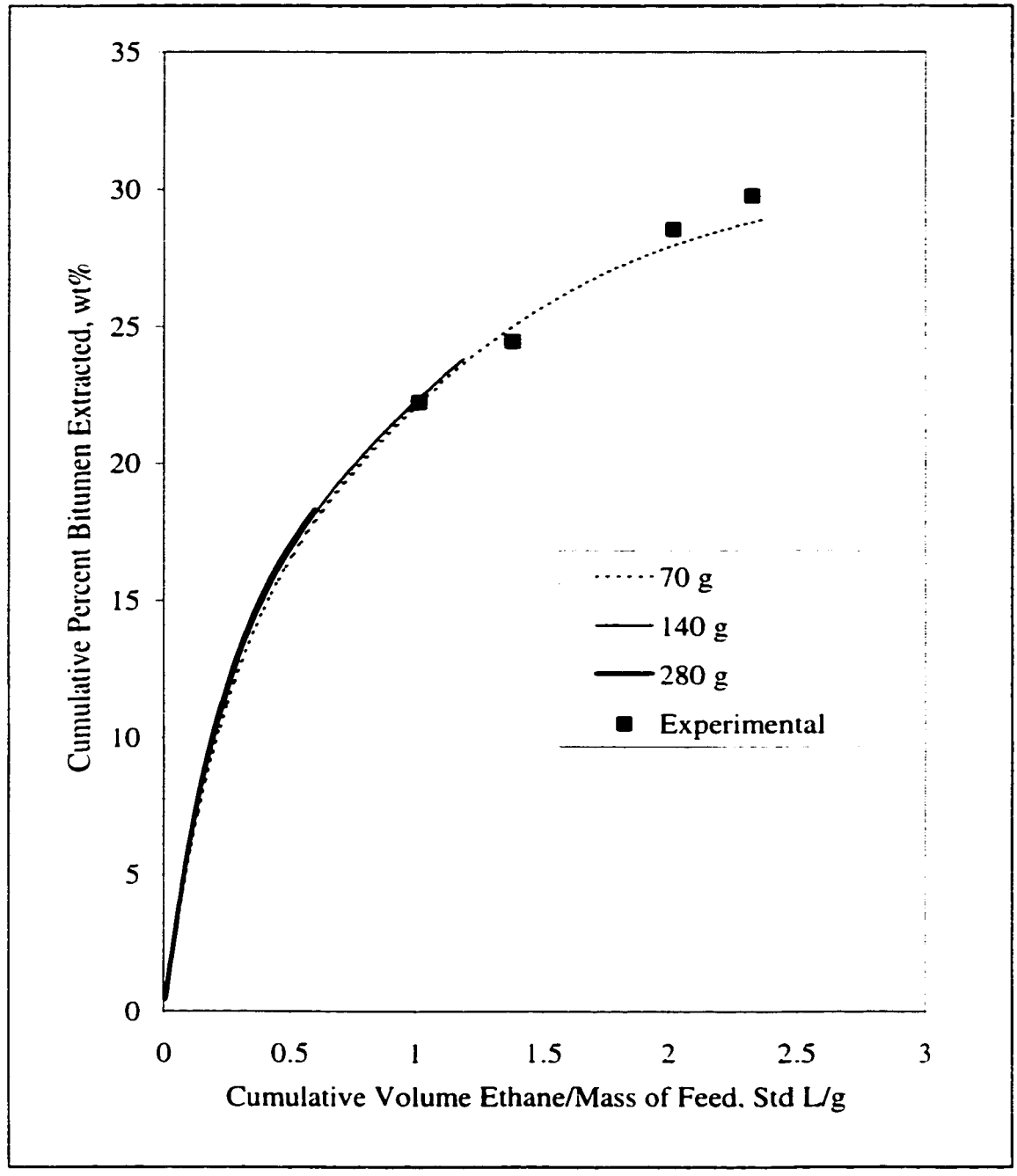

Figure 6.10 – Extraction curves produced for different amounts of bitumen feed at an extraction temperature of 47°C and 10.5 MPa.

6.3.2 Behaviour Within the Extractor

The model provided a reasonable idea of how the composition of the solvent phase changes as it flows through the extractor. Profiles of the amount of oil extracted per stage are shown in Figure 6.11. The data shows that at the beginning of the extraction, the largest amount of bitumen was extracted and that the majority of the bitumen was recovered from the first sections of the extractor. The amount of bitumen extracted from the first stage continually declined over the duration of the extraction, indicating that the bottom of the extractor was being depleted of extractable bitumen first as would be expected. This model prediction was routinely verified when the extractor was cleaned at the end of a experiment. The bitumen/sand mixture at the bottom of the extractor was much harder and more difficult to clean than higher up in the extractor indicating that the lighter components had been removed.

The amount of bitumen extracted from a given section reached a maximum at different times over the course of the extraction. In other words, the section at which the maximum occurred continually moved up the extractor as time increased. An interesting trend was observed in the increased amount of bitumen extracted at extraction times of 30 and 40 min. This observation points to the dynamic nature of the solvent-rich phase as it passed through the extractor. For example, the data at 30 minutes shows that there was an increase in the amount of bitumen extracted after Section 7. This increase may have occurred because the bitumen that had been extracted in the earlier stages changed the properties of the solvent phase enhancing its solvent properties. Therefore, the solvent was capable of extracting more bitumen in the later stages than it had been in the earlier sections.

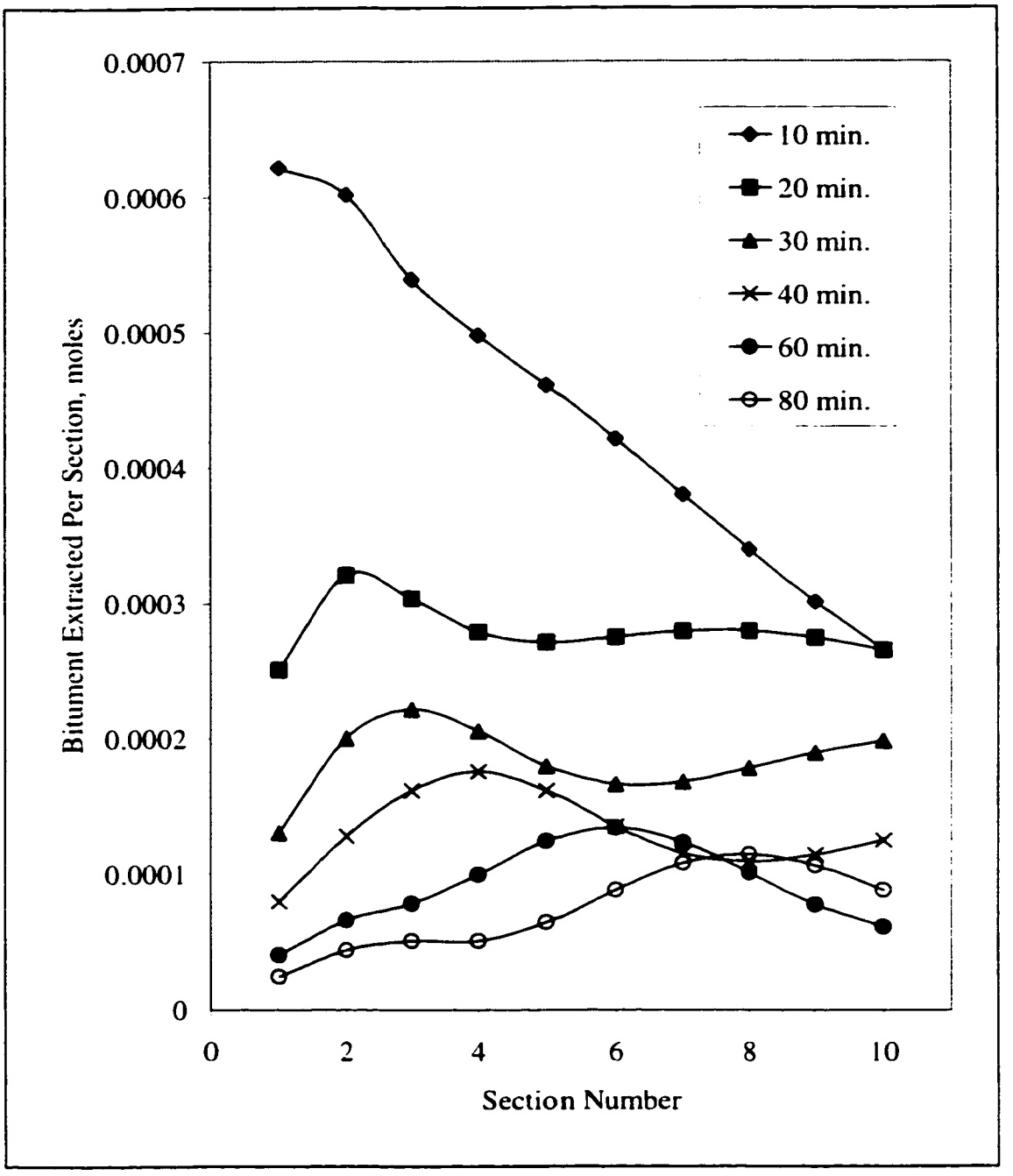

Figure 6.11 – Moles of bitumen extracted per section at different times during the course of the extraction process.

6.3.3 Trebble Binary Interaction Parameters

The binary interaction parameters calculated earlier in Section 6.2.4 using the Trebble correlation were used in the simulation to predict the extraction curves. The results from four different extraction conditions are shown in Figure 6.12 and Figure 6.13. The simulation consistently underpredicted the amount of oil that was extracted for a given volume of ethane by an average of 37.2%. The composition of extracted oil were also predicted and the average absolute relative deviation was 19.2% for compositions greater than 0.1 mole percent.

These results can be explained by examining the nature of the components used in the development of Equation 6.18. The two heaviest components used by Trebble et al. were n-decane and hexadecane while the majority of the heavier hydrocarbons used in the development of Equation 6.18 had carbon numbers in the 6 to 9 range. While hexadecane was the only component that had a molecular weight close to the lighter pseudocomponents used in this work, it was still significantly lighter than the heaviest pseudocomponents. Therefore, the systems for which Equation 6.18 accurately predicted interaction parameters are significantly lighter and behave somewhat differently than the bitumen system used in this study.

As a result, some of the interaction parameters predicted using Equation 6.18 were quite different from the parameters regressed using experimental data. The most notable were the interaction parameters for ethane and PC5 and ethane and PC1. The combination of a low interaction parameter for ethane/PC5 and a high parameter for ethane/PC1 resulted in a large reduction in the predicted amount of bitumen extracted using supercritical ethane.

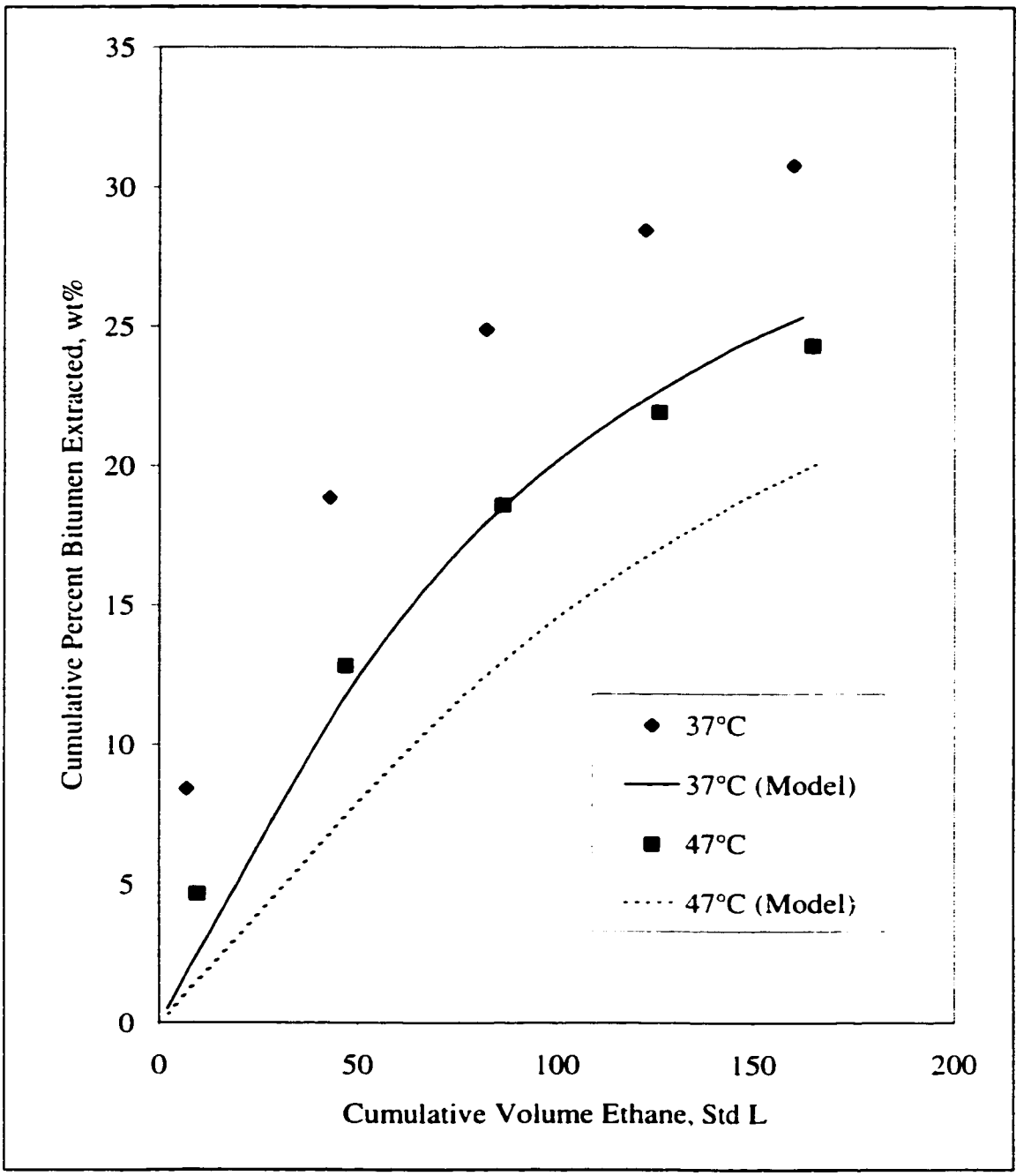

Figure 6.12 – Extraction curves predicted using the Trebble binary interaction parameters for a pressure of 10.5 MPa and temperatures of 37 and 47°C.

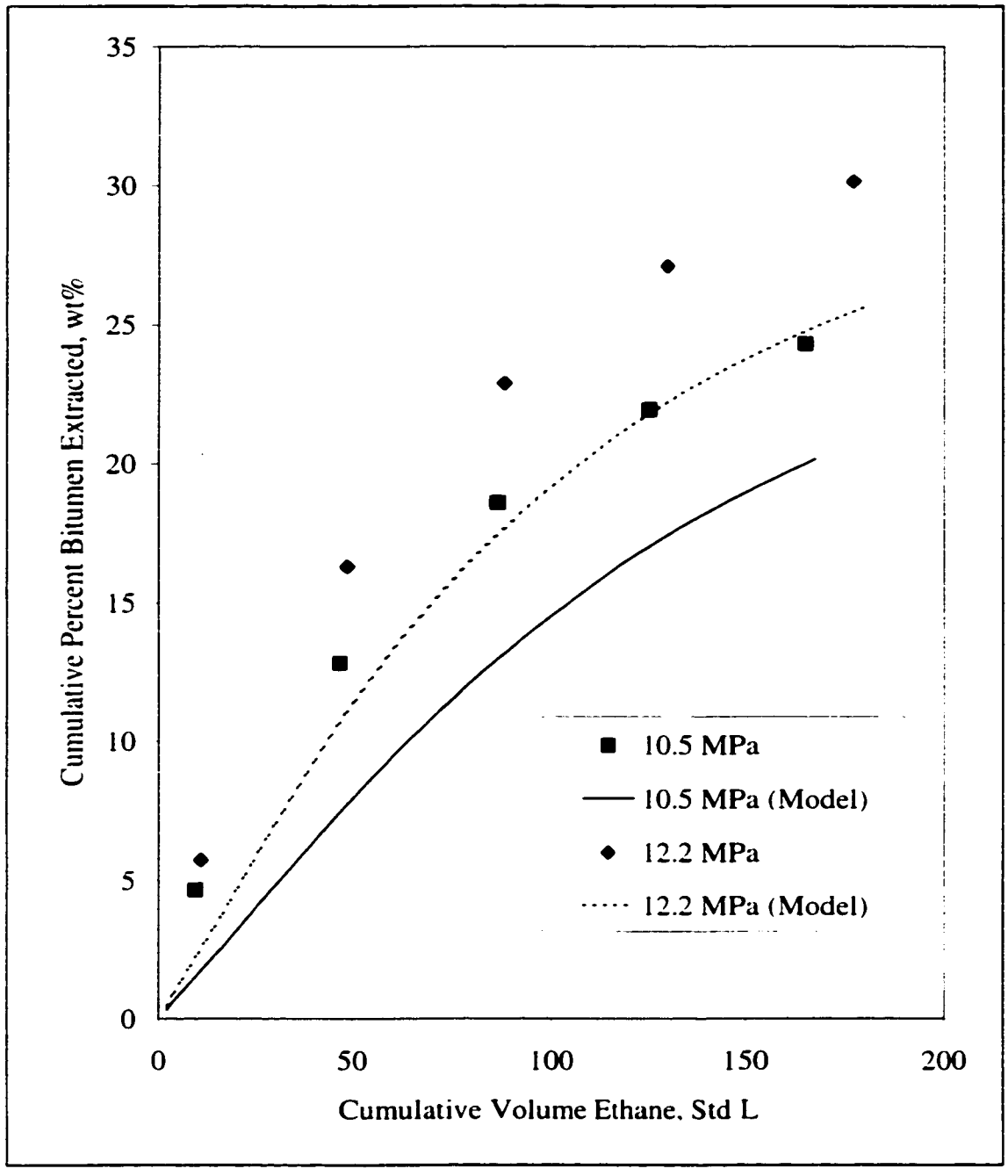

Figure 6.13 – Extraction curves predicted using the Trebble binary interaction parameters for a temperature of 47°C and pressures of 10.5 and 12.2 MPa.

6.4 Sensitivity Analysis

Experimental data has an inherent degree of uncertainty. For example, the operating temperature was not held to a fixed value over the complete extraction process but had an average standard deviation of ± 0.45°C. The binary interaction parameters used to predict the extraction behaviour in the previous section were averages of the six sets of optimised parameters. Therefore, it is useful to know which parameters have the greatest impact on model results. The sensitivity of the simulation results to variations in input data such as these is the topic of this section.

6.4.1 Variations in Temperature and Pressure

There were slight variations in the operating temperature and pressure over the course of all of the extractions performed. The average standard deviation for the extraction temperature and pressure reported in Chapter Four were ± 0.45°C and ± 0.04 MPa, respectively. The simulations were re-run adjusting the average operation conditions by one standard deviation. The results were used to calculate a percent difference between the results for the adjusted condition and the average value. The percent difference was calculated using the following equation:

$$\% \text{ Difference} = \sum_{i=1}^{N} \left(\frac{M_{ext,i}^{\pm 1\sigma} - M_{ext,i}^{avg}}{M_{ext,i}^{avg}} \right) * 100\% \qquad \text{Equation 6.21}$$

where N is the number of data points for a given extraction, $M_{ext}^{\pm\sigma}$ is the extracted mass calculated at a temperature or pressure plus or minus one standard deviation and M_{ext}^{avg} is the mass determined at the average operating conditions. The results are shown in Figure 6.14.

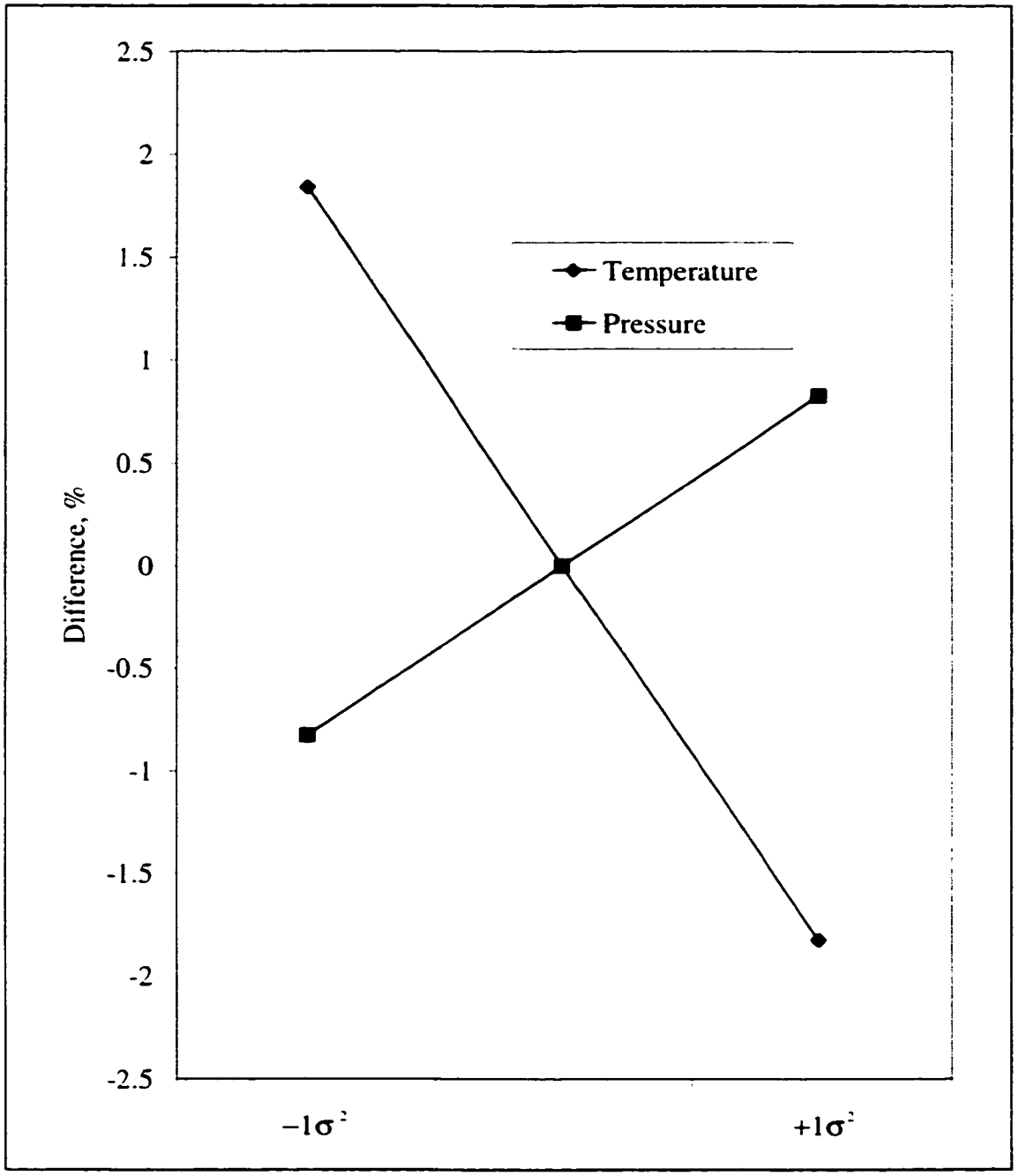

Figure 6.14 – Sensitivity of the model to changes in the extraction temperature and pressure.

Figure 6.14 shows that the simulation results are not overly sensitive to minor variations in either the temperature or pressure that occurred during the experimental process. Pressure changes of ± one standard deviation caused the model results to differ by less than 1%, while similar changes to the temperature caused the model results to vary by less than 2%. Therefore, uncertainty in the reported temperature and pressure had only a minor impact on the model results.

6.4.2 Number of Sections and Size of Time Steps

In order to simulate the supercritical extraction process, the extractor was divided into ten equal volume sections. Each of these subsections was modelled as a completely mixed stage with the solvent-rich phase entering at the bottom and moving up through successive sections. The number of sections chosen influences simulation performance in two ways. As the number of sections increased the difference between results for different numbers of sections became smaller. This is analogous to the behaviour that occurs when the number of continuous stirred tank reactors in series increases and the results approach that of a plug flow reactor. Unfortunately, as the number of sections increases so does the computational time required to complete the simulation. Computational time was an important consideration in this work due to the large number of iterations required to optimise the binary interaction parameters. Therefore, an optimum number of extractor sections was found that provided a compromise between the accuracy of the results and limiting the computational time.

Figure 6.15 shows the results of varying the number of extractor sections used by the extraction model. The extraction curves shown in this figure are for operating conditions of 47°C and 10.5 MPa and for three different numbers of extractor sections: 5, 10 (base case) and 15 are shown. As the number of segments increased, the results predicted by the model began to converge. The percent deviation between the 15 section results and

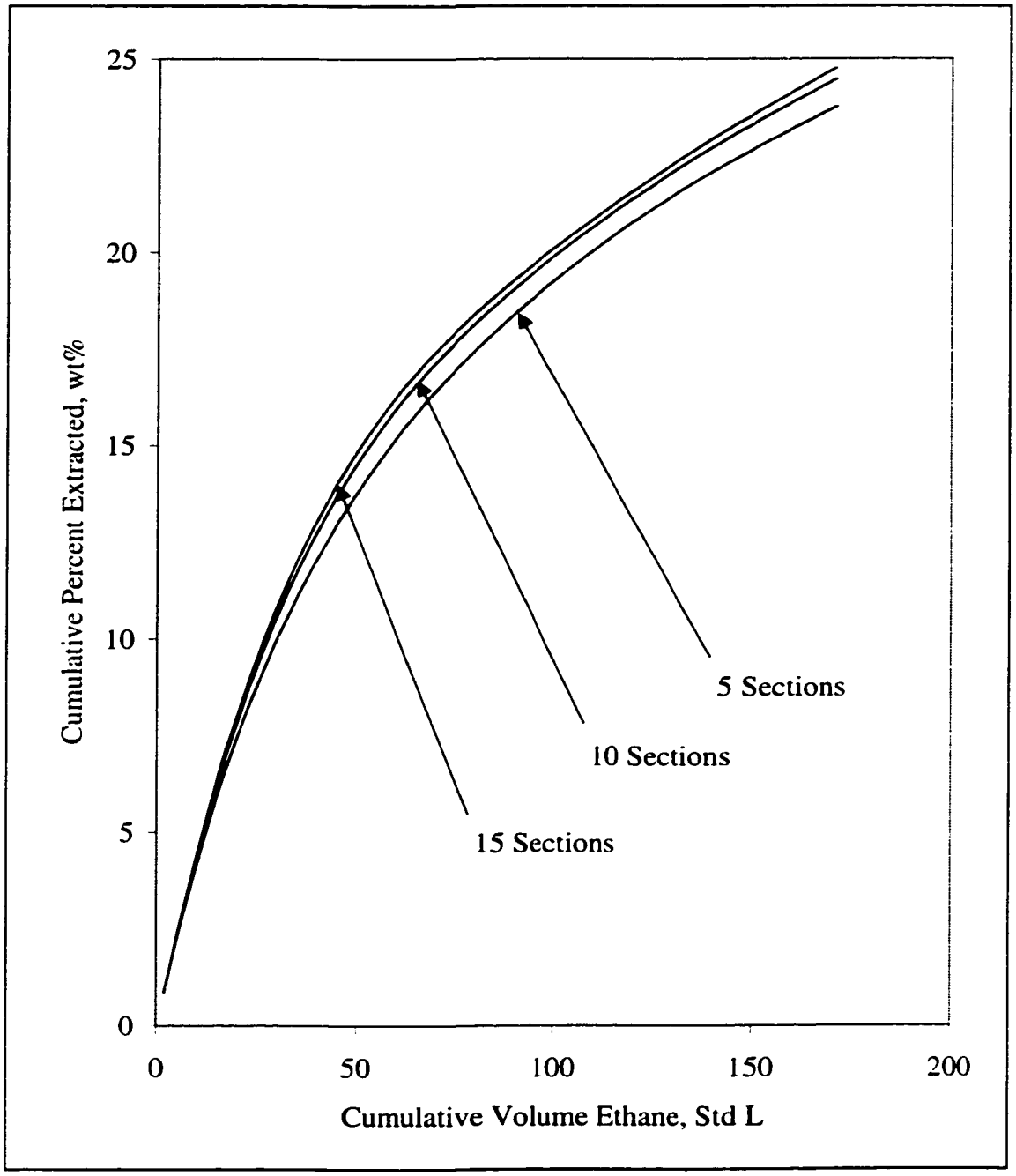

Figure 6.15 – Effect of varying the number of sections used by the model to predict the extraction curve for 47°C and 10.5 MPa.

the 10 section results was 1.3% while the deviation between the results obtained using 5 and 10 extractor sections was 3.6%.

The computational time required to complete a simulation increased as the number of extractor sections was increased. For 5 sections, the computational time was 5.93 min., which increased to 6.93 min. for 10 sections and finally to 9.23 min. for 15 sections. It should be noted that all computational times were measured using a Pentium II 333 MHz computer and Version 5.0 of Matlab®. The length of time required for the simulation increased as the number of sections increased because the number of flash calculations increased proportionately. These results show that 10 extractor sections was a suitable choice because the computational time was reduced without compromising the accuracy of the results.

The effect of varying the time step size on the predicted results was also evaluated. The size of the time step and the solvent flow rate determine the amount of ethane fed to the extractor during the simulation of the extraction process. The larger the time step, the greater the amount of ethane added per iteration. Thus the simulation would reach the ethane upper limit more quickly and the simulation would be halted. The size of the time step also determines the number of flash calculations to be performed. The smaller the time step, the greater the number of calculations.

The results from varying the time step size are shown in Figure 6.16. The same operating conditions as those used to evaluate the impact of the number of extractor sections were used. The simulations were performed using time steps of 0.5, 1.0 (base case) and 2.0 minutes. The results show that as the time step was decreased, the extraction curves began to converge. This was reflected by the fact that the percent deviation was only 0.9% between time steps of 0.5 and 1.0 min. but increased to 1.8% when the time step was increase to 2.0 min.

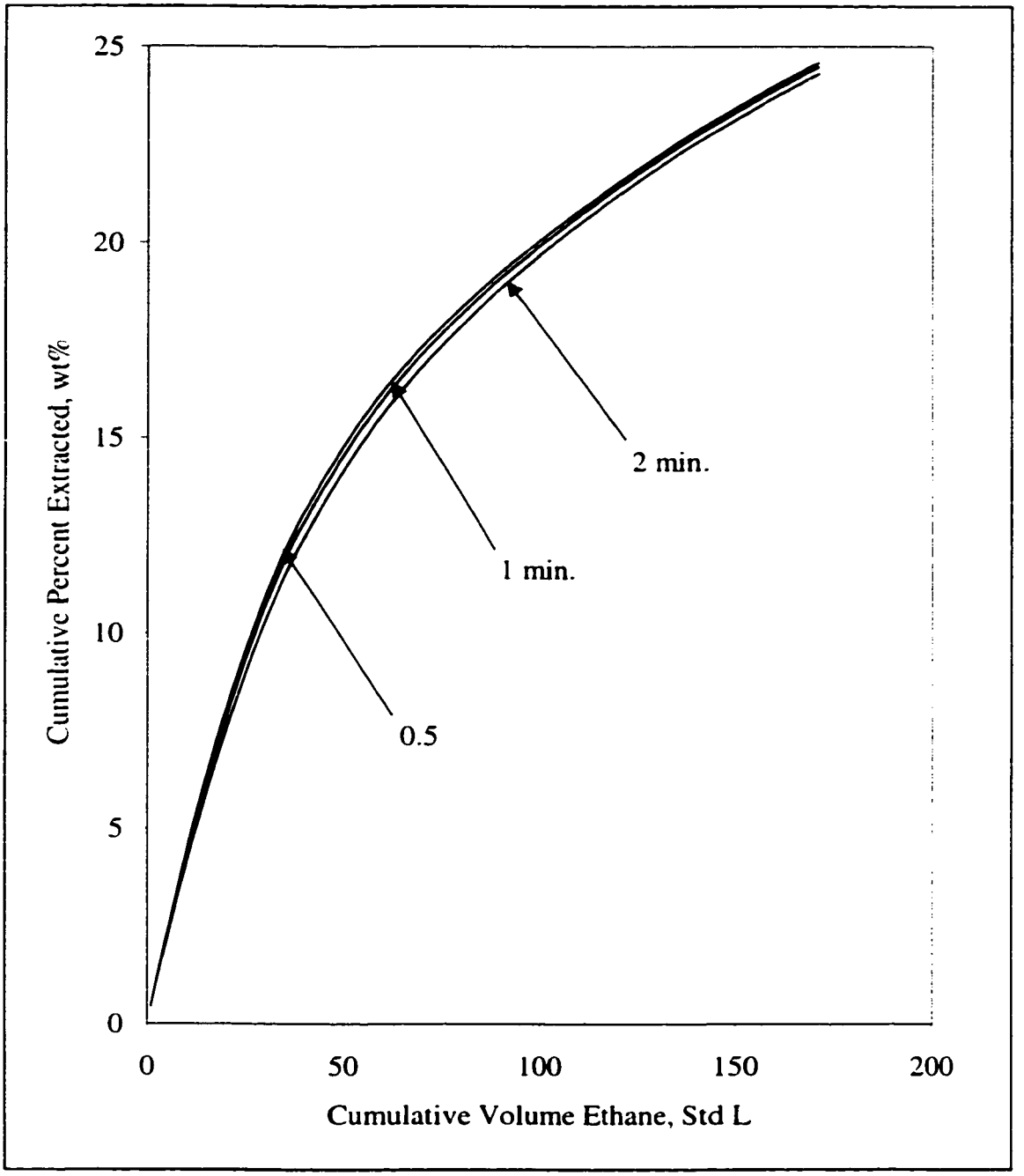

Figure 6.16 - Effect on the extraction curve for 47°C and 10.5 MPa of varying the size of the time steps used when modelling the extractor with ten sections.

Decreasing the time step size resulted in the simulation time increasing from 3.5 min. for a step size of 2 min. to over 17 min when the time step was 0.5 min. Therefore, an optimum time step size was chosen to reduce the computational time while maintaining the accuracy of the results. For this study, it appeared that a time step size of 1 minute was a suitable value meeting this criteria.

6.4.3 Variation in Interaction Parameters

An analysis was done to determine the sensitivity of the simulation results to changes in the interaction parameters. The effect of the interaction parameters on extraction results was observed by rerunning the simulation with one parameter changed by ± one standard deviation while the others were kept constant. The results from these runs are summarised in Figure 6.17. The percent differences were calculated using Equation 6.21.

The results show that the simulation was most sensitive to the interaction parameters for the second and fifth pseudocomponents. The second and fifth pseudocomponents represent the two largest segments of the bitumen at 16.04 and 55.84 wt%, respectively. Therefore, as expected, changes in either of these two parameters would have the most significant impact on the equilibrium.

These results also explain why, when the binary interaction parameters calculated using Trebble's correlation were incorporated into the simulation, the extraction curves were consistently under predicted. Figure 6.17 shows that when the interaction parameter for PC5 was low, the simulation under predicted the amount of bitumen extracted. The other interaction parameter that was quite different from the regressed parameters was the interaction parameter for ethane and PC1. However, Figure 6.17 shows that changes in this parameter had little impact on model results. Therefore, the major reason that the

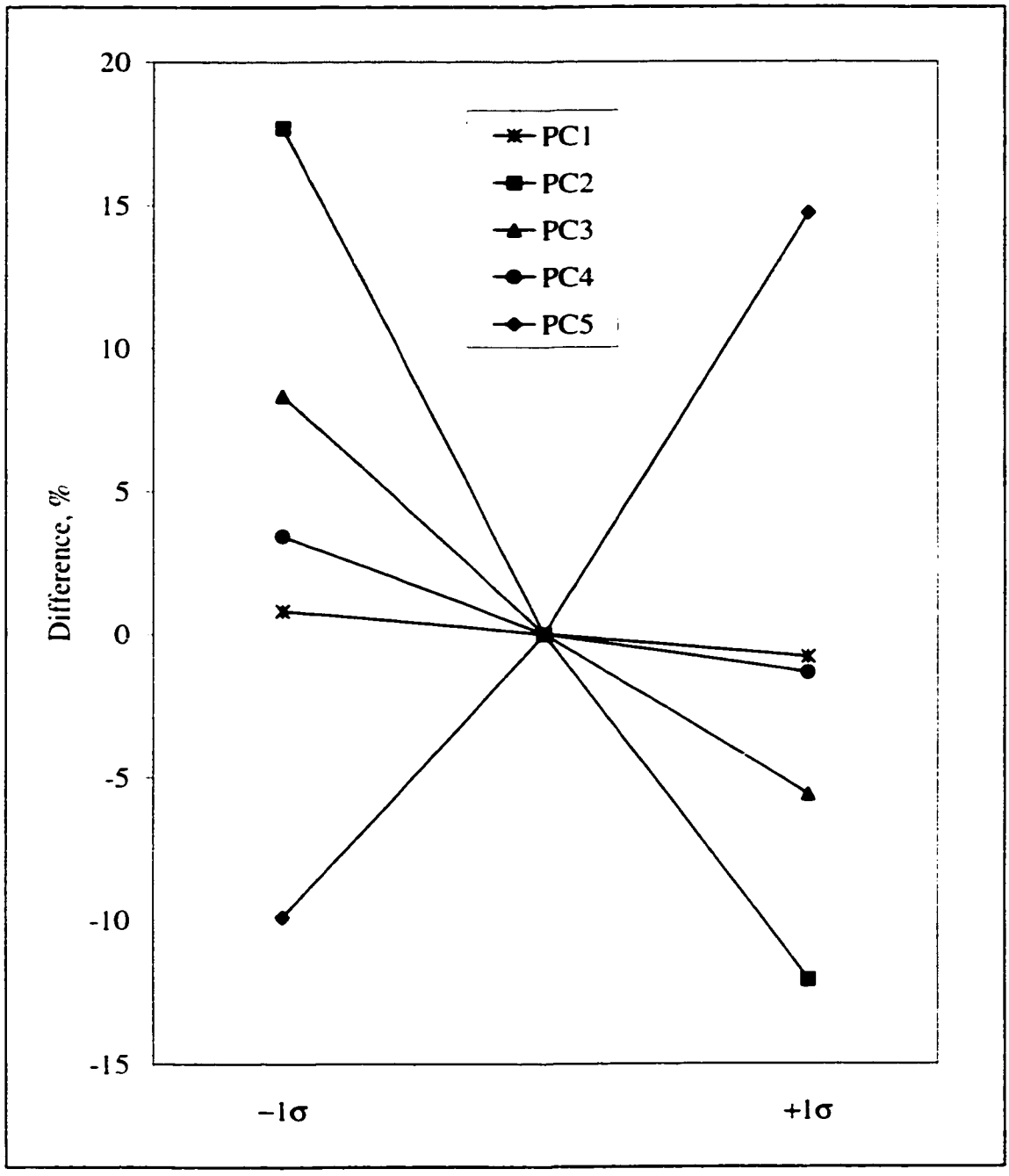

Figure 6.17 – Sensitivity of the simulation to changes in the binary interaction parameters.

results were under predicted using the Trebble correlation parameters was the prediction of the fifth interaction parameter that was too small.

6.5 Kesler-Lee Critical Properties

In Chapter 5, three methods were used to calculate the critical properties for the five pseudocomponents used to characterise the Peace River bitumen. The results from the Twu method appeared to characterise the bitumen the most accurately and thus were used in the thermodynamic calculations thus far. While the Twu data was found to be the most accurate, the Kesler-Lee correlations gave results that were also quite reasonable. Therefore, the optimisation routine was run using data at one extraction condition and the Kesler-Lee critical properties to determine how the binary interaction parameters would change if different critical properties were used for the Peace River pseudocomponents.

The optimisation routine was run using experimental data obtained at 47°C and 10.5 MPa. The interaction parameters resulting from the Twu and Kesler-Lee correlations are compared in Table 6.6.

	Kesler-Lee	Twu
PC1	0.0194	0.0050
PC2	0.0744	0.0420
PC3	0.0765	0.0420
PC4	0.0919	0.0874
PC5	0.1620	0.1500

Table 6.6 – Optimised binary interaction parameters using Twu and Kesler-Lee critical properties.

Table 6.6 shows that the optimal binary interaction parameters differed greatly depending on which set of critical property correlations was used in the simulation. The difference in the extraction curves for the two sets of data are evident in Figure 6. 18. This suggests that care must be taken to ensure that the critical properties selected to model phase behaviour for a bitumen or heavy oil system are the same as those used to calculate the interaction parameters for mixtures.

6.6 Summary

A computer program capable of modelling the extraction of Peace River bitumen using supercritical ethane was written. The simulation model used the Peng-Robinson equation of state to determine the phase behaviour of the system. Liquid densities predicted by the equation of state were improved by translating the value predicted using the method proposed by Kokal et al. The successive substitution method was used to update the equilibrium constants in the flash routine.

The model was used as the basis for determining a set of optimum binary interaction parameters for the ethane/pseudocomponent pairs. A set of parameters was found which was capable of predicting the extraction curves for a wide range of temperature and pressure conditions. The model was capable of predicting the process beyond the conditions for which the interaction parameters were determined though the accuracy decreased further away from the regressed data region.

Using optimised interaction parameters, the model was capable of predicting the extraction yields with an %AARD of 13.8%, and for component compositions greater than 0.1 mol% to within 15%. The model also provided results for changes in the amount

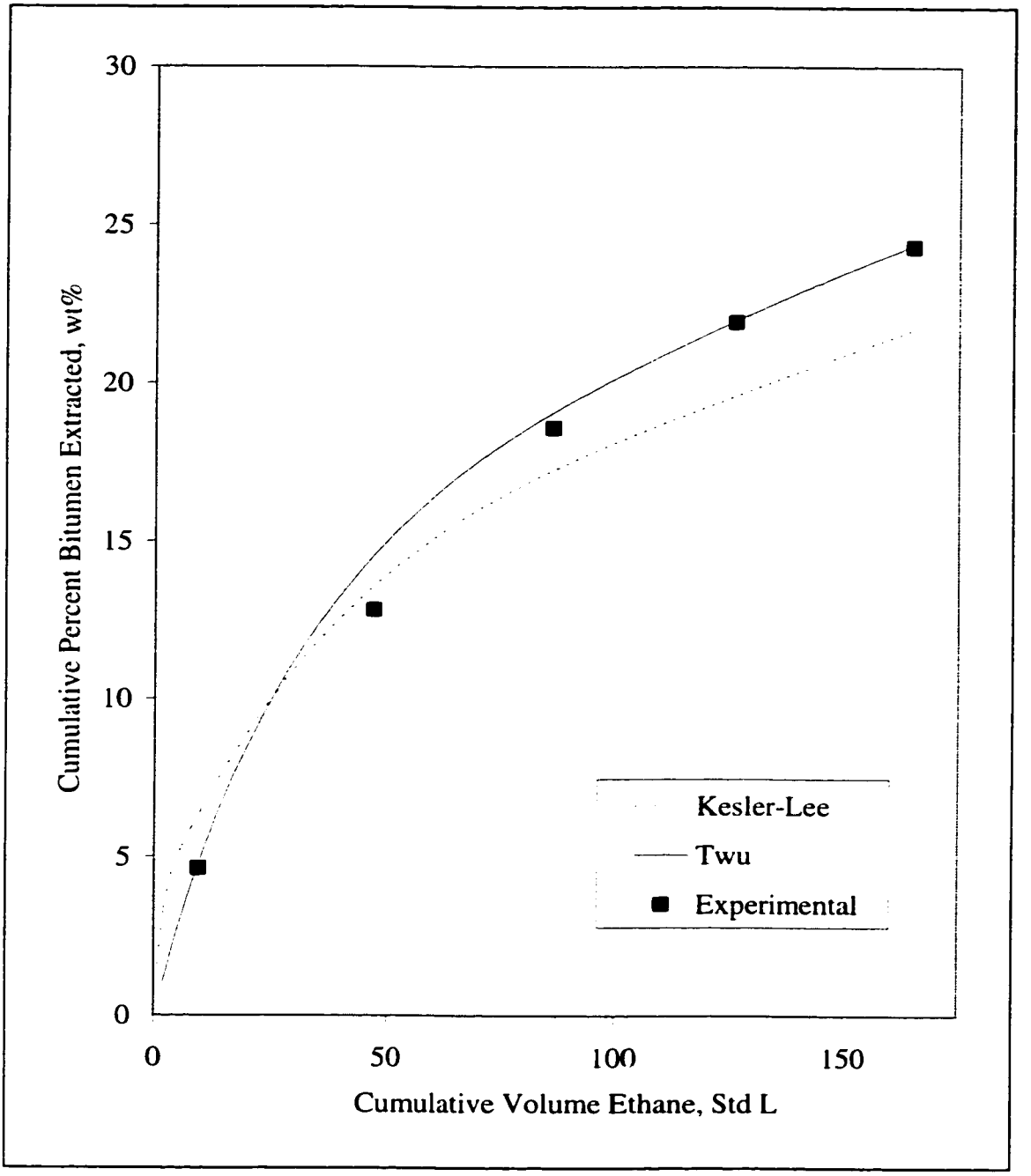

Figure 6.18 – Simulation results using optimised interaction parameters determined using both the Twu and the Kesler-Lee critical properties.

of bitumen feed and accurately predicted results for conditions beyond those used for parameter optimisation.

Binary interaction parameters were calculated using the correlation published by Trebble et al. for binary supercritical systems. The simulation consistently under predicted the extraction curves when these interaction parameters were used. This was due to the fact that the correlation was developed using hydrocarbons that were significantly lighter than the Peace River bitumen pseudocomponents used in this study.

A sensitivity analysis showed that the variation in temperature and pressure observed during the experiments had a relatively small impact on the model results. The number of sections used to model the extractor and the size of the time steps used in the simulation affected both the simulation results and the computational time required. A time step of 1 min. and modelling the extractor using 10 sections was shown to be good compromise that reduced the computational time while maintaining the fidelity of the simulation results.

The simulation was used to compare the results obtained using two different methods for characterising the bitumen. The optimised interaction parameters were shown to depend on the correlation used to calculate the critical properties. The extraction curve produced using the Twu critical properties and corresponding critical properties was more representative of the experimental results than those calculated using the Kesler-Lee critical data.

Chapter Seven

Conclusions and Recommendations

7.1 Conclusions

A review of the published literature on supercritical fluids cited that supercritical fluid technology could address a number of process issues, however, their application to industrial scale processes remains quite limited. This is primarily the result of a lack of both experimental data and accurate models capable of describing the behaviour of supercritical systems, especially those involving complex, undefined hydrocarbon mixtures such as bitumens and heavy oils.

An apparatus capable of providing accurate equilibrium data for the extraction of bitumen from a bitumen/sand mixture using supercritical solvents was designed and constructed. The experimental apparatus provided excellent pressure and temperature control, exhibited small random and systematic errors and was able to produce solubility data that was in good agreement with published values. Extensive experimental tests showed that the solvent flowed through the extractor in a plug flow manner. The assumption that the process was controlled by thermodynamic equilibrium rather than mass transfer resistances was also validated by experimental results.

Experimental results indicated that the extraction process was dependent on the operating conditions. Extraction yields could be increased either by increasing the extraction pressure or decreasing the temperature. As temperature was decreased and pressure

increased, the extracted oil became heavier and more viscous. These trends were also observed over the course of a single extraction run in which the samples obtained later in the extraction were the heaviest and most viscous. SARA analysis showed that supercritical ethane has a higher selectivity towards the saturate fraction of the bitumen. Thus, not only was the bitumen being separated from the sand, but also a degree of fractionation occurred during the extraction process.

Extractions were also conducted using supercritical carbon dioxide as the solvent in order to compare the solvent ability of supercritical ethane with another common supercritical fluid. While both solvents exhibited the same trends with respect to changes in pressure and temperature, the recoveries for ethane were significantly higher, indicating that supercritical ethane would be a much better solvent that carbon dioxide when processing complex hydrocarbon mixtures such as bitumens and heavy oils

In order to use an equation of state to model the extraction process, it was necessary to characterise the Peace River bitumen. Two methods for extrapolating the boiling point curve and three methods for estimating the critical properties of complex hydrocarbon mixtures were used to determine the critical properties, molecular weights and acentric factors of the bitumen pseudocomponents. Translated liquid volume predictions, obtained using each set of properties, were compared to the experimental liquid volumes. From this analysis, it was concluded that the Denchfield method for extrapolating the boiling point curve combined with the Twu property estimation method provided the most accurate critical properties for characterising Peace River bitumen

A computer program was developed that modelled the extraction process. The Peng-Robinson equation of state was used to determine the phase behaviour of the supercritical ethane/Peace River bitumen system. A set of optimised interaction parameters were produced and using these parameters, the model was capable of reproducing the extraction curves and compositions greater than 0.1 mol% to within 15%. The simulation

results demonstrated that it is possible to accurately model supercritical systems using an equation such as the Peng-Robinson equation of state.

7.2 Recommendations

While the bitumen recoveries using supercritical fluids found in this study were significantly lower than those obtained using the water wash method presently employed, the extract product was of particularly high quality and would require little upgrading. Therefore, the potential exists to combine supercritical extraction with another technology such as pyrolysis. The lighter fractions could be extracted using a supercritical fluid and the remaining hydrocarbon/sand mixture processed using technology typically found in the production of oil from oil shale. Experimental work would be required to determine the most efficient way of processing the residue remaining after the supercritical extraction process was completed.

Studies have been conducted in which the supercritical solvent was modified through the addition of a small amount of a second fluid such as methanol (Lu et al., 1990). The presence of the entrainer increased the solubility of various pure solutes in supercritical fluids. Therefore, an investigation of the effect of entrainers on the extraction of complex hydrocarbon mixtures using supercritical fluids would be valuable.

The simulation results performed as part of this study, showed that it was possible to model supercritical fluid/bitumen systems using the Peng-Robinson equation of state. One of the issues with this equation of state was the determination of reliable values for the binary interaction parameters between the solvent and the pseudocomponents used to characterise the bitumen. Correlations exist which are capable of providing interaction parameters for lighter hydrocarbons and supercritical fluids but these do not provide

accurate interaction parameters for heavy components. Thus, there is a need for a correlation that is able to determine binary interaction parameters for heavy hydrocarbons and supercritical solvents so that more accurate predictions can be made of the phase behaviour of these systems.

References

Altgelt, K. H. & Boduszynski, M. M. (1994). Composition and Analysis of Heavy Petroleum Fractions, Marcel Dekkar Inc., New York, New York.

ASTM (1999). Annual Book of ASTM Standards, Section 5. West Conshohocken, Pennsylvania.

Bartle, K. D., Erdem-Senetalar, A., Kadioglu, E. & Tolay, M. (1984). Sub-Critical and Super-Critical Solvent Extraction of the Avgamasya Asphaltite of South Eastern Turkey. Characterisation of Heavy Crude Oils and Petroleum Residues: Symposium International, Lyon, France, June, 217-222.

Benmekki, E. H., Kwak, T. Y. & Mansoori, G. A. (1987). Supercritical Fluids: Chemical and Engineering Principles and Applications, Squires, T. G. & Paulaitis, M. E. (Editors). American Chemical Society, Washington, DC.

Brennecke, J. F. and Eckert, C. A. (1989). Phase Equilibria for Supercritical Fluid Process Design. AIChE Journal 1989, 35, 1409-1424.

Benneker, A. H., Kronberg, A. E. & Westerterp, K. R. (1988). Influence of Buoyancy Forces on the Flow of Gases through Packed Beds at Elevated Pressures. AIChE Journal, 44, 2, 263-270.

Bentein, J. (1996). Oilsands Report. The Calgary Sun. June.

Bertucco, A., Barolo, M. & Soave, G. (1995). Estimation of Chemical Equilibria in High-Pressure Gaseous Systems by a Modified Redlich-Kwong-Soave Equation of State. Industrial and Engineering Chemistry Research, 34, 3159-3165.

Bishnoi, (1996). ENCH 427 Course Notes. Department of Chemical and Petroleum Engineering, Calgary, Alberta.

Burk, R., & Kruus, P. (1992). Solubilities of Solids in Supercritical Fluids. The Canadian Journal of Chemical Engineering, 70, April, 403-407.

Capeling, R. R., & Peggs, J. K. (1979). Experimental Steamflood Cold Lake Oil Sands. The Future of Heavy Crude Oils and Tar Sands, June 4-12, Edmonton, Alberta, Canada, 361-368.

Carberry, J. J. & Bretton, R. H. (1958). Axial Dispersion of Mass in Flow Through Fixed Beds. AIChE Journal, 4, 3, 367-375.

Cheng, J., Fan, Y. & Zhan, Y. (1994). Supercritical Propane Fractionation of Wax-Bearing Residue. Separation Science and Technology, 29, No. 14, 1779-1787.

Chung, K., Xu, C., Hu, Y. & Wang, R. (1996). Super-critical Fluid Extraction Cuts Deep into the Bottom of the Barrel. Presented at the 46th Canadian Society for Chemical Engineering Conference, Kingston, Ontario, September 29 – October 2.

Clifford, A.A. & Bartle, K. D. (1993). Supercritical Fluid Extraction. Journal of Chemical Technology and Biotechnology, 58, 307-308.

Cussler, E. L. (1984). Diffusion: Mass Transfer in Fluid Systems, Cambridge University Press, New York, New York.

Das, S. K. & Butler, R. M. (1996). Diffusion Coefficients of Propane and Butane in Peace River Bitumen. The Canadian Journal of Chemical Engineering, 74, 985-992.

Denchfield, T. (1981). Rapid Calculator Solutions: ASTM/TBP; Other Probability Problems. Oil & Gas Journal, April 27, 179-184.

Deo, M., Hwang, J. & Hanson, F. (1992). Supercritical Fluid Extraction of a Crude Oil, Bitumen-Derived Liquid and Bitumen by Carbon Dioxide and Propane. Fuel, 71, December, 1519-1526.

Dimitrelis, D. & Prausnitz, J. M. (1989). Solubilities of n-Octadecane, Phenanthrene, and n-Octadecane/Phenanthrene Mixtures in Supercritical Propane at 390 and 420 K and Pressures to 60 bar. Journal of Chemical and Engineering Data, 34, 286-291.

Donaldson, E. C., Chilingarian, G. V. & Yen, T. F., Editors (1989). Enhanced Oil Recovery, II: Processes and Operations, Elsevier Science Publishers, New York.

Dunn, S. G., Nenninger, E. H. & Rajan, V. S. V. (1989). A Study of Bitumen Recovery by Gravity Drainage Using Low Temperature Soluble Gas Injection. The Canadian Journal of Chemical Engineering, 67, 978-991.

Eastick, R. R., Svrcek, W. Y., & Mehrotra, A. K. (1992). Phase Behaviour of CO_2 – Bitumen Fractions. The Canadian Journal of Chemical Engineering, 70, 159-164.

Edgar, T. F. & Himmelblau, D. M. (1988). Optimisation of Chemical Processes. McGraw-Hill Co., New York, New York.

Eisenbach, W. O., Niemann, K. & Göttsch, P. J. (1983). Supercritical Fluid Extraction of Oil Sands and Residues from Oil and Coal Hydrogenation. Chemical Engineering at

Supercritical Conditions, Paulaitis, M. E., Penninger, J. M. L., Gray Jr., R. D. and Davidson, P. (Editors). Ann Arbor Science, Ann Arbor, Michigan.

Frauenfeld, T., Lillico, D., Jossy, C., Vilcsak, G., Rabeeh, S. & Singh, S. (1988). Evaluation of Partially Miscible Processes for Alberta Heavy Oil Reservoirs. The Journal of Canadian Petroleum Technology, 37, No. 4, 17-24.

Giese, M., Rottschäfer, K. & Vortmeyer, D. (1998). Measured and Modelled Superficial Flow Profiles in Packed Beds with Liquid Flow. AIChE Journal, 44, 2, 484-490.

Gray, M. R. (1994). Upgrading Petroleum Residues and Heavy Oils, Marcel Deckker, Inc., New York, New York.

Han, N. W., Bhakta, J. & Carbonell, R. G. (1985). Longitudinal and Lateral Dispersion in Packed Beds: Effect of Column Length and Particle Size Distribution. AIChE Journal, 31, 2, 277-288.

Han, B., Peng, D.-Y., Fu C.-T., & Vilcsak, G. (1992). An Apparatus for Phase Equilibrium Studies of Carbon Dioxide + Heavy Hydrocarbon Systems. The Canadian Journal of Chemical Engineering, 70, December, 1164-1171.

Hepler, L. G. & Hsi, C. (1989). AOSTRA Technical Handbook on Oil Sands, Bitumens and Heavy Oils, AOSTRA, Edmonton, Alberta.

Houlihan, R. (1984). An Overview of Oil Sands Extraction – Commercial Technology and New Techniques. Future of Heavy Crude and Tar Sands, 2nd International Conference, UNITAR, Caracas, Venezuela, 1076-1086.

Hoyer, G. G. (1985). Extraction with Supercritical Fluids: Why, How, and so What? Chemtech, July, 440-448.

Hwang, J., Deo, M. & Hanson, F. (1996). Dynamic Behaviour of Supercritical Fluid Extractions of a Crude Oil and its Vacuum Residue. Fuel, 75, No. 13, 1591-1595.

Hwang, J., Park, S., Deo, M. & Hanson, F. (1995). Phase Behaviour of CO_2/Crude Oil Mixtures in Supercritical Fluid Extraction System: Experimental Data and Modelling. Industrial Engineering Chemistry Research, 34, 1280-1286.

Huang, S. & Radosz, M. (1990). Phase Behaviour of Reservoir Fluids II: Supercritical Carbon Dioxide and Bitumen Fractions. Fluid Phase Equilibria, 60, 81-98.

Hyndman, A. W. (1995). Regional Development of Canada's Oil Sands. UNITAR International Conference on Heavy Crude and Tar Sands, Houston, Texas, 85-93.

Hysys Version 1.0 (1995). Hyprotech Ltd., Calgary, Alberta, Canada.

Jacobs, F. A., Donnelly, J. K., Stanislav, J. & Svrcek, W. Y. (1980). Viscosity of Gas-Saturated Bitumens. The Journal of Canadian Petroleum Technology, 19, 4, 46-50.

Johnston, K. P., Peck, D. G., & Kim, S. (1989). Modeling Supercritical Mixtures: How Predictive Is It? Industrial and Engineering Chemistry Research, 28, 1115-1125.

Johnston, K. P., Peck, D. G. & Kim, S. (1989). Modelling Supercritical Mixtures: How Predictive Is It? Industrial and Engineering Chemistry Research, 28, 1115-1125.

Johnston, K. P., Ziger, D. H., & Eckert, C. A. (1982). Solubilities of Hydrocarbon Solids in Supercritical Fluids. The Augmented van der Waals Treatment. Industrial and Engineering Chemistry Fundamentals, 21, No. 3, 191-197.

Johnston, K. P. & Eckert, C. A. (1981). An Analytical Carnahan-Starling-van der Waals Model for Solubility of Hydrocarbon Solids in Supercritical Fluids. AIChE Journal, 27, 5, 773-779.

Kershaw, J. R., & Bagnell, L. J. (1987). Extraction of Australian Coals with Supercritical Aqueous Solvents. Supercritical Fluids: Chemical and Engineering Principles and Applications, Squires, T. G. & Paulaitis, M. E. (Editors). American Chemical Society, Washington, DC.

Kesavan, S. K., Ghosh, A., Polasky, M. E., Parameswaran, V. & Lee, S. (1988). Supercritical Extraction of Stuart Oil Shale. Fuel Science and Technology International, 6, 5, 505-523.

Kesler, M. & Lee, B. (1976). Improve Prediction of Enthalpy of Fractions. Hydrocarbon Processing, March, 153-158.

Kohn, J. P., Kim,Y. J. & Pan, Y. C. (1966). Partial Miscibility Phenomena in Binary Hydrocarbon Systems Involving Ethane. Journal of Chemical and Engineering Data, 11, 3, 333-335.

Kokal, S. L. & Sayegh, S. G. (1990). Gas-Saturated Bitumen Density Predictions using the Volume-Translated Peng-Robinson Equation of State. The Journal of Canadian Petroleum Technology, 29, 5, 77-82.

Körner, J. P. (1985). Design and Construction of Full-Scale Supercritical Gas Extraction Plants. Chemical Engineering Progress, April, 63-66.

Larson, L. L., Silva, M. K., Taylor, M. A., & Orr, F. M. (1989). Temperature Dependence of $L_1/L_2/V$ Behaviour in CO_2/Hydrocarbon Systems. SPE Reservoir Engineering, February, 105-114.

Laureshen, C. (1992). ENGG 311 Course Notes. University of Calgary, Calgary, Alberta.

Levenspiel, O. (1962). Chemical Reaction Engineering. John Wiley & Sons Ltd., New York.

Lim, G., Kry, R., Harker, B. & Jha, K. (1995). Cyclic Stimulation of Cold Lake Oil Sand With Supercritical Ethane. Society of Petroleum Engineers, SPE 30298.

Lu, B. C.-Y., Zhang, D. & Sheng, W. (1990). Solubility Enhancement in Supercritical Solvents. Pure and Applied Chemistry, 62, 12, 2277-2285.accuratelyaccurately

Luque de Castro, M. D., Valcárcel, M. & Tena, M. T. (1994). Analytical Supercritical Fluid Extraction, Springer-Verlag, Heidelberg, Germany.

Lutz, U., Oelert, H. H., Glinzer, O., Lübke, M., Severin, D. (1984). Supercritical Extraction and Short-Path Distillation of Long-and Sort-Residues From Petroleum (LR and SR). Characterisation of Heavy Crude Oils and Petroleum Residues: Symposium International, Lyon, France, June, 217-222.

Madras, G., Erkey, C. & Akgerman, A. (1993). A New Technique for Measuring Solubilities of Organics in Supercritical Fluids. Journal of Chemical Engineering Data, 38, 422-423.

Magoulas, K. & Tassios, D. (1990). Thermophysical properties of n-alkanes from C_1 to C_{20} and their prediction for higher ones. Fluid Phase Equilibria, 56, 119-140.

McHugh, M. A. & Krukonis, V. J. (1994). Supercritical Fluid Extraction: Principles and Practice, 2nd Edition, Butterworths, Stoneham, MA.

McHugh, M. A. & Paulaitis, M. E. (1980). Solid Solubilities of Naphthalene and Biphenyl in Supercritical Carbon Dioxide. Journal of Chemical Engineering Data, 25, 326-329.

Megyesy, E. F. (1981). Pressure Vessel Handbook, 5th Edition. Publishing Inc., Tulsa, Oklahoma.

Mehrotra, A. K., Nighswander, J. A. & Kalogerakis, N. (1989). Data and Correlation for CO_2-Peace River Bitumen Phase Behaviour at 22-200°C. AOSTRA Journal of Research, 5, 351-358.

Mehrotra, A. K. & Svrcek, W. Y. (1985a). Viscosity, Density, and Gas Solubility Data for Oil Sand Bitumens. Part II: Peace River Bitumen Saturated with N_2, CO, CH_4, CO_2 and C_2H_6. AOSTRA Journal of Research, 1, No. 4, 269-279.

Mehrotra, A. K., Sarkar, M. & Svrcek, W. Y. (1985b). Bitumen Density and Gas Solubility Predictions Using the Peng-Robinson Equation of State. AOSTRA Journal of Research, 1, No. 4, 215-229.

Miller, K. A. (1994). Heavy Oil and Bitumen – Not Glamorous, but Often Profitable. The Journal of Canadian Petroleum Technology, 33, 4, 13-15.

Miller, M. & Kraemer, D. (1989). Observations on the Multiphase Equilibria Behaviour of CO2-Rich and Ethane-Rich Mixtures. Fluid Phase Equilibria, 44, 295-304.

Monnery, W. D. & Svrcek, W. Y. (1993). Design Two-Phase Separators Within the Right Limits. Chemical Engineering Progress, October, 53-60.

Moradinia, I. & Teja, A. S. (1987). Solubilities of Five Solid n-Alkanes in Supercritical Ethane. Supercritical Fluids: Chemical and Engineering Principles and Applications, Squires, T. G. & Paulaitis, M. E. (Editors). American Chemical Society, Washington, DC.

Mukhopadhyay, M. & Raghuram Rao, G. V. (1993). Thermodynamic Modelling for Supercritical Fluid Process Design. Industrial Engineering and Chemistry Research, 32, 922-930.

Nelson, W. (1968). Does crude boil at 1,400 °F? The Oil and Gas Journal, March 25, 125-126.

National Institute of Standards and Technology (1986). NIST Thermophysical Properties of Pure Fluids Database, Version 3.1. Gaithersburg, MD.

Oschmann, H. J., Prahl, U. & Severin, D. (1998). Separation of Paraffin From Crude Oil by Supercritical Fluid Extraction. Petroleum Science and Technology, 16, 133-143.

Parkinson, G. & Johnson, E. (1989). Supercritical Processes Win CPI Acceptance. Chemical Engineering, July, 36-39.

Pedersen, K. S., Thomassen, P. & Fredenslund, A. (1985). Thermodynamics of Petroleum Mixtures Containing Heavy Hydrocarbons. 3. Efficient Flash Calculation Procedures Using the SRK Equation of State. Industrial and Engineering Chemistry Process Design and Development, 24, 948-954.

Peters, C. J. & de Swan Arons, J. (1989). On the Relationship Between the Carbon-Number of n-Paraffins and their Solubility in Supercritical Solvents. Fluid Phase Equilibria, 52, 389-396.

Pruden, B. (1997). ENCH 619.24 – Upgrading of VTB from Heavy Oil, Bitumen and Conventional Crude. Course Notes. University of Calgary, Calgary, Alberta.

Raeissi, S., Gauter, K. & Peters, C. J. (1998). Fluid Multiphase Behaviour in Quasi-Binary Mixtures of Carbon Dioxide and Certain 1-Alkanols. Fluid Phase Equilibria, 147, 239-249.

Rance, R. W. & Cussler, E. L. (1974). Fast Fluxes with Supercritical Solvents. AIChE Journal, 20, 2, 353-356.

Riazi, M. & Al-Sahhaf, T. (1996). Physical Properties of Heavy Petroleum Fractions and Crude Oils. Fluid Phase Equilibria, 117, 217-224.

Riazi, M. & Daubert, T. (1987). Characterization Parameters for Petroleum Fractions. Industrial Engineering Chemistry Research, 26, 755-759.

Rodrigues, A. B. & Kohn, J. P. (1967). Three Phase Equilibria in the Binary System Ethane-n-Docosane and Ethane-n-Octacosane. The Journal of Chemical and Engineering Data, 12, 2, 191-193.

Rowlinson, J. S. & Swinton, F. L. (1982). Liquids and Liquid Mixtures, 3rd Edition. Butterworth & Co. Ltd, Great Britian.

Schmitt, W. J. & Reid, R. C. (1985). The Influence of the Solvent Gas on Solubility and Selectivity in Supercritical Extraction. Supercritical Fluid Technology, Elsevier Science Publishers, Amsterdam, 123-147.

Shah, Y. T., Stiegel, G. J. & Sharma, M. M. (1978). Backmixing in Gas-Liquid Reactors. AIChE Journal, 24, No. 3, 369-400.

Sheng, W. & Lu, B.C.-Y. (1990). Phase Equilibria and Volumetric Representation of Bitumen-Containing Systems. AOSTRA Journal of Research, 6, 211-218.

Speight, J. G. (1991) The Chemistry and Technology of Petroleum, 2nd Edition, Marcel Dekker, New York.

Stephan, K. & Lucus, K. (1979). Viscosity of Dense Fluids, Plenum Press, New York, New York.

Subramanian, M. & Hanson, F. V. (1998). Supercritical Fluid Extraction of Bitumens from Utah Oil Sands. Fuel Processing Technology, 55, 35-53.

Sunol, A. & Beyer, H. (1990). Mechanism of Supercritical Extraction of Coal. Industrial Engineering Chemistry Research, 29, 842-849.

Svrcek, W. Y. & Mehrotra, A. K. (1989). Properties of Peace River Bitumen Saturated with Field Gas Mixtures. The Journal of Canadian Petroleum Technology, 28, No. 2, 50-56.

Svrcek, W. Y. & Mehrotra, A. K. (1982). Gas Solubility, Viscosity and Density Measurements for Athabasca Bitumen. The Journal of Canadian Petroleum Technology, 21, 4, 31-38.

Tan, C. S. and Liou, D. C. (1989). Axial Dispersion of Supercritical Carbon Dioxide in Packed Beds. Industrial and Engineering Chemistry Research, 28, 1246-1250.

Tan, C. S. & Yu-Cherng, W. (1988). Supercritical Fluid Distribution in a Packed Column. Chemical Engineering Communications, 68, 119-131.

Taylor, L. T. (1996). Supercritical Fluid Extraction, John Wiley & Sons, Inc. New York, New York.

Trebble, M. A. & Sigmund, P. M. (1990). A Generalised Correlation for the Prediction of Phase Behaviour in Supercritical Systems. The Canadian Journal of Chemical Engineering, 68, 1033-1039.

Treybal, R. E. (1987). Mass-Transfer Operations, 3rd Edition, McGraw-Hill Publishing Co., New York, New York.

Triday, J., Smith, J. M. (1988). Dynamic Behaviour of Supercritical Extraction of Kerogen from Shale. AIChE Journal, 34, 4, 658-668.

Twu, C. (1984). An Internally Consistent Correlation for Predicting the Critical Properties and Molecular Weights of Petroleum and Coal-Tar Liquids. Fluid Phase Equilibria, 16, 137-150.

Van Konynenburg, P. & Scott, R. L. (1980). Critical lines and phase equilibria in binary van der Waals mixtures. Philos. Trans. R. Soc. London, Ser. A, 298. 495-540.

Voulgaris, M., Stamatakis, S., Magoulas, K. & Tassios, D. (1991). Prediction of Physical Properties for Non-Polar Compounds, Petroleum and Coal Liquid Fractions. Fluid Phase Equilibria, 64, 73-106.

Warzinski, R. P. (1987) Fractional Destraction of Coal-Derived Residuum. Supercritical Fluids: Chemical and Engineering Principles and Applications, Squires, T. G. & Paulaitis, M. E. (Editors). American Chemical Society, Washington, DC.

Walas, S. M. (1985). Phase Equilibria in Chemical Engineering. Butterworth-Heinemann, Stoneham, MA.

Whitson, C. H. (1983). Characterising the Hydrocarbon Plus Fractions. Society of Petroleum Engineers Journal, 23, 683-694.

Williams, D. (1981). Extraction with Supercritical Gases. Chemical Engineering Science, 36, No. 11, 1769-1788.

Yu, J., Huang, S. & Radosz, M. (1989). Phase Behaviour of Reservoir Fluids: Supercritical Carbon Dioxide and Cold Lake Bitumen. Fluid Phase Equilibria, 53, 429-438.

Appendix A

Calibration Procedures

A.1 Thermocouple Calibration

The thermocouples were calibrated using a Model F250 Precision Thermometer manufactured by Automatic Systems Laboratories Inc with a PT 100 T25-02 platinum resistance probe. The thermometer had an accuracy of ± 0.025°C at temperatures of 0°C and 100°C. The error in the probe was much less than that for the T-type special thermocouples used in this study which was ± 0.6°C.

The boiling point and melting point of water were used as reference temperatures to calibrate the thermocouples used in this work. The thermocouples were attached to the data acquisition system which recorded the temperatures. The digital thermometer and the thermocouples were placed in a beaker containing boiling water and the temperatures were recorded. This process was repeated using ice water to check the lower range of the thermocouples.

Six thermocouples were calibrated, the five shown in Figure 3.1 and a spare. The data from the calibration experiments were used to determine linear equations which corrected the temperature readings from the thermocouples so that they matched the digital thermometer values. The coefficients for each of the thermocouples are shown in Table A.1.

Thermocouple	X Variable	Intercept, °C
Pump (T1)	0.9947	0.2136
Inlet (T2)	1.0006	0.5263
Extractor (T3)	1.0009	0.3990
Outlet (T4)	1.0025	0.4537
Oven (T5)	1.0034	0.3592
Spare	1.0031	0.1669

Table A.1 – X variables and intercepts for thermocouple calibration equations.

In Table A.1, the designations in parenthesis refer to the location of the thermocouples as shown in Figure 3.1. The calibration equations were used in the QMON data acquisition system.

A.2 Pressure Transducer Calibration

The two pressure transducers were calibrated against a new Fisher-Rosemount pressure transmitter (Model #3051CA). The transducer was factory calibrated for a range of 0-4000 psia with an accuracy of ±0.075% of span. The error in this transducer was smaller than the transducers used for the experiments which was ±0.25% of span.

Calibrations were performed by connecting the three pressure transducers downstream of the pump. The pump was used to pressurise the system to six pressures ranging from 857 psia to 2645 psia. The transducers are linear voltage instruments and a voltage signal is converted to pressure readings by the data acquisition system using a linear calibration

equation. The readings from the new transducer were used to calculate the coefficients for the other two transducers. The results are summarised in Table A.2.

Transducer	X Variable, psia/V	Intercept, psia	Regression Coefficient
Pump Pressure (P1)	664.327	-658.871	0.999
Extractor Pressure (P2)	625.237	-128.443	0.999

Table A.2 – X variables and intercepts for the pressure transducer equations.

The designations in parenthesis are the pressure transducers as they are referenced in Figure 3.1. The resulting calibration equations were used by the QMON data acquisition system to measure and record the experimental pressures. The pressures were converted to MPa using a conversion factor of 0.006896 MPa/psi.

A.3 Gas Chromatographs

Two gas chromatographs were used in this work. One chromatograph was used to measure the composition of the gas exiting the extractor during the residence time distribution study. The second was used to evaluate the performance of the two phase separators used to collect the extracted bitumen downstream of the micrometer valve.

A.3.1 Residence Time Distribution Gas Chromatograph

The gas chromatograph used in the residence time distribution study was calibrated so that it could be used to measure the amount of ethane in the stream exiting the extractor. This stream was a mixture of nitrogen and ethane and varied from 0-100 mole percent ethane over the course of a distribution study.

The mole percent of ethane in the mixture was calculated by dividing the area of a detected ethane peak by the area of the peak for pure ethane. A gas chromatograph can be calibrated for a given component using this method regardless of the composition of the rest of the gas in the sample. The key to using this technique was that the sample to the gas chromatographic detector had to be the same volume for all samples. This was achieved by using a 2 mL sample loop. The gas chromatograph was calibrated using a gas mixture of known composition.

A calibration gas comprised of propylene, ethane, methane and ethylene from Matheson Gas Products Inc was used to determine the area for a mole percent of ethane less than 100%. The composition of the calibration gas is shown in Table A.3 The actual mole percent ethane was plotted as a function of measured mole percent ethane in Figure A.1.

Component	Mole Percent
Propylene	22.9% ± 0.5%
Ethane	25.0% ± 0.5%
Methane	24.2% ± 0.5%
Ethylene	Balance

Table A.3– Composition of gas used to calibrate gas chromatograph.

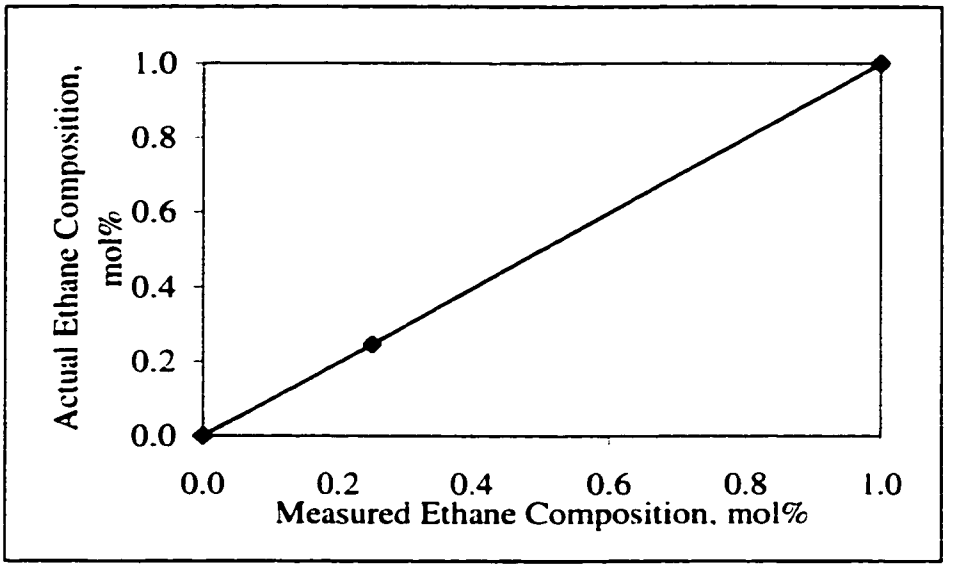

Figure A.1– Calibration plot of area count for ethane versus mole percent.

Figure A.1 revealed that the measured mole percent of ethane and the actual mole % of ethane had a linear relationship with a regression coefficient of 1.0. Therefore, the composition of ethane of the stream exiting the extractor could be determined by normalising the area of the ethane peaks using Equation A.1 shown below:

$$\% \text{ Ethane} = \frac{\text{Area for Ethane in Mixture}}{\text{Area for 100\% Ethane}} * 100\% \qquad \text{Equation A.1}$$

A.3.2 Separator Performance Gas Chromatograph

The purpose of the gas chromatograph used in the separator performance evaluation was to verify that the gas leaving the separators was pure ethane. In other words, that all of the bitumen extracted was precipitated in the separators. If the separators were working

properly, when samples of the gas exiting the separators were analysed using a gas chromatograph, the only peak produced would be for ethane.

The calibration consisted of determining the time that ethane was detected by the thermal conductivity detector. If any other peaks were present during the analysis of the separator exit gas, it would mean that the separators were not performing correctly. Neither the type of hydrocarbon nor amount detected for these peaks were important.

A.4 Wet Test Meter

The wet test meter was calibrated against a Porter mass flow controller (model 221-APASVCAA) with an accuracy of ±1% of full scale which was 0-2 standard litres per minute. The mass flow controller and the wet test meter were connected in series to a nitrogen supply. The flow rate was set using the mass flow controller and the rate measured using the wet test meter reading was recorded. The flow rate measured using the wet test meter was corrected to standard conditions using the following equations and compared to the mass flow controller rate. The equation for correcting the wet test meter flow rate to standard litres per minute is as follows:

$$\text{Acutal Flow} = (\text{Measured Flow})(\text{WTCF}) \qquad \text{Equation A.2}$$

Where,

$$\text{WTCF} = \left(\frac{P_b + \Delta P_{WTM} - P_{water}}{760\ \text{mmHg}} \right) \left(\frac{288.15\ \text{K}}{T_{water}} \right) \qquad \text{Equation A.3}$$

In Equation A.3, P_b is the barometric pressure in mmHg, ΔP_{WTM} is the pressure drop across the wet test meter in mmHg, P_{water} is the vapour pressure of water at the wet test meter temperature in mmHg and T_{water} is the wet test meter temperature.

In Figure A.2, the volumetric flow rate measured using the mass flow controller was plotted as a function of the volumetric flow rate measured using the wet test meter.

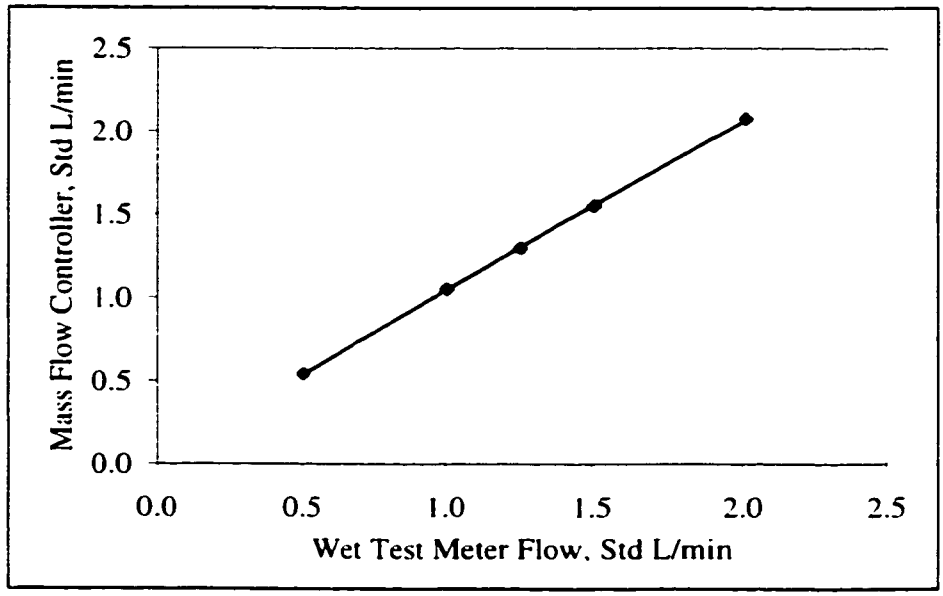

Figure A.2 – Mass flow controller volumetric flow rate versus wet test meter volumetric flow rate.

The relationship between the two measurements was linear and the data was regressed to determine the coefficients for the calibration equation. The slope and intercept for the calibration equation were 0.986 and –0.0267 respectively with a regression coefficient of 0.9998.

Appendix B

Material Data

B.1 Distillation Data

The boiling point data for the bitumen and the diluent are shown in Table B.1. The test method used was the ASTM D-2887 distillation procedure (ASTM, 1999).

Weight Percent Distilled	Diluent, °C	Peace River Bitumen, °C
I.B.P.	-2	167
5%	25	218
10%	27	257
15%	28	290
20%	34	324
25%	38	360
30%	39	399
35%	40	440
40%	46	480
45%	60	523
50%	62	584
55%	70	
60%	71	
65%	76	
70%	86	
75%	94	
80%	103	
85%	117	
90%	130	
95%	156	
F.B.P.	275	

Table B.1 – Distillation data for Peace River bitumen and diluent.

The boiling point data for the four cuts are shown in Table B.2. The test method used was the ASTM D-2887 distillation procedure (ASTM, 1999).

Simulated Distillation	Cut 1, °C	Cut 2, °C	Cut 3, °C	Cut 4, °C
I.B.P.	155	176	276	349
5%	166	204	304	382
10%	172	220	319	397
15%	178	232	329	406
20%	183	242	337	414
25%	188	251	343	420
30%	194	257	349	426
35%	197	264	355	432
40%	202	270	360	436
45%	206	276	365	441
50%	210	281	370	446
55%	214	286	376	451
60%	219	292	381	456
65%	224	298	387	461
70%	229	304	393	466
75%	235	311	400	472
80%	242	318	408	478
85%	250	327	417	486
90%	260	338	429	497
95%	276	356	448	514
F.B.P.	335	420	518	596

Table B.2 - Distillation data for the four cuts of Peace River bitumen used in this work.

It should be noted that the distillation data required to characterise the fifth cut was obtained by extrapolating the bitumen distillation curve.

B.2 Sand Data

Table B.3 contains the sieve analysis and Table B.4 is the chemical analysis as quoted in the specifications provided by the manufacturer of the sand, Target Products Ltd.

Sieve Size		Individual Percent Retained	Cumulative Percent Passing
U.S.	mm		
No.16	4.75	-	100
20	0.85	0-10	90+
30	0.60	50-70	20-45
40	0.425	15-35	2-12
50	0.300	2-12	0-2
70	0.212	-	-

Table B.3 – Sieve analysis for sand used in this study.

Chemical Compound	Composition, wt%
Silica, SiO_2	93.2 – 93.6
Alumina, Al_2O_3	3.6 – 4.6
Iron Oxide, Fe_2O_3	0.30 – 0.35
Calcium Oxide, CaO	0.25 – 0.65
Magnesium Oxide, MgO	0.08 – 0.15
Sodium Oxide, Na_2O	0.75 – 0.85
Titanium Dioxide, TiO_2	maximum
Lost on Ignition	0.3 maximum

Table B.4 – Chemical analysis of sand used in this study.

The porosity and density values of the sand were 0.4 and 1640 g/mL, respectively.

Appendix C

Simulation Code

C.1 Extraction Simulation Code

```
clear
ks = [.0054 .0422 .0445 .0865 .1494 0]  % Average T

R = 8.314;          % Universal Gas Constant
tol=1e-20;          % Tolerence for flash routine
nc = 6;             % Number of Components in system

% Properties of the components
% Pseudocomponent #1; - Twu
Tc(1) = 273.15+407.67; % Critical Temp, K
Pc(1) = 2460.1;        % Critical Pressure, kPa
w(1) = 0.42779;        % Acentric Factor
MW(1) = 159.49;        % Molecular Weight
Zra(1) = 0.260568;     % Racket compressibility factor

% Pseudocomponent #2; - Twu
Tc(2) = 273.15+488.21; % Critical Temp, K
Pc(2) = 2152.77;       % Critical Pressure, kPa
w(2) = 0.55085;        % Acentric Factor
MW(2) = 205.49;        % Molecular Weight
Zra(2) = .256162;      % Racket compressibility factor

% Pseudocomponent #3; - Twu
Tc(3) = 273.15+586.28; % Critical Temp, K
Pc(3) = 1889.57;       % Critical Pressure, kPa
w(3) = 0.72109;        % Acentric Factor
MW(3) = 287.39;        % Molecular Weight
Zra(3) = .260906;      % Racket compressibility factor

% Pseudocomponent #4; - Twu
Tc(4) = 273.15+644.04; % Critical Temp, K
Pc(4) = 1527.55;       % Critical Pressure, kPa
w(4) = 0.92916;        % Acentric Factor
MW(4) = 386.35;        % Molecular Weight
Zra(4) = .260759;      % Racket compressibility factor

% Pseudocomponent #5; - Twu - Denchfeld
```

```
Tc(5) = 273.15+901.58;  % Critical Temp, K
Pc(5) = 755.57;         % Critical Pressure, kPa
w(5) = 1.40713;         % Acentric Factor
MW(5) = 808.45;         % Molecular Weight
Zra(5) = .228996;       % Racket compressibility factor

% Ethane Data
Tc(6) = 32.28+273.15;   % Critical Temp, K
Pc(6) = 4883.8;         % Critical Pres, kPa
w(6) = 0.0986;          % Acentric Factor
MW(6) = 30.07;          % Molecular Weight
Zra(6) = 0.28329;       % Racket compressibility factor

T = 47.79+273.15;       % Extraction Temperature, K
P = 10490;              % Extraction Pressure, kPa
Q = 0.400;              % Solvent Flow Rate L/h
Tpump = 23 + 273.15;    % Pump Temperature, K

MassSand = 800;         % Mass of Sand in Feed, g
DenSand = 1640;         % Sand Density, g/L
SandPore = 0.4;         % Sand Porosity
MassOil = 140;          % Mass of Bitumen in Feed, g
DenOil = 998.5;         % Bitumen Density, g/L

VT = MassSand/DenSand;  % Volume of Sand,L
Vvoid = VT*SandPore;    % Void Volume in Sand, L
VH = MassOil/DenOil;    % Volume of Bitumen, L
VL = Vvoid - VH;        % Volume for solvent, L

% Constants for P-R EOS
apc=0.45724*(R^2)*(Tc.^2)./Pc;
bpc=0.07780*R*Tc./Pc;
alpha=(1+(0.37464+1.54226*w-0.26992*(w.^2)).*(1-(T./Tc).^(0.5))).^2;
Apc= apc.*alpha*P/(R^2*T^2);
Bpc= bpc*P/(R*T);
apc=apc.*alpha;

% Set up interaction parameter matrix
i=1;
while i<=nc;
    j=1;
    while j<=nc;
        k(i,j) = 0;
        j=j+1;
    end;
    i=i+1;
end;
k(:,nc) = ks';
k(nc,:) = ks;
i=1;
while i<=nc
  j=1;
  while j<=nc
```

```
    Aij(i,j)=(1-k(i,j))*(Apc(i)*Apc(j))^(1/2);
    j=j+1;
  end;
  i=i+1;
end;

% Flash to get density of Ethane at T and P;
phase=0;
zC2=zroot(Bpc(6), Apc(6), phase);
VC2=R*T*zC2/P;
DenC2=1/VC2;
alphapump=(1+(0.37464+1.54226*w(6)-0.26992*(w(6)^2))*(1-(Tpump/Tc(6))^(0.5)))^2;
Apump= apc(6)*alphapump/alpha(6)*P/(R^2*Tpump^2);
Bpump= bpc(6)*P/(R*Tpump);
zC2pump=zroot(Bpump, Apump, phase);
VC2pump=R*Tpump*zC2pump/P;
DenC2Pump=1/VC2pump;
Eth = (VL*DenC2);

% Initial Feed composition
wt(1) = 0.0609;        % Mass fraction of cpt 1 in feed
wt(2) = 0.1604;        % Mass fraction of cpt 2 in feed
wt(3) = 0.1209;        % Mass fraction of cpt 3 in feed
wt(4) = 0.0986;        % Mass fraction of cpt 4 in feed
wt(5) = 0.5584;        % Mass fraction of cpt 5 in feed
wt(6) = 0;             % Mass fraction of ethane in bitumen feed

% Saturate the oil (pressure up stage)
satdata = saturate(Apc, Bpc, Aij, Tc, Pc, w, MW, Zra, Eth, wt, MassOil, R, tol, P, T, nc, k, Vvoid, DenC2);
x = satdata(:,3);
y = satdata(:,1);
molheavy = sum(satdata(:,4));   % Moles of bitumen rich phase, mol
mollight = sum(satdata(:,2));   % Moles of ethane rich phase, mol

% Set up to begin to add ethane
NumSec = 10;        % Number of Sections for Extractor
Deltat = 1;         % Time Steps, minutes
NumSteps = 40/Deltat;
Ethane = 0;         % Solvent measured by wtm, mol
MassExt = 0;        % Mass Extracted, g

%Calc den for each phase
Ay=0;
Ax=0;
By=0;
Bx=0;
i=1;
while i<=nc
  j=1;
  while j<=nc
    Ay= Ay+y(i)*y(j)*Aij(i,j);
    Ax= Ax+x(i)*x(j)*Aij(i,j);
    j=j+1;
```

```
  end;
  By=By+y(i)*Bpc(i);
  Bx=Bx+x(i)*Bpc(i);
  i=i+1;
end;

%Calc den for each phase
%  Vapour z
phase=0;
zv=zroot(By, Ay, phase);
vlight=zv*R*T/P;

%  Liquid z
phase=1;
zl=zroot(Bx, Ax, phase);
Vl=zl*R*T/P;
%  Calculate shifted liquid volumes
cmix=cmixx(Tc, Pc, Zra, Bpc, Apc, T, P, x, R, nc);
Vlshift= Vl-cmix;
vheavy= Vl-cmix;

%Check vol balance
volheavy = vheavy*molheavy;
vollight = vlight*mollight;
VL = Vvoid-volheavy;

% Divide extractor into sections
volh = volheavy/NumSec;
VL = VL/NumSec;
Vvoid = Vvoid/NumSec;

% Initialize extractor data - moles of light and heavy in each section
molsh1 = satdata(:,4)/NumSec;
molsl1 = satdata(:,2)/NumSec;
molsh2 = satdata(:,4)/NumSec;
molsl2 = satdata(:,2)/NumSec;
molsh3 = satdata(:,4)/NumSec;
molsl3 = satdata(:,2)/NumSec;
molsh4 = satdata(:,4)/NumSec;
molsl4 = satdata(:,2)/NumSec;
molsh5 = satdata(:,4)/NumSec;
molsl5 = satdata(:,2)/NumSec;
molsh6 = satdata(:,4)/NumSec;
molsl6 = satdata(:,2)/NumSec;
molsh7 = satdata(:,4)/NumSec;
molsl7 = satdata(:,2)/NumSec;
molsh8 = satdata(:,4)/NumSec;
molsl8 = satdata(:,2)/NumSec;
molsh9 = satdata(:,4)/NumSec;
molsl9 = satdata(:,2)/NumSec;
molsh10 = satdata(:,4)/NumSec;
molsl10 = satdata(:,2)/NumSec;
```

```
% Begin Extraction process
% Add ethane
EthaneIn = Q/60*Deltat*DenC2Pump;
Bitmolext=[0 0 0 0 0 0];    % Moles of each cpt extracted, mol
Bitmolext=Bitmolext';
Diff=0;
i=1;
s=1;
while Ethane<=166;
  % Section one
  z = molsh1 + molsl1;
  z(6) = z(6) + EthaneIn;
  molefeed = sum(z);
  z = z'/molefeed;
  Section1 = calcsec(R, tol, Tc, Pc, Zra, w, T, P, nc, z, k, molefeed, Apc, Bpc, Aij, Vvoid);
  molsl1 = Section1(:,2);
  molsh1 = Section1(:,4);
  molext1 = Section1(:,5);

  % Section Two
  z = molsh2 + molsl2 + molext1;
  molefeed = sum(z);
  z = z'/molefeed;
  Section2 = calcsec(R, tol, Tc, Pc, Zra, w, T, P, nc, z, k, molefeed, Apc, Bpc, Aij, Vvoid);
  molsl2 = Section2(:,2);
  molsh2 = Section2(:,4);
  molext2 = Section2(:,5);

  % Section Three
  z = molsh3 + molsl3 + molext2;
  molefeed = sum(z);
  z = z'/molefeed;
  Section3 = calcsec(R, tol, Tc, Pc, Zra, w, T, P, nc, z, k, molefeed, Apc, Bpc, Aij, Vvoid);
  molsl3 = Section3(:,2);
  molsh3 = Section3(:,4);
  molext3 = Section3(:,5);

  % Section Four
  z = molsh4 + molsl4 + molext3;
  molefeed = sum(z);
  z = z'/molefeed;
  Section4 = calcsec(R, tol, Tc, Pc, Zra, w, T, P, nc, z, k, molefeed, Apc, Bpc, Aij, Vvoid);
  molsl4 = Section4(:,2);
  molsh4 = Section4(:,4);
  molext4 = Section4(:,5);

  % Section 5
  z = molsh5 + molsl5 + molext4;
  molefeed = sum(z);
  z = z'/molefeed;
  Section5 = calcsec(R, tol, Tc, Pc, Zra, w, T, P, nc, z, k, molefeed, Apc, Bpc, Aij, Vvoid);
  molsl5 = Section5(:,2);
  molsh5 = Section5(:,4);
```

```
molext5 = Section5(:,5);

% Section 6
z = molsh6 + molsl6 + molext5;
molefeed = sum(z);
z = z'/molefeed;
Section6 = calcsec(R, tol, Tc, Pc, Zra, w, T, P, nc, z, k, molefeed, Apc, Bpc, Aij, Vvoid);
molsl6 = Section6(:,2);
molsh6 = Section6(:,4);
molext6 = Section6(:,5);

% Section 7
z = molsh7 + molsl7 + molext6;
molefeed = sum(z);
z = z'/molefeed;
Section7 = calcsec(R, tol, Tc, Pc, Zra, w, T, P, nc, z, k, molefeed, Apc, Bpc, Aij, Vvoid);
molsl7 = Section7(:,2);
molsh7 = Section7(:,4);
molext7 = Section7(:,5);

% Section 8
z = molsh8 + molsl8 + molext7;
molefeed = sum(z);
z = z'/molefeed;
Section8 = calcsec(R, tol, Tc, Pc, Zra, w, T, P, nc, z, k, molefeed, Apc, Bpc, Aij, Vvoid);
molsl8 = Section8(:,2);
molsh8 = Section8(:,4);
molext8 = Section8(:,5);

% Section 9
z = molsh9 + molsl9 + molext8;
molefeed = sum(z);
z = z'/molefeed;
Section9 = calcsec(R, tol, Tc, Pc, Zra, w, T, P, nc, z, k, molefeed, Apc, Bpc, Aij, Vvoid);
molsl9 = Section9(:,2);
molsh9 = Section9(:,4);
molext9 = Section9(:,5);

% Section 10
z = molsh10 + molsl10 + molext9;
molefeed = sum(z);
z = z'/molefeed;
Section10 = calcsec(R, tol, Tc, Pc, Zra, w, T, P, nc, z, k, molefeed, Apc, Bpc, Aij, Vvoid);
molsl10 = Section10(:,2);
molsh10 = Section10(:,4);
molext10 = Section10(:,5);

gramext = MW'.*Section10(:,5);
Bitmolext = Bitmolext + Section10(:,5);
MassExt = MassExt + sum(gramext) - Section10(6,5)*MW(6);
Ethane = Ethane + Section10(6,5)*23.643;
```

```
if Ethane >8.7
 if Ethane <10.5
  s=s+1;
  [Ethane      MassExt]
  Comp_expt= [0.0342 0.0258 0.0095 0.0027 0.0008 0.9269]; % Window 1
  Comp_expt= Comp_expt';
  Comp_theo = Bitmolext/sum(Bitmolext);
  Compositions=[Comp_theo Comp_expt]
%   Diff = Diff + sum((abs(Comp_expt-Comp_theo))./Comp_expt)fs
 end;
end;

if Ethane >46.2
 if Ethane <48
  s=s+1;
  [Ethane   MassExt]
  Comp_expt= [0.0176 0.0154 0.0059 0.0017 0.0005 0.9589]; % Window 2
  Comp_expt= Comp_expt';
  Comp_theo = Bitmolext/sum(Bitmolext);
  Compositions=[Comp_theo Comp_expt]
  Diff = Diff + sum((abs(Comp_expt-Comp_theo))./Comp_expt);
 end;
end;

if Ethane >85.5
 if Ethane <86.9
  s=s+1;
  [Ethane      MassExt]
  Comp_expt= [0.0133 0.0124 0.0048 0.0014 0.0004 0.9676]; % Window 2
  Comp_expt= Comp_expt';
  Comp_theo = Bitmolext/sum(Bitmolext);
  Compositions=[Comp_theo Comp_expt]
  Diff = Diff + sum((abs(Comp_expt-Comp_theo))./Comp_expt);
 end;
end;


if Ethane >124.5
 if Ethane <126.5
  s=s+1;
  [Ethane      MassExt]
  Comp_expt= [0.0103 0.0102 0.0041 0.0012 0.0003 0.9738]; % Window 1
  Comp_expt= Comp_expt';
  Comp_theo = Bitmolext/sum(Bitmolext);
  Compositions=[Comp_theo Comp_expt]
  Diff = Diff + sum((abs(Comp_expt-Comp_theo))./Comp_expt);
 end;
end;

if Ethane >164
 if Ethane <166
  s=s+1
  [Ethane      MassExt]
```

```
        Comp_expt= [0.0084 0.0087 0.0036 0.0011 0.0003 0.9780]; % Window 1
        Comp_expt= Comp_expt';
        Comp_theo = Bitmolext/sum(Bitmolext);
        Compositions=[Comp_theo Comp_expt]
        Diff = Diff + sum((abs(Comp_expt-Comp_theo))./Comp_expt)
      end;
    end;
  massext(i) = MassExt;
  ethane(i) = Ethane;
  i=i+1;
end
%Total_Dif=Diff/(s-1)
```

Subroutines

```
% Saturate the initial feed
function data = saturate(Apc, Bpc, Aij, Tc, Pc, w, MW, Zra, Eth, wt, MassOil, R, tol, P, T, nc, k, Vvoid,
DenC2);

% Initial Moles of fractions
z = wt*MassOil./MW;
z(6) = Eth;
molefeed = sum(z);
%  Mole fraction combined feed
z=z/molefeed;

Comps=flashvol(tol, R, z, nc, k, w, Apc, Bpc, T, P, Tc, Pc, molefeed);
x = Comps(:,3);
y = Comps(:,1);
molheavy = sum(Comps(:,4));
mollight = sum(Comps(:,2));

%Calc den for each phase
Ay=0;
Ax=0;
By=0;
Bx=0;
i=1;
while i<=nc
  j=1;
  while j<=nc
    Ay= Ay+y(i)*y(j)*Aij(i,j);
    Ax= Ax+x(i)*x(j)*Aij(i,j);
    j=j+1;
  end;
  By=By+y(i)*Bpc(i);
  Bx=Bx+x(i)*Bpc(i);
  i=i+1;
end;
```

```
% Vapour z
phase=0;
zv=zroot(By, Ay, phase);
vlight=zv*R*T/P;

% Liquid z
phase=1;
zl=zroot(Bx, Ax, phase);
Vl=zl*R*T/P;
% Calculate shifted liquid volumes
cmix=cmixx(Tc, Pc, Zra, Bpc, Apc, T, P, x, R, nc);
Vlshift= Vl-cmix;
vheavy= Vl-cmix;

%Check vol balance
volheavy = vheavy*molheavy;
vollight = vlight*mollight;
VL = Vvoid-volheavy;
volexit = vollight-VL;

Ethold = Eth;
volexitold = volexit;
Eth = Eth + abs(volexit)*DenC2;

s=1;
while s<=100;
% Moles of fractions
z = wt*MassOil./MW;
z(6) = Eth;
molefeed = sum(z);
% Mole fraction combined feed
z=z/molefeed;

Comps=flashvol(tol, R, z, nc, k, w, Apc, Bpc, T, P, Tc, Pc, molefeed);
x = Comps(:,3);
y = Comps(:,1);
molheavy = sum(Comps(:,4));
mollight = sum(Comps(:,2));

%Calc den for each phase
Ay=0;
Ax=0;
By=0;
Bx=0;
i=1;
while i<=nc
  j=1;
  while j<=nc
    Ay= Ay+y(i)*y(j)*Aij(i,j);
    Ax= Ax+x(i)*x(j)*Aij(i,j);
    j=j+1;
  end;
```

```
  By=By+y(i)*Bpc(i);
  Bx=Bx+x(i)*Bpc(i);
  i=i+1;
end;

% Vapour z
phase=0;
zv=zroot(By, Ay, phase);
vlight=zv*R*T/P;

% Liquid z
phase=1;
zl=zroot(Bx, Ax, phase);
Vl=zl*R*T/P;
% Calculate shifted liquid volumes
cmix=cmixx(Tc, Pc, Zra, Bpc, Apc, T, P, x, R, nc);
Vlshift= Vl-cmix;
vheavy= Vl-cmix;

%Check vol balance
volheavy = vheavy*molheavy;
vollight = vlight*mollight;
VL = Vvoid-volheavy;
volexit = vollight-VL;

if abs(volexit)<=1e-12;
  s= 101;
else;
  Ethnew = Eth-volexit/((volexit-volexitold)/(Eth-Ethold));
  Ethold = Eth;
  volexitold = volexit;
  Eth = Ethnew;
end;
s=s+1;
end;

data = Comps;
```

C.2 Flash Code

```
function data=flashvol(tol, R, z, nc, k, w, Apc, Bpc, T, P, Tc, Pc, molefeed)

% Calculate first estimates for K using Wilson's Equation
lnK = log(Pc/P) + 5.37*(1 + w).*(1-Tc/T);
K = exp(lnK);
if K(5) <1e-15
  K(5)=1e-14;
```

```
end;

s=0;
t=1;
% Begin flash iteration process
while s<=100;

% Stability analysis i.e Q(0) and Q(1)
Beta = 0;
Q = (z.*(K - 1))./(1 + Beta*(K - 1));
Q0 = sum(Q);
Beta = 1;
Q = (z.*(K - 1))./(1 + Beta*(K - 1));
Q1 = sum(Q);
if Q0*Q1 <= 0
        Beta = beta2phs(K, z);
        NPhase = 2;
elseif Q0<=0                % Bubble pt Calc.
        Beta = 0;
        NPhase = 1;
else                        % Dew pt Calc.
        Beta = 1;
        NPhase = 1;
end;

% Calculate x and y and normalise
x = z./(1 + Beta*(K - 1));
y = K.*x;
x = x/sum(x);
y = y/sum(y);

% Calculate Amix and Bmix
i=1;
while i<=nc
  j=1;
  while j<=nc
    Aij(i,j)=(1-k(i,j))*(Apc(i)*Apc(j))^(1/2);
    j=j+1;
  end;
  i=i+1;
end;
Ay=0;
Ax=0;
By=0;
Bx=0;
i=1;
while i<=nc
  j=1;
  while j<=nc
    Ay= Ay+y(i)*y(j)*Aij(i,j);
    Ax= Ax+x(i)*x(j)*Aij(i,j);
    j=j+1;
  end;
```

```
  By=By+y(i)*Bpc(i);
  Bx=Bx+x(i)*Bpc(i);
  i=i+1;
end;

% Liquid z
phase=1;
zl=zroot(Bx, Ax, phase);
Vl=zl*R*T/P;

% Vapour z
phase=0;
zv=zroot(By, Ay, phase);
Vv=zv*R*T/P;

i=1;
while i<=nc;
% Calculate lnphi
  sumxjaij(i)=0;
  sumyjaij(i)=0;
          j=1;
          while j<=nc
    sumxjaij(i) = sumxjaij(i) + x(j)*Aij(i,j);
    sumyjaij(i) = sumyjaij(i) + y(j)*Aij(i,j);
                    j=j+1;
          end;
          lnphil(i)=Bpc(i)/Bx*(zl-1)-log(zl-Bx)+Ax/(2.828*Bx)*(Bpc(i)/Bx - 2/Ax*sumxjaij(i))
*log((zl+2.414*Bx)/(zl-0.414*Bx));
          lnphiv(i)=Bpc(i)/By*(zv-1)-log(zv-By)+Ay/(2.828*By)*(Bpc(i)/By - 2/Ay*sumyjaij(i))
*log((zv+2.414*By)/(zv-0.414*By));
  i=i+1;
end;

thetai = y.*log((y.*exp(lnphiv))./(x.*exp(lnphil)));
theta = sum(thetai);
theta2 = (theta)^2;
if theta2 <= tol
          s = 101;
else
  i=1;
  while i<=nc
    K(i) = (K(i)*(x(i)*exp(lnphil(i)))/(y(i)*exp(lnphiv(i))))^(1.0);
    i=i+1;
  end
end;
if K(5) <1e-15
  K(5)=1e-14;
end;

if t>100
          s=101;
end;
t=t+1;
```

```
end;  % end of large while loop

molesvap = molefeed*Beta;
moly = y*molesvap;
molesliq = molefeed*(1-Beta);
molx = x*molesliq;
data = [y' moly' x' molx'];
```

Subroutines

```
function Beta = beta2phs(K, z);      % Calculates the vapour fraction based on the set of K's

tolerence = 10;
Beta = 0.95;

while tolerence >= 1e-10
        q = (z.*(K - 1))./(1 + Beta*(K - 1));
        Q = sum(q);
        dq = (z.*(K - 1).^2)./((1 + Beta*(K - 1)).^2);
        DQ = -1*(sum(dq));
        Beta2 = Beta - (Q/DQ);
        tolerence = abs(Beta2 - Beta);
        Beta = Beta2;
end;
```

C.3 Optimisation Code

```
clear
ks = [0.0258 0.0338 0.0424 0.0539 0.1010];  % kij initial guess
ksopt = fmins('volstepq',ks)       % Call the extraction simulation
```

Appendix D

Raw Data

D.1 Ethane Extraction Experiments

The raw data from the bitumen extraction experiments performed are shown below:

Temp	63.35 C		
Press	10.5 MPa		
Flow	400 cm3/h		
Patm	658.3 mmHg		
T WTM	17.5 C		
Mass Bitumen	139.50 g		
Vol Expt	M sep i	M sep f	Mext
L	g	g	g
45.7	154.71	160.2	5.49
93.3	225.39	232.27	6.88
141.7	154.19	159.37	5.18
193	156.31	160.75	4.44
246	154.01	156.85	2.84
Temp	36.91 C		
Press	10.5 MPa		
Flow	400 cm3/h		
Patm	672 mmHg		
T WTM	18.5 C		
Mass Bitumen	140.3 g		
Vol Expt	M sep i	M sep f	Mext
L	g	g	g
41.1	155.99	167.8	11.81
83.9	225.25	239.89	14.64
131	155.36	163.83	8.47
178.3	154.34	159.34	5
232.6	154.44	157.72	3.28

Table D.1 – Raw experimental data.

Temp	47.79 C
Press	10.49 MPa
Flow	400 cm3/h
Patm	668.9 mmHg
T WTM	17.5 C
Mass Bitumen	140.86 g

Vol Expt L	M sep i g	M sep f g	Mext g
40.6	155.85	162.4	6.55
85.1	225.07	236.59	11.52
132.1	154.89	163.01	8.12
178.7	154.07	158.78	4.71
233.9	153.92	157.27	3.35

Temp	92.05 C
Press	10.49 MPa
Flow	400 cm3/h
Patm	663.4 mmHg
T WTM	18 C
Mass Bitumen	140.34 g

Vol Expt L	M sep i g	M sep f g	Mext g
45.8	155.88	156.82	0.94
93.7	225.35	226.86	1.51
142.2	155.22	156.83	1.61
192.1	154.5	156.02	1.52
252.5	154.6	156.6	2

Temp	47.69 C
Press	12.21 MPa
Flow	400 cm3/h
Patm	669.9 mmHg
T WTM	16.5 C
Mass Bitumen	140 g

Vol Expt L	M sep i g	M sep f g	Mext g
43.4	156.24	164.27	8.03
88.2	225.28	240.06	14.78
134.7	155.34	164.59	9.25
184.6	154.37	160.26	5.89
248.4	154.41	158.68	4.27

Temp	47.86 C
Press	7.29 MPa
Flow	400 cm3/h
Patm	665.8 mmHg
T WTM	16.5 C
Mass Bitumen	140.4 g

Vol Expt L	M sep i g	M sep f g	Mext g
41	156.34	158.76	2.42
86.3	225.37	230.99	5.62
127	155.21	160.06	4.85
175.6	154.72	158.44	3.72
238.5	154.48	158.06	3.58

Table D.1 (continued).

Temp	76.69 C		
Press	10.51 MPa		
Flow	400 cm3/h		
Patm	666.9 mmHg		
T WTM	18 C		
Mass	140.2 g		
Bitumen			
Vol Expt	M sep i	M sep f	Mext
L	g	g	g
43.5	156.06	157.82	1.76
90.5	225.6	228.96	3.36
138.2	155.08	158.05	2.97
186.3	154.21	156.72	2.51
249.5	154.62	157.71	3.09

Temp	47.92 C		
Press	15.03 MPa		
Flow	400 cm3/h		
Patm	668.4 mmHg		
T WTM	17 C		
Mass	140.2 g		
Bitumen			
Vol Expt	M sep i	M sep f	Mext
L	g	g	g
45	154.91	163.4	8.49
97.5	225.23	245.21	19.98
144	154.68	162.83	8.15
180	155.52	159.57	4.05
213	154.34	156.97	2.63

Table D.1 (continued).

Appendix E

Compositional Data

The following table presents the complete compositional data for the supercritical ethane/bitumen system. Table E.1 includes both the experimental and model compositions in terms of mole fraction.

63°C, 10.5 MPa										
	Window #1		Window #2		Window #3		Window #4		Window #5	
	Model	Expt.	Model	Expt.	Model	Expt.	Model	Expt.	Model	Expt.
Cum. Volume, Std L	16.48	16.05	55.70	55.45	95.11	95.51	138.91	137.98		175.82
Cum. Mass, g	2.80	5.49	9.25	12.37	14.33	17.55	18.17	24.83		2.84
Comp., mol fraction										
PC1	0.0123	0.0200	0.0119	0.0128	0.0104	0.0105	0.0084	0.0088		0.0076
PC2	0.0079	0.0142	0.0078	0.0094	0.0074	0.0079	0.0069	0.0070		0.0064
PC3	0.0011	0.0042	0.0011	0.0028	0.0010	0.0023	0.0009	0.0021		0.0019
PC4	0.0001	0.0010	0.0001	0.0007	0.0001	0.0006	0.0001	0.0005		0.0004
PC5	0.0000	0.0001	0.0000	0.0001	0.0000	0.0001	0.0000	0.0001		0.0001
Ethane	0.9786	0.9606	0.9792	0.9741	0.9811	0.9786	0.9837	0.9815		0.9836

47°C, 10.5 MPa										
	Window #1		Window #2		Window #3		Window #4		Window #5	
	Model	Expt.	Model	Expt.	Model	Expt.	Model	Expt.	Model	Expt.
Cum. Volume, Std L	9.36	9.46	46.85	46.90	85.79	86.45	125.09	125.66	164.50	165.01
Cum. Mass, g	5.92	6.55	19.68	18.07	25.90	26.19	29.95	30.90	33.34	34.25
Comp., mol fraction										
PC1	0.0296	0.0342	0.0207	0.0176	0.0138	0.0133	0.0098	0.0103	0.0075	0.0084
PC2	0.0307	0.0258	0.0214	0.0154	0.0166	0.0124	0.0141	0.0102	0.0125	0.0087
PC3	0.0086	0.0095	0.0053	0.0059	0.0039	0.0048	0.0032	0.0041	0.0028	0.0036
PC4	0.0011	0.0027	0.0006	0.0017	0.0004	0.0014	0.0003	0.0012	0.0003	0.0011
PC5	0	0.0008	0	0.0005	0	0.0004	0	0.0003	0	0.0003
Ethane	0.9301	0.9269	0.952	0.9589	0.9653	0.9676	0.9726	0.9738	0.9769	0.978

37°C, 10.5 MPa										
	Window #1		Window #2		Window #3		Window #4		Window #5	
	Model	Expt.	Model	Expt.	Model	Expt.	Model	Expt.	Model	Expt.
Cum. Volume, Std L	9.93	6.80	43.93	42.80	82.56	82.42	121.70	122.21	159.08	160.18
Cum. Mass, g	7.87	11.81	27.49	26.45	34.18	34.92	38.39	39.92	41.11	43.20
Comp., mol fraction										
PC1	0.0392	0.0614	0.0235	0.0228	0.0145	0.0153	0.0100	0.0114	0.0077	0.0091
PC2	0.0559	0.0541	0.0311	0.0213	0.0224	0.0150	0.0180	0.0117	0.0150	0.0097
PC3	0.0228	0.0221	0.0105	0.0090	0.0070	0.0065	0.0056	0.0053	0.0048	0.0045
PC4	0.0047	0.0080	0.0017	0.0035	0.0010	0.0025	0.0008	0.0020	0.0006	0.0017
PC5	0.0001	0.0044	0.0000	0.0017	0.0000	0.0011	0.0000	0.0009	0.0000	0.0008
Ethane	0.8774	0.8500	0.9333	0.9417	0.9550	0.9595	0.9656	0.9687	0.9719	0.9742

48°C, 12.2 MPa										
	Window #1		Window #2		Window #3		Window #4		Window #5	
	Model	Expt.	Model	Expt.	Model	Expt.	Model	Expt.	Model	Expt.
Cum. Volume, Std L	10.50	10.83	48.41	48.76	88.31	88.14	130.82	130.40	175.81	176.97
Cum. Mass, g	10.46	8.03	26.20	22.81	32.89	32.06	37.46	37.95	40.63	42.22
Comp., mol fraction										
PC1	0.0356	0.0315	0.0217	0.0188	0.0136	0.0141	0.0094	0.0108	0.0070	0.0085
PC2	0.0460	0.0276	0.0275	0.0179	0.0206	0.0142	0.0167	0.0115	0.0137	0.0095
PC3	0.0167	0.0107	0.0085	0.0073	0.0060	0.0059	0.0048	0.0049	0.0042	0.0042
PC4	0.0030	0.0038	0.0013	0.0027	0.0008	0.0022	0.0006	0.0018	0.0005	0.0016
PC5	0.0000	0.0012	0.0000	0.0009	0.0000	0.0007	0.0000	0.0006	0.0000	0.0005
Ethane	0.8985	0.9251	0.9411	0.9524	0.9590	0.9629	0.9685	0.9703	0.9746	0.9757
48°C, 7.3 MPa										
	Window #1		Window #2		Window #3		Window #4		Window #5	
	Model	Expt.	Model	Expt.	Model	Expt.	Model	Expt.	Model	Expt.
Cum. Volume, Std L	15.43	14.90	52.10	53.00	86.87	87.20	127.49	128.10	175.92	175.10
Cum. Mass, g	1.48	2.42	4.99	8.04	8.11	12.89	11.11	16.61	13.79	20.19
Comp., mol fraction										
PC1	0.0080	0.0105	0.0080	0.0098	0.0077	0.0091	0.0071	0.0078	0.0061	0.0067
PC2	0.0041	0.0070	0.0041	0.0065	0.0040	0.0066	0.0038	0.0059	0.0036	0.0053
PC3	0.0004	0.0016	0.0004	0.0016	0.0004	0.0016	0.0004	0.0014	0.0004	0.0013
PC4	0.0000	0.0004	0.0000	0.0004	0.0000	0.0004	0.0000	0.0003	0.0000	0.0003
PC5	0.0000	0.0000	0.0000	0.0000	0.0000	0.0000	0.0000	0.0000	0.0000	0.0000
Ethane	0.9875	0.9804	0.9875	0.9817	0.9879	0.9823	0.9887	0.9863	0.9899	0.9863
48°C, 15.0 MPa										
	Window #1		Window #2		Window #3		Window #4		Window #5	
	Model	Expt.	Model	Expt.	Model	Expt.	Model	Expt.	Model	Expt.
Cum. Volume, Std L	11.43	10.62	54.02	54.87	93.22	94.06	124.19	124.41	146.46	146.51
Cum. Mass, g	15.16	8.49	34.50	28.47	40.71	36.62	43.61	40.67	45.04	43.30
Comp., mol fraction										
PC1	0.0392	0.0230	0.0208	0.0133	0.0129	0.0093	0.0098	0.0075	0.0083	0.0066
PC2	0.0578	0.0323	0.0321	0.0212	0.0235	0.0161	0.0192	0.0135	0.0167	0.0121
PC3	0.0243	0.0140	0.0115	0.0100	0.0083	0.0077	0.0071	0.0067	0.0064	0.0061
PC4	0.0056	0.0054	0.0022	0.0040	0.0014	0.0032	0.0012	0.0028	0.0010	0.0026
PC5	0.0001	0.0013	0.0000	0.0010	0.0000	0.0007	0.0000	0.0006	0.0000	0.0006
Ethane	0.8730	0.9240	0.9334	0.9506	0.9538	0.9628	0.9628	0.9689	0.9674	0.9720

Appendix F

Error Analysis

F.1 Systematic Error Data

Systematic errors were calculated using the errors associated with the measurement devices and the results are shown in Table F.1.

Temp. °C	Press. MPa	Error in Value	Mass g	Volume Std L	Oil/Gas g/Std L	Absolute Deviation	Absolute Rel Dev
48	7.3	Expt Value	8.17	52.6	0.1553		
		+0.01/+0.01	8.19	52.61	0.1557	0.0004	0.0023
		+0.01/-0.01	8.19	52.59	0.1557	0.0004	0.0026
		-0.01/+0.01	8.15	52.61	0.1549	0.0004	0.0026
		-0.01/-0.01	8.15	52.59	0.1550	0.0004	0.0023
48	15	Expt Value	36.62	93.1	0.3933		
		+0.01/+0.01	36.64	93.11	0.3935	0.0002	0.0004
		+0.01/-0.01	36.64	93.09	0.3936	0.0003	0.0007
		-0.01/+0.01	36.6	93.11	0.3931	0.0003	0.0007
		-0.01/-0.01	36.6	93.09	0.3932	0.0002	0.0004
48	15	Expt Value	18.07	49.3	0.3665		
		+0.01/+0.01	18.09	49.31	0.3669	0.0003	0.0009
		+0.01/-0.01	18.09	49.29	0.3670	0.0005	0.0013
		-0.01/+0.01	18.05	49.31	0.3661	0.0005	0.0013
		-0.01/-0.01	18.05	49.29	0.3662	0.0003	0.0009
48	15	Expt Value	20	141.1	0.1417		
		+0.01/+0.01	20.02	141.11	0.1419	0.0001	0.0009
		+0.01/-0.01	20.02	141.09	0.1419	0.0002	0.0011
		-0.01/+0.01	19.98	141.11	0.1416	0.0002	0.0011
		-0.01/-0.01	19.98	141.09	0.1416	0.0001	0.0009
					Average	0.00029	0.00128

Table F.1 - Data used to calculate the systematic error of the experimental apparatus.

The error in the balance was 0.01 g and the wet test meter had an error of 0.01 L. These errors were used with four experimental data points to determine the variation in the oil to gas ratio calculated using Equation 3.7. The designations in the third column refer to how the variables in Equation 3.7 were adjusted. For example, "–0.01/+0.01" means the balance values were reduced by 0.01 g and the wet test volume was increased by 0.01 L.

F.2 Random Error Data

The random errors in the experimental data presented in Chapter 3 were determined using the Equation 3.7 and the data in Table F.2.

Temp. °C	Press. MPa	Window #	Mass g	Volume Std L	Oil/Gas g/Std L	Average	Absolute Deviation	Absolute Rel Dev
63	10.5	2	11.44	67.00	0.171		0.006	0.035
			11.52	62.90	0.183		0.006	0.035
			11.50	65.00	0.177	0.177	0.000	0.000
63	10.5	4	19.66	142.50	0.138		0.002	0.017
			20.79	146.90	0.142		0.001	0.008
			20.00	141.10	0.142	0.140	0.001	0.009
47	10.5	2	19.09	48.60	0.393		0.021	0.057
			18.07	49.30	0.367		0.005	0.014
			16.76	47.10	0.356	0.372	0.016	0.043
47	7.3	2	8.17	52.60	0.155		0.001	0.004
			8.04	51.50	0.156		0.001	0.009
			7.55	49.40	0.153	0.155	0.002	0.012
47	7.3	3	12.18	88.50	0.138		0.005	0.037
			12.93	92.00	0.141		0.002	0.017
			12.89	85.50	0.151	0.143	0.008	0.054
47	15.0	3	36.46	93.20	0.391		0.002	0.004
			36.62	93.10	0.393		0.004	0.010
			35.70	93.00	0.384	0.389	0.006	0.014
						Average	0.005	0.021

Table F.2 – Data used to determine the random experimental error.